

**COLLAGEN-BASED SCAFFOLDS FOR
TISSUE ENGINEERING
OF SMALL-DIAMETER BLOOD VESSELS**

Laura Buttafoco

Members of the Committee:

Promotors:	Prof. Dr. J. Feijen	University of Twente
	Prof. Dr. I. Vermes	University of Twente
Assistant promotor:	Dr. A.A. Poot	University of Twente
Referent:	Dr. P.J. Dijkstra	University of Twente
Members:	Prof. Dr. W. Kruijer	University of Twente
	Prof. Dr. J.F.J. Engbersen	University of Twente
	Prof. Dr. Ir. I.H. Koole	University of Maastricht
	Dr. T.H. van Kuppevelt	University of Nijmegen

The research described in this thesis was financially supported by the IOP Senter, Den Haag, The Netherlands, Project number IIE00003

This publication was sponsored by the Nederlandse Vereniging voor Biomaterialen en Tissue Engineering (NTBE).

Collagen-based scaffolds for tissue engineering of small-diameter blood vessels.

By Laura Buttafoco

Ph.D. Thesis, University of Twente, Enschede, The Netherlands, 2005.

With references and with summary in English, Dutch and Italian.

ISBN 90-365-2135-1

Copyright © L. Buttafoco 2005

All rights reserved.

Cover design by Marco Buttafoco and Alessandra Scerch.

Printed by Print Partners Ipskamp, Enschede, The Netherlands, 2005.

**COLLAGEN-BASED SCAFFOLDS FOR
TISSUE ENGINEERING
OF SMALL-DIAMETER BLOOD VESSELS**

DISSERTATION

to obtain

the doctor's degree at the University of Twente,

on the authority of the rector magnificus,

prof. dr. W.H.M. Zijm,

on account of the decision of the graduation committee,

to be publicly defended

on Friday, 18th February 2005 at 13.15

by

Laura Buttafoco

born on 14th December 1975

in Rome, Italy

This dissertation has been approved by:

Promotors: Prof. dr. J. Feijen
 Prof. dr. I. Vermes
Assistant promotor: Dr. A.A. Poot

*“In those whom I like
I can find no common denominator;
In those whom I love I can:
They all make me smile”
(W.H. Auden)*

To those who can make me smile ☺

*“Non so trovare alcun comun denominatore
in coloro che mi piacciono;
so trovarlo in coloro a cui voglio bene:
sanno farmi sorridere”
(W.H. Auden)*

A tutti coloro che mi fanno sorridere ☺

Acknowledgments

Those who bring sunshine into the lives of others cannot keep it for themselves

(J. M. Barrie)

These past four years would have probably been completely different if Prof. Feijen would not have given me the possibility to work in his group. It is for this reason that my first acknowledgments go to him, also for having created such a nice environment around me. The discussions we had, especially during this last year, were always very inspiring. I also always enjoyed the almost yearly ever-joyful sneertfest.

Of course I would like to thank also my co-promotor, Prof. Vermes. It was always nice to discuss things with you, always smiling and encouraging also in the most stressful periods. Though the topic of this research is for certain aspects far from your interests you were always ready to give a helpful hand when needed. Thank you for that!

Almost each of the staff members of PBM contributed in a way or another to the development of this project. Piet, without doubts you were the one who mostly helped me throughout these four years and not only in working matters. You trusted me, giving me the freedom to choose, sometimes also in the wrong direction. I have learnt a lot from that and from the interesting discussions we had together almost daily: you were always interested in my work. I especially thank you for all the time you dedicated to reading many of the chapters of this dissertation. I appreciated a lot that for certain topics you openly admitted you did not know and you never hesitated going back to the library to study and help me out in the most intricate matters. Not everyone would have done it! At the same time, I thank you for having arranged all the paperwork for me when I moved here and for having tried to make me integrate in The Netherlands organizing dinners at your place (thanks also to Jenny) and short trips. You indeed contributed to make me feel at home also in Enschede and I really enjoyed it!

André, during this years we had regular meetings to keep each other updated, but I could always also just pop in your office if I had questions. Being my assistant-promotor your share of

responsibilities increased a lot in the last months of this project. Thanks for the accuracy with which you read this thesis and for having turned the “Summary” into the “*Samenvatting*”.

Dirk, thanks for the fruitful discussions we had together, regarding chapter 8.

Maybe this project would not have been there without the financial support of the IOP Senter (Den Haag) and indeed without the project meetings, I would not have had the possibility to cooperate with the people of the group of Toin van Kuppevelt in the University of Nijmegen. Willeke, without your elastin this thesis would not have the contents it has today. It was nice to cooperate with you, I appreciated your always-quick answers to my emails and, thanks to you, I have also learnt a bit about proteins purifications. I wish you all the best in your new job! Toin van Kuppevelt you were the only one always present at every IOP meeting: thanks for your never lacking interest in this work and for having accepted to be a member of this PhD committee.

Ernst van Eck and prof. Kentgens, Chapter 5 would not be part of this thesis without your help. Solid state NMR was almost unknown to me when I came to Nijmegen asking for some measurements. It took some time, but at the end I think we managed in making a nice piece of work. Thanks for the time you spent explaining me the “mysteries” of CP/MAS ^{13}C NMR!

Paula, I certainly owe you a special thank. We spent a long time in figuring out “the right” bioreactor and, when the set up was finally completed, the exhausting work begun. From then on the alarm clock started ringing at 7.30 a.m. also in the weekend, but it was always pleasant to know that you would have also been there. I was amazed to hear how many sports you play in the weekend, but at least I could explain why you were so good in spear throwing in Cairns. In Kuranda, it was fun to play the didgeridoo: we made a nice concert (?!?).

Niels *prutser* and Niel B. without your work chapters 4 and 8 would not be here. I really enjoyed having you as students and I have learned a lot in a very pleasant way. It was fun also to watch Ajax-A.S.Roma together, being shown around Nijverdaal, eating *pannencoeken*, brownies and all the dinners that followed. Thanks!!!

Zlata, John, Clemens, Hetty, Karin, Genevieve, Gerda and Cindy the work would not have been so smooth here without you. Thanks for your efficiency and for your always present “smiling” support.

Mark (Smithers) I would like to thank you especially for your expertise in SEM, but also for the nice chats we had during the measurements. I came out of your office always knowing a bit more

about my samples but also about (English or Italian) football, squash, food and gossips about all the people who came and measure with you ;-)

My life in the office would surely have been duller without the company of the people I shared it with. QinPu, when you arrived you were so reserved and formal that you used to bow everytime I entered the office. Who would have thought that you would have come with me and Francesca S. to the “tropical night” in Hengelo? It was fun! Fenghua, *little girl*, we had a lot of nice chats together and indeed a lot of delicious (but strange looking) tea. Eating with chopsticks is not a secret anymore for me, thanks to you and Zhiyuan, but still I think that little Eric will learn better than me in a shorter time! Christine with your arrival the office was full again and officially became “the chicken room”. Suddenly we also starting smelling soup at any time of the day...Your solar, but also a bit clumsy character brought a lot of smiles in the office. With Ingrid also the candy-box came. It was nice to know that you can always take a *snoepje* when you feel like! Thanks for the nice chit-chats girls ☺

Pri, we shared the office for basically the all 4 years. Your being always full of life and your friendship contributed in making it a great time! You introduced me to many typical aspects of dutch life going from birthdays, to eating stampot, to being totally addicted to your agenda...even my appointments can be found in yours! I am honoured you chose me as your paranimf and extremely glad that you accepted to be on stage once more with me!

Also together with Ype, we organized a lot of nice things together: a boat-weekend in Frisland (that was really great, you even arranged the sun ;-)), short holidays in Italy and even in Australia. Hey guys, when are we going for the next holiday? By the way, Ype, I will miss your satisfied face when I address you with “*Ciao bello!!!*”... Thanks also for the “weight-lifting” exercise every time I used the Zwick. You, Wilco and Edwin really had a lot of patience with me!!!!

Karin, you were there when I was an Erasmus and again when I came as a PhD. Together we always had a lot of fun, no matter where we were. In one of our evenings together, you met the love of your life, Wimpie, and in a few months you both moved to South Africa. I am really happy you are both having a wonderful time overthere! Bas, together with Karin, you were one of my best tea-mates. After she left, we kept the habit, though we had to abandon it after a while ☹ It is always nice to chat with you, no matter in which language or about what and, you know? You are the one who gave me the only book in dutch I have ever read in my life! *Dankje!*

I owe a lot also to the other (former) colleagues of the PBM, RBT, STEP and MTP groups: Zhiyuan (hope you don't mind I still mention you among the colleagues, now that you are part of the staff), BoonHua (and your never ending talks/gossips), Zhang (always very helpful), Lanti (good luck with collagen), Wei (virtually you are one of my roommates, but Priscilla never allowed you to effectively become one!), Martijn (pity that you left), Chao (finally a Chinese with an easy name to remember), Mark t.B. (the real *tucker*), Mark A. (always ready to give me a hand), Kannika (the sweet Thai girl), Monique (the perfect organizer of the girls' nights), Ewa (how can you bake all those nice cakes?), *Ninoska* (my gym preferred companion), Kinsuk, Pratip and Vipin (good humor bringing trio), Giorgio (it was great playing in the waves of the blue sea in Nice with you and Enrica and the narghilé idea was also fun), Margie, Ana and Audrey (the first ones who introduced me into the "party-society" of Enschede), Menno (my preferred tennis-mate...to loose with and a very good guide for dutch festivals and events...but does it always have to rain then?), Marina and Sandra (finally some solar mediterranean spirit also in this side of the building). Mediterranean spirit is something that never lacked in the SMCT group...Marta, Francesca C., Olga, Alessio, Mitchell, Fernando and Lourdes (hey girl *que tal?*) I enjoyed your company always a lot! Playing Twister, dancing, having tons of good food and always fun are the things which come to my mind when I think about you!

I could easily write a separate thesis for all the wonderful people I met during these years living in Calslaan. Jaco, you were one of the first and indeed one of the best friends I made during these years! No one could ever make a cooler snow-man than the one we made together... I could not think of better companions than you and Mauro to travel. Our "*peperépé-trips*" to Paris, London, Belgium, The Netherlands and also at home, in Rome, were simply great. Very soon we will come to South Africa, it is a promise ;-)

Calslaan would not have been the same without the Indians. Anil, you were the first and the one I had the most difficult conversations with. It took me sometime, but at the end I managed to get used to your accent! Nidhi, you were the only Indian girl I had the pleasure to know. It is always very nice to chat with you! I will be always more than happy to spend a *gandu* week end with you *gandus*...Dhanya (the wise married guy, teaching useful (???) Marathi words to innocent (!?!)) Italians in his spare time), Vinit (the ever smiling, sweet guy), Saba (the one of the best present ever...no one could do better!), Suresh (the womaniser !?!), Chaitya (the "surprise" guy...hey this year is going to be one to remember!), Akash (or Suresh :-P). It was always a lot of fun and the

kaju kathali, chicken tandoori, mattar paneer, laddoo were always delicious ☺. But please stop trying to kill pasta cooking it in the indian way :-P!!!! Charu, you belong to this eccentric group as well, but you deserve separate thanks for having been closer than the others to me, having cooked a bit less spicy for me, having taught to me a lot about Indian culture and becoming a very good *pizzaiolo!*

It was really pleasant to share the flat also with you, Phuong, Ha, Geng and Chi (always smiling and cooking delicious food), Wei (tall), Wei (short) and Yan (I enjoyed our interesting conversations in the kitchen!), Jiong (the weirdest Chinese ever...not cooking and talking a bit of Italian!), Raffael (the only guy who, while talking in French, English and Dutch all together, can also add an Italian joke! How can I forget your “*Buongiorno Principessa*” every morning?), Hany (one of the greatest eater of my pizza...I can still hear your bright laughter around), Julien (despite your efforts I will be never good in french and you must have realized it when I told you “*Salut*” because you sneezed!), Peter (my best *cocopal* night-chatter...I am happy I have started to read that book...*sladke sny* ☺), Doris (now I really need to come to hug Hannah and Greta: congratulations!), Paula (definitely I think you have some joints more than me...it is impossible to dance samba like you!), Camilo (my official Spanish teacher), Anand (always very polite).

Truzzi (Fra S.), *Kullatje* (Fra de R.), Anna, officially you were never my flat-mates but in reality you were much more than that! *Truzzi* you have been my best mate for small cultural trips around The Netherlands. Den Haag, the exhibition of van Gogh and Gauguin and many other smaller things we visited around The Netherlands would have not been the same without your company. It is always fun to chat with you, no matter if during one of those long dutch rainy evenings when none of the two wanted to get soaked biking back (“No way...*é una roba da chiodi!*”), or at 35°C eating a fresh and juicy water melon in the Isle of Elba. Anna, coming from Rimini you could not be anyone else than the party, party, party and more party girl!!! No matter where or why, when you were around it was party-time almost every night! It has always been unbelievable how fast you could turn from a sleeping-mood, already wearing your pyjama, to a dancing/drinking one... 5 min and you were already on the bike! Together with Miriam, the Sicilians, Raffael and Marcela we always had a lot of fun! It was great to spend the New Year together again this year ☺! *Kullatje*, together we went through good, hard, but especially “stupid” times! Just to mention some: “the conquer of Boekelo” (?!?) skating, the fight in the foam in a freezing, but officially “tropical” night, baking “Laura Brown” cakes, dancing on the notes of Nabucco in a carnival

night in Maastricht, organizing a wonderful trip to Nice, during which we spent the first night in a 4 star Mc Donald's in the internationally famous city of Holzwickede (!!?) and especially the development of a new language: Kullese..."*Ehy cica, I'm happy a number che sarai mijn paranimf ☺*". Just a question: how will you manage to invite people for dinner at MY place when I will move out?

Most of the fun would not have been there without all the sporting events (tennis, swimming, horseback riding, gym, triathlons), the borrels, the olie-bollen, the SinterKlaas parties and especially without Marcela (hola Marcela now I am ready for a party weekend in Amsterdam...coming!!!), the Sicilians, Carlo (ehy *ingeniere*, you were one of the best trio-team-mates in the triathlon...*baciamo le mani!*), Marco (missing our salsa party) and Andrea (the more serious guy!), *Dorotina*, Sune, Maia and Kazu-san (with the ultimately cool parties, the tennis matches and the fun in the swimming pool), Cristiano, Vittorio and Elena (nice bbq at your place...it is always a cosy Italian corner there!!).

I would not have known many wonderful corners in Twente, without the special biking trips together with you, Wim. You are a unique kind of person, always full of brilliant and bizarre ideas, a very good company no matter if for a dinner, a theatre performance, an open-air activity or just a tea. When I think of you, the jelly fish, Giovanni the juggler, the old old man, Enea and Dido, your sweet mum or the always happy Karin come to my mind and make me smile ☺. Thanks a lot for having shown to me also this side of The Netherlands!

Also back in Italy there are a lot of people who really deserve my gratitude. *Cri*, *Anto* and now also *Elisa* (*i mitici topolini* with your unique way of ordering French fries...), *Giada* (*ciao bruttona!* What about the football team then?) and *Gabriele*, your life changed a lot in these last four years, with the marriage and all the rest, but you never forgot to include me as an active part of it ☺! Your mails and sms, as well those from *Vale* (a friend, my friend...but it was really a pity that you never managed to come here in all these years), *Cristiano* (I am *un pupazzetto*, a cartoon ok, but in that photo of yours you gave me when I left, you don't look less funny!!) *Juá* (the busy guy of the group) and *Flavia* (will we manage to meet before next Christmas this year?) always made me feel there with you! Thanks a lot guys also for having tried to keep up to my crazy rhythms when, coming there, I tried to see everyone and do thousands things at the same time and in the few days I had.

D.D.P.M. it is great to have you around all the time. And *Puzzola* I can already imagine your puzzled face during the PhD ceremony. *Penserai ancora di voler fare chimica?*

Mamma, without your encouragement, I don't know whether I would have come here in Enschede for four years. It sounded like such a long time far from everyone...But you know it, *come fai, fai bene* and you were right also this time: *t.v.t.b.!*

Ciccio in these years, there was hardly a day when you did not fill me with emails and sms, also just to say hi! You indeed are my preferred "taxi-driver" from or to the airport, assistant for technical/computer problems (the cover would not be here without you!), companion to play fool (which were the names of the reindeers?) and especially *il mio dolce fratellino mostriciattolo*. Now can I have a small (!?) space back in your (!?) room ☺?

Mauro I don't know how many times we took off and landed to spend some time together, but for all these years it always felt like we were much closer than what geography was showing. Maybe what Gibran says is really true "There is no distance save that which the soul does not span in fancy. And when the soul shall span that distance, it becomes a rhythm in the soul." And this was the most pleasant rhythm ever! Ehy *beautiful moro* who else could I see knocking at my door wrapped up with 5m red ribbon, as an unexpected human-gift for my birthday?

Thanks a lot people for all the special moments you offered me...you will always be welcome in Rome or wherever else I will be!

Laura ☺

Contents

Chapter 1	General introduction	3
Chapter 2	The tissue-engineered small-diameter artery	9
Chapter 3	First steps towards tissue engineering of small-diameter blood vessels: preparation of flat scaffolds of collagen and elastin by means of freeze drying	41
Chapter 4	Electrospinning of collagen and elastin for tissue engineering applications	67
Chapter 5	A solid-state ¹³ C CP/MAS NMR study of collagen/elastin assemblies	91
Chapter 6	Development of a bioreactor for tissue engineering of small-diameter blood vessels: design of a pulsatile flow system	121
Chapter 7	Dynamic versus static smooth muscle cell culture in tubular collagen/elastin matrices for vascular tissue engineering	139
Chapter 8	Preparation of porous hybrid structures based on P(DLLAcoTMC) and collagen for tissue engineering of small-diameter blood vessels	165
Summary		189
Samenvatting		193
Sommario		199
Curriculum Vitae		205

Chapter 1

General Introduction.

*The grand aim of all science is
to cover the greatest number of empirical facts by logical deduction
from the smallest number of hypotheses or axioms.
(A.Einstein)*

Introduction.

Atherosclerosis is one of the main causes of death and morbidity in the Western society [1]. Synthetic blood vessels prostheses are successfully being used for large-diameter vascular reconstruction. However, until now, no functional small-diameter (< 6 mm) artificial blood vessel is available, due to thrombus formation early after implantation. Although endothelial cell seeding in small-diameter vascular prosthesis improves the patency to some extent, this approach has not resulted in large-scale clinical applications. Therefore, tissue engineering of small-diameter vascular constructs is an expanding area of research. The ideal tissue-engineered vascular construct should be prepared from a biocompatible material that degrades and resorbs at a controlled rate, to match cell and tissue ingrowth *in vitro* and/or *in vivo*. The material should be processable into a porous tubular scaffold with interconnected pores, which allows cell adhesion, thus providing a suitable environment for cell growth and transfer of nutrients, gases and metabolic end products. The mechanical properties of the resulting construct should match those of a native artery, especially in terms of compliance, to avoid the development of intima hyperplasia after implantation and subsequent vascular failure.

In the past, many attempts to produce a successful tissue-engineered small-diameter vascular construct have been made using either collagen gels [2-5] or synthetic materials [6-8]. Processing of synthetic polymers is generally easy and allows the development of structures with initial burst

pressures comparable to those required for the intended application. However, achieving the necessary cell proliferation and matrix synthesis is still a challenge. In addition, polymer degradation products can alter the local cellular environment and thus cell function, preventing the development of a proper vascular construct. Collagen gel-based scaffolds ensure good cell adhesion and proliferation necessary for the preparation of tissue-engineered constructs, but their application is limited because their mechanical properties do not match the needed requirements.

Aim and structure of this thesis.

It is the aim of this thesis to evaluate the potential use of collagen-based scaffolds for tissue engineering of small-diameter blood vessels. Many of the concepts being pursued up to now rely on the incorporation of cells into collagen gels. However, as stated above, collagen gels do not match the required mechanical properties because they lack the high tensile strength of the organized collagen fibres present in blood vessels. By combining insoluble collagen with insoluble elastin, we expect to modify the material properties and to match the requirements for the preparation of constructs for replacement of atherosclerotic small-diameter blood vessels. Incorporation of elastin in the collagen scaffolds may allow the preparation of constructs having viscoelastic properties similar to those of a native artery.

Alternatively, collagen was combined with poly(D,L-lactide)co(1,3-trimethylene carbonate), P(DLLAcoTMC), thus forming a hybrid structure. Hybrids of natural and synthetic materials are advantageous since they are known to benefit from suitable mechanical properties and low costs of the synthetic polymer as well as appropriate cellular interactions within the natural material.

This thesis is divided into three parts. The introductory part, **Chapter 2** provides a literature overview of the different tissue engineering approaches to address the problem of atherosclerosis in small-diameter blood vessels. The requirements of tissue-engineered vascular constructs and the motivation behind the selection of a combination of collagen with either elastin or P(DLLAcoTMC) for this application are discussed. The potential advantages of collagen/elastin scaffolds or P(DLLAcoTMC)-collagen hybrid matrices over the approaches described in literature are also addressed.

The second part of this thesis deals with the preparation and subsequent characterization of porous scaffolds of collagen and elastin. In **Chapter 3**, the characterization of flat porous scaffolds of insoluble collagen type I and insoluble elastin prepared by freeze drying, is described. The influence of freezing temperature and of crosslinking with a carbodiimide in the presence or absence of a diamine spacer on the morphological and physical properties of the scaffolds is evaluated. Smooth muscle cells (SMC) could be successfully grown throughout the (crosslinked) matrices.

In **chapter 4** the production of non-woven meshes of soluble collagen type I and/or soluble elastin by electrospinning, is addressed. Scaffolds with a high porosity and large surface area, which can be stabilized by crosslinking with a carbodiimide, are obtained. Smooth muscle cells could be successfully grown on top of the non-woven meshes.

Chapter 5 deals with the evaluation of the interactions occurring in freeze-dried assemblies of soluble collagen and elastin by means of cross-polarization magic angle spinning ^{13}C solid-state NMR. Mixing these two components does not induce conformational changes in the separate proteins. However, the analyses of the carbon spin-lattice relaxation times in the rotating frame for collagen/elastin samples revealed significantly different mobilities for the distinct parts of the amino acid residues as compared to those measured for the single components. Proton spin-lattice relaxation times in the rotating frame revealed that the various amino acid residues behave exactly in the same way, independently from the protein they belong to. No separate domains are present in collagen/elastin assemblies. These measurements were performed at two degrees of hydration, since it is known that water plays an important role in the conformations and properties of these proteins. The observed changes in mobility especially for the C_β of Ala and C_α of HyPro, can be attributed to the formation of hydrophobic interactions and hydrogen bonds in collagen/elastin mixtures.

The development of a bioreactor and its applications in tissue engineering of small-diameter blood vessels is addressed in the last part of this thesis. The description of the bioreactor and the investigation of its fluid dynamical properties are reported in **chapter 6**. The developed system allows to reproduce arterial pressure and pulses. Moreover, a laminar flow of culture medium in the lumen of the vessels ensures homogeneous diffusion of nutrients, gases and metabolic end products in the constructs.

Porous tubular collagen/elastin scaffolds prepared by freeze drying have been used to culture SMC in the dynamic environment provided by the bioreactor. The morphological and physical characteristics of the vessels before and after culture for different time periods are described in **chapter 7**. Constructs potentially suitable for further (*in vivo*) applications are obtained.

Chapter 8 deals with the preparation of porous tubular scaffolds of P(DLLAcoTMC) by melt spinning and fibre winding. Hybrid matrices have been prepared by introducing a collagen micro sponge in the scaffolds by dipping in a collagen type I suspension, followed by freeze drying. Resulting hybrid scaffolds have suitable structural stability to be applied for SMC culture in the bioreactor system. After culturing under dynamic conditions, constructs with mechanical properties similar to those of a human artery mesenterica are obtained.

Most of the work described in this thesis has been or will be submitted for publication [9-14].

References.

1. Lusis, A.J., Atherosclerosis. Nature, 2000. 407(6801): 233-241.
2. Berglund, J.D., Mohseni, M.M., Nerem, R.M. and Sambanis, A., A biological hybrid model for collagen-based tissue engineered vascular constructs. Biomaterials, 2003. 24(7): 1241-1254.
3. L'Heureux, N., Pâquet, S., Labbè, R., Germain, L. and Auger, F.A., A completely biological tissue-engineered human blood vessel. Faseb J., 1998. 12(1): 47-56.
4. Seliktar, D., Black, R.A., Vito, R.P. and Nerem, R.M., Dynamic mechanical conditioning of collagen-gel blood vessel constructs induces remodeling in vitro. Ann. Biomed. Eng., 2000. 28(4): 351-362.
5. Weinberg, C.B. and Bell, E., A blood vessel model constructed from collagen and cultured vascular cells. Science, 1986. 231: 397-400.
6. Pennings, A.J., Knol, K.E., Leenslag, J.W. and Van der Lei, B., A two-ply artificial blood vessel of polyurethane and poly(L-lactide). Colloid Polym. Sci., 1990. 268: 2-11.
7. Soldani, G., Panol, G., Sassen, H.F., Goddard, M.B. and Galletti, P.M., Small diameter polyurethane polydimethylsiloxane vascular prostheses made by a spraying, phase-inversion process. J. Mater. Sci.-Mater. Med., 1992. 3(2): 106-113.

8. Niklason, L.E., Gao, J., Abbott, W.M., Hirschi, K.K., Houser, S., Marini, R. and Langer, R., Functional arteries grown in vitro. *Science*, 1999. 284(5413): 489-493.
9. Buttafoco, L., Engbers-Buijtenhuijs, P., Poot, A.A., Dijkstra, P.J., Daamen, W.F., van Kuppevelt, T.H., Vermes, I. and Feijen, J., First steps towards tissue engineering of small-diameter blood vessels: preparation of flat scaffolds of collagen and elastin by means of freeze-drying. *Submitted to J. Biomed. Mat. Res.*
10. Buttafoco, L., Kolkman, N.G., Engbers-Buijtenhuijs, P., Poot, A.A., Dijkstra, P.J., Vermes, I. and Feijen, J., Electrospinning of collagen and elastin for tissue engineering applications. *Submitted to Biomaterials.*
11. Buttafoco, L., van Eck, E., Dijkstra, P.J., Kentgens, A. and Feijen, J., Solid-state ^{13}C CP/MAS NMR analyses of collagen/elastin mixtures. *Submitted to Biopolymers.*
12. Buttafoco, L., Engbers-Buijtenhuijs, P., Poot, A.A., Dijkstra, P.J., Vermes, I. and Feijen, J., Development of a bioreactor for tissue engineering of small-diameter blood vessels: design of a pulsatile flow system. *Submitted to Biotechnol. Bioeng.*
13. Buttafoco, L., Engbers-Buijtenhuijs, P., Poot, A.A., Dijkstra, P.J., Vermes, I. and Feijen, J., Dynamic vs. static smooth muscle cell culture in tubular collagen/elastin matrices for vascular tissue engineering. *Submitted to Biomaterials.*
14. Buttafoco, L., Boks, N.P., Engbers-Buijtenhuijs, P., Grijpma, D.W., Poot, A.A., Dijkstra, P.J., Vermes, I. and Feijen, J., Preparation of porous hybrid structures based on P(DLLAcoTMC) and collagen for tissue engineering of small-diameter blood vessels. *Submitted to J. Biomed. Mat. Res.*

Chapter 2

The Tissue-Engineered Small-Diameter Artery.

It can sometimes be easier to repair a damaged automobile than the vehicle's driver because the former may be rebuilt using spare parts, a luxury that human beings simply have not enjoyed
(D. Mooney, *Scientific American* 1999)

Introduction: tissue engineering.

Atherosclerosis, diabetes, cirrhosis, hepatitis and other afflictions kill or disable millions of people every year by deteriorating their organs in time. In the U.S. alone, thousands of people die annually waiting for a transplant and many thousands more never even make it onto a waiting list. Tissue engineering is an interdisciplinary field that applies the principles of engineering and life sciences towards the reconstruction or development of biological substitutes that restore, maintain or improve tissue functions [1]. Three different approaches are generally chosen to achieve a successful fabrication of new, physiologic, functioning tissue: guided tissue regeneration using engineered matrices, injection of cells or use of cells seeded on or within matrices [2]. The last two methods are most commonly used. Injection or infusion of cells avoids potential surgical complications and allows manipulation of the cells before use [3-5]. However, rejection and loss of functions are the possible drawbacks of this technique [1]. In the most frequently used approach, cells are seeded on a (synthetic or natural) polymeric scaffold and grown *in vitro*. The resulting tissue-engineered material is implanted in the appropriate anatomic location, thus defining a three-dimensional space for the development of new tissue with suitable structure and function [6] (Fig. 2.1).

The impact area of tissue engineering is very broad and in the future the developments in this field could greatly reduce the need for organ transplantation and also accelerate the discovery of new

drugs that may cure patients [7]. At present, dermis [8, 9], epidermis [10], articular cartilage [11, 12] and bone [13] have been successfully reconstructed *in vivo*. However, before translating scientific discoveries into “off the shelf” organs to treat millions of patients, many challenges have still to be addressed. These include identifying expandable sources of suitable cells, developing new scaffolding materials, scaling up the production of that particular tissue and last but not least, discovering ways to preserve the produced tissue and prevent immune rejection [14].

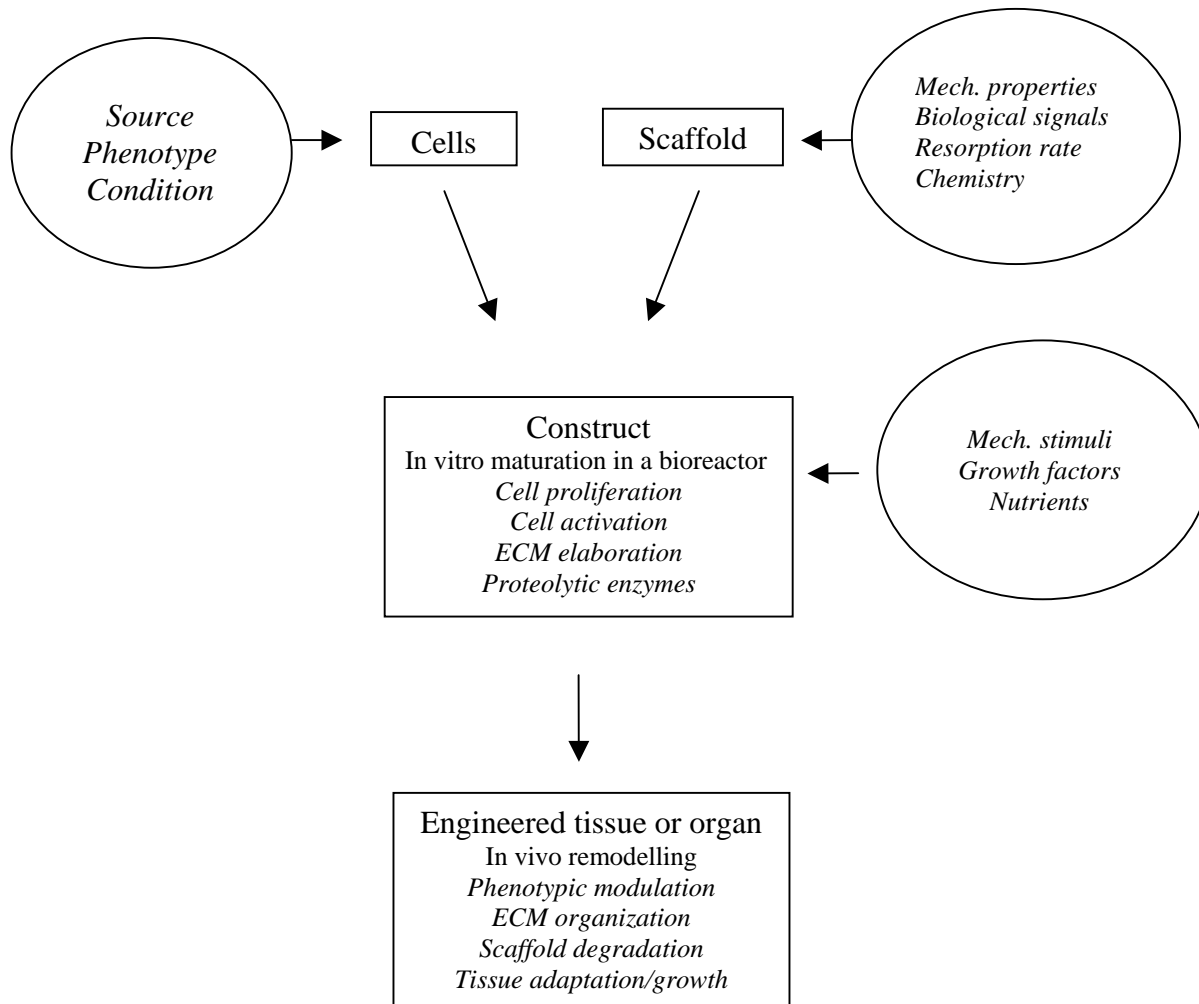


Figure 2.1. Schematic description of a typical tissue engineering approach. In the first step, differentiated or undifferentiated cells are seeded on a bioresorbable scaffold and then the construct is matured *in vitro* in a bioreactor. During maturation, the cells proliferate and synthesize extra-cellular matrix (ECM) to form new tissue. In the second step, the construct is implanted in the appropriate anatomical position, where remodelling *in vivo* is intended to re-establish the normal tissue/organ structure and function. The key variables in the principal components – cells, scaffold and bioreactor - are indicated.

Blood vessels: function and morphology.

The function of blood vessels is to carry blood from and to the heart and to and from tissues and organs. In order to serve every part of the body, blood vessels form a branched system of arteries and veins with a complex structure that varies from site to site within the circulatory system.

In general, blood vessels consist of three concentric layers (Fig. 2.2):

- the intima. It forms the layer closest to the blood flow and consists of a lining of endothelial cells (EC) attached to a connective tissue bed of basement membrane and matrix molecules. Inactivated EC prevent activation of coagulation and complement factors and inhibit adherence of leukocytes and platelets. Moreover, it acts as a mechanical barrier to solutes and solvents in plasma and takes part in the regulation of vasomotor tone, growth and vascular remodelling. The EC layer is adjacent to the internal elastic lamina, which is a band of elastic tissue, separating the intima from the media, mainly found in larger arteries.

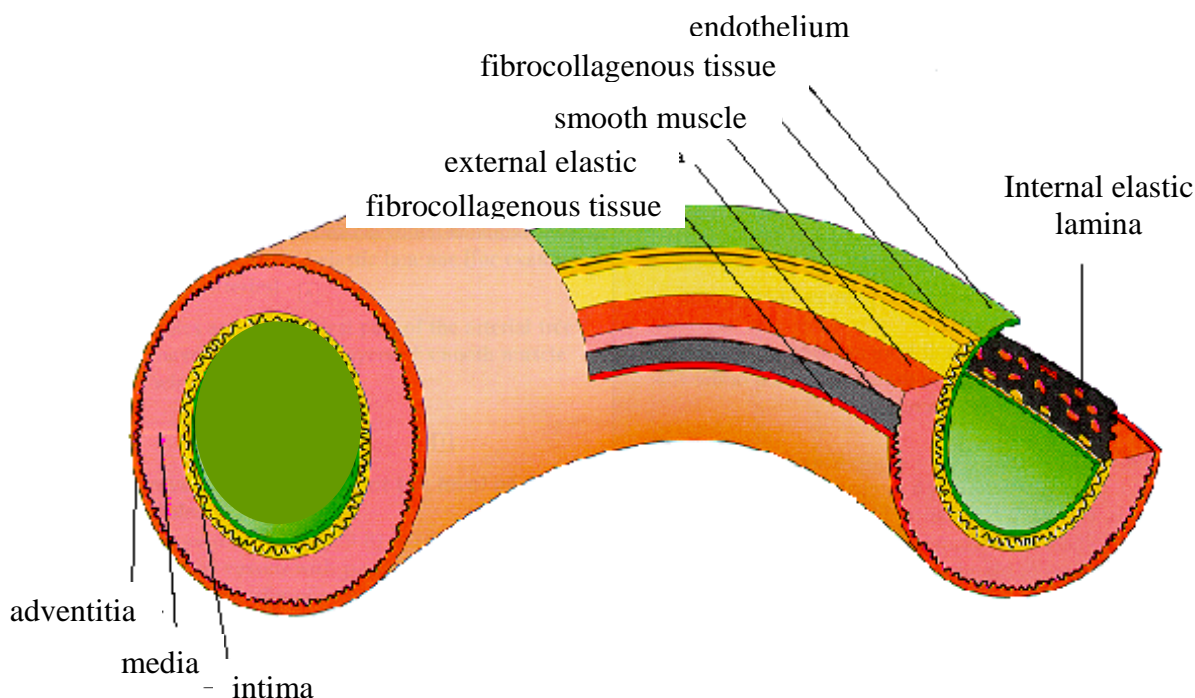


Figure 2.2. Schematic representation of a blood vessel. Its three-layered structure and the main components can be distinguished. The inner layer is the intima, consisting of a lining of endothelial cells attached to a connective tissue bed of basement membrane and matrix molecules; the media, in which the intermediate layers mostly consist of smooth muscle cells organized concentrically, with bands or fibres of elastic tissue; the outer layer, the adventitia, contains collagenous ECM with fibroblasts, blood vessels and nerves.

- the media. It contains a dense population of concentrically organized smooth muscle cells (SMC), with bands or fibres of elastic tissue. It contributes to the mechanical stability of the vessel wall, for example allowing the contraction and relaxation in response to the pulsatile blood flow. The external elastic lamina separates the media from the adventitia.

- the adventitia. It comprises collagenous extracellular matrix (ECM) containing fibroblasts, blood vessels and nerves and mainly functions to add rigidity and form to the blood vessel.

The composition of blood vessels is mainly determined by the mechanical stresses they are subjected to. The overall ratio and architecture of SMC, collagen and elastin fibres ultimately determine their performance. The mechanical properties critical for the correct function of a blood vessel include tensile stiffness, (visco)elasticity and compressibility [15]. Collagen provides the tensile stiffness, elastin the elastic properties, proteoglycans contribute to the compressibility and combined with collagen and elastin, are responsible for the viscoelasticity. This complex mixture of molecules and their particular organization is a fundamental prerequisite for the correct function of a blood vessel.

Unfortunately, atherosclerotic vascular diseases, including peripheral vascular and coronary artery disease, are the major cause of mortality and morbidity in the United States, Europe and other Western countries [16]. In the U.S. alone, cardiovascular diseases were responsible for 38.5% of all deaths in 2001. This year, an estimated 1.2 million Americans will have a new or recurrent coronary attack. These alarming statistics from the American Heart Associations' Heart Disease and Stroke Statistics – 2004 Update demonstrate that cardiovascular diseases clearly pose the greatest risk to life for both men and women. Different studies have revealed many important environmental and genetic risks factor associated with atherosclerosis and it is now clear that this is a progressive disease characterized by the accumulation of lipids and fibrous elements in the arteries, thus altering the morphology and the functionality of a blood vessel.

Atherosclerosis: development and consequences.

The initial stage of atherosclerosis is characterized by the accumulation of excessive amounts of cholesterol-rich lipids derived from the blood, beneath the endothelial lining of the blood vessel. This accumulation leads to the formation of a fatty streak. The disease progresses as SMC within the blood vessel wall migrate from the muscular layer of the blood vessel to a position on top of

the lipid accumulation, just beneath the endothelium. Here SMC continue to divide and enlarge, producing atheromas, benign tumours of SMC within the blood vessel wall. Together the lipid-rich core and the overlying SMC form a plaque. The plaque progressively bulges into the lumen of the vessel as it continues to develop and thus narrows the opening through which blood can flow. The physiology of EC that line the inner wall of the vessel is also altered during the development of atherosclerosis, further contributing to vessel narrowing. The ability of the EC to release nitric oxide, a local chemical messenger that causes relaxation of the SMC becomes impaired. Relaxation causes the vessel to dilate, but, because of reduced nitric oxide release, atherosclerotic vessels cannot dilate as readily as normal.

A thickening plaque also interferes with nutrients transfer for the cells of the involved arterial wall, leading to degeneration of the wall in the vicinity of the plaque. The damaged area is then invaded by fibroblasts (scar tissue forming cells), which form a collagen-rich connective tissue fibrous cap. In the later stages of the disease, Ca^{2+} often precipitates in the plaque (Fig. 2.3).

A vessel so afflicted becomes hard and poorly distensible, a condition normally defined as “hardening of the arteries”. This morphological variation also results in altered blood flow patterns, which together with inflammatory substances can weaken the plaque and lead to its rupture. If this happens, tissue factors will interact with clot-promoting elements in the blood, causing a thrombus to form. This pathology attacks arteries throughout the body, but the most serious consequences involve damage of the vessels of the brain and of the heart. In the brain, atherosclerosis is the prime cause of strokes, whereas in the heart it brings about myocardial ischemia and its complications [17, 18].

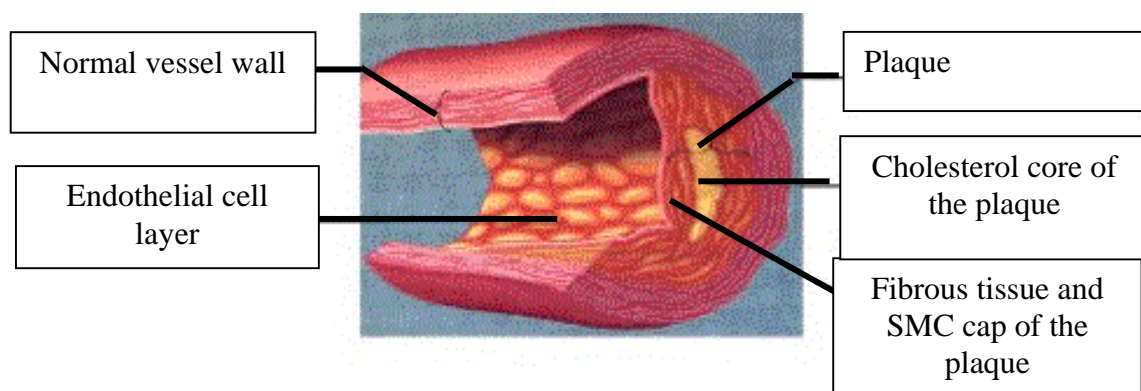


Figure 2.3. *Schematic representation of an atherosclerotic blood vessel.*

Synthetic vascular grafts.

The search for a solution to the problem of atherosclerosis and thus the creation of artificial vascular substitutes dates back to Voorhes *et al.* who successfully developed the first graft [19], a hand-woven fabric made of Vinyon N. The use of this vessel in a clinical study as arterial prosthesis [20], revealed the importance of using porous woven fabrics as vascular grafts and since then, grafts based on textile technology started to be used as replacement vessels.

A variety of knitted or woven materials have been tested for this purpose including nylon, Teflon, poly(ethylene terephthalate) (Dacron) and expanded (tetrafluoroethylene) (ePTFE) [21-25]. Vascular grafts were developed and successfully used for reconstruction of large-calibre arteries (diameter > 6 mm) [26, 27]. Precoating these grafts with proteins, such as albumin, collagen type I or fibrin improves graft healing [28]. Long-term anticoagulant treatment and administration of platelet inhibitors enhances the patency of these vascular grafts up to more than 10 years post-implantation [29]. Unfortunately, when used in the coronary system, as small-diameter vessels substitutes, these materials induced thrombotic events, which rapidly close off the vessel [22, 29-31].

Significant efforts have been made to improve the performance of synthetic vascular grafts as small-diameter prostheses, by interacting the synthetic polymers with subendothelial components (*i.e.* elastin-solubilized peptides) [32] or using surface grafting of matrix components and immobilization of bioactive molecules [33]. However, more detailed *in vivo* studies are needed to confirm the results obtained up to now.

Autologous veins and arteries as blood vessel replacements.

Autologous veins and arteries have been extensively used as blood vessel replacements and current surgical therapy especially for diseased vessels less than 6 mm in diameter, involves bypass grafting with such autologous arteries or veins [34].

Bypassing the left anterior descending coronary artery with an internal mammary artery graft resulted in one of the most durable coronary revascularizations [35]. Also autologous veins have proved to be durable and versatile arterial substitutes. Saphenous veins can be considered as the reference material for reconstructive surgery of medium- and small-diameter arteries [36]. In the

lower extremity, long-term results with saphenous vein bypass of infrapopliteal and pedal arteries have been excellent, resulting in patency rates as high as 80% after 5 years [37].

However, though common practice, this surgical approach has many complications. Arterial conduits have restricted dimensions and are limited in supply. Venous conduits lack vasomotor tone and may have varicose degenerative alterations which will eventually lead to the formation of aneurysms in the higher pressure arterial circulation [38].

Tissue engineering of small-diameter vascular grafts.

During the last years, the interest of most laboratories has shifted towards the engineering of blood vessel substitutes that exhibit all the functional characteristics of a normal blood vessel, giving rise to the use of biomaterials colonized by different cell types, *i.e.* tissue engineering [39]. The challenge of vascular tissue engineering is to design a tubular structure with a diameter of 1-6 mm, which remains patent in a low blood flow configuration, without inducing anastomotic hyperplasia and connective tissue growth on the luminal surface, thus supporting the formation of a thin, stable and mature neointima.

Endothelialization of synthetic vascular grafts.

Bioadhesion of thrombotic and coagulum masses on the luminal side of the graft, followed by scale formation of minerals in the blood stream, are the major problems encountered in the development of small-diameter synthetic vascular grafts [40]. The introduction of a non-thrombogenic layer, resembling the one present at the interface of a natural blood vessel, was used as a possible way to prevent thrombosis. This layer was formed on the luminal side of the artificial grafts, by endothelial cell lining [41, 42]. Despite the initial difficulties related to the necessity of using autologous EC to avoid immunologic complications [43], recently Zilla *et al.* have provided strong evidence that autologous endothelial cell lining improves the patency of small-diameter vascular grafts [44-46]. In particular, implantation in the infrainguinal position of endothelialized ePTFE grafts in 136 patients resulted in a patency rate of 62.8% after 7 years. A patency rate of 65% after 9 years was found for endothelialized ePTFE grafts implanted in the femoropopliteal position.

Protein-based scaffolds.*Collagen-based vascular scaffolds.*

Collagen: structure and functions. In the body, collagen is the main structural protein. It provides strength and structural stability to various tissues, like skin, cartilage, bone, tendons and also functions as mediator in many biological functions, like binding, migration, growth of cells and interaction with proteins and proteoglycans [47-52]. At least 19 different types of collagen have been identified, but the major fibre-forming types are type I, II and III, which constitute approximately 70% of the body collagen. In particular, blood vessels are composed for 60% of collagen type I and for 30% of type III. The remaining 10% includes fibrillar collagen type V, microfibrillar collagen type IV, basement membrane collagen type IV and VIII and fibril-associated collagens with interrupted triple helix types XII and XIV [53].

The basic subunit of collagen is tropocollagen, a rod-like molecule with a length of 300 nm, a diameter of 1.5 nm and a molecular weight of about 300 kDa. Collagen is characterised by helical domains and short non-helical portions (telopeptides) at both ends of the molecule. The helical region consists of three polypeptide α -chains, of about 1000 residues each. A typical repeating peptide sequence Gly-X-Y, in which X and Y are mainly proline and hydroxyproline, is characteristic of these α -chains (Fig. 2.4). In particular, the presence of glycine every third residue allows the formation of the triple helix. This conformation is stabilized by hydrogen bonds and by

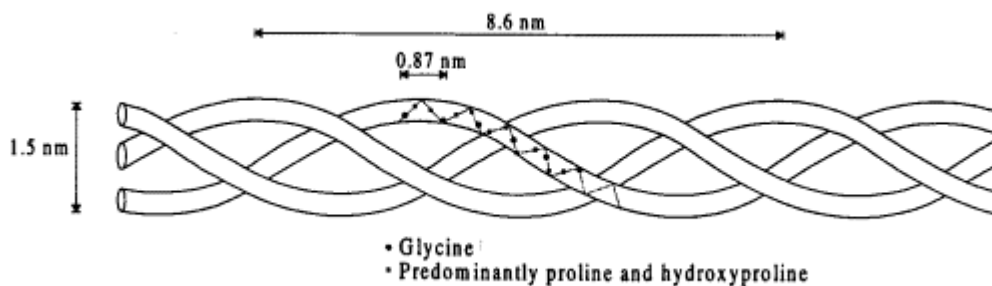


Figure 2.4. *The triple helix of collagen. Collagen is formed by three individual α -chains that are crosslinked biosynthetically and folded to form a triple helix with a molecular weight of approximately 300 kDa, a length of approximately 300 nm and a diameter of 1.5 nm.*

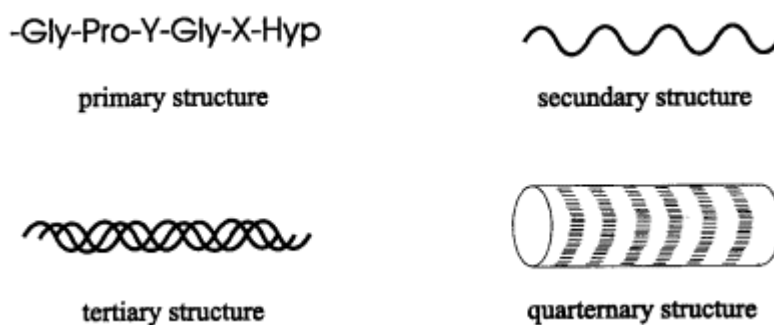


Figure 2.5. *The molecular architecture of the fibre forming collagens. Collagen domains have an amino acid sequence (primary structure) rich in Gly, Pro and Hyp. This arranges in a helix (secondary structure), which generates a symmetrical pattern of three left-handed helical α -chains, which consist of about 1000 amino acids. Three individual α -chains are folded together to form a triple helix (tertiary structure). Further aggregation of the triple helices leads to the development of an axial periodicity, the D-period (quaternary structure).*

the residues of proline and hydroxyproline. These two amino acids direct the chain conformation locally by the rigidity of their ring structures. Also the formation of covalent inter- and intra-molecular crosslinks, as a result of oxidative deamination of lysine and hydroxylysine residues, contributes to the structural integrity of tropocollagen and to its supramolecular assembly [54-59] (Fig. 2.5).

The good mechanical [60] and biological properties [61] of collagen, as well as its biocompatibility and biodegradability have resulted in a frequent use of this protein for biomedical applications [62, 63]. Collagen can be readily purified not only from animal tissues, such as skin and tendons, but also from human tissues, such as placenta. Moreover, recent studies have demonstrated the feasibility of producing recombinant human collagen [64, 65]. This can be reconstituted into fibrils that can be formulated into porous structures, membranes or gels, with the same techniques currently used with animal-derived collagen, thus yielding scaffolds meeting the requirements of different biomedical applications. For example, if used in tissue engineering, recombinant collagen would allow the creation of human tissue based on a human matrix, thus eliminating the risks of prions and viruses which can derive from xenogenic materials [66].

Collagen: applications in vascular tissue engineering.

Weinberg and Bell were the first to report on a functional biological substitute as tissue-engineered vascular graft [67]. Their model was comprised of vascular cells embedded in a reconstituted collagen gel matrix and arranged in a multi-layered structure that resembled that of an artery (Fig. 2.6). In this way, the feasibility of creating tubular structures with an adventitia-like layer made from fibroblasts and collagen, a media-like layer composed of SMC and collagen and an intima-like EC monolayer was demonstrated. In particular, cultured SMC were well differentiated and secreted collagen into the extracellular space, whereas the endothelial lining was quite similar to the natural one. However, in order to withstand physiological pressure, these constructs required support sleeves made of Dacron. Burst strengths of only 10 mmHg were reported in the absence of this synthetic support.

The mechanical strength of the engineered grafts was improved by L'Heureux *et al.*, using a culturing technique that allowed to contract the collagen gel over a central mandrel without adhering to it [68]. However, these constructs exhibited burst strengths lower than 120 mmHg, still not sufficient to withstand arterial pressure.

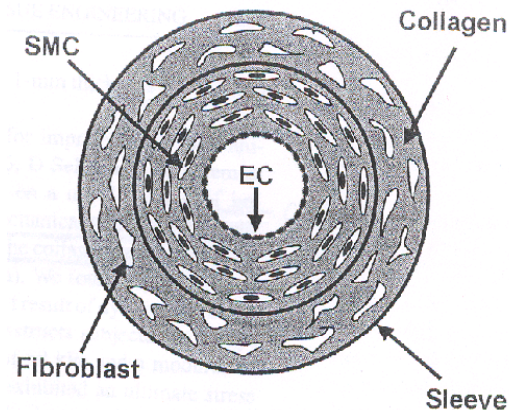


Figure 2.6. Schematic representation of the collagen-based construct developed by Weinberg *et al.* [67]. The construct contains an adventitia-like layer made of fibroblasts and collagen, a media-like layer composed of SMC and collagen and an intima-like EC monolayer. Dacron sleeves were used for structural reinforcement.

Constructs prepared with a similar technique, but with different initial collagen gel concentrations, showed comparable burst strengths [69, 70]. The rupture pressure of these vessels was shown to be dependent on the initial collagen concentration. Scaffolds prepared with 0.625 mg of collagen per ml of solution had burst strengths of 50 mmHg, whereas vessels made with 1.25 or 2.5 mg of collagen per ml of solution ruptured at 110 mmHg. These tubular constructs composed of autologous vascular cells and collagen were implanted as a venous substitute in the canine posterior vena cava. More than 50% of the grafts remained patent throughout the implantation period and, after 6 months, structural and functional restoration of the venous system were completed. However, also in this case, the presence of a Dacron mesh was essential for the success of the experiment [71].

The first totally biological vascular graft with a burst strength comparable to that of human vessels, was created by L'Heureux *et al.* [72]. A cohesive cellular sheet was prepared by culturing human vascular SMC in the presence of ascorbic acid and successively placing the resulting construct around a tubular support to produce the media of the vessel. A similar sheet of human fibroblasts was wrapped around the media to provide the adventitia. After maturation, the tubular support was removed and EC were seeded in the lumen (Fig. 2.7). The resulting tissue-engineered blood vessel featured a well-defined, three-layered organization and many ECM proteins,

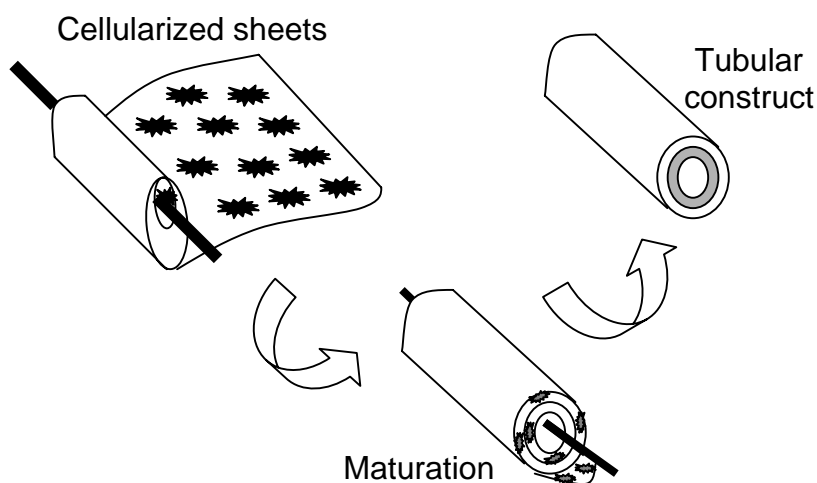


Figure 2.7. Schematic representation of the cell self-assembly model used by L'Heureux *et al.* [72]. Vascular cells are cultured to form a continuous sheet of cells and ECM and then rolled over a central mandrel. The construct is matured for 10 weeks to allow cell organization into the mechanically stable tubular construct.

including elastin. The complete vessel had burst strength of 2000 mmHg. Short-term grafting experiments in a canine model demonstrated good handling and suturability characteristics, but low patency rates of 50% after 7 d implantation.

The concept of magnetic alignment during collagen fibrillogenesis also proved to be favourable for the properties of collagen-based constructs. Circumferential orientation of collagen fibrils in a media-equivalent was achieved using the orientating effects of a strong magnetic field during collagen fibrillogenesis, which was induced while creating the construct. Circumferential orientation of the entrapped SMC was subsequently achieved via cell contact guidance, *i.e.* induced SMC orientation along orientated fibrils [73, 74]. Cell, as well as fibre orientation, are important issues in tissue engineering of blood vessels, since the circumferential orientation of SMC and structural proteins, like collagen, in the media layer are important for both vasoactivity and structural integrity [43].

Despite the increasing efforts made in this field, one of the main limitations of the application of collagen gels in mechanically demanding applications, like tissue engineering of blood vessels, is their insufficient stiffness and strength. Recently, however, Girton *et al.* were able to achieve significant stiffening and strengthening of collagen gel constructs by means of glycation [75]. Glycation is a non-enzymatic, and thus cell-tolerated, crosslinking method that is brought about by reducing sugars, like glucose and ribose. After several weeks of culture, tubular collagen constructs grown in medium containing 30 mM ribose had a circumferential tensile modulus of 1025 kPa compared with only 63 kPa for constructs cultured in normal medium. Similarly, the circumferential tensile strength of constructs cultured in medium containing 30 mM glucose was 165 kPa, compared with 42 kPa for constructs cultured in normal medium. From these data, burst strength values of approximately 225 mmHg were predicted for constructs with wall thickness of 1 mm and outer diameter of 3 mm, cultured in high-ribose content medium.

The use of temporary biological support sleeves is another possible alternative to improve the burst strength of an engineered vessel [76]. Support sleeves are able to impart the necessary mechanical integrity while providing cells with the opportunity to secrete, reorganize and develop the ECM. The main advantage is that the cellular compartments strengthen over time, while the support is remodelled and eventually incorporated into the construct. Sleeve supports made of dehydrated collagen type I gels were constructed first and the combined with a second cell-seeded layer of collagen to generate the construct-sleeve hybrid. These were used as such or after

crosslinking with glutaraldehyde, ultraviolet or dehydrothermal treatments. After *in vitro* culture with neonatal human dermal fibroblasts, the ultimate stress of constructs with uncrosslinked or glutaraldehyde treated sleeves was 20-fold and 121-fold higher than unreinforced control constructs, respectively. Moreover, it was shown that the function of cells was not altered by the incorporation of the biological sleeve. By tailoring the rates of development and degradation so that the construct always matches at least the necessary minimum strength requirements, it might be possible to implant the graft after abbreviated culture periods and allow the remodelling and development to continue *in vivo*.

Unfortunately, despite the numerous efforts to improve the mechanical properties of tissue-engineered small-diameter blood vessels based on collagen gels, the use of these constructs is still limited by their poor mechanical integrity.

Elastin-based vascular scaffolds.

Elastin: structure and function. Elastin is the extracellular matrix protein responsible for the resilience of many tissues, like skin or lungs. The elastic fibre keeps its elastic properties up to extensions of about 140% [77] and is the most abundant protein of large arteries that are subjected to a high pulsatile pressure generated by cardiac contraction. However, elastin is also found in smaller arteries and in veins [78]. Elastin contributes to the compliance of blood vessels at physiological pressure, acting as a recoil protein that stretches with the vessel at each pulse and then pulls it back to its original diameter [79]. In the general case, elastic fibres are arranged in rather thick and concentric wavy layers called elastic lamellae, distributing stress uniformly through the media. Each concentric elastic lamella alternates with a physically connected concentric ring of SMC to form lamellar units [77]. *In vivo*, elastin not only ensures the maintenance of vascular tone, but is also responsible for the control of SMC function [80], thus having a fundamental role in natural arteries.

The soluble precursor of elastin is tropoelastin, a highly hydrophobic protein having a molecular weight of 72 kDa. After being secreted into the extracellular space by SMC and fibroblasts [81], tropoelastin becomes highly cross-linked into a rubber-like network (insoluble elastin), due to the activity of the copper-requiring enzyme lysyl oxidase. Desmosine and isodesmosine crosslinks are the most frequently occurring, however their distribution remains unknown [82]. The possible

sequence of events leading to the formation of insoluble elastin, starting from its soluble precursor, tropoelastin, is shown in Fig. 2.8.

Elastin is a highly hydrophobic protein, forming fibres, which are able to recoil after stretching.

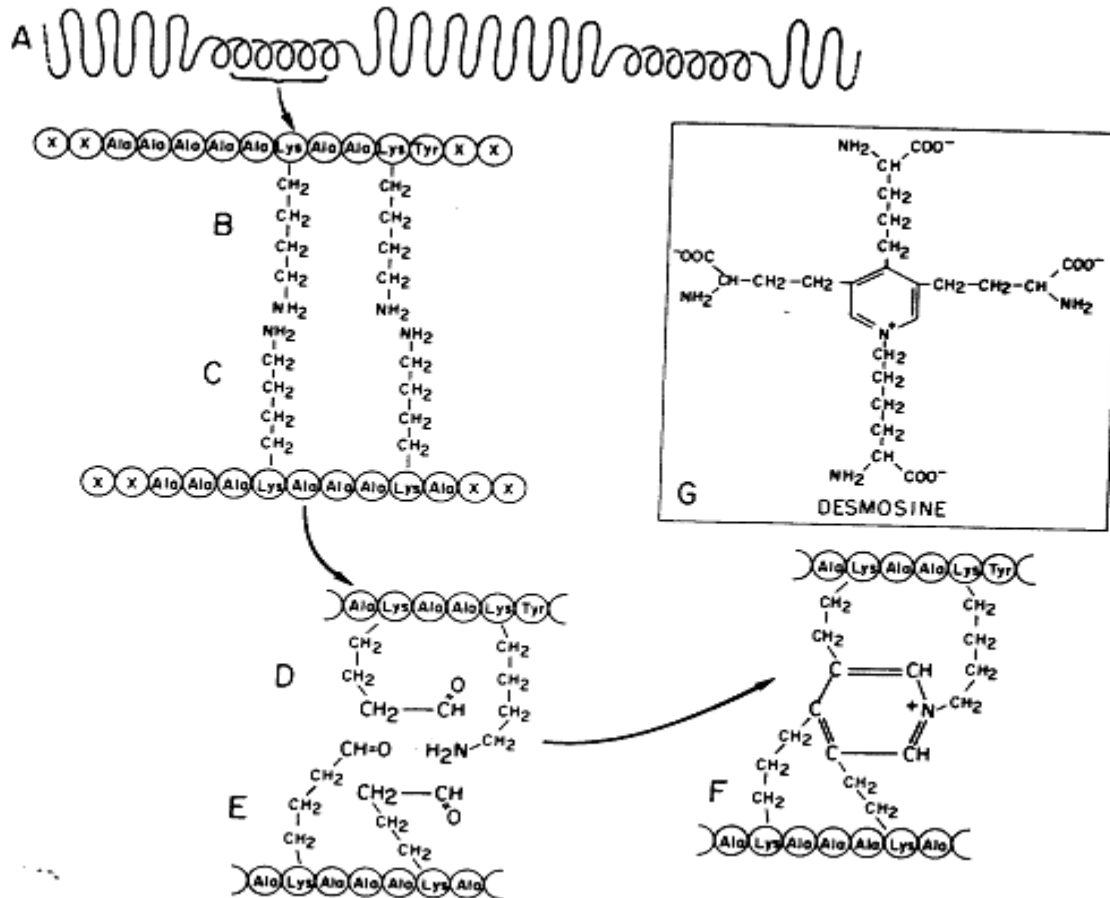


Figure 2.8. Crosslinking of soluble elastin into insoluble elastin. In A the polypeptide chains of tropoelastin consist of elastic large loops (mainly composed of hydrophobic amino acids) alternating with inelastic smaller loops (mostly composed of polyAla sequences interspersed with Lys residues). B and C show the opposition of two crosslinking sites on different chains, with the probable position of the lysine side chains before the oxidative removal of the ϵ -amino groups. In B, two alanine residues separate the two lysine residues; in C there are three alanines. In D and E, aldehydes have replaced three of the four ϵ -amino group of the lysine side chains, which are now folded to indicate their probable contribution to the desmosine ring structure. In F, the pyridium ring of desmosine has been formed with its resonating double bonds. In G shows a desmosine molecule free from peptide linkages to the elastin polypeptide chains. With isodesmosine, the lysine-derived side chain opposite the nitrogen in para is moved to the ortho position.

Dry elastin is brittle, whereas the water-swollen protein is highly elastic. This is explained by the fact that water acts like a plasticizer for the polymer, thus significantly raising the conformational entropy of the protein [83, 84]. This is a fundamental aspect of elastin elasticity, but its explanation in structural terms is still unclear [85-87].

Elastin: applications in vascular tissue engineering.

In contrast to collagen, elastin-containing constructs are rarely used in tissue engineering applications, mostly because of the laborious purification procedure of this protein [88]. A few possible approaches to include elastin in tissue-engineered substitutes have been reported and include use of:

- intact elastin (and collagen) scaffolds obtained from a digested animal artery [89, 90];
- scaffolds woven from natural elastin or elastin mimetic fibres [91, 92];
- molecularly-defined scaffolds of collagen, elastin and glycosaminoglycans [93];
- genetically modified cells or growth factors to exhibit elevated production and assembly of elastin [94-96].

However, up to now, despite the fundamental role of elastin in natural blood vessels, elastic fibres were present only in a few engineered vascular constructs [72, 97].

The absence of elastin and thus the lack of the appropriate viscoelasticity, may be one of the reasons why, even though many of the tubular constructs engineered up to now have sufficient strength, none of them has mechanical properties that mimic those of natural blood vessels [98].

Acellular vascular scaffolds.

An alternative approach to produce vascular grafts is one where an acellular construct is implanted and thereafter recruits cells from the surrounding host tissue. Small intestine submucosa (SIS), a cell free 100 μm thick collagen layer derived from the small intestine, is generally considered as a good candidate for this approach, due to its suitable mechanical properties and healing characteristics. The compliance (percent of diameter increase for a pressure rise from 80 to 120 mmHg) of SIS grafts with diameters of 5.5 or 8 mm, was on average 4.6% or 8.7%, respectively. These values are slightly lower than those measured for a carotid or femoral artery,

but four times the compliance of a typical vein graft [99]. The compliance match between a graft and the vessel it is replacing is important to predict the behaviour of that particular construct once implanted *in vivo*. It has been shown that stiffer (less compliant) grafts induce arterial hypertrophy at the anastomotic sites due to the local high pulsatile stress. Hypertrophy causes an early failure of the vascular graft, a failure that occurs much later with isocompliant or more compliant grafts [100, 101]. Rolled SIS implanted in the canine carotid artery remained patent for 120 d and showed the formation of a cellularized neointima with a confluent EC monolayer already after 28 d of implantation [102].

Similar experiments with a rabbit arterial bypass model also demonstrated the feasibility of the acellular approach. Grafts composed of porcine SIS and coated with a thin layer of bovine collagen on the luminal side had sufficient mechanical integrity for implantation. In particular, the burst pressure was 1000 mmHg and the suture retention was twice the surgical requirement [97]. Although the possibility of using xenogeneic cells for tissue repair is still controversial because of the potential risks of transmission of animal pathogens to humans, xenogeneic materials might constitute a temporary solution while a human donor becomes available or while the tissue regenerates on its own [7].

The potentials of using a xenogeneic acellularized matrix have been investigated by Bader *et al.* [103]. In their work these authors developed an alternative xenotransplantation method, in which all viable xenogeneic cells were removed and the residual matrix was sterilized. In this way, the requirements for immunosuppression inherent with xenogeneic transplantation may be reduced. Acellularized porcine vessels cultured with human EC and myofibroblasts in a bioreactor showed promising results. During culture, myofibroblasts migrated into positions formerly occupied by the xenogeneic cells and a 100% EC lining was observed on the inner surface of the graft. Longer, *in vivo* animal trials have to be performed before confirming the applicability of this approach.

Acellular human dermal matrix was also employed as a small-diameter vascular substitute. Acellular dermis rolled into a tube, with the dermal-epidermal junction on the inside, yielded vessels with a patency superior to that observed with ePTFE substitutes. However, 40% of the grafts exhibited aneurysms around the longitudinal suture line [104].

In conclusion, if acellular methodologies, on one hand, offer some advantages over the cellular approach because of the difficulties in isolating and expanding autologous human cells, on the

other they can lead to thrombogenesis. Moreover, recruiting cells into an acellular vascular construct can be a daunting task, since the process of *in vivo* vascular cell migration is poorly understood. As a consequence, engineering acellular matrices into vascular constructs is likely several years from clinical application.

Synthetic polymer-based vascular scaffolds.

The advantages of using synthetic polymer scaffolds in tissue engineering of small-diameter blood vessels, are mostly related to the possibility of better controlling the material properties (*e.g.* strength, degradation, porosity and microstructure) of synthetic materials as compared to natural materials [105]. However, in the former case, often, surface modification or addition of growth factors is necessary to induce cell attachment [106, 107].

Up to now, the most widely used polymers for biomedical applications are the poly(α -hydroxy acids) of the aliphatic polyesters, like polyglycolic or polylactic acid [108]. Unfortunately, the tubular grafts made from these materials are stiff, which restricts their use for construction of vascular prostheses, unless combined with other polymers.

The biocompatibility of some polyurethanes makes them good candidates to tailor the flexibility and resorbability of polylactide-based grafts. Two-layered artificial vascular grafts of polylactide and polyurethane remained patent for 1 year, when implanted in the rat abdominal aorta and did not exhibit any aneurysmal formation [109]. Highly porous, distensible, gel-like tubular scaffolds suitable for engineering small-diameter blood vessels were also fabricated by combining spraying and phase-inversion of thermodynamically unstable solutions of biocompatible polyurethane and polydimethylsiloxane blends over a sliding and rotating mandrel. Stable luminal surfaces, absence of anastomotic hyperplasia and deposition of collagen were observed after 8 weeks of implantation in the rat abdominal aorta [110].

Copolymerisation of lactic and glycolic acid is a possible approach to tailor the degradation times and the mechanical properties of matrices potentially suitable for tissue engineering of small-diameter blood vessels. Porous tubular devices fabricated by means of salt leaching from a 50/50 copolymer of D,L-lactic and glycolic acid were stable to large radial compressional forces (150 mN) *in vitro* and also upon implantation in the artery mesenterica of rats [111]. Their

potential use in tissue engineering applications was further shown by the finding that SMC and EC seeded onto these devices *in vitro*, formed a tubular tissue with appropriate cell distribution [112]. In a leading work in this area, Niklason *et al.* [34] cultured bovine aorta SMC in polyglycolic acid based tubular scaffolds and placed them in a pulsatile flow bioreactor, mimicking the stresses experienced by blood vessels *in vivo*. After 8 weeks of culture, the bioresorbable mesh had been partially replaced by a SMC intermediate layer. EC were then seeded onto the luminal side, thus forming the second of the three layers typical of a natural blood vessel (Fig. 2.9). The resulting construct was able to withstand a pressure higher than 2000 mmHg and, when implanted into the right saphenous artery of miniature swine, remained patent up to 4 weeks. Combining the structural support of a biodegradable scaffold with the benefits of a dynamically stimulated culture was particularly important for the success of the prepared construct.

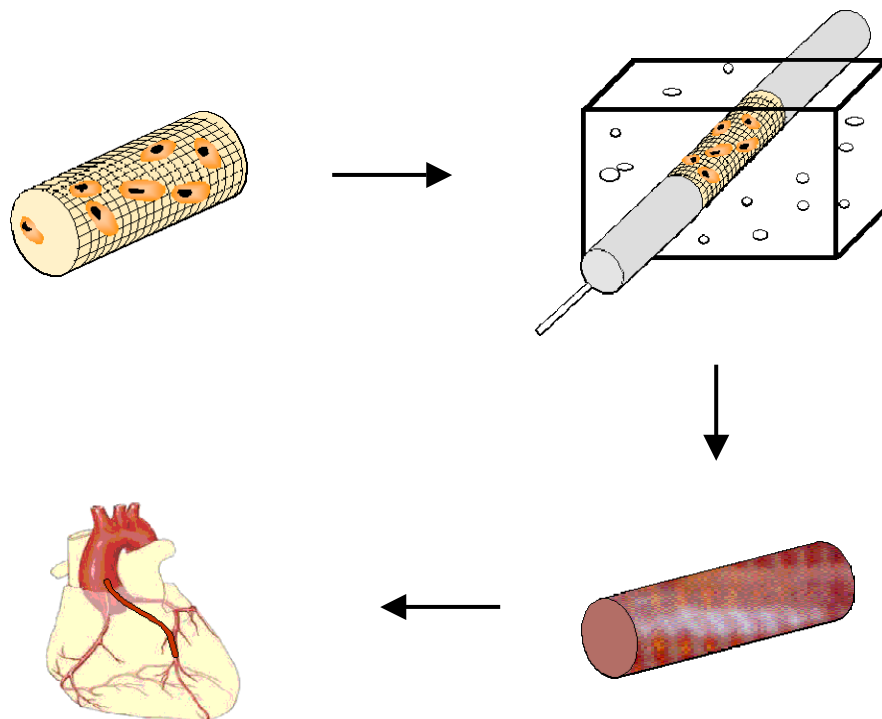


Figure 2.9. Schematic representation of the culture model used by Niklason *et al.* [34]. SMC are cultured on a tube of biodegradable polymer mesh and then the construct is placed in a bioreactor. After 2 months of culture SMC have completely replaced the polymer scaffold. A lining of endothelial cell is added and the construct is ready for heart surgery.

A similar approach was used to fabricate vascular grafts from a non-woven polyglycolic acid mesh coated with a layer of poly-4-hydroxybutyrate and seeded with ovine vascular myofibroblasts and endothelial cells. Grafts with inner diameter of 5 mm, were cultured 4 d in static conditions, after which they were grown in a bioreactor up to 28 d. Histology showed viable, dense tissue in all samples, with confluent smooth inner surfaces. The mechanical properties of the constructs comprised supra-physiological burst strength and suture retention appropriate for surgical implantation [113].

Though seeding of synthetic polymer scaffolds has often resulted in excellent burst pressures [34], achieving the necessary cell proliferation and matrix synthesis is still a challenge. In addition, polymer degradation products can alter the local cellular environment and thus the cell function, preventing the development of a proper vascular construct [114].

Hybrid scaffolds.

The production of hybrid scaffolds of natural and synthetic polymers constitutes a suitable alternative to benefit simultaneously from the two different components. In general, hybrid porous grafts can be more easily shaped by using a synthetic polymer as mechanical skeleton. The synthetic component will also confer better mechanical properties to the resulting scaffolds. Moreover, incorporation of cell adhesive proteins or growth factors will be facilitated by blending with the natural polymer during composite formation [115-117].

In vascular tissue engineering, using hybrid grafts reinforced with an elastomeric synthetic mesh, yielded stronger hybrid tissues with a better compliance matching with native arteries. Promising results have been obtained with hybrid vascular prostheses (diameter 3-6 mm) composed of bovine SMC and collagen type I reinforced with a knitted fabric mesh of segmented polyester [118, 119]. Poly(carbonate-urea)urethanes have also been used in the production of permanent scaffolds [120]. In this approach, either poly(urethane)-nylon meshes or segmented poly(urethane) films were used to wrap an inner collagen gel layer previously seeded with SMC and EC. After implantation into canine carotid arteries for 1 month, all nylon-containing grafts were dilated due to loosening of the mesh, resulting in loss of EC and thrombus formation. In contrast, grafts made with poly(urethane) films developed a well-organized neoarterial wall composed of a confluent EC monolayer and

medial tissue containing SMC. Moreover, slight thrombus formation and minimal tissue ingrowth were observed 6 months after implantation.

More recently, in a similar approach, microporous segmented poly(urethane) films were used to enwrap collagen type I meshes seeded with autologous circulating progenitor EC and successively implanted in dog carotid arteries. After 3 months implantation the grafts were still patent, their inner layer was covered with a confluent monolayer of EC, whereas SMC and fibroblasts could be observed in the medial and adventitial layer, respectively [121].

Despite the promising results obtained till now, further investigation is needed before clinical application of hybrid vascular grafts can take place.

Bioreactors for vascular tissue engineering.

In native blood vessels, the arterial wall has a specific hierarchic structure in which cells have a regular orientation. This arrangement ensures the vessel to function most efficiently. Ideal tissue-engineered vascular grafts should thus have a morphology and organization analogous to that of native tissue. It has been documented that in native blood vessels, cellular orientation is induced by the dynamic environment to which vascular cells are exposed because of the pulsatile blood flow [122]. Due to the possibility of creating a dynamic culture environment, bioreactors have not only the potential to improve the quality of the engineered tissues but also the technological means to reveal the fundamental mechanisms of cell function in a three-dimensional scaffold [123]. It was thus discovered that mechanical stimulation induces not only orientation but also phenotypic modulation of SMC. Vascular smooth muscle tissues engineered *in vitro* with static culture techniques may not be functional, because this typically reverts SMC from a contractile to a synthetic phenotype. On the contrary, pulsatile strain and shear stress enhance vascular SMC proliferation [124-126].

Different kinds of bioreactors and experimental conditions have been analysed during the years by different groups in order to facilitate proliferation and migration of cells in scaffolds developed as tissue-engineered blood vessels. Dynamic conditions are normally generated by compressed air supply [113, 127] and luminal flow is obtained either with buffer or culture medium [34, 72, 103, 127-129]. In all cases, temperature, pH, exchange of gases and mechanical stimuli are strictly regulated and controlled.

One of the first applications of bioreactors in vascular tissue engineering was reported by L'Heureux *et al.* [72], who used perforated PTFE tubular mandrels inside growing blood vessels to provide luminal flow of culture medium and mechanical support. A more detailed description is given by Niklason *et al.* [34]. Culturing of SMC in PLGA tubular structures under static conditions resulted in fragile constructs not suitable for the intended application. Improved mechanical properties and better cellular organization were instead found when the same constructs were cultured in bioreactors providing flow through the lumen of the constructs via distensible silicone tubing. Continuous pulsatile flow periodically stretched the silicone tubing, applying cyclic strain to the cell-polymer construct (5% pulse strain at 165 beats/min). After 8 wk, the silicone tubing was removed and the flow of the medium was applied directly through the cultured vessels. All pulsed vessels had a burst strength greater than native human saphenous veins, similar wall thickness and collagen content as native arteries. Grafts cultured under the described pulsatile conditions with autologous SMC and EC were implanted in the right saphenous artery of Yucatan miniature swine. After 4 wk the grafts were still open and had a highly organized cellular structure. Minimal inflammation was found. On the contrary, analogous non-pulsed grafts remained open for only 3 wk and then developed thrombosis.

Similarly, studies performed on rat tail collagen type I gel and chitosan scaffolds cultured with SMC revealed that mechanical conditioning during culture leads to improved properties of tissue-engineered blood vessel constructs in terms of histological organization and mechanical strength. In particular, after 4 and 8 d of culture, the yield stress of dynamically conditioned constructs was significantly higher than that of static controls, with values increasing up to 200%. Dynamic conditioning also improved the material modulus of the constructs. After 8 d of culture, dynamically stimulated samples showed a 108% higher modulus than static controls. In the former vessels, a highly oriented SMC population was observed dispersed through the wall of the tissue [125, 127].

Recent work in the field of vascular tissue engineering offers promising new approaches to the design and manufacture of small-diameter vascular grafts. However, such work is still in its early stages and many steps have to be done before tissue-engineered vessels can be used in clinical applications.

Conclusions.

Collagen has proven to be highly valuable in the biomedical field, but, unfortunately, available tissue-engineered small-diameter blood vessels based on collagen do not match the needed requirements, especially in terms of compliance and burst strength. Combining collagen and elastin holds promises for use in tissue engineering of small-diameter blood vessels, as together these two proteins allow the production of scaffolds having viscoelastic mechanical properties very similar to those of a native artery. Mechanical characteristics suitable for vascular tissue engineering applications could be also obtained with hybrid scaffolds of poly(D,L-lactide)co(1,3-trimethylene carbonate) (P(DLLAcoTMC)) and collagen. A hybrid of natural and synthetic materials would benefit from suitable mechanical properties and low costs of the synthetic polymer as well as appropriate cellular interactions of the natural occurring material.

Constructs, which could be further used for vascular tissue engineering applications, were produced by culturing SMC in the above mentioned scaffolds in a pulsatile flow bioreactor developed in our laboratories.

References.

1. Langer, R. and Vacanti, J.P., Tissue Engineering. *Science*, 1993. 260(5110): 920-926.
2. Fuchs, J.R., Nasser, B.A. and Vacanti, J.P., Tissue engineering: A 21st century solution to surgical reconstruction. *Ann. Thorac. Surg.*, 2001. 72(2): 577-591.
3. McGill, T.J., Lund, R.D., Douglas, R.M., Wang, S., Lu, B. and Prusky, G.T., Preservation of vision following cell-based therapies in a model of retinal degenerative disease. *Vision Res.*, 2004. 44(22): 2559-2566.
4. Foster, G.A. and Stringer, B.M.J., Cell-based therapies for Parkinson's disease. *Drug Discovery Today*, 2004. 1(1): 43-49.
5. Melo, L.G., Gnechi, M., Pachori, A.S., Wang, K. and Dzau, V.J., Gene- and cell-based therapies for cardiovascular diseases: current status and future directions. *Eur. Heart J.*, 2004. 6(Supplement 5): E24-E35.
6. Rabkin, E. and Schoen, F.J., Cardiovascular tissue engineering. *Cardiovasc. Pathol.*, 2002. 11(6): 305-317.

7. Griffith, L.G. and Naughton, G., Tissue Engineering- Current Challenges and Expanding Opportunities. *Science*, 2002. 295: 1009-1016.
8. Galassi, G., Brun, P., Radice, M., Cortivo, R., Zanon, G.F., Genovese, P. and Abatangelo, G., In vitro reconstructed dermis implanted in human wounds: degradation studies of the HA-based supporting scaffold. *Biomaterials*, 2000. 21(21): 2183-2191.
9. Dantzer, E. and Braye, F.M., Reconstructive surgery using an artificial dermis (Integra): results with 39 grafts. *Brit.J. Plastic Surg.*, 2001. 54(8): 659-664.
10. O'Connor, N.E., Mulliken, J.B., Banks-Schlegel, S., Kehinde, O. and Green, H., Grafting of burns with cultured epithelium prepared from autologous epidermal cells. *Lancet*, 1981. 317(8211): 75-78.
11. Temenoff, J.S. and Mikos, A.G., Review: tissue engineering for regeneration of articular cartilage. *Biomaterials*, 2000. 21(5): 431-440.
12. Cancedda, R., Dozin, B., Giannoni, P. and Quarto, R., Tissue engineering and cell therapy of cartilage and bone. *Matrix Biol.*, 2003. 22(1): 81-91.
13. Malizos, K.N., Dailiana, Z.H., Kirou, M., Vragalas, V., Xenakis, T.A. and Soucacos, P.N., Longstanding nonunions of scaphoid fractures with bone loss: successful reconstruction with vascularized bone grafts. *J. Hand Surg.*, 2001. 26(4): 330-334.
14. Lavine, M., Roberts, L. and Smith, O., Bodybuilding: the bionic human. *Science*, 2002. 295: 995.
15. Zhou, J. and Fung, Y.C., The degree of nonlinearity and anisotropy of blood vessels elasticity. *Proc. Natl. Acad. Sci.*, 1997. 94: 14255-14260.
16. Lusis, A.J., Atherosclerosis. *Nature*, 2000. 407(6801): 233-241.
17. Kaul, S. and Lindner, J.R., Visualizing coronary atherosclerosis in vivo: thinking big, imaging small. *J. Am. College Cardiol.*, 2004. 43(3): 461-463.
18. Trion, A. and van der Laarse, A., Vascular smooth muscle cells and calcification in atherosclerosis. *Am. Heart J.*, 2004. 147(5): 808-814.
19. Voorhes, The use of tubes of Vinyon N cloth in bridging arterial defects. *Ann. Surg.*, 1950. 135: 332-336.
20. Blakemore, A.H. and Voorhes, A.B., The use of tubes constructed from Vinyon 'N' cloth in bridging arterial defects. *Experimental and clinical. Ann. Surg.*, 1954. 140: 324-334.

21. Harrison, J.H., Synthetic materials as vascular prostheses: II. A comparative study of nylon, dacron, orlon, ivalon sponge and teflon in large blood vessels with tensile strength studies. *Am. J. Surg.*, 1958. 95(1): 16-24.
22. Sasajima, T., Inaba, M., Goh, K., Yamazaki, K., Yamamoto, H., Azuma, N., Akasaka, N. and Kubo, Y., 28.12 Biological fate of Dacron vascular prostheses in human subjects: the possibility of achieving endothelial coverage. *Cardiovasc. Surg.*, 1997. 5(Supplement 1): 147.
23. Post, S., Kraus, T., Muller-Reinartz, U., Weiss, C., Kortmann, H., Quentmeier, A., Winkler, M., Husfeldt, K.J. and Allenberg, J.R., Dacron vs polytetrafluoroethylene grafts for femoropopliteal bypass: a prospective randomised multicentre trial. *Eur. J. Vasc. Endovasc. Surg.*, 2001. 22(3): 226-231.
24. Harrison, J.H., Synthetic materials as vascular prostheses: I. A comparative study in small vessels of nylon, dacron, orlon, ivalon sponge and teflon. *Am. J. Surg.*, 1958. 95(1): 3-15.
25. Greenwald, S.E. and Berry, C.L., Improving vascular grafts: the importance of mechanical and haemodynamic properties. *J. Pathol.*, 2000. 190(3): 292-299.
26. Auguste, K.I., Quinones-Hinojosa, A. and Lawton, M.T., The tandem bypass: subclavian artery-to-middle cerebral artery bypass with dacron and saphenous vein grafts. Technical case report. *Surg. Neurol.*, 2001. 56(3): 164-169.
27. Johansen, K.H. and Watson, J.C., Dacron femoral-popliteal bypass grafts in good-risk claudicant patients. *Am. J. Surg.*, 2004. 187(5): 580-584.
28. Hirt, S.W., Aoki, M., Demertzis, S., Siclari, F., Haverich, A. and Borst, H.G., Comparative in vivo study on the healing qualities of four different presealed vascular prostheses. *J. Vasc. Surg.*, 1993. 17(3): 538-545.
29. Bos, G.W., Poot, A.A., Beugeling, T., Feijen, J. and van Aken, W.G., Small-diameter vascular graft prostheses: current status. *Arch. Physiol. Biochem.*, 1998. 2: 100-115.
30. Esquivel, C.O. and Blaisdell, F.W., Why small caliber vascular grafts fail: a review of clinical and experience and the significance of the interaction of blood at the interface. *J. Surg. Res.*, 1986. 41: 1-15.

31. Shirkey, A.L., Beall, J., Arthur C. and DeBakey, M.E., The problem of small vessel grafting and the flexion crease: a comparison between autogenous vein and dacron grafts. *Am. J. Surg.*, 1963. 106(4): 558-565.
32. Bonzon, N., Lefebvre, F., Ferre, N., Daculsi, G. and Rabaud, M., New bioactivation mode for vascular prostheses made of Dacron(R) polyester. *Biomaterials*, 1995. 16(10): 747-751.
33. Chandy, T., Das, G.S., Wilson, R.F. and Rao, G.H.R., Use of plasma glow for surface-engineering biomolecules to enhance blood compatibility of Dacron and PTFE vascular prosthesis. *Biomaterials*, 2000. 21(7): 699-712.
34. Niklason, L.E., Gao, J., Abbott, W.M., Hirschi, K.K., Houser, S., Marini, R. and Langer, R., Functional arteries grown in vitro. *Science*, 1999. 284(5413): 489-493.
35. Cameron, A., Davis, K.B., Green, G. and Schaff, H.V., Coronary bypass surgery with internal-thoracic-artery grafts - Effects on survival over a 15-year period. *N. Engl. J. Med.*, 1996. 334(4): 216-219.
36. Canham, P.B., Finlay, H.M. and Boughner, D.R., Contrasting structure of the saphenous vein and internal mammary artery used as coronary bypass vessels. *Cardiovasc. Res.*, 1997. 34(3): 557-567.
37. Belkin, M., Conte, M.S., Donaldson, M.C., Mannick, J.A. and Whittemore, A.D., Preferred strategies for secondary infrainguinal bypass - lessons learned from 300 consecutive reoperations. *J. Vasc. Surg.*, 1995. 21(2): 282-295.
38. Edelman, E.R., Vascular tissue engineering: designer arteries. *Circ. Res.*, 1999. 85(12): 1115-1117.
39. Citron, P. and Nerem, R.M., Bioengineering: 25 years of progress-but still only a beginning. *Technol. Soc.*, 2004. 26(2-3): 415-431.
40. Baier, R.E., Physical and biomechanical issues in graft design. *Sem. Vasc. Surg.*, 1999. 12: 8-17.
41. Magometschnigg, H., Kadletz, M., Vodrazka, M., Dock, W., Grimm, M., Grabenwoger, M., Minar, E., Staudacher, M., Fenzl, G. and Wolner, E., Prospective clinical-study with in vitro endothelial-cell lining of expanded polytetrafluoroethylene grafts in crural repeat reconstruction. *J. Vasc. Surg.*, 1992. 15(3): 527-535.

42. Wilson, J.M., Birinyi, L.K., Salomon, R.N., Libby, P., Callow, A.D. and Mulligan, R.C., Implantation of vascular grafts lined with genetically modified endothelial cells. *Science*, 1989. 244(4910): 1344-1346.
43. Nerem, R.M. and Seliktar, D., Vascular tissue engineering. *Ann. Rev. Biomed. Eng.*, 2001. 3: 225-243.
44. Zilla, P., Endothelialization of vascular grafts. *Curr. Op. Cardiol.*, 1991. 6(6): 877-886.
45. Meinhart, J.G., Deutsch, M., Fischlein, T., Howanietz, N., Froschl, A. and Zilla, P., Clinical autologous in vitro endothelialization of 153 infrainguinal ePTFE grafts. *An. Thorac. Surg.*, 2001. 71(5, Supplement 1): S327-S331.
46. Deutsch, M., Meinhart, J. and Zilla, P., Graft endothelialization by in vitro lining. *Atherosclerosis*, 2000. 151(1): 93.
47. Tzaphlidou, M., The role of collagen and elastin in aged skin: an image processing approach. *Micron*, 2004. 35(3): 173-177.
48. Plenz, G.A.M., Deng, M.C., Robenek, H. and Volker, W., Vascular collagens: spotlight on the role of type VIII collagen in atherogenesis. *Atherosclerosis*, 2003. 166(1): 1-11.
49. Janicki, J.S. and Brower, G.L., The role of myocardial fibrillar collagen in ventricular remodeling and function. *J. Cardiac Fail.*, 2002. 8(6, Part 2): S319-S325.
50. Wang, X., Bank, R.A., TeKoppele, J.M. and Mauli Agrawal, C., The role of collagen in determining bone mechanical properties. *J. Orthop. Res.*, 2001. 19(6): 1021-1026.
51. Vouyouka, A.G., Pfeiffer, B.J., Liem, T.K., Taylor, T.A., Mudaliar, J. and Phillips, C.L., The role of type I collagen in aortic wall strength with a homotrimeric $[[\alpha]1(I)]_3$ collagen mouse model. *J. Vasc. Surg.*, 2001. 33(6): 1263-1270.
52. Lees, S. and Davidson, C.L., The role of collagen in the elastic properties of calcified tissues. *J. Biomech.*, 1977. 10(8): 473-475.
53. Jacob, M.P., Badier-Commander, C., Fontaine, V., Benazzoug, Y., Feldman, L. and Michel, J.B., Extracellular matrix remodeling in the vascular wall. *Pathol. Biol.*, 2001. 49(4): 326-332.
54. Nimni, M.E., Collagen: molecular structure and biomaterial properties, in *Encyclopedia handbook of biomaterials and bioengineering materials*, M. Deheler, Editor. 1995: New York. 1229-1243.

55. Ottani, V., Raspanti, M. and Ruggeri, A., Collagen structure and functional implications. *Micron*, 2001. 32(3): 251-260.
56. Ottani, V., Martini, D., Franchi, M., Ruggeri, A. and Raspanti, M., Hierarchical structures in fibrillar collagens. *Micron*, 2002. 33(7-8): 587-596.
57. Hulmes, D.J.S., Building collagen molecules, fibrils, and suprafibrillar structures. *J. Struct. Biol.*, 2002. 137(1-2): 2-10.
58. Gelse, K., Poschl, E. and Aigner, T., Collagens-structure, function, and biosynthesis. *Adv. Drug Deliv. Rev.*, 2003. 55(12): 1531-1546.
59. Brodsky, B. and Ramshaw, J.A.M., The collagen triple-helix structure. *Matrix Biol.*, 1997. 15(8-9): 545-554.
60. Gentleman, E., Lay, A.N., Dickerson, D.A., Nauman, E.A., Livesay, G.A. and Dee, K.C., Mechanical characterization of collagen fibers and scaffolds for tissue engineering. *Biomaterials*, 2003. 24(21): 3805-3813.
61. Barnes, M.J. and Farndale, R.W., Collagens and atherosclerosis. *Exp. Gerontol.*, 1999. 34(4): 513-525.
62. Cavallaro, J.F. and Kemp, P.D., Collagen fabrics as biomaterials. *Biotechnol. Bioeng.*, 1994. 43: 781-791.
63. Lee, C.H., Singla, A. and Lee, Y., Biomedical applications of collagen. *Intern. J. Pharmac.*, 2001. 221(1-2): 1-22.
64. Bulleid, N.J., John, D.C.A. and Kadler, K.E., Recombinant expression systems for the production of collagen. *Biochem. Soc. Trans.*, 2000. 28: 350-353.
65. Yang, C.L., Hillas, P.J., Baez, J.A., Nokelainen, M., Balan, J., Tang, J., Spiro, R. and Polarek, J.W., The application of recombinant human collagen in tissue engineering. *Biodrugs*, 2004. 18(2): 103-119.
66. Hellman, K.B., honstead, J.P. and Vincent, C.K., Adventitious agents from animal-derived raw materials and production systems. *Dev. Biol. Stand.*, 1996. 88: 231-234.
67. Weinberg, C.B. and Bell, E., A blood vessel model constructed from collagen and cultured vascular cells. *Science*, 1986. 231: 397-400.
68. L'Heureux, N., Germain, L. and Labbe`, R., In vitro construction of a human blood vessel from cultured vascular cells: a morphologic study. *J. Vasc. Surg.*, 1993(17): 499-509.

69. Hirai, J., Kanda, K., Oka, T. and Matsuda, T., Highly oriented, tubular hybrid vascular tissue for a low pressure circulatory system. *ASAIO J.*, 1994. 40(3): M383-M388.
70. Hirai, J. and Matsuda, T., Self-organized, tubular hybrid vascular tissue composed of vascular cells and collagen for low-pressure-loaded venous system. *Cell Transplant.*, 1995. 4(6): 597-608.
71. Hirai, J. and Matsuda, T., Venous reconstruction using hybrid vascular tissue composed of vascular cells and collagen: Tissue regeneration process. *Cell Transplant.*, 1996. 5(1): 93-105.
72. L'Heureux, N., A completely biological tissue-engineered human blood vessel. *Faseb J.*, 1998. 12(1): 47-56.
73. Tranquillo, R.T., Self-organization of tissue-equivalents: the nature and role of contact guidance, in cell behaviour: control and mechanism of motility. 1999, Portland Press Ltd: London. 27-42.
74. Tranquillo, R.T., Girton, T.S., Bromberek, B.A., Triebes, T.G. and Mooradian, D.L., Magnetically oriented tissue equivalent tubes: application to a circumferentially orientated media equivalent. *Biomaterials*, 1996. 17(3): 349357.
75. Girton, T.S., Oegema, T.R. and Tranquillo, R.T., Exploiting glycation to stiffen and strengthen tissue equivalents for tissue engineering. *J. Biomed. Mat. Res.*, 1999. 46(1): 87-92.
76. Berglund, J.D., Mohseni, M.M., Nerem, R.M. and Sambanis, A., A biological hybrid model for collagen-based tissue engineered vascular constructs. *Biomaterials*, 2003. 24(7): 1241-1254.
77. Faury, G., Function-structure relationship of elastic arteries in evolution: from microfibrils to elastin and elastic fibres. *Pathol. Biol.*, 2001. 49(4): 310-325.
78. Rosenbloom, J., Abrams, W.R. and Mecham, R., Extracellular-Matrix .4. The elastic fiber. *Faseb J.*, 1993. 7(13): 1208-1218.
79. Mitchell, S.L. and Niklason, L.E., Requirements for growing tissue-engineered vascular grafts. *Cardiovasc. Pathol.*, 2003. 12(2): 59-64.
80. Li, D.Y., Brooke, B., Davis, E.C., Mecham, R.P., Sorensen, L.K., Boak, B.B., Eichwald, E. and Keating, M.T., Elastin is an essential determinant of arterial morphogenesis. *Nature*, 1998. 393(6682): 276-280.

81. Strauss, B.H. and Rabinovitch, M., Adventitial fibroblasts - Defining a role in vessel wall remodeling. *Am. J. Respir. Cell Mol. Biol.*, 2000. 22(1): 1-3.
82. Debelle, L. and Tamburro, A.M., Elastin: molecular description and function. *Int. J. Biochem. Cell Biol.*, 1999. 31(2): 261-272.
83. Anrady, A.L. and Mark, J.E., Thermoelasticity of swollen elastin networks at constant composition. *Biopolymers*, 1980. 19: 849-855.
84. Lillie, M.A. and Gosline, J.M., The viscoelastic basis for the tensile strength of elastin. *Intern. J. Biol. Macromol.*, 2002. 30(2): 119-127.
85. Pasquali-Ronchetti, I., Fornieri, C., Baccarani-Contri, M. and Quaglino, D., Ultrastructure of elastin. *Ciba Found. Symp.*, 1995. 192: 31-42; discussion 42-50.
86. Weis-Fogh, T. and Andersen, S.O., New molecular model for the long-range elasticity of elastin. *Nature*, 1970. 225: 718-721.
87. Anwar, R., Primary structure of insoluble elastin. *Methods Enzymol.*, 1982. 82 Part A: 606-615.
88. Daamen, W.F., Hafmans, T., Veerkamp, J.H. and van Kuppevelt, Comparison of five procedures for the purification of insoluble elastin. *Biomaterials*, 2001. 22(14): 1997-2005.
89. Lu, Q., Ganesan, K., Simionescu, D.T. and Vyavahare, N.R., Novel porous aortic elastin and collagen scaffolds for tissue engineering. *Biomaterials*, 2004. 25(22): 5227-5237.
90. Goissis, G., Suzigan, S., Parreira, D.R., Maniglia, J.V., Braile, D.M. and Raymundo, S., Preparation and characterization of collagen-elastin matrices from blood vessels intended as small diameter vascular grafts. *Artif. Organs*, 2000. 24(3): 217-223.
91. Huang, L., McMillan, R.A., Apkarian, R.P., Pourdeyhimi, B., Conticello, V.P. and Chaikof, E.L., Generation of synthetic elastin-mimetic small diameter fibers and fiber networks. *Macromolecules*, 2000. 33(8): 2989-2997.
92. Boland, E.D., Matthews, J.A., Pawlowski, K.J., Sompson, D.G., Wnek, G.E. and Gary, L., Electrospinning collagen and elastin: preliminary vascular tissue engineering. *Frontiers Biosci.*, 2004. 9: 1442-1432.
93. Daamen, W.F., van Moerkerk, H.T.B., Hafmans, T., Buttafoco, L., Poot, A.A., Veerkamp, J.H. and van Kuppevelt, T.H., Preparation and evaluation of molecularly-defined collagen-elastin-glycosaminoglycan scaffolds for tissue engineering. *Biomaterials*, 2003. 24(22): 4001-4009.

94. Johnson, D.J. and Keeley, F.W., Factors affecting the production of insoluble elastin in aortic organ-cultures. *Connect. Tissue Res.*, 1990. 24(3-4): 277-288.
95. Sutcliffe, M.C. and Davidson, J.M., Effect of static stretching on elastin production by porcine aortic smooth-muscle cells. *Matrix*, 1990. 10(3): 148-153.
96. Davidson, J.M., Zoia, O. and Liu, J.M., Modulation of transforming growth factor β_1 stimulated elastin and collagen production and proliferation in porcine vascular smooth-muscle cells and skin fibroblasts by basic fibroblast growth factor, transforming growth factor-Alpha, and insulin-like growth factor-I. *J. Cell. Physiol.*, 1993. 155(1): 149-156.
97. Huynh, T., Abraham, G., Murray, J., Brockbank, K., Hagen, P.O. and Sullivan, S., Remodeling of an acellular collagen graft into a physiologically responsive neovessel. *Nature Biotechnol.*, 1999. 17(11): 1083-1086.
98. Nerem, R.M., Critical issues in vascular tissue engineering. *Inter. Congress Series*, 2004. 1262: 122-125.
99. Roeder, R., Wolfe, J., Lianakis, N., Hinson, T., Geddes, L.A. and Obermiller, J., Compliance, elastic modulus, and burst pressure of small-intestine submucosa (SIS), small-diameter vascular grafts. *J. Biomed. Mater. Res.*, 1999. 47(1): 65-70.
100. Seiffert, K.B., Albo, D. and Knowlton, H., Effect of elasticity of prosthetic walls on patency of small diameter arterial prosthesis. *Surg. Forum*, 1979(3): 206-208.
101. Clark, R.E., Apostolou, S. and Kardos, L.J., Mismatch of mechanical properties as a cause of arterial prosthesis thrombosis. *Surg. Forum*, 1976. 27: 208-209.
102. Badylak, S., Kokini, K., Tullius, B. and Whitson, B., Strength over time of a resorbable bioscaffold for body wall repair in a dog model. *J. Surg. Res.*, 2001. 99(2): 282-287.
103. Bader, A., Steinhoff, G. and Strobl, K., Engineering of human vascular aortic tissue based on a xenogenic starter matrix. *Transplant.*, 2000. 70(1): 7-14.
104. Inoue, Y., Anthony, J.P., Leon, P. and Young, D.M., Acellular human dermal matrix as a small vessel substitute. *J. Reconst. Microsurg.*, 1996. 12(5): 307-311.
105. Van de Velde, K. and Kiekens, P., Biopolymers: overview of several properties and consequences on their applications. *Polymer Testing*, 2002. 21(4): 433-442.
106. Greisler, H.P., Gosselin, C., Ren, D., Kang, S.S. and Kim, D.U., Biointeractive polymers and tissue engineered blood vessels. *Biomaterials*, 1996. 17(3): 329-336.

107. Bujan, J., Garcia-Honduvilla, N. and Bellon, J.M., Engineering conduits to resemble natural vascular tissue. *Biotechnol. Appl. Biochem.*, 2004. 39: 17-27.
108. Gogolewski, S. and Pennings, A.J., Biodegradable materials of polylactides. Porous biomedical materials based on mixtures of polylactides and polyurethanes. *Makromol. Chem., Rapid Commun.*, 1982. 3: 839-845.
109. Pennings, A.J., Knol, K.E., Leenslag, J.W. and Van der Lei, B., A two-ply artificial blood vessel of polyurethane and poly(L-lactide). *Colloid Polym. Sci.*, 1990. 268: 2-11.
110. Soldani, G., Panol, G., Sasken, H.F., Goddard, M.B. and Galletti, P.M., Small diameter polyurethane polydimethylsiloxane vascular prostheses made by a spraying, phase-inversion process. *J. Mater. Sci.-Mater. Med.*, 1992. 3(2): 106-113.
111. Mooney, D.J., Breuer, M.D., McNamara, M.D., Vacanti, J.P. and Langer, R., Fabricating tubular devices from polymers of lactic and glycolic acid for tissue engineering. *Tissue Eng.*, 1995. 1(2): 107.
112. Mooney, D.J., Mazzoni, C.L., Breuer, C., McNamara, K., Hern, D., Vacanti, J.P. and Langer, R., Stabilized polyglycolic acid fibre-based tubes for tissue engineering. *Biomaterials*, 1996. 17(2): 115-124.
113. Hoerstrup, S.P., Zund, G., Sodian, R., Schnell, A.M., Grunfelder, J. and Turina, M., Tissue engineering of small caliber vascular grafts. *E. J. Cardio-Thorac. Surg.*, 2001. 20(1): 164-169.
114. Nerem, R.M. and Ensley, A.E., The tissue engineering of blood vessels and the heart. *Am. J. Transplant.*, 2004. 4: 36-42.
115. Chen, G.P., Ushida, T. and Tateishi, T., A biodegradable hybrid sponge nested with collagen microsponges. *J. Biomed. Mat. Res.*, 2000. 51(2): 273-279.
116. Chen, G.P., Ushida, T. and Tateishi, T., Fabrication of PLGA-collagen hybrid sponge. *Chem. Lett.*, 1999(7): 561-562.
117. Chen, G.P., Ushida, T. and Tateishi, T., A hybrid network of synthetic polymer mesh and collagen sponge. *Chem. Commun.*, 2000(16): 1505-1506.
118. Kobashi, T. and Matsuda, T., Fabrication of branched hybrid vascular prostheses. *Tissue Eng.*, 1999. 5(6): 515-524.
119. Kobashi, T. and Matsuda, T., Fabrication of compliant hybrid grafts supported with elastomeric meshes. *Cell Transplant.*, 1999. 8(5): 477-488.

120. He, H.B. and Matsuda, T., Arterial replacement with compliant hierarchic hybrid vascular graft: Biomechanical adaptation and failure. *Tissue Eng.*, 2002. 8(2): 213-224.
121. He, H.B., Shirota, T., Yasui, H. and Matsuda, T., Canine endothelial progenitor cell-lined hybrid vascular graft with nonthrombogenic potential. *J. Thorac. Cardiovasc. Surg.*, 2003. 126(2): 455-464.
122. Kanda, K., Matsuda, T. and Oka, T., In vitro reconstruction of hybrid vascular tissue. Hierarchic and oriented cell layers. *ASAIO J.*, 1993. 39(3): M561-M565.
123. Martin, I., Wendt, D. and Heberer, M., The role of bioreactors in tissue engineering. *Trends Biotechnol.*, 2004. 22(2): 80-86.
124. Lee, A.A., Graham, D.A., Dela, C.S., Ratcliffe, A. and Karlon, W.J., Fluid shear stress-induced alignment of cultured vascular smooth muscle cells. *J. Biomech. Eng.*, 2002. 124(1): 37-43.
125. Kanda, K. and Matsuda, T., Mechanical stress-induced orientation and ultrastructural change of smooth muscle cells cultured in three-dimensional collagen lattices. *Cell Transplant.*, 1994. 3(6): 481-492.
126. Jeong, S.I., Kwon, J.H., Lim, J.I., Cho, S.W., Jung, Y., Sung, W.J., Kim, S.H., Kim, Y.H., Lee, Y.M. and Kim, B.S., Mechano-active tissue engineering of vascular smooth muscle using pulsatile perfusion bioreactors and elastic PLCL scaffolds. *Biomaterials*, 2005. 26(12): 1405-1411.
127. Seliktar, D., Black, R.A., Vito, R.P. and Nerem, R.M., Dynamic mechanical conditioning of collagen-gel blood vessel constructs induces remodeling in vitro. *Ann. Biomed. Eng.*, 2000. 28(4): 351-362.
128. Surowiec, S.M., Conklin, B.S., Li, J.S., Lin, P.H., Weiss, V.J., Lumsden, A.B. and Chen, C., A new perfusion culture system used to study human vein. *J. Surg. Res.*, 2000. 88(1): 34-41.
129. Conklin, B.S., Surowiec, S.M., Lin, P.H. and Chen, C., A simple physiologic pulsatile perfusion system for the study of intact vascular tissue. *Med. Eng. Phys.*, 2000. 22(6): 441-449.

Chapter 3

First Steps Towards Tissue Engineering of Small-Diameter Blood Vessels: Preparation of Flat Scaffolds of Collagen and Elastin by Means of Freeze Drying*.

The real voyage of discovery consists not in seeking new landscapes but in having new eyes
(M. Proust)

Abstract.

Porous scaffolds composed of collagen or collagen and elastin have been prepared by freeze drying at temperatures between -18 and -196 °C. All scaffolds had a porosity of 90-98% and a homogeneous distribution of pores. Freeze-drying at -18 °C afforded the best collagen and collagen/elastin matrices with average pore sizes of 340 and 130 μm , respectively. After 20 successive cycles up to 10% of strain, collagen/elastin dense films had a total degree of strain recovery of 70 ± 5 %, which was higher than that of collagen films (42 ± 6 %). Crosslinking of collagen/elastin matrices either in water or ethanol/water (40% v/v), was carried out using a carbodiimide (EDC) in combination with a succinimide (NHS), in the presence or absence of a diamine (J230) or by reaction with butanediol diglycidylether (BDGE) followed by EDC/NHS. Crosslinking with EDC/NHS or

* Buttafoco L.¹, Engbers-Buijtenhuijs P.^{1,2}, Poot A.A.¹, Dijkstra P.J.¹, Daamen W.F.³, van Kuppevelt T.H.³, Vermes I.^{1,2}, Feijen J.¹

Submitted to J. Biomed. Mat. Res.

¹ Department of Polymer Chemistry and Biomaterials, Faculty of Science and Technology and Institute of Biomedical Technology (BMTI), University of Twente, Enschede, P.O. Box 217, 7500 AE, The Netherlands,

² Department of Clinical Chemistry, Medical Spectrum Twente Hospital, Enschede, P.O.Box 50000, 7500 KA, The Netherlands,

³ Department of Biochemistry 194, NCMLS, University Medical Centre Nijmegen, P.O.Box 9101, 6500 HB, Nijmegen, The Netherlands.

J230/EDC/NHS resulted in matrices with improved mechanical properties as compared to non-crosslinked matrices, whereas sequential crosslinking with the diglycidylether and EDC/NHS yielded very fragile scaffolds. Ethanol/water was the preferred solvent in the crosslinking process due to its ability to preserve the open porous structure during crosslinking. Smooth muscle cells were seeded on top and into the (crosslinked) scaffolds and could be expanded after 14 d of culturing.

Introduction.

Atherosclerosis, a disease which affects large-, small- and medium-sized arteries, is the main cause of coronary occlusion, stroke, aortic aneurysms and gangrene and therefore one of the major causes of death in the Western society [1, 2]. Atherosclerotic lesions in the arterial wall are characterized by excessive deposition of lipids surrounded by extracellular matrix (ECM), smooth muscle cells (SMC) and covered with a fibrous cap. This deposit can grow in size and can become large enough to inhibit the flow of blood. These problems can partly be solved by the use of blood vessel prostheses when large-diameter vessels have to be replaced. In case of small-diameter blood vessels no adequate methods are available today. A promising approach to solve this problem is to make use of tissue-engineered blood vessels.

In tissue engineering the principles of life science and engineering are combined in an attempt to restore, maintain or enhance the function of tissues or organs [3, 4]. The ability of cells to adhere, proliferate and differentiate on a scaffold, the production of new ECM components, the degradation of the scaffold and the regeneration of the appropriate tissue are key issues which have to be taken into consideration [5, 6]. Especially for the development of a tissue-engineered blood vessel the scaffold has to have sufficient burst strength and elasticity to withstand the forces during dynamic culturing. After *in vitro* culturing, the construct has to be strong enough to withstand the blood pressure and to remodel into a non-thrombogenic functional blood vessel [1, 7].

During the past 25 years many attempts have been made to obtain tissue-engineered blood vessel substitutes by using either synthetic [7-10] or natural materials [11-14]. Only recently, a successful clinical application of tissue-engineered blood vessels has been documented [15]. A tubular construct prepared from poly(ϵ -caprolactone-co-lactic acid) reinforced with woven polyglycolic acid has been seeded with cells isolated from the peripheral vein of a 4 year old girl affected with pulmonary artresia. After 10 d of culture this tissue-engineered construct was

transplanted in the pulmonary artery. After 7 months, the patient was still doing good, with no evidence of graft occlusion or aneurismal changes.

Blood vessels can be considered as viscoelastic tubes. Their diameter is maintained by the balance between the elasticity and strength imparted by all the different components of the wall and the applied transmural pressure. The composition of the wall of a particular artery is dependent on its function [16]. The presence of SMC ensures the maintenance of the vascular tone due to their ability to contract and relax [17]. Moreover, in all arteries, both elastic (elastin) and fibrous (collagen) components can be found. The former are responsible for the elastic behaviour of the vessel, while the latter limit its extensional ability and prevent the vessel from bursting. The engineering of blood vessels from collagen/elastin matrices has been investigated in the past, but either decellularized matrices [18] or soluble proteins [19, 20] have been used.

Collagen is one of the most abundant proteins in the ECM. In the body it is present in most of the organs or in parts of them. Its main function is to keep specialized cells together in discrete units. In this way, it prevents organs/tissues from tearing or loosing their functional shape, when they are exposed to sudden movements [21]. The structure of elastin is still a matter of debate, but it is generally agreed that elastin is the functional component of the elastic fibre. Elastin is characterized by its high durability and ability to deform reversibly, which makes it responsible for the elasticity and resilience of many tissues [22-25]. Moreover, Li *et al.* have reported a regulatory function of elastin during arterial development. Elastin seems to be responsible for the control of SMC function and for the stabilization of the arterial structure [26].

Our approach aims at developing a small-diameter tissue-engineered blood vessel resembling a native artery in both composition and physical properties. Insoluble type I collagen from bovine Achilles tendons and insoluble elastin from equine ligamentum nuchae have been used as the basic constituents of the tissue-engineered scaffold. Scaffold preparation and stabilization through crosslinking have been investigated. The (crosslinked) scaffolds have been fully characterized from a morphological and physical point of view. SMC were seeded on the (crosslinked) scaffolds and the resulting constructs were analysed by means of histology.

Materials and methods.

All chemicals and materials were purchased from Sigma & Aldrich (Zwijndrecht, The Netherlands) unless stated otherwise.

Preparation of porous structures.

A 1% w/v suspension of type I insoluble collagen derived from bovine Achilles tendon (University of Nijmegen, The Netherlands, purification procedure as in [27]) was swollen overnight at 6 °C in 0.05 M acetic acid. The resulting suspension was homogenised first with a Philips Blender for 4 min and then for 15 min at 4 °C with an Ultra-Turrax T25 (IKA Labortechnik, Staufen, Germany). The suspension was filtered through a 20 denier nylon filter (average pore size 30 µm) and then degassed at 0.1 mbar (Edwards, oil vacuum pump). Parts of the resulting suspension were frozen for 16 h at temperatures varying between –18 °C and –80 °C. The cooling rate was not controlled. After freezing, samples were freeze-dried for 24 h. Subsequently, the effect of the freezing temperature on the morphology of the samples was evaluated with scanning electron microscopy (SEM) as described below.

Insoluble type I collagen and insoluble elastin derived from equine ligamentum nuchae (University of Nijmegen, The Netherlands; purification procedure as in [28]) were mixed in 0.25 M acetic acid in order to obtain a suspension containing 1% w/v of each of the components. The resulting suspension was homogenized as described above but the filtration step was omitted to avoid loss of thick elastin fibres. Parts of the resulting suspension were frozen at temperatures varying between –18 °C and –80 °C, after which the samples were freeze-dried for 24 h.

Crosslinking.

Freeze-dried collagen and collagen/elastin samples were crosslinked with a water-soluble carbodiimide in the presence or absence of a Jeffamine spacer (J230). A third method to crosslink these materials comprised crosslinking with a diglycidylether followed by a reaction with the carbodiimide.

In the first method N-(3-dimethylaminopropyl)-N'-ethylcarbodiimide hydrochloride (EDC) in the presence of N-hydroxysuccinimide (NHS) was used to activate carboxylic acid groups. This combination limits the occurrence of secondary reactions and induces crosslinking with free primary amine groups [27]. Flat freeze-dried disc-shaped specimens with a diameter

of 5-6 cm and a thickness of approximately 3-4 mm, were incubated (215 ml per gram of sample) for 30 min in a 2-morpholinoethane sulfonic acid (MES) buffer (0.05 M, pH 5.5). Crosslinking was carried out by the addition of EDC (2.3 g) and NHS (0.56 g) per gram of collagen/(elastin) (molar ratio of EDC/NHS = 2.5). The reaction was performed for 2 h at room temperature. After removal of the crosslinking solution, samples were incubated for 2 h in 0.1 M sodium phosphate (pH = 7.4). A further washing step was performed with demineralized MilliQ water. The total incubation time was 2 h, during which water was exchanged every 30 min. The crosslinked matrices were frozen at the same temperature used to prepare the native scaffolds, and subsequently freeze-dried for 24 h.

Crosslinking reactions in the presence of poly(propylene glycol)-bis-(2-aminopropyl ether) (J230) were performed by first placing the freeze-dried scaffolds in a MES buffer (0.05M, pH 5.5) containing J230 (0.062 M) at room temperature for 30 min. Subsequently, EDC (5.75 g/g of protein) and NHS (1.38 g/g of protein) were added and crosslinking was performed overnight at room temperature (molar ratio of J230 : EDC : NHS = 2.1 : 1 : 0.4). The samples were then rinsed with sodium phosphate buffer (0.1M, pH 7.4) and demineralised MilliQ water and subsequently freeze-dried as described above.

In the third approach, butanediol diglycidylether (BDGE) was used as a crosslinking agent. Freeze-dried samples were first incubated in a MES buffer (0.05 M, pH 4.5) for 30 min and then transferred to a solution of BDGE (4% v/v) in MES buffer (0.05M, pH 4.5). The reaction was terminated after 10 d by washing with 0.1 M sodium phosphate at pH 7.4 and then with demineralised MilliQ water. Subsequently, samples were crosslinked with EDC/NHS (molar ratio of EDC/NHS = 2.5). Crosslinking was carried out for 2 h in MES buffer (0.05 M, pH 5.5) containing EDC (2.3 g/g of protein) and NHS (0.56 g/g of protein) per gram of collagen/(elastin). The samples were then rinsed in sodium phosphate (0.1M, pH 7.4) and demineralised MilliQ water and finally freeze-dried as described above.

Crosslinking applying the procedures as described above was also carried out using ethanol/water (40% v/v) instead of water as a solvent. The washing step was also performed with ethanol/water (40% v/v). The total washing time was 2 h, during which the medium was exchanged every 30 min. Finally the samples were rinsed for 10 min with demineralised MilliQ water.

The effect of crosslinking on the volume shrinkage and mass retention of the samples after freeze-drying was evaluated using the following equations:

$$\text{Volume shrinkage (\%)} = [1 - (V / V_0)] * 100 \quad (3.1)$$

where V is the volume of the scaffold after crosslinking and V_0 is the original volume;

$$\text{Mass retention (\%)} = (\text{mass}_{\text{after crosslinking}} / \text{mass}_{\text{before crosslinking}}) * 100 \quad (3.2)$$

Characterization of scaffolds.

Determination of primary amine group content.

The concentration of free primary amine groups present in (crosslinked) collagen and collagen/elastin samples was determined using 2,4,6-trinitrobenzenesulfonic acid (TNBS) according to the following procedure.

Samples of approximately 5 mg were incubated for 30 min in an aqueous solution of NaHCO_3 (1 ml, 4% w/v). Then a solution of TNBS (1 ml, 0.5% w/v) in the same aqueous NaHCO_3 solution was added and the mixture was incubated at 40 °C for 2 h. After the addition of HCl (3 ml, 6 M) samples were hydrolysed at 60 °C for 90 min. The reaction mixture was diluted with demineralised MilliQ water (5 ml), cooled to room temperature and the absorbance at 420 nm was measured using a Varian Cary 300 Bio spectrophotometer. A blank was prepared using the same procedure, except that HCl was added prior to the TNBS solution. The absorbance was correlated to the concentration of free amino groups using a calibration curve obtained with glycine (stock solution: glycine (10 mg) in an aqueous NaHCO_3 solution (100 ml, 4% w/v)).

Amino acid analysis [28].

Samples of approximately 3 mg were weighed, placed in glass tubes and to each glass tube 0.5 ml of 6 M HCl was added. The tubes were immediately put on dry ice in order to prevent oxidation. Tubes were evacuated and sealed with a flame. The hydrolysis was performed for 21 h in an oven at 110 °C. After hydrolysis the tubes were opened and placed on NaOH pellets *in vacuo* overnight, in order to eliminate remaining HCl and to dry the samples. The residues were dissolved in 1 ml of 0.01 M HCl. Subsequently a 5-sulphosalicylic acid

solution (18.8% w/v, Fluka Chemie AG, Buchs, Switzerland) containing norleucine as an internal standard was added to the hydrolysed samples. Separation of the amino acids was performed by column ion exchange chromatography using a Biochrome 20 amino acid analyser (Amersham Pharmacia Biotech) and lithium buffers with increasing pH.

Denaturation temperature.

The denaturation temperature of (crosslinked) collagen and collagen/elastin samples was measured using differential scanning calorimetry (DSC 7, Perkin Elmer, Norwalk, CT). Samples of approximately 5-10 mg were swollen overnight in 50 μ l of PBS (pH 7.4) in high-pressure capsules. Samples were heated from 20 $^{\circ}$ C to 90 $^{\circ}$ C at a heating rate of 10 $^{\circ}$ C/min. A sample containing 50 μ l of PBS (pH 7.4) was used as a reference. The onset of the endothermic peak, which indicates denaturation of the collagen triple helix, was recorded as the denaturation temperature.

Mechanical properties.

Stress-strain properties of flat freeze-dried scaffolds (length 15mm, width 5 mm) were determined using a ZWICK Z020 tensile tester (Zwick, Ulm, Germany), with a load cell of 10 N, and an elongation speed of 5 mm/min. Flat specimens were cut from the scaffolds and swollen in PBS (pH 7.4) for 30 min prior to analysis. The thickness of the samples in the test area was measured at three different points using an electronic micrometer (Mitutoyo, Tokyo, Japan) and was always approximately 4 mm. The E-modulus was always calculated at strains lower than 1%.

Films of collagen or collagen/elastin were cast from protein suspensions on a Teflon plate using a casting knife. The films were subsequently air-dried and used to determine the degree of strain recovery of the specimens. Films 10 x 30 mm and an average thickness of 0.02 mm were tested with the same set up as described above and subjected to 20 successive cycles with an upper strain of 10 % of the initial length of the sample. The degree of strain recovery after 2, 5, 10 and 20 cycles and the total degree of strain recovery after 20 cycles were determined using the following equations [29]:

$$R_r(N) = \frac{\varepsilon_m - \varepsilon_p(N)}{\varepsilon_m - \varepsilon_p(N-1)} \quad (3.3)$$

$$R_{r,tot} = \frac{\varepsilon_m - \varepsilon_p(N)}{\varepsilon_m} \quad (3.4)$$

where ε_m is the applied strain and ε_p the residual strain in the tension free state.

Structure and morphology.

The structure and morphology of the samples were studied by means of histological techniques and scanning electron microscopy (SEM), respectively.

Freeze-dried samples were embedded in paraffin and parallel and cross-sections were stained with the Masson Trichrome technique (methylene blue staining of collagen (blue) and acid fuchsin staining of elastin (pink)).

The surface morphology of the scaffolds was examined using SEM. Samples ($n = 5 \pm \text{s.d.}$) were freeze-dried before analysis and then sputter coated with gold in a Polaron E5600 sputter coater. Images were recorded with SEM (Leo Gemini 1550 FEG-SEM) at different acceleration voltages.

Average pore sizes were obtained after measuring the dimensions of 10 pores chosen at random in the samples. The porosity of the scaffolds was calculated by determining the volume (V) and the mass (m) of the scaffolds. The porosity is defined as:

$$p (\%) = [1 - (d / d_p)] * 100 \quad (3.5)$$

where d is the density of the scaffold and d_p is the density of the polymer.

Cell culture.

Human smooth muscle cells (SMC) were isolated from umbilical veins by a collagenase digestion method as described previously [30]. Sub-confluent cultures of SMC were harvested by trypsinisation (2 min, 0.125% trypsin/0.05% EDTA). Cells were centrifuged at 300 g for 10 min at 21 °C and resuspended in culture medium (Dulbecco's Modified Eagle's Medium containing 10% (v/v) human serum, 10% (v/v) foetal bovine serum, 50 U/ml penicillin and 50 µg/ml streptomycin). Cells were counted with a Bürker hemacytometer. In order to stimulate cell attachment and growth in between the collagen and elastin fibres of the scaffold, cells were seeded using a filtration procedure. Scaffolds were sterilised with ethanol/water 70% (v/v), washed 3 times with PBS and then placed on top of a filter flask (filter pore size: 0.20 µm).

Aliquots of 40 μl of cell suspension (10^6 cells per 20 ml) were seeded on top of the scaffolds. Filtration seeding was carried out by applying a small pressure difference between the two sides of the scaffolds. The filtration cycle was repeated 12 times till a final concentration of 200000 cells/ cm^2 (normalised to the surface area of the scaffolds) was reached. Scaffolds were transferred to 24-wells TCPS culture dishes, secured with Viton O-rings (Eriks, Alkmaar, The Netherlands) and cells were subsequently cultured for 14 d in culture medium under static conditions in an incubator at 37 °C in a humidified atmosphere containing 5% CO_2 . The culture medium was refreshed every 2-3 d. After culturing, the resulting scaffolds containing SMC were fixed with formalin, impregnated with paraffin, cut into transverse sections and stained using the Elastic von Gieson (EG) method at the Laboratory of Pathology Oost Nederland according to standard procedures. In particular, collagen was stained pink, elastin black and the nuclei of the cells brown [30]. The number of cells present on or in the scaffolds after 14 d of culture was determined by the CyQuant method as previously described [30].

Results and discussion.

Porous scaffolds obtained by freeze drying collagen suspensions have a structure and a morphology which are highly dependent on the freeze drying conditions [31]. Although the porosity of the scaffolds in all cases was between 90 and 97%, the size of the pores decreased with decreasing freeze drying temperature [27, 32]. At lower temperatures the freezing process is faster and ice crystals do not have enough time to increase in dimensions. In particular, samples freeze-dried at -196 °C collapsed, due to the extremely high speed of freezing and subsequent solid-liquid phase separation process. At higher temperatures pore sizes were easily controlled and at -35 °C scaffolds had pores of 110 ± 10 μm . Their size increased to 200 ± 20 μm at -22 °C and to 480 ± 20 μm at -5 °C. All the scaffolds prepared by this technique had a very homogeneous distribution of the pores throughout the matrix.

Freeze drying suspensions composed of collagen and elastin (weight ratio 1:1) afforded porous structures for which the average pore size also increased with increasing freeze drying temperatures (Fig. 3.1a,b). The porosity of the scaffolds was only slightly affected by the presence of elastin and typical values were around 90%. Also in this case, collapsed structures were obtained upon freeze-drying at -196 °C. However, the presence of elastin gave a decrease in the average size of the pores formed at higher freeze-drying temperatures.

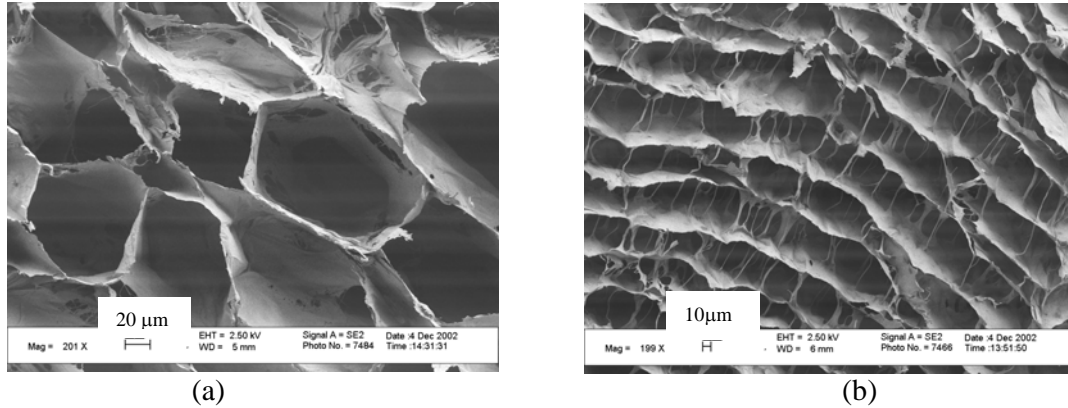


Figure 3.1. SEM pictures of cross-sections of collagen/elastin structures (weight ratio 1:1) obtained by freeze drying at different temperatures. (a) Sample frozen at $-18\text{ }^{\circ}\text{C}$ (scale bar $30\mu\text{m}$); (b) sample frozen at $-50\text{ }^{\circ}\text{C}$ (scale bar $10\mu\text{m}$).

At $-18\text{ }^{\circ}\text{C}$ the average pore size of the collagen/elastin scaffolds was $130 \pm 30\ \mu\text{m}$ compared to $340 \pm 20\ \mu\text{m}$ of the collagen scaffolds. This can be due to the concentration of collagen/elastin suspensions used, which was twice that of collagen suspensions in weight per volume. An increase in the solute concentration is known to decrease the pore size of the obtained freeze-dried matrices [30]. Moreover, elastin fibres have a much larger diameter ($4\ \mu\text{m}$) than collagen fibres ($200\ \text{nm}$) and this may also have influenced the resulting pore size. It has been reported that pore sizes between 5 and $100\ \mu\text{m}$ are sufficient to ensure exchange of oxygen and nutrients in a $10\ \text{mm}$ thick matrix (porosity $\sim 99\%$) [33] and that SMC can still migrate in pores having a size up to $10\ \mu\text{m}$ [34]. Based on these data, in further studies collagen(/elastin) scaffolds were prepared by freeze drying at $-18\text{ }^{\circ}\text{C}$.

Another interesting feature noticed when a mixture of the proteins was freeze-dried, was the ability of collagen to enwrap and bridge elastin fibres (Fig. 3.2a,b). Moreover, the long fibres of collagen and the short fibres of elastin seem to follow the same spatial direction in the assembly (Fig. 3.2c,d). This assembly of the proteins was expected to have a beneficial influence on the mechanical properties of the initial construct. This could be illustrated by comparing the degree of strain recovery of dense films of collagen and of collagen and elastin (weight ratio 1:1), prepared by casting suspensions on a PET surface and subsequent air-drying. After 20 cycles up to 10% of strain, the degree of strain recovery of collagen/elastin films levelled off to $70 \pm 5\%$, which is much higher than that recorded for collagen films ($42 \pm 6\%$) under the same conditions (Table 3.1).

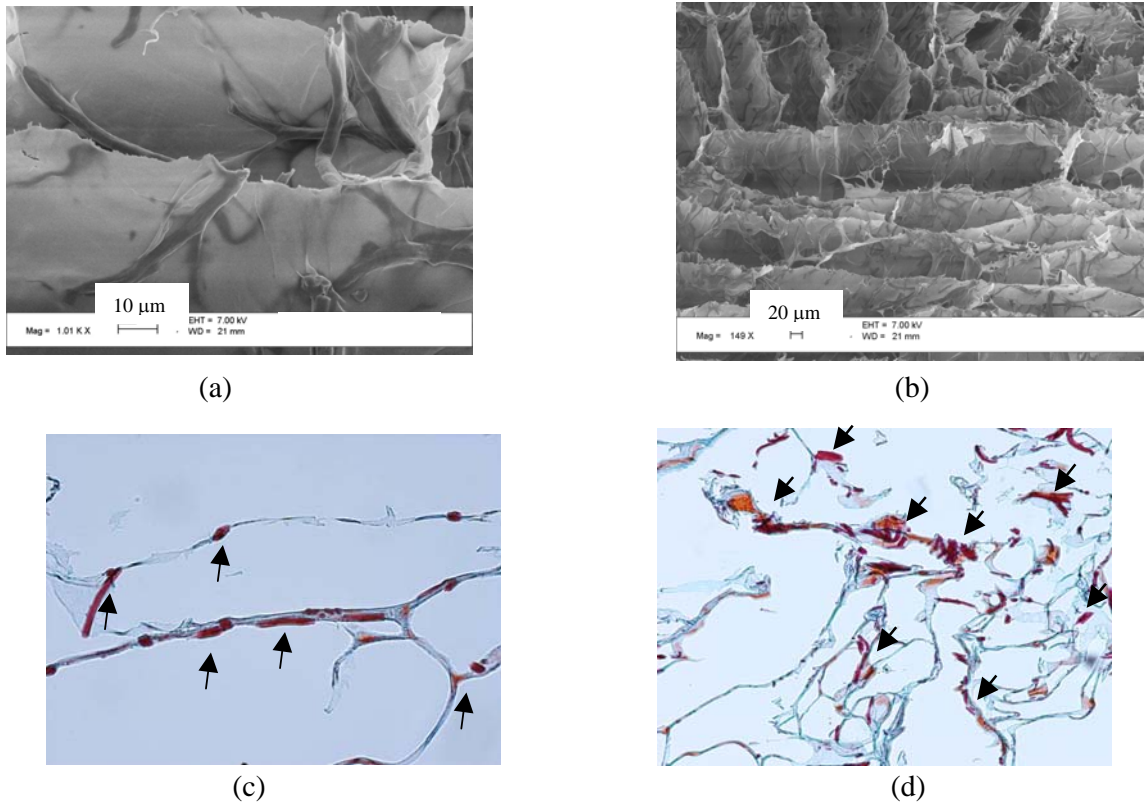


Figure 3.2. SEM pictures of cross sections of a collagen/elastin matrix (weigh ratio 1:1) obtained by freeze-drying: (a) scale bar 10 μm ; (b) scale bar 20 μm ; the largest fibres are made of elastin, while the rest of the structure is collagen. Histological cross sections of a collagen/elastin matrix: (c) magnification 25X; (d) magnification 10X; elastin fibres are indicated by arrows.

Table 3.1. Degree of strain recovery (%) of films composed of collagen or collagen/elastin (weight ratio 1:1).

Degree of strain recovery (%) [*]	Collagen	Collagen/elastin
R _r (2)	90 ± 3	96 ± 1
R _r (5)	97 ± 0	99 ± 1
R _r (10)	99 ± 1	100 ± 0
R _r (20)	100	100 ± 0
R _r (tot)	42 ± 6	70 ± 5

^{*} Values in brackets represent the number of the performed cycles.

R_r (tot) is the total degree of strain recovery obtained when the length of the specimen after the last cycle is compared with its original one.

It is anticipated that in tubular porous scaffolds aggregation of collagen and elastin will also enhance the mechanical properties with respect to collagen scaffolds thus avoiding long-term deformation during *in vitro* culturing.

Crosslinking of collagen(/elastin)-based materials is necessary to obtain matrices with improved mechanical properties suitable for *in vitro* culture of SMC and subsequent implantation. Crosslinking of collagen or collagen/elastin samples with EDC/NHS involves activation of free carboxylic acid groups of glutamic and aspartic acid residues and subsequent formation of peptide bonds upon reaction with the free amino groups of lysine and hydroxylysine residues. In this way no additional chemical entities are introduced and stable amide linkages are formed. The addition of NHS is advantageous not only because it prevents the formation of side products but also because it increases the reaction rate [35]. When freeze-dried collagen samples were crosslinked in water with EDC/NHS and subsequently freeze-dried at $-18\text{ }^{\circ}\text{C}$, a porosity of 81% was obtained. This value is lower than that of the freeze-dried native collagen scaffolds (98%). Moreover, shrinkage to 15% of their original volume was observed and this resulted in a decrease of the average pore size from 340 to approximately 190 μm (Table 3.2). It is well known that shrinkage of polymer matrices upon lyophilization can be reduced by the use of alcohols. In particular, Zhang *et al.* [36] have reported a decrease in the shrinkage of poly(α -hydroxy acids)-hydroxyapatite foams, when a solution of poly(α -hydroxy acids) containing homogeneously dispersed hydroxyapatite powder was freeze-dried at temperatures between -5 and $-10\text{ }^{\circ}\text{C}$ in ethanol instead of water. Moreover, the higher viscosity of ethanol when compared to water can be another factor influencing the shrinkage of these structures [37]. The use of ethanol/water as a solvent in the crosslinking reactions did not give collagen scaffolds having morphological characteristics significantly different from those obtained after crosslinking in water.

Upon crosslinking collagen/elastin composites with EDC/NHS in water and subsequent freeze drying, a complete collapse of the pores was observed. On the contrary, when collagen/elastin scaffolds were crosslinked in ethanol/water, a porosity of 90% was retained, shrinkage was 56% instead of 68% for crosslinking performed in water and scaffolds with an average pore size of 60 μm were obtained (Table 3.2). These results show that the high shrinkage of collagen/elastin samples to about one third of their original volume observed upon crosslinking in water, can partly be circumvented by the use of ethanol/water during crosslinking. Moreover, ethanol is known to be inactive towards carbodiimides at room temperature and these results indicate that the reagents can more easily penetrate the scaffolds, thus crosslinking

Table 3.2. Morphological characteristics of freeze-dried crosslinked collagen or collagen/ elastin samples. Volume shrinkage and mass retention have been calculated from the equations (3.1) and (3.2), respectively.

<i>Parameter</i> <i>Sample</i>	Crosslinking method	Porosity (%)	Pore size (μm)	Shrinkage (%)	Mass retention (%)
Collagen	Native	98	340 ± 20	-	-
	EDC/NHS (H ₂ O)	81	190 ± 10	85	93
	EDC/NHS (EtOH/H ₂ O)	75	180 ± 15	91	88
	J230 (H ₂ O)	55	5 ± 1	50	92
	J230 (EtOH/H ₂ O)	76	9 ± 3	74	93
	BDGE (H ₂ O)	40	5 ± 1	91	95
	BDGE (EtOH/H ₂ O)	86	6 ± 3	91	94
Collagen/Elastin	Native	90	130 ± 30		
	EDC/NHS (H ₂ O)	-*	-*	68	90
	EDC/NHS (EtOH)	90	60 ± 40	56	100
	J230 (H ₂ O)	-*	-*	76	90
	J230 (EtOH/H ₂ O)	90	30 ± 20	47	100
	BDGE (H ₂ O)	-*	-*	70	100
	BDGE (EtOH/H ₂ O)	90	10 ± 5	55	100

Pore size has been measured from SEM pictures by averaging the size of ten pores taken at a random. J230 stands for J230/EDC/NHS crosslinking and BDGE for BDGE-EDC/NHS.

* Collapsed structures

them more thoroughly. The higher crosslink density of collagen/elastin samples after EDC/NHS crosslinking in ethanol/water as compared to water is illustrated by the concentration of residual amino groups (25 nmol/mg vs. 85 nmol/mg) (Table 3.3).

Table 3.3. Free amino group content (nmol/mg) of (crosslinked) collagen (/elastin) samples as determined by the TNBS assay ($n = 3 \pm s.d.$).

Crosslinking method	Collagen	Collagen:Elastin
None	333 \pm 1	110 \pm 20
EDC/NHS (H ₂ O)	- *	85 \pm 10
EDC/NHS (EtOH)	89 \pm 1	25 \pm 1
J230 (H ₂ O)	- *	130 \pm 30
J230 (EtOH)	240 \pm 20	127 \pm 3
BDGE/EDC/NHS (H ₂ O)	- *	33 \pm 1
BDGE/EDC/NHS (EtOH)	82 \pm 3	44 \pm 3

* Not determined

Crosslinking of freeze-dried collagen samples in water using EDC/NHS in the presence of a Jeffamine spacer induced 50% shrinkage of the scaffolds and resulted in samples with an average pore size of 5 μm . The use of ethanol/water (40% v/v) as solvent yielded scaffolds that retained 26% of their original volume but the average pore size (9 μm) was similar. Crosslinking of collagen/elastin scaffolds in water under the same conditions resulted in scaffolds retaining 24% of their original volume and a complete collapse of the porous structure was observed. On the contrary, when crosslinking was performed using ethanol/water (40% v/v) as a solvent, the scaffolds shrank to 53% of their original volume and an average pore size of 30 μm was obtained (Table 3.2).

Crosslinking collagen samples in water first with BDGE and then with EDC/NHS resulted in shrinkage of the scaffolds up to 91% and as a consequence, the average pore size also decreased to 5 μm . These results were not significantly affected by the use of ethanol/water (40% v/v) as a solvent. Also in this case, crosslinking of collagen/elastin samples under the same conditions in water, resulted in structures that shrank to 30% of their original dimensions. Shrinkage was somewhat reduced using ethanol/water and samples with small pore sizes of 10 μm were obtained (Table 3.2). In all the experiments performed, crosslinking either in water or in ethanol does not cause significant mass loss of the samples (Table 3.2).

As expected, formation of crosslinks in the matrix increased the denaturation temperature (T_d) of the samples (e.g. a native sample of collagen has a T_d of 53 $^{\circ}\text{C}$, which increased to 78 $^{\circ}\text{C}$ after crosslinking in ethanol/water) (Fig. 3.3). Elastin is a thermally stable protein [38] and no

transitions were observed in the temperature range used in this study (25 - 90 °C). When collagen/elastin samples were crosslinked with EDC/NHS, the same reaction mechanism was operative as in the crosslinking of collagen. Elastin was crosslinked concurrently with collagen because of the presence of free carboxylic acid (Glu, Asp) and free amine groups (Lys, Hylys) containing α -amino acids (Table 3.4). Under the same conditions, when crosslinking with EDC/NHS was carried out, the percentage of amino groups involved in the reaction was the same for both collagen and collagen/elastin scaffolds (~74%) when ethanol/water (40% v/v) was used as a solvent (Table 3.3). From thermal analyses it is evident that the denaturation temperatures of EDC/NHS crosslinked collagen and collagen/elastin samples using ethanol/water are similar (Fig. 3.3).

When the crosslinking procedure is performed in the presence of poly(propylene glycol)-bis-(2-aminopropyl ether) (J230), crosslinks are formed between two pendant carboxylic acid residues and amino groups of the Jeffamine, with formation of amide bonds. As expected, because of the presence of EDC/NHS, zero-length crosslinks will be formed as well. Collagen/elastin scaffolds crosslinked in ethanol/water with EDC/NHS in the

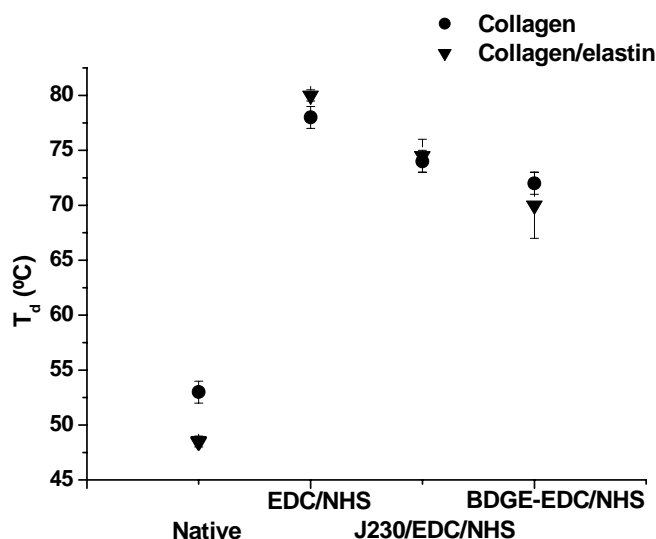


Figure 3.3. Thermal behaviour of collagen and collagen/elastin scaffolds freeze-dried at -18 °C and crosslinked in three different ways using ethanol/water (40% v/v) as solvent. Analyses have been performed on samples swollen in PBS overnight ($n = 3 \pm s.d.$).

Table 3.4. Amino acid analyses of collagen or elastin samples (numbers of amino acids are expressed per 1000 amino acid residues) ($n = 3 \pm s.d.$).

Amino acids	Collagen	Elastin*
Asp/Asn	32 ± 2	5 ± 0
Glu/Gln	58 ± 3	19 ± 1
Hylys	15 ± 3	0
Lys	35 ± 1	7 ± 1

*Obtained results are comparable with those found in literature [28].

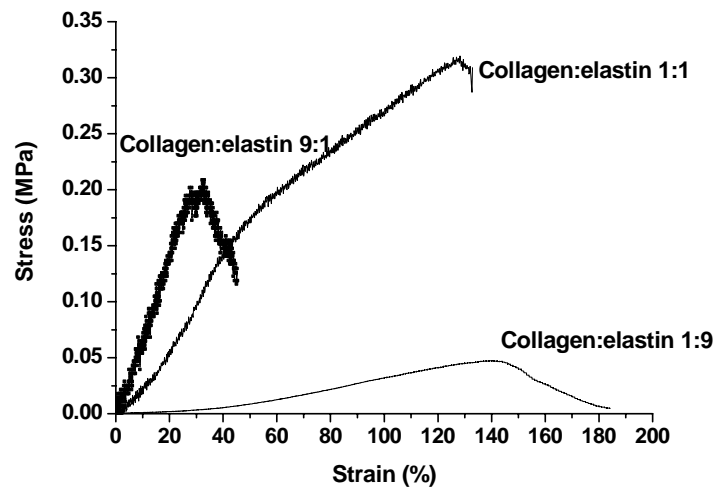
N.B. Number of amino acids = [(moles of one particular amino acid) / (total moles of amino acids in the compound)] * 1000

presence of J230 have a denaturation temperature of 75 °C, which is lower than observed for analogous matrices crosslinked with only EDC/NHS (80 °C). Moreover, the concentration of free amino groups found after crosslinking of collagen/elastin scaffolds in the presence of J230 (127 ± 3 nmol/mg) is higher than the concentration of free amino groups present in uncrosslinked scaffolds (110 ± 20 nmol/mg). J230 can also react only at one side leading to dangling chains containing amino end-groups. Since dangling groups destabilize helical structures, the denaturation temperature will be decreased. It is concluded that a fraction of J230 has not reacted on both sides during crosslinking of the structures in the presence of EDC/NHS.

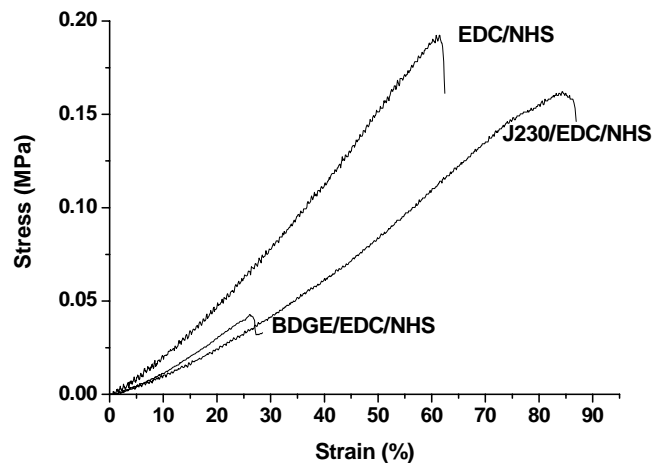
When butanediol diglycidylether (BDGE) is used as a crosslinker in an acidic environment (pH 4.5), carboxylic acid groups of glutamic and aspartic acid residues react with the bisepoxy compound. At this pH, approximately half of the carboxylic acid groups are deprotonated ($pK_a = 4.4 - 4.6$). A nucleophilic attack of the carboxylic anion on the protonated epoxide groups will result in the formation of an ester linkage. Crosslinking with BDGE in an acidic environment is known to proceed with a very low reaction rate and is accompanied by masking reactions (*e.g.* partial hydrolysis of the epoxy groups) [39]. In previous research, dermal sheep collagen has been crosslinked with butanediol diglycidylether (BDGE) affording materials that are soft and have a high elongation at break [37]. However, crosslinking of collagen/elastin freeze-dried samples with BDGE resulted in extremely fragile materials. In an attempt to improve the properties of the resulting scaffolds, in a second step, additional crosslinks were introduced by activating remaining carboxylic acid groups with EDC/NHS and *in situ* reaction with free amine groups. At the end of the process, 82 ± 3 and 44 ± 3 nmol/mg free amino

groups were present in collagen and in collagen/elastin samples, respectively (Table 3.3). The denaturation temperatures of the two different materials had comparable values of 72 °C for collagen and 70 °C for collagen/elastin. However, the samples remained fragile. The difference observed between the results reported in literature and those obtained in the present study might result from a different degree of structural organization of fibres in the matrices, but this was not studied in further detail. Formation of dangling groups after coupling of one epoxide group and hydrolysis of the other epoxide groups may also have an influence on the final properties of the resulting material. In view of the mechanical properties required for the intended application, a substantial degree of elasticity, this crosslinking method was not considered suitable to prepare scaffolds.

It was envisaged that the mechanical performance of the scaffolds is influenced by the presence of elastin. This could be verified by comparing stress-strain curves representative for scaffolds comprising different ratios of the two proteins (9:1, 1:1 and 1:9), having a porosity of approximately 90% and pore sizes between 60 and 110 μm (Fig. 3.4a). As expected, scaffolds containing a higher percentage of collagen had a higher E-modulus. Increasing the content of elastin enhanced the elongation at yield. Like in native tissues, elastin is responsible for the behaviour of the scaffolds at low strains, while at higher strains more and more collagen fibres become fully extended and take up most of the load [16]. In our previous work, the mechanical properties of porous scaffolds prepared from collagen/elastin suspensions by freeze drying at $-80\text{ }^{\circ}\text{C}$, have been described [40]. Constructs with pore sizes ranging from 20 to 100 μm , depending on the ratio of collagen to elastin were obtained. Increasing the ratio of elastin to collagen yielded scaffolds with a higher elongation at yield (elongation at yield increased to almost 150% for collagen/elastin = 1:9), but did not influence the yield stress in a significant way. The E-modulus decreased from 0.42 MPa (weight ratio collagen to elastin 9:1) to 0.24 MPa (weight ratio collagen to elastin 1:1) (Table 3.5). For tissue engineering small-diameter blood vessels, moduli in the range of several MPa are required. This was verified by measuring in exactly the same way as described above, the mechanical properties of native healthy artery mesenterica of man. The obtained results were in agreement with those reported in literature [41]. Therefore, in the present study, the porosity and the pore size of the scaffolds were controlled by freezing the above mentioned collagen and elastin suspensions at $-18\text{ }^{\circ}\text{C}$. Freeze drying afforded collagen/elastin 9:1 and 1:9 samples with a porosity of 95 and 87% and an average pore size of $110 \pm 40\text{ }\mu\text{m}$ and $60 \pm 30\text{ }\mu\text{m}$, respectively, comparable to the collagen/elastin 1:1 specimens. Also in this case, the yield strain increased with increasing elastin content from 60% (collagen/elastin 9:1) to 108% (collagen/elastin 1:1) and levelled off



(a)



(b)

Figure 3.4. Mechanical properties of freeze-dried collagen/elastin scaffolds frozen at -18°C . (a) Comparison of representative curves of scaffolds having three different collagen and elastin ratios; (b) comparison of representative curves of collagen/elastin scaffolds (weight ratio 1:1) crosslinked in three different ways using ethanol/water (40% v/v) as solvent. Analyses have been performed at 37°C , after swelling the samples in PBS for 30 min.

at high elastin content to 130% (collagen/elastin 1:9). The values of yield stress were in the same range of 0.05 to 0.3 MPa.

The E-modulus of these three materials increased with increasing collagen content from 2.0 to 5.3 MPa, thus being in the range observed for native arteries (Table 3.5). The increase in stiffness observed by changing the freezing temperature from -80 to -18 °C may be related to the more regular structure obtained at higher temperatures. Samples having a weight ratio of collagen to elastin 1:1 can be considered suitable for *in vitro* culture of SMC, which requires both elasticity and stiffness if performed in a dynamic environment mimicking the one experienced by blood vessels *in vivo*.

Crosslinking these scaffolds further improved their mechanical properties in terms of E-modulus (Fig. 4b), which increased to approximately 8 MPa, when EDC/NHS was used in presence or absence of J230. All the crosslinked scaffolds revealed a lower elongation at yield than uncrosslinked samples, whereas the capacity to withstand load was hardly altered (yield stress is 0.26 ± 0.08 MPa for freeze-dried collagen/elastin scaffolds crosslinked with EDC/NHS in ethanol/water). In particular, an elongation at yield of approximately 30% was observed for EDC/NHS crosslinked scaffolds, while the lower yield strain was less evident when the crosslink spacer J230 was used (elongation at yield = 60%) (Table 3.6).

Since, as observed for native artery mesenterica, an elongation of approximately 80% is needed for tissue engineering, crosslinking with EDC/NHS in presence of J230 can be considered the optimal crosslinking method among the analysed ones.

Table 3.5. *Mechanical properties of freeze-dried collagen/elastin scaffolds frozen at -80 and -18 °C and having three different collagen to elastin ratios. Analyses have been performed at 37 °C, after swelling the samples in PBS for 30 min ($n = 3 \pm s.d.$).*

Freezing T (°C)	Collagen to elastin ratio	E-Modulus (MPa)	Yield stress (MPa)	Yield strain (%)
- 80**	9:1	0.42 ± 0.1	0.067 ± 0.006	125
	1:1	0.24 ± 0.06	0.063 ± 0.02	140
	1:9	-*	-*	150
- 18	9:1	5.3 ± 0.3	0.20 ± 0.01	60 ± 20
	1:1	3.5 ± 0.1	0.3 ± 0.01	108 ± 14
	1:9	2.0 ± 0.1	0.050 ± 0.001	130 ± 10

* Not determined

** Data from reference [40]

Table 3.6. Mechanical properties of freeze-dried collagen/elastin (weight ratio 1:1) scaffolds frozen at -18°C and crosslinked in three different ways using ethanol/water (40% v/v) as solvent. Analyses have been performed at 37°C , after swelling the samples in PBS for 30 min ($n = 3 \pm \text{s.d.}$).

Crosslinking method	E-Modulus (MPa)	Yield stress (MPa)	Yield strain (%)
EDC/NHS	8.0 ± 0.2	0.26 ± 0.08	35 ± 20
J230/EDC/NHS	8.3 ± 0.1	0.22 ± 0.08	60 ± 15
BDGE-EDC/NHS	2.0 ± 0.5	0.06 ± 0.02	15 ± 5

Preliminary cell culturing experiments performed with native, EDC/NHS and J230/EDC/NHS crosslinked scaffolds having porosity of 90% and pore sizes in the range of 30 to 60 μm (Table 3.2), showed that the cells were still viable after 14 d of culturing. Filtration seeding favoured the growth of SMC not only on the surface of the scaffolds but also inside the freeze-dried (crosslinked) porous collagen/elastin matrices. Native or EDC/NHS crosslinked collagen/elastin scaffolds contained approximately $1.5 \cdot 10^6$ cells, while $9 \cdot 10^5$ cells were found on J230/EDC crosslinked specimens. Moreover, a low density of cells was observed inside the J230/EDC/NHS crosslinked scaffolds, whereas cells proliferated inside native and EDC/NHS crosslinked matrices (Fig 3.5a-d). This may be an indication that the density of cells present in these matrices is dependent on the size of the pores. Collagen/elastin scaffolds crosslinked in the presence of a diamine spacer have the smallest size of pores ($30 \pm 20 \mu\text{m}$). However, also the chemical nature of J230 or the presence of dangling group as a consequence of crosslinking with J230/EDC/NHS may have altered the ability of SMC to adhere to and migrate in these particular scaffolds. Further investigations are currently being performed.

Conclusions.

Homogeneous porous scaffolds of insoluble collagen and elastin, having an average pore size larger than 100 μm and porosities ranging from 90 to 98 %, were prepared by means of freeze drying. The aggregation and assembly of these two proteins in the scaffolds ensured an

improvement in terms of mechanical properties compared to collagen scaffolds, affording

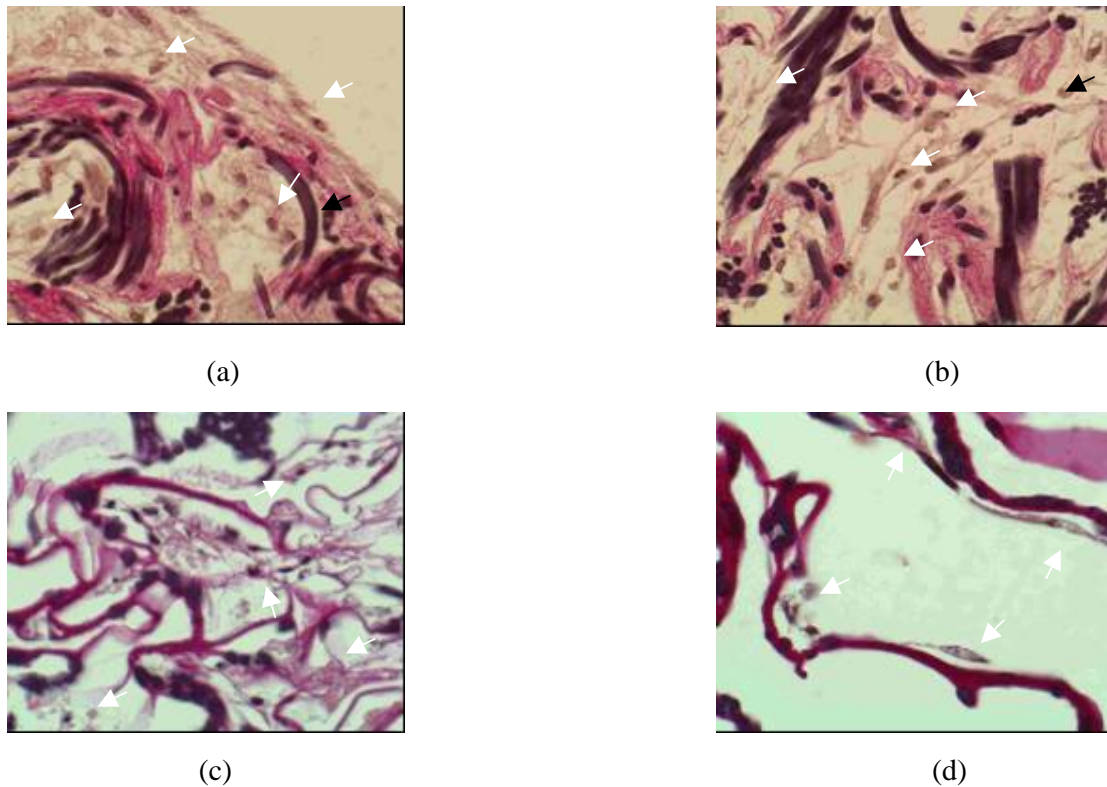


Figure 3.5. *Histological cross sections of freeze-dried (crosslinked in ethanol (40 %v/v)) samples of collagen/elastin cultured with SMC for 14 days. SMC are indicated by an arrow. SMC on top and inside an uncrosslinked scaffold (a); SMC inside the three-dimensional matrices of uncrosslinked (b), EDC/NHS (c) or J230/EDC/NHS (d) crosslinked scaffolds. Magnification is 50X in all the pictures.*

materials having a higher elongation at yield and a higher degree of total strain recovery. In particular, a weight ratio of collagen to elastin 1:1 afforded scaffolds having suitable mechanical properties for *in vitro* SMC culture and subsequent implantation. Freeze-dried scaffolds crosslinked with different methods improved their resistance to mechanical stimuli. Ethanol/water (40% v/v) was chosen as preferred crosslinking solvent in order to preserve porosity after crosslinking. Crosslinking with EDC/NHS or EDC/NHS in the presence of J230 resulted in matrices with suitable mechanical properties, applicable for the tissue engineering of blood vessels. Preparation of (crosslinked) collagen/elastin constructs seeded with SMC and cultured for 14 d has been achieved. Preliminary experiments have resulted in (crosslinked)

scaffolds with SMC not only on the surface but also inside the three-dimensional (crosslinked) matrices. In particular, this was observed especially in scaffolds crosslinked with EDC/NHS, whereas the introduction of a Jeffamine spacer caused a reduction in the density of cells observed inside the constructs.

Use of porous tubular scaffolds prepared in analogous way is currently under investigation for tissue engineering of small-diameter blood vessels.

References

1. Ratcliffe, A. and Niklason, L.E., in *Reparative Medicine: Growing Tissues and Organs*, 210, New York Acad. Sci., New York, 2002
2. Schmidt, C.E. and Baier, J.M., *Acellular vascular tissues: natural biomaterials for tissue repair and tissue engineering*. *Biomaterials*, 21, 2215, 2000
3. Berry, S., Honey I've shrunk biomedical technology! *Trends Biotechnol.*, 20, (1), 3, 2002
4. Griffith, L.G. and Naughton, G., *Tissue engineering - Current challenges and expanding opportunities*. *Science*, 295, 1009, 2002
5. Rabkin, E. and Schoen, F.J., *Cardiovascular tissue engineering*. *Cardiovasc. Pathol.* 11, (6), 305, 2002
6. Hutmacher, D., *Scaffold design and fabrication technologies for engineering tissues-state of the art and future perspectives*. *J. Biomat. Sci. Polymer Ed.*, 12, (1), 107, 2001
7. Hoerstrup, S.P., Zund, G., Sodian, R., Schnell, A.M., Grunenfelder, J., and Turina, M., *Tissue engineering of small caliber vascular grafts*. *E. J. Cardio-Thorac. Surg.* 20, (1), 164, 2001
8. Weinberg, C.B. and Bell, E., *A blood vessel model constructed from collagen and cultured vascular cells*. *Science*, 231, 397, 1986
9. Seifalian, A.M., Salacinski, H.J., Tiwari, A., Edwards, A., Bowald, S., and Hamilton, G., *In vivo biostability of a poly(carbonate-urea)urethane graft*. *Biomaterials*, 24, (14), 2549, 2003
10. Niklason, L.E., Gao, J., Abbott, W.M., Hirschi, K.K., Houser, S., Marini, R., and Langer, R., *Functional arteries grown in vitro*. *Science*, 284, (5413), 489, 1999
11. Bader, A., Steinhoff, G., and Strobl, K., *Engineering of human vascular aortic tissue based on a xenogenic starter matrix*. *Transplant.*, 70, (1), 7, 2000

12. L'Heureux, N., A completely biological tissue-engineered human blood vessel. *Faseb J.*, 12, (1), 47, 1998
13. Campbell, J.H., Efendy, J.L., and Campbell, G.R., Novel vascular graft grown within recipient's own peritoneal cavity. *Circ. Res.*, 85, (12), 1173, 1999
14. Berglund, J.D., Mohseni, M.M., Nerem, R.M., and Sambanis, A., A biological hybrid model for collagen-based tissue engineered vascular constructs. *Biomaterials*, 24, (7), 1241, 2003
15. Shin'oka, T., Imai, Y., and Ikada, Y., Transplantation of a tissue-engineered pulmonary artery. *N. Engl. J. Med.*, 344, (7), 532, 2001
16. Fung, Y.C., Mechanical properties and remodeling of blood vessels, in Fung, *Biomechanics. Mechanical Properties of Living Tissues*, Springer Ed., 1999.
17. Ogle, B.M. and Mooradian, D.L., The role of vascular smooth muscle cell integrins in the compaction and mechanical strengthening of a tissue-engineered blood vessel. *Tissue Eng.*, 5, (4), 387, 1999
18. Goissis, G., Suzigan, S., Parreira, D.R., Maniglia, J.V., Braile, D.M., and Raymundo, S., Preparation and characterization of collagen-elastin matrices from blood vessels intended as small diameter vascular grafts. *Artif. Organs*, 24, (3), 217, 2000
19. Lefebvre, F., Gorecki, S., Bareille, R., Amedee, J., Bordenave, L., and Rabaud, New artificial connective matrix-like structure made of elastin solubilized peptides and collagens: elaboration, biochemical and structural properties. *Biomaterials*, 13, (1), 28, 1992
20. Takahashi, K., Nakata, Y., Someya, K., and Hattori, M., Improvement of the physical properties of pepsin-solubilized elastin-collagen film by crosslinking. *Biosci. Biotechnol. Biochem.*, 63, (12), 2144, 1999
21. Nimni, M.E., *Encyclopedia handbook of biomaterials and bioengineering materials*, (Deheler, M.), 1229, New York, 1995
22. Sandberg, L.B., Soskel, N.T., and Leslie, J.G., Elastin structure, biosynthesis, and relation to disease states. *N. Engl. J. Med.*, 304, (10), 566, 1981
23. Faury, G., Function-structure relationship of elastic arteries in evolution: from microfibrils to elastin and elastic fibres. *Pathol. Biol.*, 49, (4), 310, 2001
24. Debelle, L. and Tamburro, A.M., Elastin: molecular description and function. *Int. J. Biochem. Cell Biol.*, 31, (2), 261, 1999
25. Pasquali-Ronchetti, I., Fornieri, C., Baccarani-Contri, M., and Quaglino, D., Ultrastructure of elastin. *Ciba Found. Symp.*, 192, 31, 1995

26. Li, D.Y., Brooke, B., Davis, E.C., Mecham, R.P., Sorensen, L.K., Boak, B.B., Eichwald, E., and Keating, M.T., Elastin is an essential determinant of arterial morphogenesis. *Nature*, 393, (6682), 276, 1998
27. Pieper, J.S., Oosterhof, A., Dijkstra, P.J., Veerkamp, J.H., and van Kuppevelt, T.H., Preparation and characterization of porous crosslinked collagenous matrices containing bioavailable chondroitin sulphate. *Biomaterials*, 20, (9), 847, 1999
28. Daamen, W.F., Hafmans, T., Veerkamp, J.H., and van Kuppevelt, Comparison of five procedures for the purification of insoluble elastin. *Biomaterials*, 22, (14), 1997, 2001
29. Lendlein, A., Schmidt, A.M., and Langer, R., AB-polymer networks based on oligo(epsilon-caprolactone) segments showing shape-memory properties. *Proc. Natl. Acad. Sci. USA*, 98, (3), 842, 2001
30. Buijtenhuijs, P., Buttafoco, L., Daamen, W.F., vanKuppevelt, T.H., Poot, A.A., Dijkstra, P.J., deVos, R.A.I., Sterk, L.M.T., Geelkerken, R.H., Feijen. J., and Vermes.I., Tissue engineering of blood vessels: characterisation of smooth muscle cells for culturing on collagen and elastin based scaffolds. *Biotechnol. Appl. Biochem.*, 9, (2), 141, 2004
31. Schoof, H., Apel, J., Heschel, I., and Rau, G., Control of pore structure and size in freeze-dried collagen sponges. *J. Biomed. Mat. Res.*, 58, (4), 352, 2001
32. Kang, H.W., Tabata, Y., and Ikada, Y., Fabrication of porous gelatin scaffolds for tissue engineering. *Biomaterials*, 20, (14), 1339, 1999
33. Yannas, I.V., Tissue regeneration templates based on collagen-glycosaminoglycan copolymers. *Adv. Pol. Sci.*, 122, (26), 219, 1995
34. Simpson, D.G., Bowlin, G.L., Wnek, G.E., Stevens, P.J., Carr, M.E., Matthews, J.A., and Rajendram, S., Electroprocessed collagen, in US patent & Trademark Office. 2001, 20020090725, US, 39.
35. Dijkstra, P.J., Olde Damink, L., and Feijen. J., Chemical stabilization of collagen based biomaterials. *Cardiovasc. Pathol.*, 5, (5), 295, 1993
36. Zhang, R. and Ma, P.X., Poly(alpha-hydroxyl acids)/hydroxyapatite porous composites for bone-tissue engineering. I. Preparation and morphology. *J. Biomed. Mat. Res.*, 44, 446, 1999
37. Matsuda, K., Suzuki, S., Isshiki, N., and Ikada, Y., Re-freeze dried bilayer artificial skin. *Biomaterials*, 14, (13), 1030, 1993
38. Banda, M.J., Werb, Z., and McKerrow, Elastin degradation. *Methods Enzymol.*, 144, 288, 1987

39. Zeeman, R., Dijkstra, P.J., van Wachem, P.B., van Luyn, M.J.A., Hendriks, M., Cahalan, P.T., and Feijen, J., Successive epoxy and carbodiimide cross-linking of dermal sheep collagen. *Biomaterials*, 20, (10), 921, 1999
40. Daamen, W.F., van Moerkerk, H.T.B., Hafmans, T., Buttafoco, L., Poot, A.A., Veerkamp, J.H., and van Kuppevelt, T.H., Preparation and evaluation of molecularly-defined collagen-elastin-glycosaminoglycan scaffolds for tissue engineering. *Biomaterials*, 24, (22), 4001, 2003
41. Ozolanta, I., Teter, G., Purinya, B., and Kasyanov, V., Changes in the mechanical properties, biochemical contents and wall structure of the human coronary arteries with age and sex. *Med. Eng. Phys.*, 20, (7), 523, 1998

Chapter 4

Electrospinning of Collagen and Elastin for Tissue Engineering Applications*.

*We will either find a way or make one
(Hannibal)*

Abstract.

Meshes of collagen, elastin or collagen and elastin were successfully prepared by means of electrospinning aqueous solutions of these proteins. The morphology of the obtained fibres was dependent on the flow rate, the applied electric field, the collecting distance and the composition of the starting solutions. In all cases the addition of PEO ($M_w = 8 \cdot 10^6$) and NaCl was necessary to spin continuous and homogeneous fibres. Collagen and elastin could be electrospun separately or in a mixture. In this latter case, fibres in which the single components could not be distinguished by SEM were obtained. Increasing the elastin content resulted in fibres having diameters increasing from 220 to 600 nm. In all cases, a flow rate of the solution between 30 and 69 $\mu\text{l}/\text{min}$ and a distance between the needle tip and the collecting plate of 20 to 30 cm proved to be ideal for the collection of dry fibres. The voltage necessary to obtain a continuous production of fibres was dependent on the composition of the starting solution, but always between 10 and 25 kV. Under these conditions, non-woven meshes could be formed and a certain degree of orientation of the fibres constituting the mesh was obtained by using a rotating tubular mandrel as collector. Collagen/elastin (1:1) meshes were stabilized by crosslinking in ethanol/water (70% v/v) with N-(3-dimethylaminopropyl)-N'-ethylcarbodiimide

* Buttafoco L.¹, Kolkman N.G.¹, Engbers-Buijtenhuijs P.^{1,2}, Poot A.A.¹, Dijkstra P.J.¹, Vermes I.^{1,2}, Feijen J.¹

Submitted to Biomaterials

¹ Department of Polymer Chemistry and Biomaterials, Faculty of Science and Technology and Institute of Biomedical Technology (BMTI), University of Twente, Enschede, P.O. Box 217, 7500 AE, The Netherlands,

² Department of Clinical Chemistry, Medical Spectrum Twente Hospital, Enschede, P.O.Box 50000, 7500 KA, The Netherlands.

hydrochloride (EDC) and N-hydroxysuccinimide (NHS). This treatment afforded materials with a high thermal stability ($T_d = 79\text{ }^\circ\text{C}$) and did not alter their original morphology. Moreover, upon crosslinking PEO and NaCl were fully leached out. Smooth muscle cells were cultured on electrospun crosslinked scaffolds for 14 d and formed a confluent layer of cells on top of the meshes.

Introduction.

Polymer fibres having diameters ranging from a few nanometers up to some microns can be successfully used in a wide variety of applications, like reinforcements in nanocomposites [1], nanowires and nanotubes [2] and tissue engineering [3-5]. In particular, fibres can be useful in vascular tissue engineering, since an artery can be regarded as a fibre-reinforced structure composed of a protein fibre network and cells, which determine the particular mechanical properties of that vessel [6].

In a native blood vessel, the two most abundant proteins are collagen and elastin. Together with smooth muscle cells (SMC), they confer to its wall strength, elasticity and ability to retain its shape. In particular, SMC ensure the maintenance of the vascular tone due to their capability to contract and relax [7], collagen is responsible for the resistance to rupture [8], whereas elastin confers the necessary elasticity. This combination prevents irreversible deformation of the vessels due to the pulsatile blood flow [9]. In a previous study, it was shown that porous scaffolds can be prepared from insoluble collagen and insoluble elastin as matrices for tissue engineering of blood vessels [10]. Such scaffolds were prepared by freezing collagen and elastin suspensions at $-18\text{ }^\circ\text{C}$ and successive freeze drying. Matrices having a porosity of approximately 90% were thus obtained and subsequently crosslinked.

Electrospinning of soluble collagen and soluble elastin is a suitable method to prepare scaffolds with high porosity and surface area for tissue engineering of small-diameter blood vessels. Electrospinning, a suitable technique for the production of small-diameter fibres, has been developed in the first half of the 20th century [11], but only recently Reneker and coworkers have investigated the process in more detail [12, 13], demonstrating its versatility. Briefly, in electrospinning, a polymer solution is fed through a thin needle opposite to a collecting plate or target. When a high voltage is applied to the solution, a jet is formed as soon as the applied electric field strength overcomes the surface tension of the solution. When travelling towards the grounded collecting plate, the jet becomes thinner as a consequence of solvent evaporation and fibres are formed. Splaying of the fibres because of splitting of the jet, can occur as well.

The fibres are deposited on the grounded target as a non-woven highly porous mesh [14]. Placing a rotating collector between the needle and the grounded plate allows deposition of the fibres on the collector with a certain degree of alignment [5, 15]. The possibility to produce meshes with a high surface area makes electrospinning an ideal solution for applications which require seeding of cells, like vascular tissue engineering [16]. Moreover, the architecture of the produced non-woven meshes is similar to that found in most natural extra-cellular matrices thus enhancing the applicability of these scaffolds [5].

Up to now, electrospinning of collagen type I from weak acid aqueous solutions has been described. Though fibres could not be spun from 1-2% wt collagen solutions, fibre formation was accomplished by adding high molecular weight PEO (900 kDa), which increases the viscosity of the solution, thus leading to stable jets. Uniform fibres were produced by adding sodium chloride to the starting solution. However, crystals of NaCl were observed at the surface of the fibres at high salt concentrations. Optimal conditions were achieved when a 2% wt collagen-PEO (1:1 weight ratio) solution containing 34 mM NaCl was spun at 18 kV. Fibres having an average diameter of 100-150 nm were obtained at these conditions [17].

Although electrospinning of native elastin fibres has not been documented, aqueous solutions of elastin-mimetic peptide polymers have been spun from an 81 kDa recombinant protein, based upon the repeating elastomeric peptide sequence of elastin (Val-Pro-Gly-Val-Gly)₄(Val-Pro-Gly-Lys-Gly) obtained using genetic engineering and microbial protein expression [18]. Fibres having a diameter of 400-450 nm were produced from aqueous solutions without any additives. The concentration of the solutions largely influenced the morphology of the obtained fibres. Beaded fibres, thin filaments or fibres with a ribbon-like appearance were produced at concentrations of 5 and 20%, respectively. Only at concentrations between 10 and 15% w/v predominantly long and uniform fibres were obtained. Recently, electrospinning of tubular scaffolds of soluble collagen type I, type III or soluble elastin from solutions of 1,1,1,3,3,3 hexafluoro-2-propanol (HFP) has been documented [19]. Collagen type I fibres with a diameter of 0.1-4.6 μm and the typical 7 nm banded appearance were obtained from solutions with a protein concentration of 3-10% w/v. Spinning collagen type III solutions at a concentration of 8.3% w/v yielded fibres with diameters of 250 ± 150 nm. Concentrations of 20-30% w/v of elastin in HFP were required to produce elastin fibres. These had diameters of 1.1 ± 0.7 μm . Non-woven fibrous meshes were spun also from HFP solutions containing 40% collagen type I, 40% collagen type III and 20% elastin (total protein concentration = 0.083 g/ml). The collagen and elastin could not be distinguished by atomic force microscopy. It was thus concluded that the actual composition of each fibre is

an even distribution of the two proteins in the original blend. The obtained scaffolds were then crosslinked by exposure to glutaraldehyde vapours, after which preliminary cell culture experiments were performed. Culturing of smooth muscle cells followed by endothelial cells culture in a rotating cell culture system yielded constructs characterized by complete infiltration, with SMC and an intima consisting of endothelial cells.

In the present study, soluble collagen type I from calf skin and soluble elastin from bovine neck ligament were electrospun from aqueous acidic solutions, thus avoiding the use of organic solvents. The influence of solution viscosity, surface tension and ratio of the two components on the morphology of the resulting fibres was investigated. Produced scaffolds were stabilized by means of crosslinking. This process was essential to obtain a suitable substrate for tissue engineering applications. Up to now, only glutaraldehyde has been investigated as crosslinker of electrospun collagen-based structures [19]. However, it is known that glutaraldehyde treated materials are cytotoxic [20]. As an alternative, in this study, N-(3-dimethylaminopropyl)-N'-ethylcarbodiimide hydrochloride (EDC), in the presence of N-hydroxysuccinimide (NHS), was used as crosslinker [21]. Smooth muscle cells were seeded on the crosslinked scaffolds and the resulting constructs were analysed by means of histology.

Materials and Methods

All chemicals and materials were purchased from Sigma & Aldrich (Zwijndrecht, The Netherlands) unless stated otherwise.

Preparation of protein solutions.

Solutions of collagen type I from calf skin (Elastin Products Company Inc., USA) and/or elastin from bovine neck ligament (Elastin Products Company Inc., USA) were prepared by dissolving the proteins for 5-6 h in 10 mM hydrochloric acid, at room temperature. The concentration of collagen, elastin or a mixture of collagen and elastin in the solutions was varied from 1 to 5% w/v. The weight ratio of collagen and elastin in the mixed solutions was either 3:1, 2:1, 1:1, 1:2 or 1:3. To all solutions high molecular weight poly(ethylene oxide) (PEO, $M_w = 8 \cdot 10^6$) at a concentration of 5 g/100 ml and sodium chloride to a final concentration of 42.5 mM were added.

Surface tension.

The surface tension of the mixed collagen and elastin solutions having a weight ratio of the two components equal to 3:1, 2:1, 1:1, 1:2 or 1:3 and total protein concentrations of 3 or 4% w/v was measured with the Wilhelmy plate method using a Krüss Tensiometer K12 (Krüss, Germany). Briefly, a platinum plate was immersed in the solution and then pulled up at a constant speed. The force needed to pull the plate out of the solution was measured for 1 min and then converted to a surface tension value [22]. All measurements were performed at 25 ± 1 °C. The platinum plate was cleaned with water, ethanol and finally with a flame before each measurement.

Viscosity.

The viscosity of protein solutions (5% w/v) containing collagen and elastin in a weight ratio of 3:1, 2:1, 1:2 or 1:3 was measured by means of rheology (US200 Rheometer, Messtechnik, Ostfildern, Germany). All solutions also contained PEO ($M_w = 8 \cdot 10^6$) at a concentration of 5 g/100 ml. A 1° cone/plate system having a diameter of 50 mm was used. The viscosity (η) was measured at shear rates varying from 0.05 to 100 s^{-1} . All measurements were performed at 25 ± 1 °C.

Electrospinning.

A 50 ml syringe (Perfusor-Spritze OPS, B-Braun, Melsungen, Switzerland) was filled with the protein/PEO solution and connected to a syringe pump (Perfusor E Secura, B-Braun, Melsungen, Switzerland) in a horizontal mount. The solution was pushed through a silicon tube (Nalgene 50; 1.6 mm ID x 3.1 mm OD, New York, USA) into a capillary blunt steel needle (21G 1½; 0.8 mm ID x 40 mm length) at a constant speed (between 30 and 69 $\mu\text{l}/\text{min}$). The steel needle was connected to an electrode of a high voltage supply (Bertan Associates Inc., 230-30 R). A steel ring with the same charge was placed at the same height and perpendicular to the needle tip, to stabilize the jet and direct it downwards. A grounded aluminium plate (6 x 6 cm) was placed at 20-30 cm distance from the needle tip to collect the fibres. Fibres were also collected on a rotating silicone tube (3.1 mm outer diameter x 6 cm length) placed between the grounded aluminium plate and the needle tip (Fig. 4.1). The collecting time of the fibres was varied between 30 and 240 min.

The electric potential necessary to start the spinning process (V_{start}) and thus to form a jet, was determined for all prepared solutions at a flow rate of 30 $\mu\text{l}/\text{min}$. Experiments were performed

by slowly increasing the applied potential until the cone formed and the jet was initiated from its apex. Similarly, the value of the potential at which the jet ceases (V_{stop}) was determined by forming the jet and slowly decreasing the potential until the jet ceased.

Crosslinking of the electrospun fibres.

Electrospun fibres were crosslinked using a mixture of N-(3-dimethylaminopropyl)-N'-ethylcarbodiimide hydrochloride (EDC) and N-hydroxysuccinimide (NHS) [23]. Electrospun samples (4 x 4 cm) were incubated for 30 min in a 2-morpholinoethane sulfonic acid (MES) buffer in ethanol/water (70% v/v) (0.05 M, pH 5.5) (215 ml per gram of sample).

Crosslinking was carried out in the same buffer containing EDC (2.3 g/g of sample) and NHS (0.56 g/g of protein) (molar ratio of EDC/NHS = 2.5) under the same conditions. The reaction was performed for 2 h at room temperature. After removal of the crosslinking solution, samples were incubated for 2 h in sodium phosphate (0.1 M, pH = 7.4). A further washing step was performed with ethanol/water (70% v/v). The total incubation time was 2 h, during which the ethanol/water mixture was changed every 30 min. The crosslinked matrices were frozen at $-35\text{ }^{\circ}\text{C}$ and subsequently freeze-dried for 24 h.

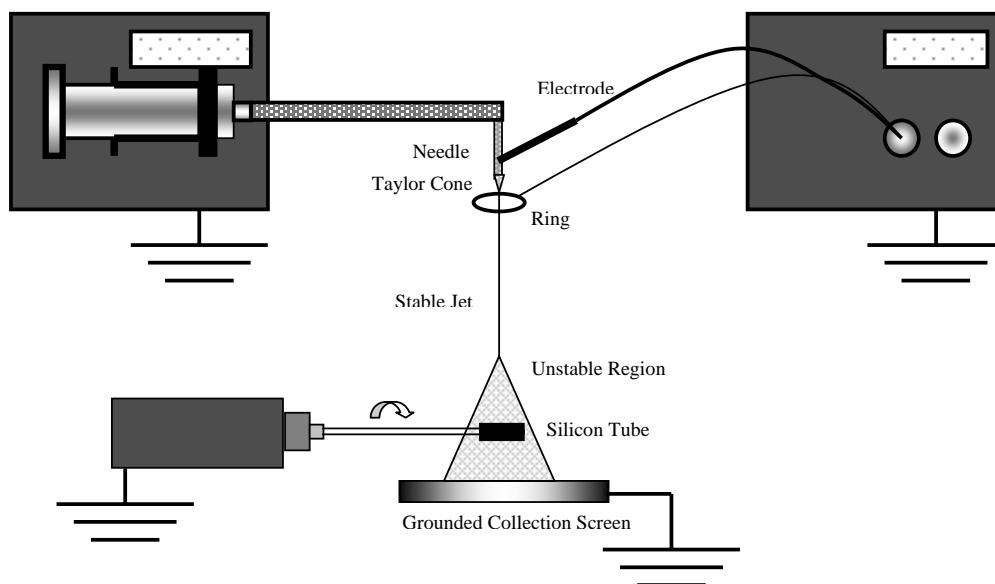


Figure 4.1. *Experimental set up of the electrospinning system.*

Differential scanning calorimetry.

Thermal properties of the electrospun (crosslinked) fibres were determined by means of differential scanning calorimetry (DSC) (DSC 7, Perkin Elmer, Norwalk, CT, USA). Samples of 5-10 mg were placed in high-pressure pans and heated from 25 °C to 180 °C at 25 °C/min.

The same analysis was performed on 5-10 mg samples swollen in 50 µl of PBS (pH = 7.4) overnight and heated from 25 to 90 °C at 25 °C/min. A sample containing 50 µl of PBS (pH = 7.4) was used as a reference.

The onset of the endothermic peak was recorded as the denaturation temperature of collagen or as the melting temperature of crystalline PEO, respectively.

Morphology.

Freeze-dried samples were sputter coated with gold in a Polaron E5600 sputter coater prior to analysis. Images were recorded with SEM (Leo Gemini 1550 FEG-SEM) at different acceleration voltages (0.5-4 kV). The diameter distribution of the electrospun fibre was determined by measuring at least 20 fibres at a random.

Determination of primary amino groups.

The concentration of free primary amine groups present in (crosslinked) non-woven meshes of collagen/elastin was determined using 2,4,6-trinitrobenzenesulfonic acid (TNBS) according to the following procedure.

Samples of approximately 5 mg were incubated for 30 min in an aqueous solution of NaHCO₃ (1 ml, 4% w/v). Then, the mixture was incubated at 40 °C for 2 h in a solution of TNBS (1 ml, 0.5% w/v) in 4% w/v NaHCO₃. After the addition of HCl (3 ml, 6 M) samples were hydrolysed at 60 °C for 90 min. The reaction mixture was diluted with demineralised MilliQ water (5 ml), cooled to room temperature and the absorbance at 420 nm was measured using a Varian Cary 300 Bio spectrophotometer. A blank was prepared using the same procedure, except that HCl was added prior to the TNBS solution. The absorbance was correlated to the concentration of free amino groups using a calibration curve obtained with glycine (stock solution: glycine (10 mg) in an aqueous NaHCO₃ solution (100 ml, 4% w/v)).

Smooth muscle cell seeding and histology.

Smooth muscle cells were isolated from umbilical veins by a collagenase digestion method as previously described [24]. Sub-confluent cultures of SMC were harvested by trypsinisation

(2 min, 0.125% trypsin/0.05% EDTA), centrifuged at 300 g for 10 min at 21 °C and resuspended in culture medium (Dulbecco's Modified Eagle's Medium containing 10% v/v human serum, 10% v/v foetal bovine serum, 50 U/ml penicillin and 50 µg/ml streptomycin). Cells were counted with a Bürker hemacytometer and seeded on top of the sterilised scaffolds with a final density of 200.000 cells/cm². Scaffolds having a diameter of 6 mm, were sterilised with ethanol/water (70% v/v), washed 3 times with PBS, placed in a 96 wells TCPS culture dishes and secured with Viton O-rings (Eriks, Alkmaar, The Netherlands). Cells were subsequently cultured for 14 d in culture medium under static conditions in an incubator at 37 °C, in a humidified atmosphere containing 5% CO₂. The culture medium was refreshed every 2-3 d. After culturing, the resulting constructs were fixed with formalin, impregnated with paraffin, cut into transverse sections and stained using the Elastic von Giesson (EG) method at the Laboratory of Pathology Oost Nederland according to standard procedures. In particular, collagen stains pink, elastin black and the nuclei of cells brown.

Results and discussion.

In the electrospinning process, the protein solution is fed through a steel needle connected to a high voltage power supply. Under the influence of the high electric field, a droplet of the protein solution at the capillary tip is deformed into a conical shape, the Taylor cone. In the droplet the mutual charge repulsion causes a repulsive force, which opposes the surface tension. Above a critical value of electric field strength, the repulsive force exceeds the surface tension and a charged jet is produced [25]. The jet is directed to a grounded plate and during its travel in air the simultaneous effects of stretching the fibre and evaporation of solvent cause the fibre diameter to decrease and the fibre to dry. The morphology of the fibres, collected at the plate as a non-woven mesh, is influenced by several parameters, like the solvent used, the strength of the electric field applied, the flow rate and the collecting distance [25, 26]. In general, volatile solvents like chloroform or 1,1,1,3,3,3-hexafluoro-2-propanol (HFP) are quite suitable for electrospinning polymeric fibres [5, 19, 27], but solvents with a high boiling point, like N,N-dimethylformamide, can be used as well [28]. In the electrospinning of protein solutions to prepare meshes to be used as scaffolds for tissue engineering applications, water is the preferred solvent. In this way, residual amounts of organic solvents associated with the fibres can be avoided and possible problems related to the interaction between the organic solvent and seeded cells can be prevented [17, 18].

Preliminary experiments revealed that, independent of the conditions used, continuous fibres could not be spun from acidic aqueous solutions of pure collagen. It is known that by addition of sodium chloride to the solution, formation of fibres by electrospinning becomes possible due to the increase in solution conductivity [17]. Moreover, the presence of NaCl can induce hydrophobic interactions in or between the protein molecules and thus contribute to the production of continuous fibres [29]. The higher net charge increases the force exerted on the jet [30] and at a concentration of 42.5 mM NaCl and spinning voltages between 10 and 25 kV, fibre formation was observed. However, continuous jets could not be produced and only short beaded fibres were obtained. This latter phenomenon is known to be favoured by the presence of a high electric field, which leads to capillary breakup of the electrospinning jet [31].

Increasing the viscosity of the spinning solution is a way to overcome the formation of beads [32] and a suitable polymer for this purpose is poly(ethylene oxide) (PEO). Addition of this polymer with M_w of $8 \cdot 10^6$ to the protein solution, which also contained 42.5 mM NaCl, allowed a much better control over fibre formation. The voltages necessary to obtain a continuous fibre were dependent on the weight ratio of collagen to PEO. Collagen solutions (2% w/v) containing 42.5 mM sodium chloride, having a collagen to PEO weight ratio of 1:2 and spun at 21 kV, afforded the formation of a continuous jet. However, the collected fibres were not completely dry and resulted in meshes of highly fused fibres. Increasing the weight ratio between collagen and PEO to 1:1 or 3:1 required higher potentials of 22 and 23.5 kV, respectively. However, at a collagen to PEO weight ratio of 3:1 beaded and highly fused fibres were obtained. Obviously, under these conditions the water evaporation from the fibres was not complete. Dry fibres entirely devoid of beads and with a narrow diameter distribution (average fibre diameter = $0.40 \pm 0.05 \mu\text{m}$) were produced at a weight ratio of collagen to PEO equal to 1:1. In all cases, sodium chloride crystals were present at the surface of the electrospun fibres (Fig. 4.2a).

Although full concentration ranges were not investigated in detail, a concentration of 5% w/v of PEO, 2% w/v of collagen, a weight ratio of collagen to PEO of 1:1 and a concentration of 42.5 mM of sodium chloride enabled successful spinning of collagen fibres. The processing parameters were further optimised and, with the described set up (inner diameter of the capillary tip = 0.8 mm), a flow rate of 69 $\mu\text{l}/\text{min}$ appeared optimal. SEM analyses of the non-woven meshes revealed the presence of the D-period, characteristic of the native collagen fibril structure [8], thus showing that electrospinning does not alter the natural

tendency of collagen to organize itself through fibrillogenesis into a fibrillar structure* (Fig. 4.2b).

In tissue engineering of blood vessels, collagen constructs have a limited applicability due to lack of structural integrity when subjected to intraluminal physiological pressure [33, 34]. Elastin is known to confer compliance to a blood vessel [35, 36] and recently we have shown that dense films composed of insoluble elastin and insoluble collagen (weight ratio 1:1) have a much higher degree of strain recovery than dense collagen films [10].

Preliminary experiments were performed to produce fibres from soluble elastin isolated from bovine neck ligament. As with collagen solutions, addition of NaCl at a concentration of 42.5 mM and PEO ($M_w = 8 \cdot 10^6$) at a concentration of 1% w/v were necessary to obtain a continuous jet. At elastin concentrations of 5% wt and ratios of elastin to PEO equal to 5:1, it was possible to spin fibres at a voltage of 10kV and a flow rate of 50 $\mu\text{l}/\text{min}$. These fibres had an average thickness of 0.5 μm , comparable to the thickness of fibres spun from elastin synthetic mimetic peptides [18]. The fibres have a rough surface and appear to be composed of 5-10 nm wide filaments, oriented parallel to their longitudinal axis (Fig. 4.3a,b), similarly to native elastin fibres [18]. As with collagen, the elastin molecules appear to preserve the ability to self organize into the native structure during fibre formation in the electrospinning process.

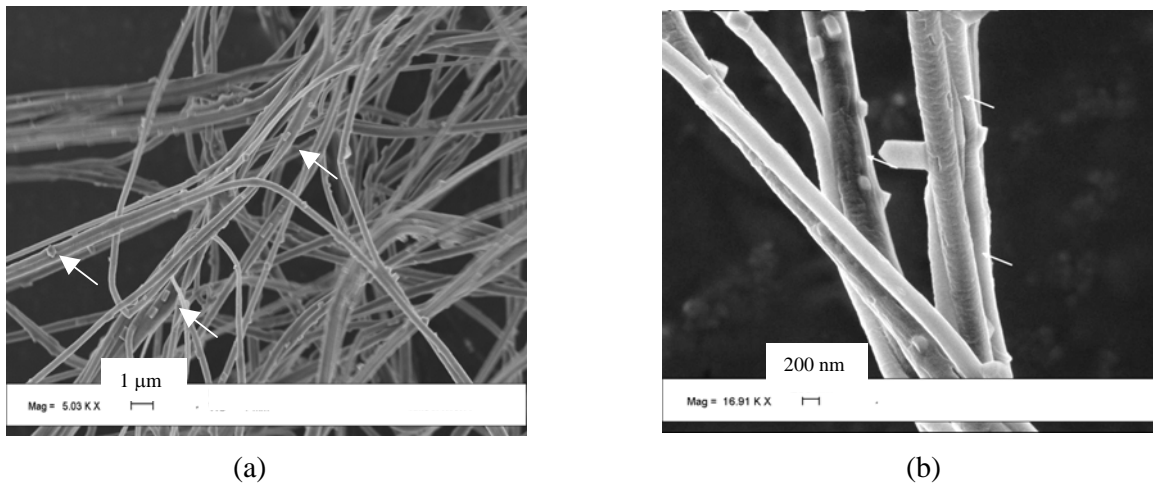


Figure 4.2. SEM images of collagen/PEO fibres. Collagen concentration is 2% w/v, collagen:PEO weight ratio is 1:1. Fibres have been spun at 22 kV, with a flow rate of 69 $\mu\text{l}/\text{min}$ and a collecting distance of 25 cm. Spun solutions contain 42.5 mM NaCl (indicated by arrows). (a) The narrow distribution of diameters of the fibres is visible. Scale bar is 1 μm ; (b) the D-period visible in the fibres is indicated by arrows. Scale bar is 200 nm.

* The diameter of the electrospun collagen fibres is comparable with that of a native collagen fibril.

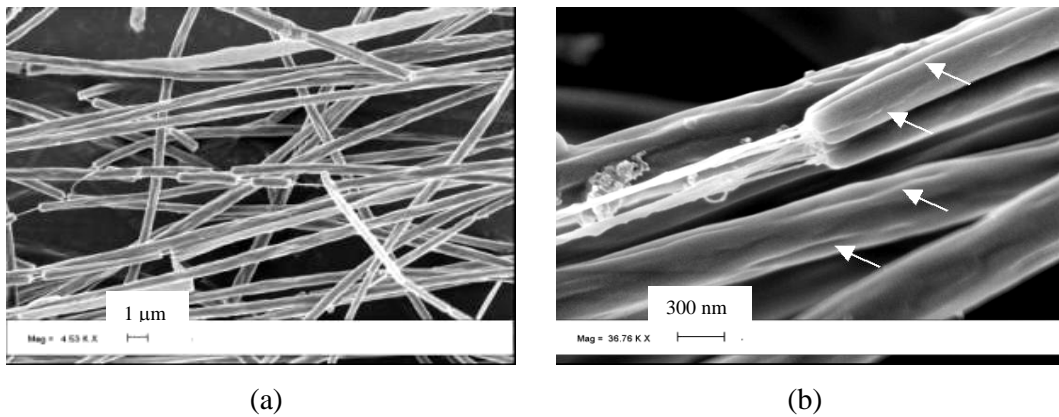


Figure 4.3. SEM image of (a) elastin/PEO fibre. Scale bar is 1 µm; (b) detail of elastin/PEO fibres. Scale bar is 300 nm. Elastin concentration is 5% w/v and elastin:PEO weight ratio is 5:1. Spun solutions contain 42.5 mM NaCl. Fibres have been spun at 10 kV, with a flow rate of 50 µl/min. Collecting distance is 25 cm. Filament-like folds are indicated by arrows.

The elastin/PEO fibres were easily produced, but difficult to collect because of substantial splaying. Splaying occurs when the radial forces derived from the electrical charges carried by the jet, overcome the cohesive forces in the jet itself. The single jet divides into many charged jets before reaching the collecting plate. Splaying thus yields unusual small diameter fibres [37].

In the arterial wall, collagen and elastin are both present and constitute together with the extracellular matrix and the cells, a fibre-reinforced composite structure of which the mechanical properties are mainly determined by the fibrous network. The presence of both proteins is necessary to confer the vessel its strength but also its elasticity [38].

Aqueous solutions comprising collagen, elastin (weight ratios are 3:1, 2:1, 1:1, 1:2 or 1:3) and PEO (0.5% wt), having total protein concentrations between 1 and 5% w/v, could be spun at voltages of 10-30 kV and yielded continuous fibres. As observed for spinning of the single proteins, the presence of PEO and NaCl was essential to form a continuous non-beaded fibre. In the used set up, a flow rate of 30 µl/min proved to be optimal for all compositions. A collecting distance of 20-30 cm was most suitable to ensure complete drying of the fibre before collection. If the solvent was not completely evaporated, a film without a recognizable fibrous structure was obtained.

As expected, the surface tension of the spun solution had a very important influence on the diameter of the obtained fibres, since the formation of the jet is the result of the balance between surface tension and electrostatic charge repulsion. Decreasing the surface tension of

the spinning solution also favoured the formation of fibres without beads [39]. The surface tension of the protein solutions decreased with increasing elastin content (Fig. 4.4a,b). For example, collagen/elastin solutions with a weight ratio of 2:1 and a total protein concentration of 3% w/v had a surface tension of 53.3 mN/m and this decreased to 46.2 mN/m when the elastin content was increased to a weight ratio of 1:3 (total protein concentration 4% w/v). In order to continuously spin a homogeneous non-beaded collagen/elastin fibre, the voltage applied had to be increased with increasing surface tension of the spinning solution (Fig. 4.4a,b). It was not possible to continuously process solutions with a surface tension of 59.5 mN/m (weight ratio of collagen to elastin = 3:1) because of the high potential of 26 kV needed at these conditions. These high potentials cause abundant sparking in the system. Monitoring the viscosity as a function of the shear rate revealed that collagen/elastin solutions behave as pseudoplastic polymers, of which the viscosity decreases with increasing shear rate. This can be a consequence of breaking up of the interactions between the two proteins (*e.g.* hydrophobic interactions and hydrogen bonds) at increasing shear rates. In particular, at

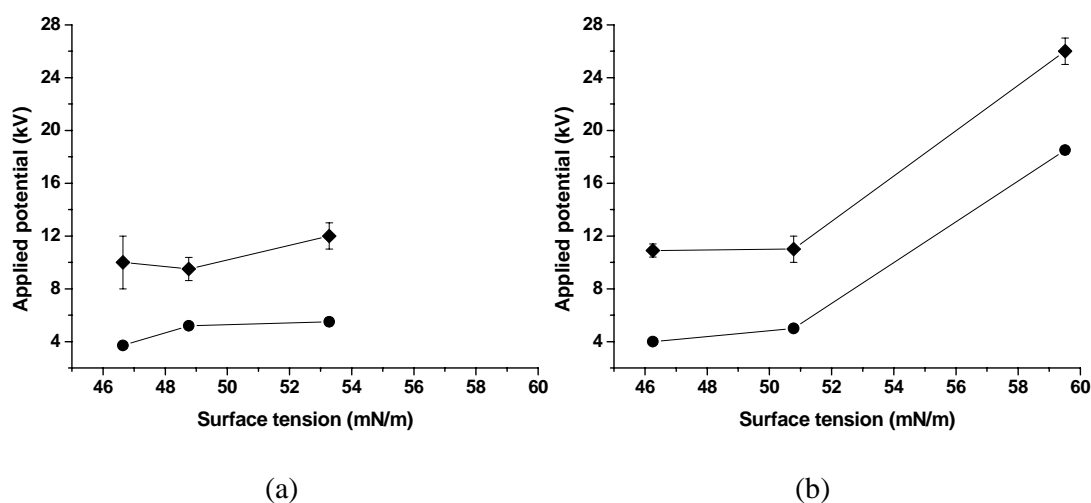


Figure 4.4. Relationship between the potential needed to start (◆) or to stop (●) the spinning process and the surface tension of the spinning solution containing various ratios of collagen to elastin, 0.5% w/v PEO and 42.5 mM NaCl. The weight ratios of collagen to elastin used are (points from left to right in the graphs): (a) 1:2, 1:1, 2:1 with a final total protein concentration of 3% w/v and (b) 1:3, 1:1, 3:1 with a final total protein concentration of 4% w/v. Flow rate is in all cases 30 $\mu\text{l}/\text{min}$.

higher collagen to elastin ratios of 2:1 and 3:1 the observed shear thinning effect is more pronounced than observed at higher elastin content (collagen to elastin weight ratio of 1:2 and 1:3).

The viscosity of a polymer solution depends on a possible orientation of polymer molecules with respect to the direction of the flow. At low shear rates, molecules with preferred conformations that are long and thin (like the triple helix of collagen) are not oriented very well in the direction of the flow and have large effective cross-sections, leading to a relatively high viscosity. However, at high shear rates, the molecules align with the flow, giving much smaller effective cross-sections and thus much lower viscosities. On the contrary, more globular molecules (like the ones expected at high elastin concentrations) are less oriented relative to the direction of the flow and the decrease in viscosity with shear rate is less pronounced.

In all cases, an increase in the collagen to elastin ratio, at a constant total protein concentration, led to more viscous solutions (Fig. 4.5). Viscosity significantly influenced the morphology of the spun fibres. A higher collagen concentration (collagen:elastin = 1:1) and thus a higher viscosity, ensured the formation of completely round fibres, whereas at lower viscosities (collagen:elastin = 1:3) completely flat fibres were obtained (Fig. 4.6 a,b,c). A similar behaviour was observed by Huang *et al.* [18] when electrospinning fibres of synthetic elastin mimetic peptides from aqueous solutions. They showed that increasing the elastin concentration resulted in the formation of flat, ribbon-shaped fibres, which were occasionally

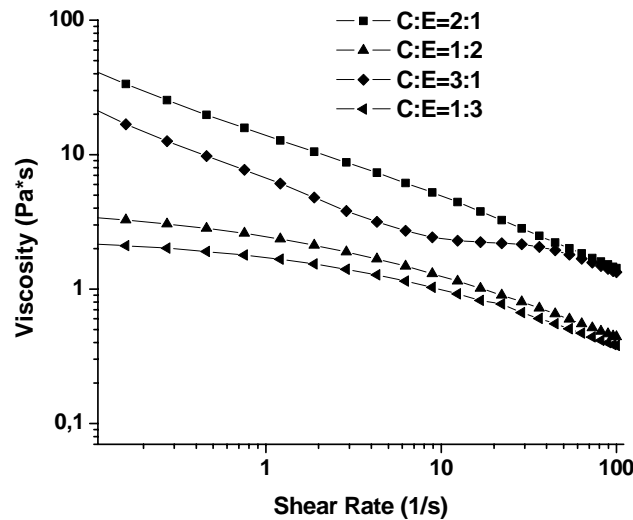


Figure 4.5. Viscosity of 5% wt solutions with different collagen to elastin weight ratios (C:E) as a function of shear rate. All solutions contain 5% (w/v) PEO.

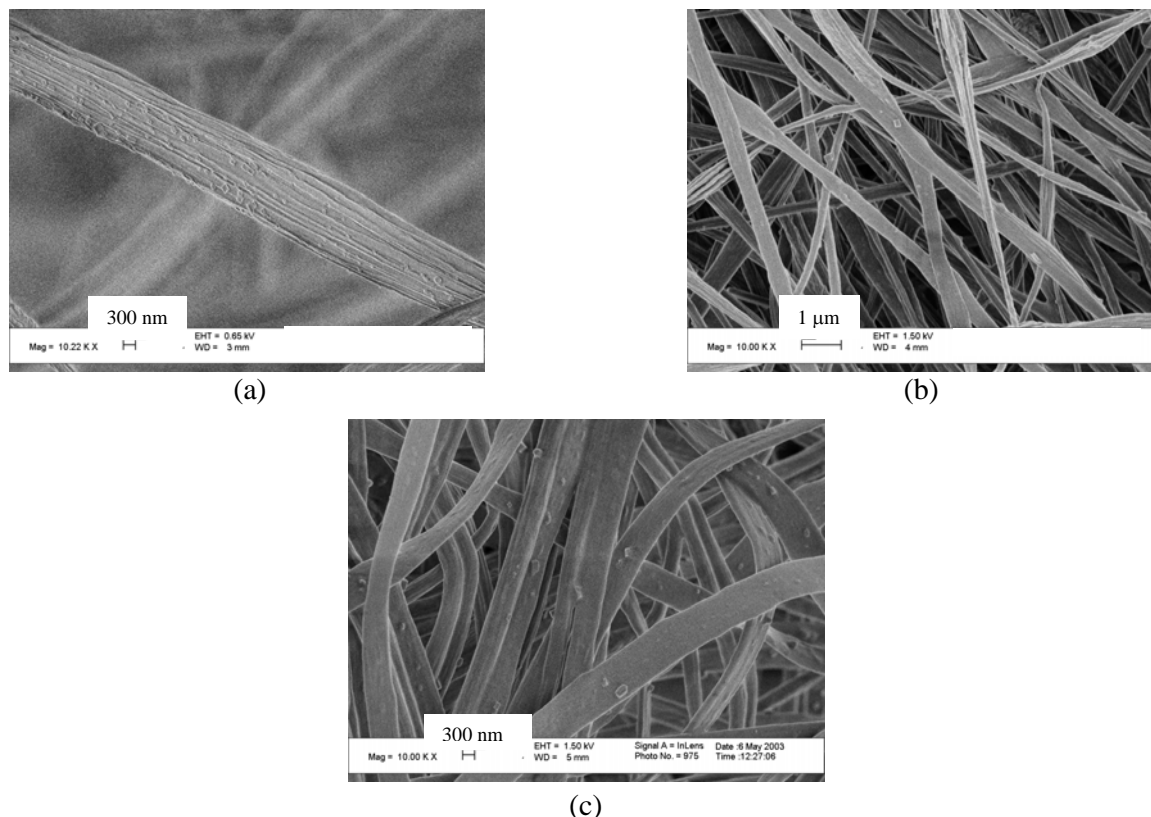


Figure 4.6. *Dependence of the morphology of the fibres on the initial composition of the spinning solution: weight ratio collagen to elastin is (a) 1:1 (scale bar is 300 nm); (b) 1:2 (scale bar is 1 μm); (c) 1:3 (scale bar is 300 nm). All spun solutions contain 0.5% w/v PEO and 42.5 mM NaCl. All the fibres were spun at 22 kV, collected at a distance of 20 cm.*

twisted during spinning and deposition. This phenomenon was related to the molecular self-assembly processes of the elastin analogue, which demonstrates a temperature dependent conformational transition from a less to a more ordered state upon increasing the temperature. This inverse temperature behaviour is attributed to hydrophobic collapse and expulsion of water molecules associated with the non-polar side chains of the molecule [40]. The increase in temperature occurring at the needle because of the high electric field applied, can facilitate hydrophobic mediated polypeptide folding and molecular self-assembly. Moreover, it has to be taken into account that at higher viscosities, the deformation imparted by electric fields on the spun jet is larger and more round and smoother fibres can be produced [30]. A decrease in the collagen to elastin weight ratio from 2:1 to 1:3 in the spinning solution resulted in an increase in the average fibre diameter from 220 to 600 nm (Fig. 4.7 and 4.8a-c). This could be a consequence of the decrease in surface tension caused by the addition of elastin

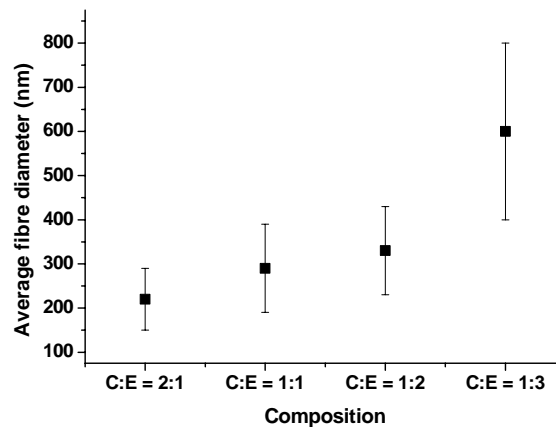


Figure 4.7. Dependence of the average fibre diameter on the collagen to elastin weight ratio in the spinning solution. All the fibres were spun under the same conditions (applied potential 22 kV; collecting distance 20 cm; PEO content 0.5% w/v; NaCl 42.5 mM). The total protein concentration is 3% w/v except for the collagen to elastin weight ratio 1:3, for which it is 4% w/w.

(e.g. collagen/elastin solutions having weight ratios of 2:1 and 2:2 have a surface tension of 53.2 and 50.7 mN/m, respectively), since it is known that the formation and diameter of the jet is determined by the balance between the surface tension and the electrostatic charge repulsion [39]. Increasing the collecting time from 30 to 240 min afforded denser non-woven meshes [4], but did not significantly influence the thickness of the produced scaffolds.

Since tubular scaffolds are needed to tissue engineer blood vessels, the possibility to produce non-woven tubular structures composed of collagen and elastin electrospun fibres was investigated. A mandrel rotating with a velocity of 5 cm/s was placed between the needle tip and the collecting plate and used as an additional collector. Dry, non-woven tubular meshes were thus formed. Moreover, it was observed that the fibres collected on the rotating mandrel had a certain degree of orientation (Fig.4.9). It is expected that varying the rotating speed can further influence the degree of orientation of the fibres obtained in the produced scaffolds.

Electrospinning of collagen/elastin mixtures afforded fibres lacking the morphological characteristics, like the D-period of collagen or the filament-like folds of elastin, which were observed when the single proteins were spun separately. As a consequence, it was not possible

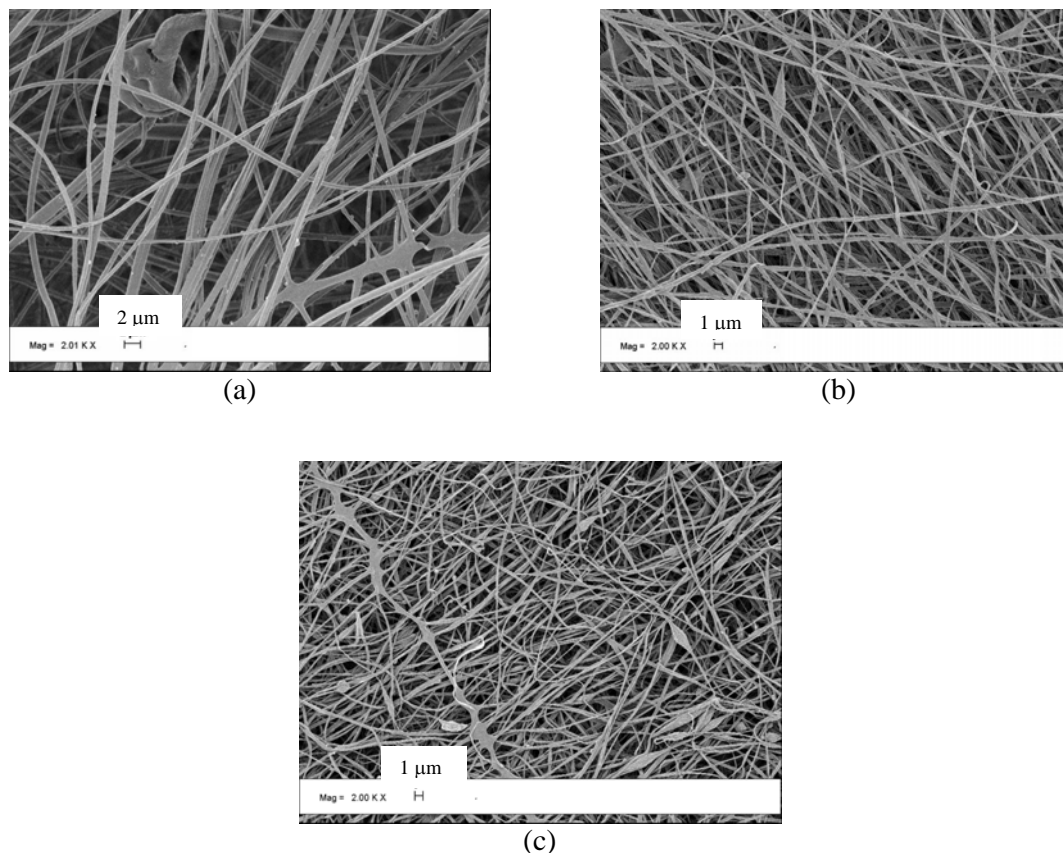


Figure 4.8. Dependence of the fibre diameter on elastin content in the electrospinning of collagen/elastin solutions: (a) weight ratio of collagen to elastin = 1:3 ($d = 600$ nm) (protein concentration 4% w/v; scale bar 2 μm); (b) collagen to elastin = 1:2 ($d = 330$ nm) (protein concentration 3% w/v; scale bar 1 μm); collagen to elastin = 2:1 ($d = 220$ nm) (protein concentration 3% w/v; scale bar 1 μm). All the fibres were spun at 22 kV, and collected at a distance of 20 cm. All the solutions contain 0.5% w/v PEO and 42.5 mM NaCl.

to distinguish the proteins in the fibre. It was thus hypothesized that the composition along each fibre is an even distribution of the collagen and elastin in the original blend, in agreement with the work of Boland *et al.* [19]. At all the explored collagen to elastin weight ratios, sodium chloride crystals were present at the surface of the fibres (Fig. 4.10).

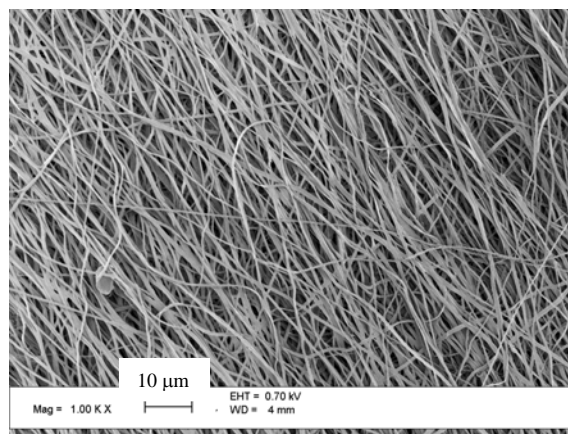


Figure 4.9. SEM picture of partially oriented collagen/elastin fibres obtained by spinning at 22 kV a solution with a weight ratio of collagen to elastin equal to 1:1 (total protein concentration 3% w/v) and containing 0.5% w/v PEO and 42.5 mM NaCl. Collecting distance was 20 cm. Scale bar is 10 μm.

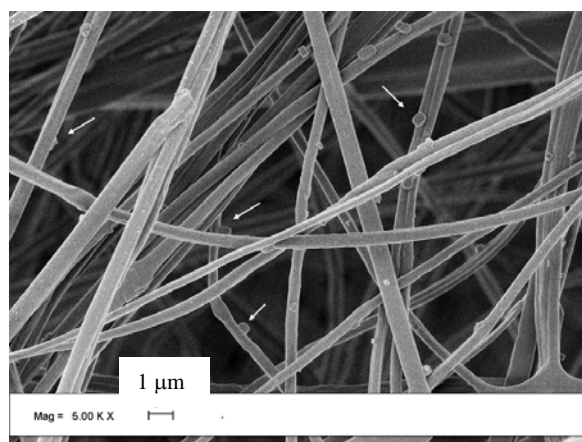


Figure 4.10. SEM image of fibres of collagen/elastin (weight ratio 1:3, total protein concentration 4% w/v), spun from an aqueous solution containing 0.5 wt% PEO and 42.5 mM NaCl, at 22 kV. Collecting distance was 25 cm. Crystals of sodium chloride are indicated by arrows. Scale bar is 1 μm.

When the electrospun fibres were placed in water, dissolution took place instantaneously. For any type of application (*e.g.* tissue engineering), crosslinking of the protein fibres is thus a requisite. Therefore, non-woven collagen/elastin/PEO meshes were crosslinked using a soluble carbodiimide (EDC) in the presence of N-hydroxysuccinimide (NHS) in ethanol/water (70% v/v).

In a previous study, we have shown that the use of diluted ethanol as a solvent in the crosslinking of scaffolds prepared from insoluble collagen and elastin with EDC/NHS, does not alter the final crosslinking density as compared to crosslinking in water [10]. Crosslinking of collagen/elastin samples with EDC/NHS involves the activation of free carboxylic acid groups of glutamic and aspartic acid residues and subsequent formation of amide bonds upon reaction with the free amino groups of lysine and hydroxylysine residues. In this way no additional chemical entities are introduced and stable amide linkages are formed. The addition of NHS is advantageous not only because it prevents the formation of side products but also because it increases the reaction rate [21].

The degree of crosslinking was estimated by determining both the denaturation temperature and the residual amount of free amine groups of (non-)crosslinked samples. Formation of crosslinks in the collagen/elastin spun matrices increased the denaturation temperature (T_d) of the samples. All the spun fibres had a T_d of 47 °C before crosslinking and of 79 °C afterwards. As a consequence of crosslinking, the amount of free amino groups present in the samples decreased (Fig. 4.11). Independent of the weight ratio of collagen to elastin, the relative percentage of free amino groups left after crosslinking of the fibres was decreased to approximately 30% of the original value. These results are comparable with those obtained by performing the same reaction with freeze-dried scaffolds of insoluble collagen and elastin [10].

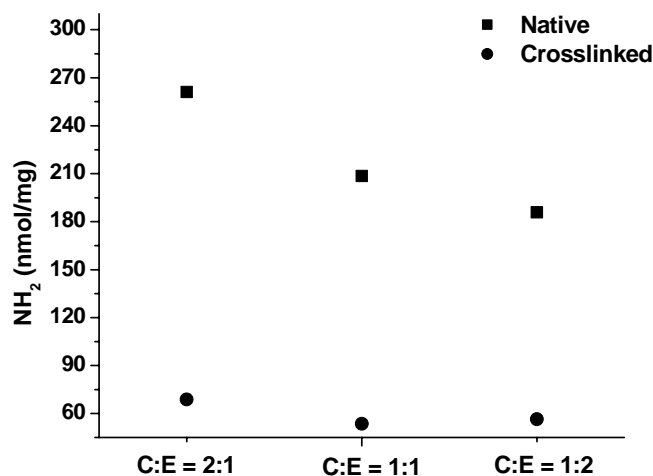


Figure 4.11. Concentration of free amino groups in electrospun collagen elastin (C:E) fibres with different weight ratios of the two proteins, before and after crosslinking with EDC/NHS.

In the DSC thermograms of dry uncrosslinked fibres, it was possible to clearly observe a melting transition of the PEO at 60 °C. After crosslinking, the melting transition of PEO was not present anymore, which implies that PEO was leached from the fibres. Moreover, by means of SEM, it was verified that no NaCl crystals were present at the surface of the fibres after EDC/NHS crosslinking. Unexpectedly, despite the removal of NaCl and PEO, the morphology of the fibres after crosslinking was not altered (Fig 4.12). Crosslinked collagen/elastin scaffolds with different weight ratios (2:1, 1:1, 1:2, 1:3) of the two proteins were cultured with SMC for 14 d. In all cases, the formation of a confluent multi-layer of SMC, growing on top of each other was observed by means of histology (Fig. 4.13).

The possibility to electrospin collagen and elastin solutions into fibres composed of an homogeneous blend of the two proteins can lead to the production of scaffolds with extraordinary properties, completely different from those observed in analogous mixtures of the insoluble proteins, for which the separate contributions can always be well distinguished. Evaluation of the specific interactions occurring in or between soluble collagen and soluble elastin and theoretically resulting in formation of collagenous fibrillar structures and aggregation of collagen and elastin might result in a better understanding of the potential of the application of collagen/elastin electrospun scaffolds in different fields, like tissue engineering. Further investigations are actually being performed in this direction.

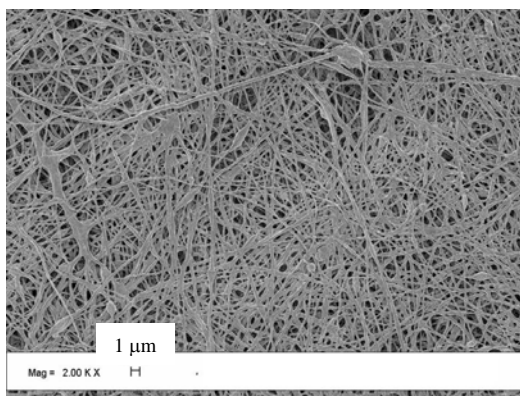


Figure 4.12. SEM image of EDC/NHS crosslinked fibres of collagen/elastin (weight ratio 2:1, total protein concentration 3% w/v), spun from an aqueous solution containing 0.5 wt% PEO and 42.5 mM NaCl at 22 kV. Collecting distance was 25 cm. Crystals of sodium chloride are no longer visible in the sample. Scale bar is 1 μm.

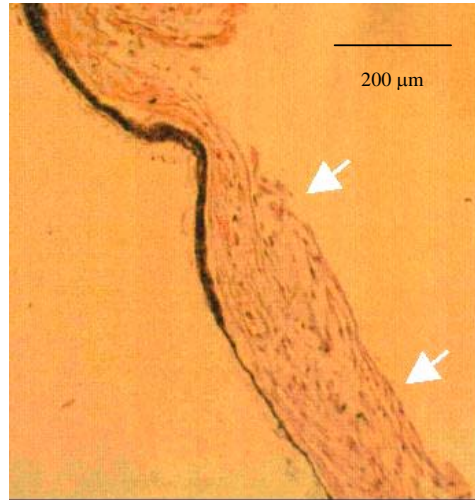


Figure 4.13. *Histological section of an electrospun EDC/NHS crosslinked collagen/elastin mesh (weight ratio 2:1, total protein concentration 3% w/v), spun from an acidic aqueous solution containing 0.5 wt% PEO and 42.5 mM NaCl at 22 kV and cultured with SMC for 14 d. A very thick SMC layer is visible on top of the scaffold and is indicated by arrows. Magnification is 100 X.*

Conclusions.

Electrospinning was used as a successful technique to produce non-woven meshes from aqueous solutions of collagen type I and/or elastin. In all cases, the addition of PEO and NaCl was necessary to spin homogeneous and continuous fibres. Composition of the solution, net charge density and applied electric field were parameters influencing the morphology of the obtained fibres. Spinning collagen/elastin solutions yielded meshes composed of fibres with diameters ranging from 220 to 600 nm. Stable scaffolds were prepared by crosslinking with EDC/NHS. After crosslinking, scaffolds completely devoid of PEO and NaCl were obtained. Smooth muscle cells were successfully cultured on crosslinked scaffolds and a confluent layer of cells was observed after 14 d on the surface of the different meshes.

One of the advantages of electrospinning aqueous solution of collagen and/or elastin is the formation of scaffolds with high porosity and surface area, two essential requisites for tissue engineering. Electrospinning solutions of the two proteins separately from each other can also give the possibility to produce multi-layered scaffolds with controlled morphology and/or mechanical properties. Moreover, in this study, it has been shown that fibres, in which the two proteins cannot be distinguished, can be electrospun from a mixture of collagen and elastin. This may result in fibres with extraordinary mechanical properties, different from those

observed in analogous mixtures of the insoluble proteins. Further investigations are currently being done in this direction.

Acknowledgments.

M. Smithers is thanked for the SEM images. R. de Vos and L. Sterks are kindly acknowledged for performing the histological analyses.

References.

1. Huang, Z.M., Zhang, Y.Z., Kotaki, M. and Ramakrishna, S., A review on polymer nanofibers by electrospinning and their applications in nanocomposites. *Comp. Sci. Technol.*, 2003. 63: 2223-2253.
2. Hu, J., Odom, T.W. and Lieber, C.M., Chemistry and physics in one dimension: synthesis and properties of nanowires and nanotubes. *Acc. Chem. Res.*, 1999. 32(5): 435-445.
3. Deitzel, J.M., Kosik, W., McKnight, S.H., Beck Tan, N.C., DeSimone, J.M. and Crette, S., Electrospinning of polymer nanofibers with specific surface chemistry. *Polymer*, 2002. 43(3): 1025-1029.
4. Khil, M.S., Kim, H.Y., Kim, M.S., Park, S.Y. and Lee, D.R., Nanofibrous mats of poly(trimethylene terephthalate) via electrospinning. *Polymer*, 2004. 45(1): 295-301.
5. Xu, C.Y., Inai, R., Kotaki, M. and Ramakrishna, S., Aligned biodegradable nanofibrous structure: a potential scaffold for blood vessel engineering. *Biomaterials*, 2004. 25(5): 877-886.
6. Fung, Y.C., Mechanical properties and Active Remodeling of Blood Vessels, in *Biomechanics. Mechanical Properties of Living Tissues*, Springer, Editor. 1999.
7. Ogle, B.M. and Mooradian, D.L., The role of vascular smooth muscle cell integrins in the compaction and mechanical strengthening of a tissue-engineered blood vessel. *Tissue Eng.*, 1999. 5(4): 387-402.
8. Nimni, M.E., Collagen: molecular structure and biomaterial properties, in *Encyclopedia handbook of biomaterials and bioengineering materials*, M. Deheler Ed. 1995: New York. 1229-1243.
9. Debelle, L. and Alix, A.J.P., The structures of elastins and their function. *Biochimie*, 1999. 81(10): 981-994.

10. Buttafoco, L., Engbers-Buijtenhuijs P., Poot A.A., Dijkstra P.J., Daamen W.F., van Kuppevelt T.H., Vermes I., Feijen I., First steps towards tissue engineering of small-diameter blood vessels: preparation of flat scaffolds of collagen and elastin by means of freeze drying, *Submitted to J. Biomed. Mat. Res.*
11. Formhals, A., Process and apparatus for preparing artificial threads. 1934: USA.
12. Reneker, D.H. and Chun, I., Nanometre diameter fibres of polymer, produced by electrospinning. *Nanotechnol.*, 1996. 7: 216-223.
13. Reneker, D.H., Yarin, A.L., Fong, H. and Koombhongse, S., Bending instability of electrically charged liquid jets of polymer solutions in electrospinning. *J. Appl. Phys.*, 2000. 87(9): 4531-4547.
14. Bowlin, G.L., Electrospinning collagen scaffolds. *Sci. Med.*, 2002: 292-293.
15. Deitzel, J.M., Kleinmeyer, J., Harris, D. and Beck Tan, N.C., The effect of processing variables on the morphology of electrospun nanofibers and textiles. *Polymer*, 2001. 42(1): 261-272.
16. Li, W.J., Laurencin, C.T., Cateson, E.J., Tuan, R.S. and Ko, F.K., Electrospun nanofibrous structure: A novel scaffold for tissue engineering. *J. Biomed. Mat. Res.*, 2002. 60(4): 613-621.
17. Huang, L., Nagapudi, K., Apkarian, R.P. and Chaikof, E.L., Engineered collagen-PEO nanofibers and fabrics. *J. Biomat. Sci. Polymer Edn.*, 2001. 12(9): 979-993.
18. Huang, L., McMillan, R.A., Apkarian, R.P., Pourdeyhimi, B., Conticello, V.P. and Chaikof, E.L., Generation of synthetic elastin-mimetic small diameter fibers and fiber networks. *Macromolecules*, 2000. 33(8): 2989-2997.
19. Boland, E.D., Matthews, J.A., Pawlowski, K.J., Sompson, D.G., Wnek, G.E. and Gary, L., Electrospinning collagen and elastin: preliminary vascular tissue engineering. *Front. Biosci.*, 2004. 9: 1442-1432.
20. Vanwachem, P.B., Vanluyn, M.J.A., Damink, L., Dijkstra, P.J., Feijen, J. and Nieuwenhuis, P., Biocompatibility and tissue regenerating capacity of cross-linked dermal sheep collagen. *J. Biomed. Mater. Res.*, 1994. 28(3): 353-363.
21. Vanluyn, M.J.A., Vanwachem, P.B., Damink, L.O., Dijkstra, P.J., Feijen, J. and Nieuwenhuis, P., Relations between in vitro cytotoxicity and cross-linked dermal sheep collagens. *J. Biomed. Mater. Res.*, 1992. 26(8): 1091-1110.
22. Shaw, D.J., Introduction to Colloid & Surface Chemistry. 4th ed, B. Heinemann. 2000, Oxford. 306.

23. Olde Damink, L.H.H., Dijkstra, P.J., van Luyn, M.J.A., van Wachem, P.B., Nieuwenhuis, P. and Feijen, J., Cross-linking of dermal sheep collagen using a water-soluble carbodiimide. *Biomaterials*, 1996. 17(8): 765-773.
24. Buijtenhuijs, P., Buttafoco, L., Poot, A.A., Dijkstra, P.J., deVos, R.A.I., Sterk, L.M.T., Geelkerken, B.R.H., Feijen, J. and Vermes, I., Tissue engineering of blood vessels: characterisation of smooth muscle cells for culturing on collagen and elastin based scaffolds. *Biotechnol. Appl. Biochem.*, 2004. 9(2): 141-149.
25. Doshi, J. and Reneker, D.H., Electrospinning process and applications of electrospun fibers. *J. Electrostat.*, 1995. 35(2-3): 151-160.
26. Bognitzki, M., Czado, W., Frese, T., Schaper, A., Hellwig, M., Steinhart, M., Greiner, A. and Wendorff, J.H., Nanostuctured fibers via electrospinning. *Adv. Mat.*, 2001. 13(1): 70-72.
27. Huang, L., Apkarian, R.P. and Chaikof, E.L., High-resolution analysis of engineered type I collagen nanofibers by electron microscopy. *Scanning*, 2001. 23(6): 372-375.
28. Pawlowski, K.J., Belvin, H.L., Raney, D.L., Su, J., Harrison, J.S. and Siochi, E.J., Electrospinning of a micro-air vehicle wing skin. *Polymer*, 2003. 44(4): 1309-1314.
29. Buttafoco, L., vanEck, E., Dijkstra, P.J., Kentgens, A., Feijen, J., A solid-state ¹³C NMR study of collagen/elastin assemblies. *Submitted to Biopolymers*.
30. Fong, H., Chun, I. and Reneker, D.H., Beaded nanofibers formed during electrospinning. *Polymer*, 1999. 40(16): 4585-4592.
31. Demir, M.M., Yilgor, I., Yilgor, E. and Erman, B., Electrospinning of polyurethane fibers. *Polymer*, 2002. 43(11): 3303-3309.
32. Jin, H.J., Fridrikh, S.V., Rutledge, G.C. and Kaplan, D.L., Electrospinning bombyx mori silk with poly(ethylene oxide). *Biomacromolecules*, 2002. 3: 1233-1239.
33. L'Heureux, N., A completely biological tissue-engineered human blood vessel. *Faseb J.*, 1998. 12(1): 47-56.
34. Weinberg, C.B. and Bell, E., A blood vessel model constructed from collagen and cultured vascular cells. *Science*, 1986. 231: 397-400.
35. Nerem, R.M., Critical issues in vascular tissue engineering. *Inter. Congress Series*, 2004. 1262: 122-125.
36. Faury, G., Function-structure relationship of elastic arteries in evolution: from microfibrils to elastin and elastic fibres. *Pathol. Biol.*, 2001. 49(4): 310-325.
37. Frenot, A. and Chronakis, I.S., Polymer nanofibers assembled by electrospinning. *Curr. Opin. Coll. Interf. Sci.*, 2003. 8(1): 64-75.

38. Mitchell, S.L. and Niklason, L.E., Requirements for growing tissue-engineered vascular grafts. *Cardiovasc. Pathol.*, 2003. 12(2): 59-64.
39. Fridrikh, S.V., Yu, J.H., Brenner, M.P. and Rutledge, G.C., Controlling the fiber diameter during electrospinning. *Phys. Rev. Lett.*, 2003. 90(14).
40. Li, B., Alonso, D.O.V. and Daggett, V., The molecular basis for the inverse temperature transition of elastin. *J. Molec. Biol.*, 2001. 305(3): 581-592.

Chapter 5

A Solid-State ^{13}C CP/MAS NMR Study of Collagen/Elastin Assemblies*.

In these matters the only certainty is that nothing is certain

(Pliny the Elder)

Abstract.

^{13}C CP/MAS solid state NMR was used to investigate the interactions between soluble collagen and soluble elastin at two different degrees of hydration (10 ± 1 and 22 ± 1 % w/w). Despite the fact that, in freeze-dried collagen/elastin specimens, the domains of the separate proteins could not be distinguished by SEM, combining collagen and elastin did not induce any significant chemical shift in the recorded spectra as compared to those of the single components. At 10 ± 1 % w/w hydration, $T_{1\rho}$ relaxation times of all protons of collagen/elastin samples were longer than those found for the separate proteins. At 22 ± 1 % w/w hydration the observed differences in ^1H $T_{1\rho}$ between collagen/elastin samples and the separate proteins were smaller. In all cases the $T_{1\rho}$ values could be obtained from mono-exponential curves, thus indicating that there are no separate domains in the sample. Carbon $T_{1\rho}$ measurements resulted in a broad range of values. At approximately 10 % w/w hydration, long relaxation times of approximately 50-55 ms for the carbonyl carbons were indicative for restricted backbone mobility of collagen/elastin samples. Values of 18.5-38.5 ms in the aliphatic region showed that these groups are more mobile than the carbonyl C-atoms, but still less mobile than in the separate components. Increasing the water content to

* L. Buttafoco¹, E. van Eck², A.A. Poot¹, P.J. Dijkstra¹, A. Kentgens², J. Feijen¹

Submitted to Biopolymers

¹ Department of Polymer Chemistry and Biomaterials, Faculty of Science and Technology and Institute of Biomedical Technology (BMTI), University of Twente, Enschede, P.O. Box 217, 7500 AE, The Netherlands,

² Department of Physical Chemistry, Solid State NMR, University of Nijmegen, Toernooiveld 1, 7525 ED Nijmegen, The Netherlands.

22 ± 1 % w/w resulted in longer $T_{1\rho}$ for parts of the carbonyl C-atoms of collagen/elastin samples, whereas the ^{13}C $T_{1\rho}$ of all the other carbon atoms (except C_β from Ala) decreased as compared to the specimens at 10 ± 1 % w/w hydration. The longer relaxation times observed for the C_β of Ala in collagen/elastin mixtures as compared to the relaxation times in the free proteins indicate the presence of hydrophobic interactions between the two proteins. The lower mobility of the side chains carbons of the hydrophilic residues observed in the mixture as compared to the single components suggests the possible occurrence of hydrogen bonding.

Introduction.

Collagen and elastin are two of the most abundant naturally occurring proteins [1, 2]. In the body, they confer strength and elasticity to different tissues and thus ensure stability and functionality [3-5].

At least 19 different types of collagen have been identified, but the major fibre-forming types are type I, II and III, which constitute approximately 70% of the body collagen. Collagen is composed of three individual α -chains of about 1000 residues each, forming a triple helix with a molecular weight of 300 kDa, a length of 280 nm and a diameter of 1.5 nm. Triple helices assemble in microfibrils and ultimately into fibrillar structures with a characteristic axial periodicity, the D-period. Short non-helical segments (telopeptides) are found at both ends of the protein molecule [6, 7]. In the body, the main function of collagen is to confer stiffness and strength to tissues, thus preventing their failure or rupture.

The structure of elastin is still a matter of debate [8, 9], but this protein is generally considered to be amorphous and to lack the typical spatial organization of collagen. The soluble precursor of elastin is tropoelastin, mainly composed of hydrophobic amino acids. Tropoelastin also contains lysine residues, which are able to form intermolecular crosslinks. Elastin can be considered as a three-dimensional network having 60-70 amino acids between crosslinks and confers tissues their elasticity.

The development of high-resolution solid-state NMR gave the possibility to investigate the structure and the conformation of natural or synthetic collagen or elastin, depending on their source, level of hydration and temperature [10-12]. The role of the different amino acids in the collagen triple helix was thus investigated in detail using collagen-like polypeptides and showing that some residues (*i.e.* guanidinium group of arginyl residues or hydroxyproline) give a major contribution to its stabilization [13, 14]. Due to the dynamic nature of the first

hydration shell of the collagen-like triple helix, it was suggested that water molecules play a role in the triple helix to triple helix assembly [15]. The elucidation of the structure-function relationship of elastin appeared more difficult and was often approached using either elastin-like synthetic polypeptides or soluble α -elastin. In all cases, the presence of more than one conformation of the polypeptide chains has been suggested [16-18].

In collagen isolated from bovine Achilles tendons, increasing hydration was reported to have a much stronger effect on the amplitude of the molecular dynamics than increasing temperature [19]. The protein backbone, essentially rigid in the dry sample, gains significant mobility as hydration increases. An even more drastic increase in mobility is observed for the C_γ of HyPro. Similarly, water of hydration of elastic fibres is known to play a critical role in the structure and function of this protein, as verified by the significant changes in the spectral intensities in the aliphatic region when 70 % of the water in hydrated insoluble elastin from bovine ligamentum nuchae is removed [17]. Comparable results have also been found with elastin mimetic polypeptides, for which extraordinary molecular flexibility has been reported even at moderate water contents of 20-30 % [10].

In conclusion, up to now high-resolution solid-state NMR has been mostly used to investigate the structure of collagen and elastin and the way water contributes to their stability and functionality. In this study, cross polarization magic angle spinning (CP/MAS) solid-state ^{13}C NMR was used in an attempt to determine the existence and the nature of the interactions occurring between soluble collagen type I and soluble elastin. For this purpose, collagen from calf skin and elastin from bovine neck ligament have been mixed and successively freeze dried. The spectra obtained from collagen/elastin samples were then compared with those derived from the single components and differences were evaluated. The influence of the degree of hydration on the nature of these interactions was investigated as well.

^{13}C CP/MAS high-resolution solid-state NMR spectra were obtained by spinning the sample at an angle of 54.7° to the direction of the magnetic field. This removes the broadening caused by the chemical shift anisotropy and, in conjunction with high power proton decoupling, also removes the effects of the strong dipole-dipole interactions. Cross-polarisation serves to enhance the signal by transferring magnetisation from the abundant protons to the rare ^{13}C spins as well as reducing the cycle time of the experiment, since one only has to wait for protons to reach Boltzmann equilibrium instead of the generally much longer ^{13}C spin-lattice relaxation times [20].

The effect of hydration on the mobility of the protein backbone and side chains and thus on the interaction between collagen and elastin was investigated calculating the cross relaxation times

(T_{1S}) from the CP curves of some of the specimens. Measurements of both proton and carbon relaxation times in the rotating frame ($T_{1\rho}$) were performed to investigate in more detail the effect of hydration on the mobility of the samples. $T_{1\rho}$ of collagen/elastin samples were measured and then compared with the relaxation times of the single components. These relaxation times are sensitive to motions in the kHz regime and have been used extensively to characterize synthetic [21-24] or natural polymers [25, 26].

Materials and methods.

Sample preparation.

Soluble collagen type I from calf skin (Elastin Products Company Inc., USA) and soluble elastin from bovine neck ligament (Elastin Products Company Inc., USA) were dissolved at a concentration of 1% (w/v) in MilliQ water for 2 h at room temperature, after which the solutions were frozen at -18 °C and finally freeze-dried overnight.

A mixed collagen/elastin solution (weight ratio 1:1) was prepared exactly in the same way, frozen at -18 °C and freeze-dried overnight.

Both collagen and elastin dehydrated by freeze-drying to constant weight, contain 10% wt structural water [27, 28]. These freeze-dried proteins were rehydrated by exposure to a humidified atmosphere (100% humidity). The time needed to obtain the desired hydration level of approximately 20% wt, was approximately 6 h for collagen and 8 h for elastin.

The water content was determined as following:

$$H_2O(\%) = \frac{(w_h - w_d)}{w_d} \times 100 \quad (5.1)$$

where w_h is the weight of the sample (in mg) after exposure to a humidified atmosphere (hydrated sample) and w_d is the weight of the freeze-dried sample. For this calculation the contribution of water of hydration was neglected and 10 % hydrated samples were considered as dry.

^{13}C CP/MAS NMR.

Solid-state ^{13}C NMR spectra of freeze-dried soluble collagen type I, soluble elastin and collagen/elastin (weight ratio 1:1) were obtained at approximately 23 °C using either a

Chemagnetics/Varian CMX-400 or a CMX-600 Infinity Spectrometer equipped with a 6 mm HX probe. Approximately 100 mg of the sample was loaded into a Pencil II 6 mm rotor. The spectra were recorded using variable amplitude CP and XiX proton decoupling [29] (Fig. 5.1a). The RF field strengths used for the CP were 52 kHz for protons with a ramp of 5% and 45 kHz for carbon. XiX decoupling was performed at a field strength of 50 kHz and 445.3 μs pulse lengths. Magic angle spinning at 6.4 kHz was used to avoid overlap of spinning side bands with the isotropic resonances. CP contact times of 0.5 ms were used for all analysed samples. The recycle delay was 5 s. The ¹³C chemical shifts were referenced with respect to the CH₂ peak of adamantane as an external reference at 38.7 ppm relative to TMS. Spectra were accumulated 1000-2000 times in order to achieve a sufficient signal to noise ratio.

The cross relaxation times (T_{IS}) were measured from the data of the CP curves at approximately 23 °C, using an RF field strength of 40-50 kHz. The contact times were varied from 0.02 to 2 ms. T_{IS} were calculated from [20]:

$$M(\tau) = M \left(1 - e^{-\frac{\tau}{T_{IS}}} \right) \times e^{-\frac{\tau}{T_{1\rho}}} \quad (5.2)$$

where τ is the contact time, T_{1ρ} the spin-lattice relaxation time in the rotating frame, M a constant and M(τ) the signal intensity.

The relaxation times in the rotating coordinate system (T_{1ρ}) of both ¹³C and ¹H nuclei were also measured at approximately 23 °C. The proton T_{1ρ} was obtained via the carbons, using the pulse sequence displayed in figure 5.1b. Prior to CP the proton magnetisation was spin-locked for a variable time τ (50 μs - 50 ms) using an RF field strength of 50 kHz. For the ¹³C T_{1ρ} measurements, after CP, the spinlock was performed on the ¹³C channel with an RF field strength of 50 kHz. During this time, the proton decoupling was switched off (Fig. 5.1c).

All relaxation time spectra were processed using MatNMR, which was also used to deconvolute signals into Lorentzian curves (MatNMR is a toolbox for processing NMR/EPR data under MATLAB and can be freely downloaded at <http://matnmr.sourceforge.net>). All T_{1ρ} relaxation time data, calculated from the amplitude of the deconvoluted signals, could be described satisfactorily by mono-exponential decays.

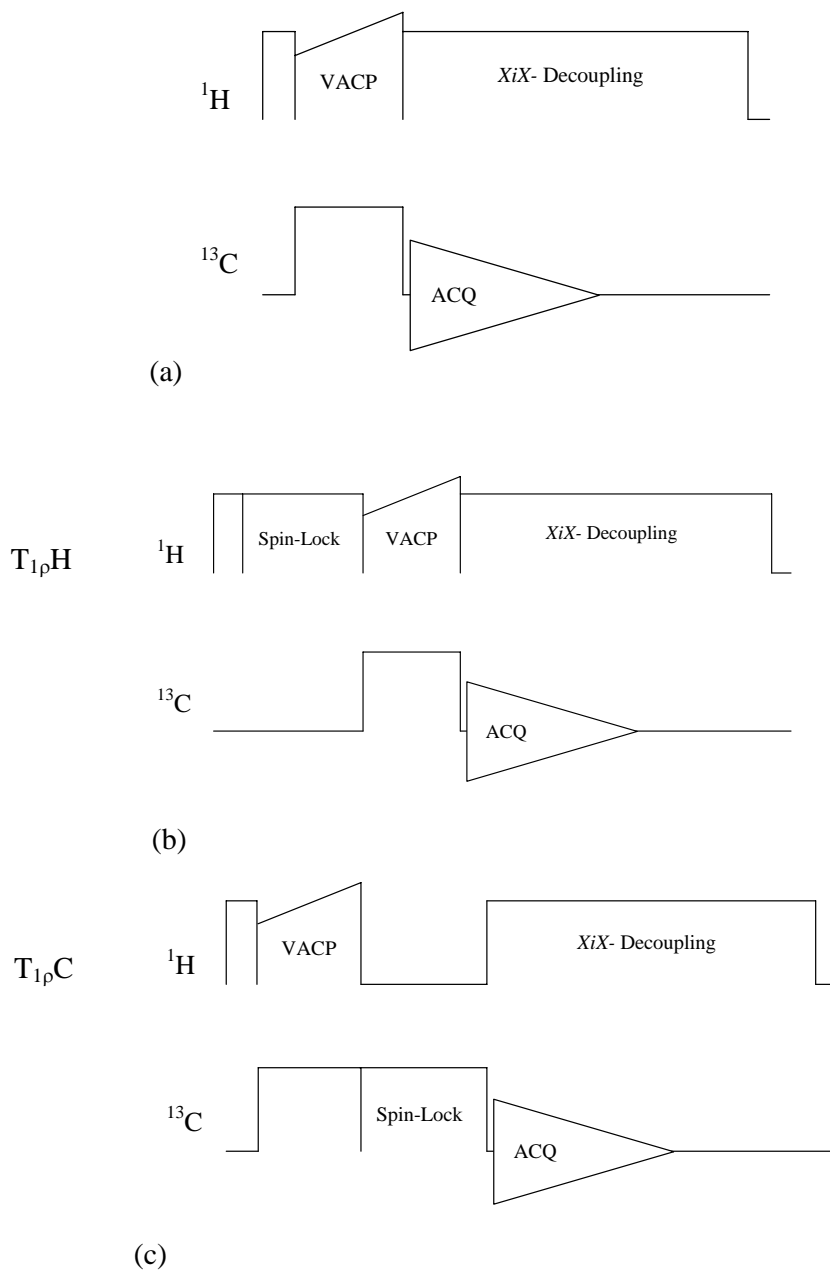


Figure 5.1. Schematic representation of the different CP/MAS ^{13}C NMR experiments performed. The spectra were recorded using variable amplitude CP and XiX proton decoupling (a); the proton $T_{1\rho}$ was obtained via the carbons, spin-locking the proton magnetization for a variable time and then performing the CP (b); in ^{13}C $T_{1\rho}$ measurements the spin-lock was performed on the ^{13}C channel, after CP was performed. During this time, the proton decoupling was switched off (c).

Results and discussion.

Spectral assignment.

Collagen.

Figure 5.2 shows a ^{13}C CP/MAS NMR spectrum of freeze-dried soluble collagen type I from calf skin containing $10 \pm 1\%$ w/w of water. The obtained ^{13}C CP/MAS NMR spectra resemble those of collagen fibres from bovine tendons and skin previously reported [19, 30, 31]. The peak assignment was carried out using the resonances of C atoms in amino acids [32], proteins and peptides [31, 33] (Table 5.1).

The peak with the highest intensity at 43.3 ppm was thus assigned to the C_α of glycine (Gly), which represents one third of the amino acids present in collagen [6] (Table 5.2). Based on the literature data, the peaks at 48 and 50 ppm were assigned to the C_α of alanine (Ala) and the peak at 59.6 ppm to the C_α of proline (Pro) and hydroxyproline (HyPro).

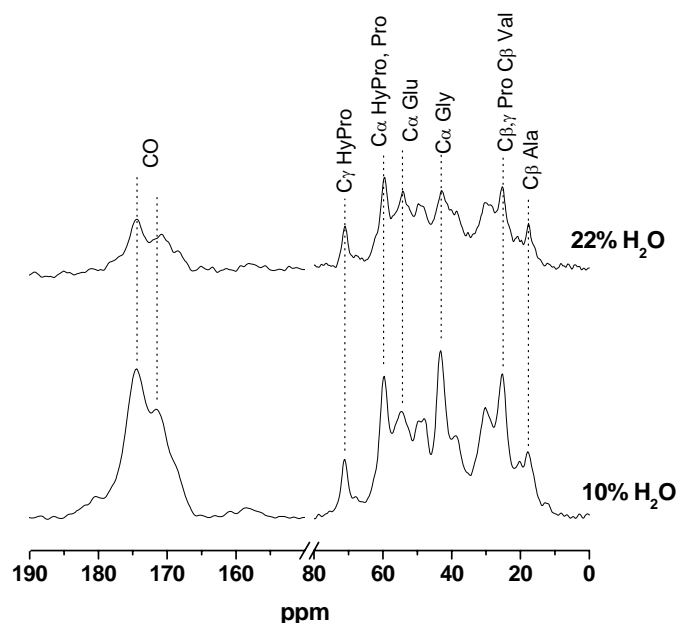


Figure 5.2. ^{13}C CP/MAS NMR spectra of soluble collagen type I from calf skin. The analysed specimens were $(10 \pm 1)\%$ w/w and $(22 \pm 1)\%$ w/w hydrated. The spectra were recorded at approximately $23\text{ }^\circ\text{C}$. The most prominent peaks were assigned according to values reported in literature [32] (18 ppm: C_β Ala; 25.5 ppm: $\text{C}_{\beta,\gamma}$ Pro, C_β Val; 43.3 ppm: C_α Gly; 54.6 ppm: C_α Glu; 59.6 ppm: C_α Pro, HyPro; 71.0 ppm: C_γ HyPro; 171.0 and 174.6 ppm: CO).

A characteristic feature of collagen is the presence of a peak at 71.0 ppm, belonging to the C_γ of HyPro. The carbonyl groups (CO) give a broad signal at around 174 ppm that appears to consist of at least two different resonances. In particular, the shoulder at 171 ppm is believed to originate from those amino acids not present in α -helical segments, *i.e.* valine, isoleucine, serine and threonine [33]. The splitting of the carbonyl signal is also considered a strong indication for the presence of the native structure of collagen [34].

Table 5.1. Selected ^{13}C chemical shifts in amino acids, proteins and peptides.

Carbon type	Chemical shift (ppm)			
	Amino acids [32]	(Pro-Gly-Pro) _n (triple helix)[31]	Collagen fibril (bovine tendon) [31]	Elastin* [33]
C_β (Ala)	18-21	-	16	16
$C_{\beta,\gamma}$ (Pro), C_β (Val)	25-30	25-29	24-29	25-30
C_α (Gly)	42	43	43	41
C_α (Ala)	48-50	-	50	53
C_α (Glu)	55	n.d.	n.d.	n.d.
C_α (Pro, HyPro)	59	60	58	60
C_γ (HyPro)	71	-	70	-
Carbonyl (C=O)	168-175	168-174	167-174	172-173- 176**

* Elastin from bovine neck ligament

** 172 ppm: Gly; 173 ppm: Val, Ser, Ile and Thr; 176 ppm: attributed to carbonyl resonances in α -helical segments.

Table 5.2. *Amino acid content of soluble collagen and soluble elastin. Values are expressed per 1000 residues*.*

Amino Acid	Soluble Collagen	Soluble Elastin
HyPro	88 ± 7	11 ± 1
Asp	56 ± 3	10 ± 2
Thr	20 ± 1	2 ± 3
Ser	30 ± 1	0
Glu	79 ± 1	20 ± 2
Pro	123 ± 3	130 ± 2
Gly	324 ± 1	330 ± 5
Ala	115 ± 3	292 ± 3
Val	Internal standard	Internal standard
Ile	16 ± 1	23 ± 1
Leu	32 ± 2	111 ± 7
Tyr	6 ± 1	15 ± 3
Phe	19 ± 1	38 ± 2
Lys	36 ± 4	7 ± 2
Arg	55 ± 4	7 ± 1

* Values have been measured according to the procedure described in [35].

Fibrillogenesis was verified by SEM analysis of the freeze-dried collagen, which revealed the presence of the D-period, typical of the native structure of this protein (Fig. 5.3).

Collagen contains approximately 10% w/w of water, which cannot be removed by freeze drying [27]. This structural water takes part in the extensive hydrogen bonded network involving especially the HyPro residues. Per triplet Gly-X-Y, with Y generally being HyPro, six water molecules are hydrogen bonded, thus stabilizing the triple helix. Increasing the water content from an initial 10 ± 1 to 22 ± 1 % w/w resulted in slight peak narrowing (Fig. 5.2), which can be considered as an indication of reorganization of conformationally disordered portions of the triple helix. As a consequence of hydration, the CP efficiency decreased, as evidenced by the decrease in intensity of the signals, which is an indication of the increased mobility of main and side chain atoms in collagen. The relative

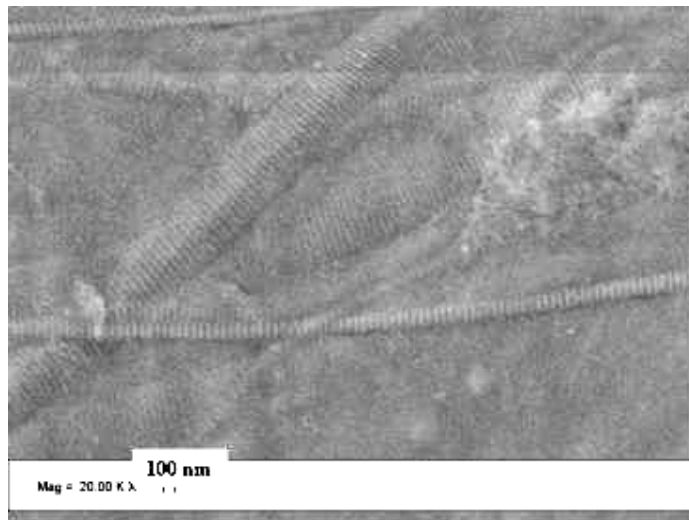


Figure 5.3. SEM image of a sample of freeze-dried soluble collagen type I from calf skin, showing the typical D-period present. Scale bar is 100 nm.

intensities of the single resonances were also affected and peaks having approximately the same degree of resolution were obtained. If a substantial conformational change is induced in collagen by the presence of water molecules, signals may shift up to 5 ppm. The magnitude of the chemical shift depends on the changes in local conformation of the amino acid residues in the protein, as defined by the torsion angles and the hydrogen bonds [34].

However, only minor chemical shifts were observed upon increasing the hydration level of collagen to 22 ± 1 % w/w. The resonance of the C_{α} of Gly shifted from 43.3 to 42 ppm, whereas even less significant chemical shifts were observed for the C_{α} of Glu at 54.1 ppm and C_{γ} of HyPro at 71.6 ppm. Hence, the increased hydration level does not induce large conformational changes in the collagen local conformation of di- and tri-peptide segments.

It is known that ^{13}C NMR chemical shifts of solid peptides are not influenced by any long range order, such as packing of helices or β -sheets, unless the rotational angles ϕ , ψ , or χ are affected [33]. Upon hydration, the polypeptide chains appear to become more mobile as shown by the increased resolution of the carbonyl resonances and the decrease in CP efficiency.

Elastin.

Compared to collagen, the interpretation of the amino acid sequence, macromolecular conformation and assembly of elastin polypeptide chains is much more difficult and its structure has not been clearly solved yet. Most chain segments adopt the energetically most

favourable conformation and in the overall structure type I and II β -turns, α -helical parts and random (unfolded) structures are reported to be present [8, 9, 16].

As for collagen, the average concentration of structural water molecules in elastin can be considered to be in the order of 10% w/w. However, this percentage increases when the molecule is stretched and decreases upon recoiling [28]. Figure 5.4 shows the ^{13}C CP/MAS NMR spectrum obtained from samples of freeze-dried soluble elastin with a degree of hydration of 10 ± 1 % w/w. In elastin, one of the most prominent peaks in the aliphatic region belongs to the methyl C_β atom of alanine, at approximately 18.9 ppm. The abundance of Ala in this protein (Table 5.2), (elastin is constituted for approximately 26% of Ala [36, 37]) determines the hydrophobic nature typical of elastin. In the aliphatic region six well distinguishable peaks corresponding to the carbons of Gly, Val, Glu and Pro can be assigned [18]. The carbonyl peak at approximately 173 ppm can be deconvoluted into two

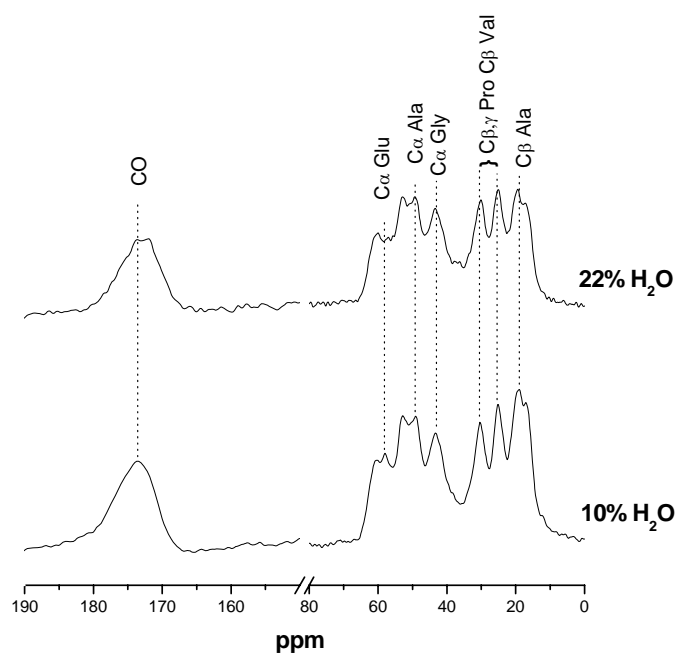


Figure 5.4. ^{13}C CP/MAS NMR spectra of soluble elastin from bovine neck ligament. The analysed samples were $(10 \pm 1)\%$ w/w and $(22 \pm 1)\%$ w/w hydrated. The spectra were recorded at approximately 23 °C. The most prominent peaks were assigned according to values reported in literature [30] (18.9 ppm: C_β Ala; 25.5 ppm: $\text{C}_{\beta,\gamma}$ Pro, C_β Val; 43.6 ppm: C_α Gly; 49.6 ppm: C_α Ala; 57.5 ppm: C_α Glu; 172.5 and 175.0 ppm: CO).

peaks, thus suggesting that more than one type of secondary structure is present, due to the tendency of most chain segments to adopt the energetically most favourable conformation.

Increasing the water content to 22 ± 1 % w/w did not induce any chemical shift of the peaks (Fig. 5.4), demonstrating the hydrophobic nature of this protein.

Collagen/elastin mixtures.

Mixing collagen and elastin (weight ratio 1:1) solutions and subsequent freeze drying up to a 10 ± 1 % w/w water content, yields a homogeneous material. SEM analysis of this material revealed a structure devoid of the characteristic D-period of the collagen fibrils. Recently, it was shown that fibres electrospun from aqueous solutions containing collagen type I and elastin also lack the characteristic D-period of collagen and filament-like organization of elastin [38, 39]. The ^{13}C CP/MAS NMR spectrum of collagen/elastin appears as a superposition of the spectra of collagen and elastin (Fig. 5.5). In this spectrum, the peaks originating from C_β of Ala and C_α of HyPro and Pro, typical for collagen and elastin, respectively, can still be clearly identified. Therefore, one can conclude that mixing collagen and elastin does not significantly alter the local molecular structure of these proteins [19], since no significant changes in the chemical shifts are observed as compared to the single components. A certain degree of peak broadening was observed only in the C_γ of HyPro at 71.2 ppm. Broadening of the peaks is known to be a clear sign of aggregation of polymers [40, 41], as reported by Nishiyama *et al.* for soluble collagen after binding to conditioned dentin [42]. However, the peak broadening observed in this case is minor, thus suggesting only a physical interaction between the two proteins.

The CP efficiency of a collagen/elastin mixture is not significantly altered at a higher water content of 22 ± 1 % w/w (Fig. 5.5). In the aliphatic region, eight peaks are easily distinguishable in collagen/elastin samples. In particular the peaks originating from the C_β of Ala, typical for elastin, and from the C_γ of HyPro, typical for collagen, are still clearly visible. Moreover, at this higher hydration level, the shoulder present at 171.7 ppm, originating from the carbonyl peak of the collagen moiety is better resolved. In amorphous synthetic polymers, a change in the amplitude of a certain signal is due to the averaging of isotropic chemical shift values of different sub-conformations. In contrast, in polypeptides this effect is mainly due to enhanced efficiency of the ^1H decoupling, related to increased molecular mobility [17, 19, 43].

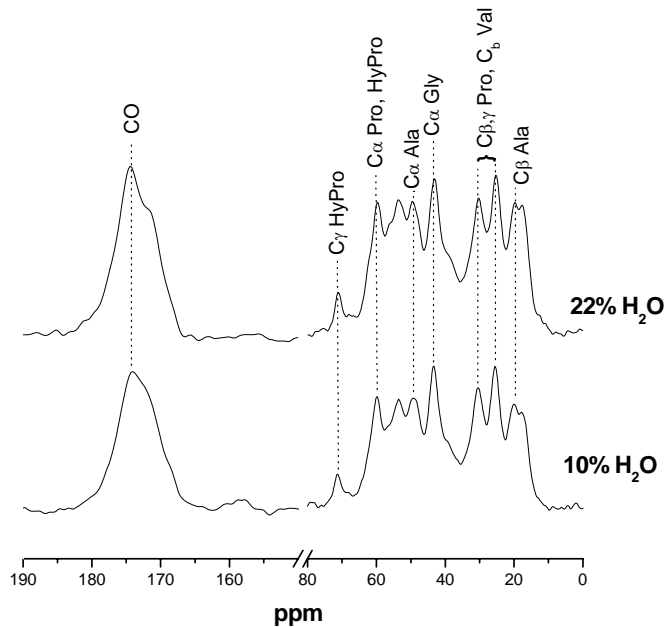


Figure 5.5. ^{13}C CP/MAS NMR spectra of soluble collagen and elastin (weight ratio 1:1). The analysed samples were $(10 \pm 1)\%$ w/w and $(22 \pm 1)\%$ w/w hydrated. The spectra were recorded at approximately 23°C . The most prominent peaks were assigned according to values reported in literature [32] (18.2 ppm: C_βAla ; 25.9 ppm: $\text{C}_{\beta,\gamma}\text{Pro}$, C_βVal ; 43.9 ppm: $\text{C}_\alpha\text{Gly}$; 49.7 ppm: $\text{C}_\alpha\text{Ala}$; 60.4 ppm: $\text{C}_\alpha\text{Pro}$, HyPro ; 71.2 ppm: $\text{C}_\gamma\text{HyPro}$; 172.2 and 175.3 ppm: CO).

Relaxation times: T_{1S}

Relaxation time measurements can be used as an efficient method to investigate the interactions between (macro)molecules. The cross-relaxation time (T_{1S}) describes the rate of transfer magnetization between ^1H and ^{13}C and is proportional to the square of the average of the dipolar coupling ($\langle D_{\text{CH}} \rangle^2$). This means that it is sensitive to both the distribution of protons around carbons, as the dipolar coupling is proportional to $1/r^3$, and local motions which affect averaging of the dipolar coupling.

In this study the cross-relaxation time was calculated for collagen and collagen/elastin samples with $10 \pm 1\%$ w/w water and for collagen or elastin $22 \pm 1\%$ w/w hydrated (Table 5.3).

Collagen T_{1S} .

The cross-relaxation time T_{1S} of the most characteristic groups in collagen was determined from the CP curves (Table 5.3). At $10 \pm 1\%$ w/w hydration, the C_γ of HyPro has the lowest T_{1S}

of $60 \pm 15 \mu\text{s}$, which verifies the high mobility of this residue as well as the possibility to easily have dipolar coupling between the carbon atoms and the protons. Longer T_{1S} times of $140 \pm 40 \mu\text{s}$ are instead observed for the C_{β} of Ala, implying that the coupling between carbons and protons are strongly reduced in the methyl rotor. Even longer times are found for the carbonyl C-atoms, which have no protons available for coupling. Increasing the hydration level to $22 \pm 1 \%$ w/w revealed an increase in the T_{1S} of C_{β} of Ala, C_{γ} of HyPro and CO, thus showing the significance of the effect of hydration on the mobility of collagen.

Elastin T_{1S} .

At hydration levels of $22 \pm 1 \%$ w/w, elastin shows T_{1S} times comparable to those measured for collagen under the same conditions. The presence of two T_{1S} times for the C_{β} of Ala in the $22 \pm 1 \%$ w/w hydrated elastin indicates that the alanine residues in this protein are present in two different motional environments, probably related to random coil and more ordered β -sheet structures. A similar behaviour has been reported for *Nephila Clavipes* dragline silk [44]. The T_{1S} times observed for the two different C_{β} atoms of Ala in the two different motional environments are the same, thus showing that the local motions in the scale of a C-H bond are the same, independent of the position of Ala in the molecule.

Table 5.3. Longitudinal relaxation times of C_{β} of Ala (18 ppm), C_{γ} of HyPro (71 ppm) and CO (171-175 ppm) of differently hydrated collagen, elastin or collagen/elastin samples.

<i>a.a. residue</i> <i>Sample</i>	T_{1S} (μs)		
	C_{β} Ala	C_{γ} HyPro	CO
Collagen ($10 \pm 1 \%$ w/w H_2O)	140 ± 40	60 ± 15	590 ± 40 600 ± 40
Collagen ($22 \pm 1 \%$ w/w H_2O)	300 ± 100	70 ± 30	1400 ± 200 1000 ± 200 1220 ± 150
Elastin ($22 \pm 1 \%$ w/w H_2O)	490 ± 140 490 ± 140	-	1300 ± 200
Collagen/elastin ($10 \pm 1 \%$ w/w H_2O)	190 ± 60	65 ± 20	660 ± 70

Collagen/elastin T_{1S} .

In the collagen/elastin mixture (weight ratio 1:1), at a water content of 10 ± 1 % w/w, the T_{1S} times of the C_{β} of Ala, C_{γ} of HyPro and CO groups are approximately the same as for collagen at the same hydration level. This shows that the local motions of C_{β} of Ala, C_{γ} of HyPro and CO are not altered by the addition of elastin to collagen samples. Moreover, these various atoms have the same cross-relaxation times independently from the protein they belong to.

Relaxation times: $T_{1\rho}$

In order to investigate possible interactions occurring between collagen and elastin also the spin-lattice relaxation times in the rotating frame ($T_{1\rho}$) of the single proteins and of the protein mixture were compared. Relaxation measurements, such as determination of ^{13}C and ^1H $T_{1\rho}$ values, are useful in identifying the dynamics (in the kHz regime) of the main and side chains of the proteins. However, it has to be taken into account that the rotating frame field applied must be sufficiently strong to overcome dipolar interactions, but not too strong so as to prevent probe deterioration due to heating effects. The pulse schemes to perform these relaxation measurements are shown in Fig. 5.1. A typical curve showing the dependence of $T_{1\rho}$ (and other relaxation times T_1 and T_2) on the correlation time τ_c is shown in figure 5.6. The correlation time corresponds to a characteristic decay for the particular motion involved.

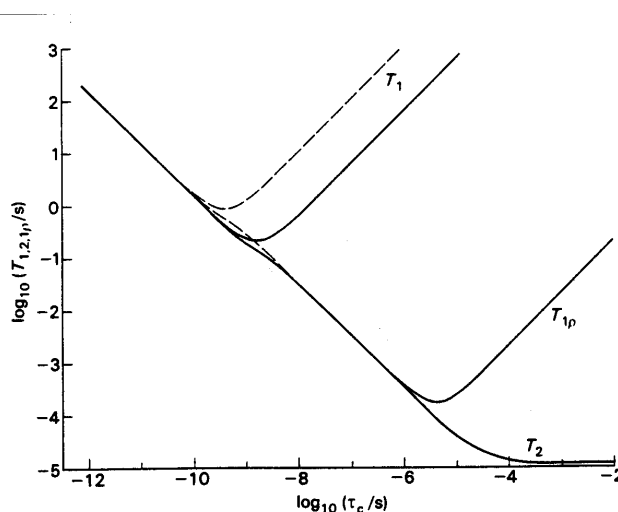


Figure 5.6. Dependence of T_1 , T_2 and $T_{1\rho}$ on the correlation time τ_c . The solid lines are calculated for a spectral frequency of 100 MHz, whereas the dashed lines show deviations for frequencies of 400 MHz. If τ_c increases sufficiently to become of the order of the inverse of the transition frequency, a minimum is reached. At higher magnetic fields T_1 and $T_{1\rho}$ increase again.

The $T_{1\rho}$ or spin-lattice relaxation time in the rotating frame has been a very useful tool in the analyses of polymer structures. The change in mobility may permit the identification of inhomogeneities in the structure and molecular packing of distinct regions in the molecule [22, 45]. In addition to pinpointing differences in the local dynamics of the various proteins, relaxation time values are also useful to confirm the mobility effects anticipated with ^{13}C CP/MAS NMR spectra and T_{1S} measurements for the proteins. Since the method used for preparation of the samples and their thermal history is known to lead to variations in $T_{1\rho}$ [23], in this study, all the samples were processed exactly in the same way in order to obtain results not affected by variations in these parameters (see Sample preparation in Materials and Methods).

Collagen ^1H $T_{1\rho}$

A typical series of spectra obtained from the measurement of the proton rotating frame spin-lattice relaxation times $T_{1\rho}$ of collagen samples containing $10 \pm 1\%$ w/w water is shown in figures 5.7 and 5.8a. In collagen samples hydrated at $10 \pm 1\%$ w/w, proton $T_{1\rho}$ measurements yielded values of approximately 5 ms for all protons, independent of the particular amino acid they belong to (Fig 5.8 and Table 5.4). Slightly shorter proton $T_{1\rho}$ values were found for the more hydrophilic amino acid residues. In particular, ^1H $T_{1\rho}$ of HyPro, had a value of 3 ± 0.8 ms, indicating its high mobility. If domains within the sample are small, rapid

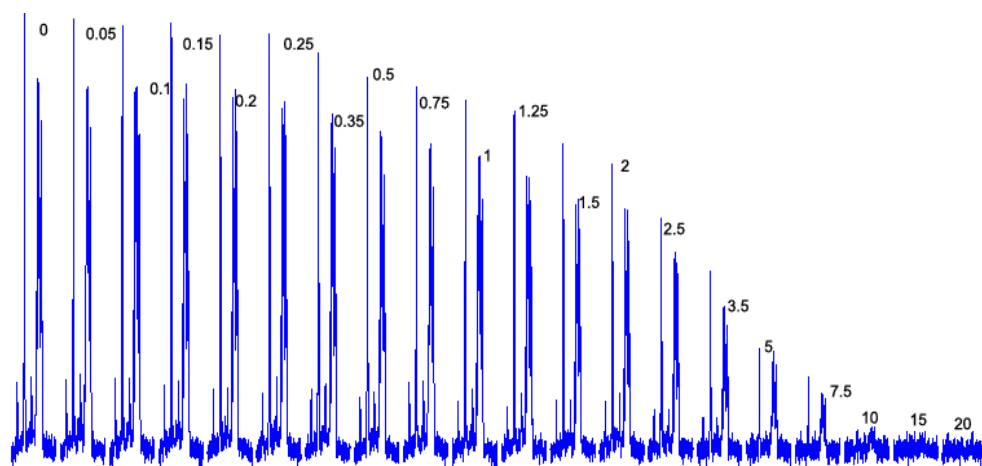


Figure 5.7. Horizontal stack plot of the different spectra of proton $T_{1\rho}$ obtained by varying the spin-lock time from 0.05 to 50 ms during a ^{13}C CP/MAS NMR experiment of freeze-dried soluble collagen, $(10 \pm 1)\%$ w/w hydrated. All measurements were performed at approximately 23 °C. The spin-lock time used is indicated in ms next to each spectrum.

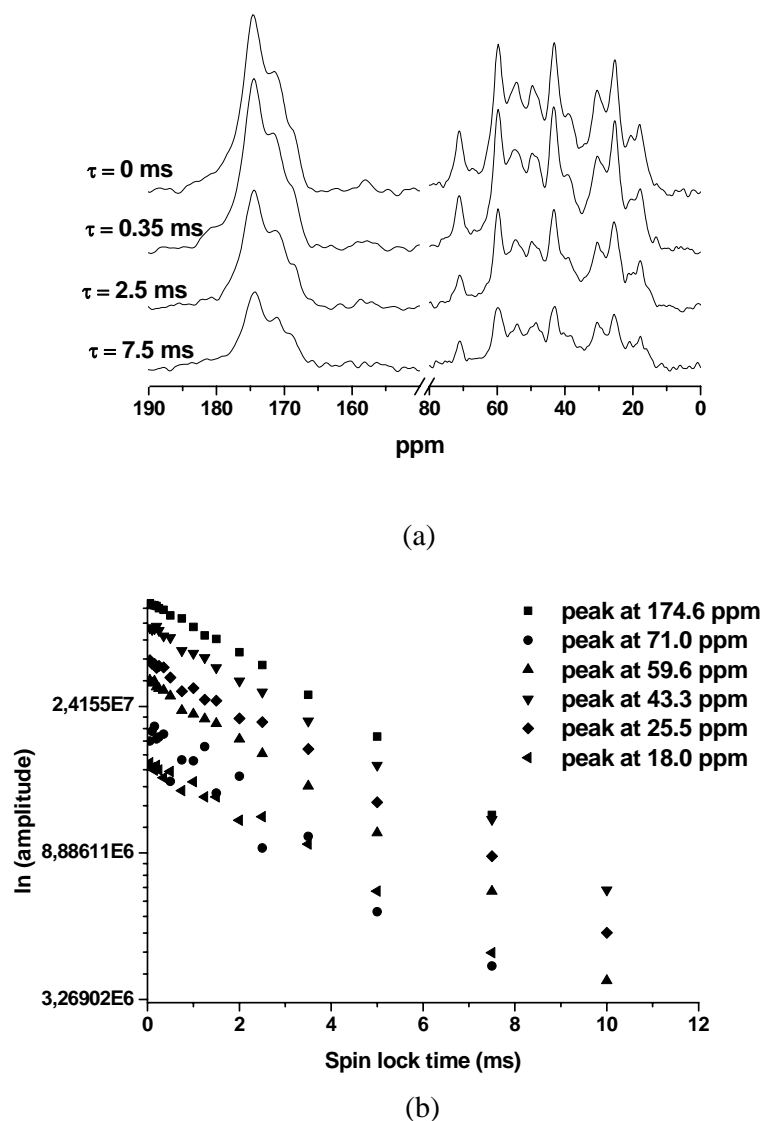


Figure 5.8. (a) Typical spectra of soluble collagen, (10 ± 1)% w/w hydrated, obtained measuring the ^1H $T_{1\rho}$ spin-lattice relaxation times in the rotating frame for different spin-lock times; (b) mono-exponential linear fit of the peaks of the most representative amino groups present in collagen (18 ppm: C_β Ala; 25.5 ppm: $C_{\beta,\gamma}$ Pro, C_β Val; 43.3 ppm: C_α Gly; 59.6 ppm: C_α Pro, HyPro; 71.0 ppm: C_γ HyPro; 174.6 ppm: CO). All measurements were performed at approximately 23 °C.

^1H NMR spin diffusion leads to a single value for the proton $T_{1\rho}$ measured via each carbon [45]. As a consequence, it can be concluded that in collagen all the protons experienced the same chemical surrounding thus verifying the expected homogeneity within the analysed

sample. It is known from studies on the dielectric relaxation time of collagen over a wide range of temperatures that this relaxation time and therefore the local mobility of this protein is highly dependent not only on temperature but also on its degree of hydration [46, 47].

The ^1H $T_{1\rho}$ values decreased to approximately 3 ms when the hydration level was increased from 10 ± 1 to 22 ± 1 % w/w (Table 5.4). Furthermore it was found that at these conditions all the protons of the collagen molecules experience the same chemical environment similar to that observed when only structural water is present.

Elastin ^1H $T_{1\rho}$

At 10 ± 1 % w/w hydration, the protons of elastin have spin-lattice relaxation times in the rotating frame of approximately 5 ms. These values are comparable to those observed in collagen samples having the same water content (Table 5.4) and equal to the ^1H $T_{1\rho}$ values found for lyophilised insoluble elastin [17], α -elastin [48], synthetic elastin mimetic polypeptides [45] or Nephila Clavipes silk [44]. A proton $T_{1\rho}$ value as low as 5 ms implies that the molecule is homogeneous at scales of approximately 3 nm, as shown in a structural study on membrane proteins [49]. This domain size indicates that the organized domains (*i.e.* α -helix and ordered β -structures) are interspersed with the disorganized portions in the protein.

Increasing the water content to 22 ± 1 % w/w did not alter the spin-lattice relaxation times in the rotating frame of elastin protons. This was a clear indication of the rather weak interaction of elastin with water, which was already hypothesized from the ^{13}C CP/MAS NMR spectra of elastin. No changes in CP efficiency were observed by increasing the water content from 10 ± 1 % w/w to 22 ± 1 % w/w. These results are further supported by the rather small percentage ($< 5\%$) of amino acids in elastin that have polar side groups (Table 5.2).

Collagen/elastin ^1H $T_{1\rho}$

At 10 ± 1 % w/w hydration, the collagen/elastin samples showed proton spin-lattice relaxation times in the rotating frame longer than those found in the separate components (Table 5.4). In particular, the $T_{1\rho}$ of the C_γ of the HyPro, typical of collagen, increased from 3 to 7 ms, thus showing a substantial decrease in mobility of that particular residue after aggregation with elastin. The same trend was observed for the $T_{1\rho}$ of the C_β of Ala, typical of elastin, which increased from approximately 5 to approximately 9 ms. In all cases, the $T_{1\rho}$ values were

Table 5.4. Rotating frame spin-lattice proton relaxation time ($^1\text{H } T_{1\rho}$) for collagen, elastin and collagen/elastin samples (weight ratio 1:1) having different degrees of hydration. All relaxation data could be satisfactorily described by mono-exponential decays. Multiple values are expressed when a peak could be deconvoluted in more than one Lorentzian lineshape.

Shift (ppm)	Carbon type	$^1\text{H } T_{1\rho}$ of 10% hydrated samples (ms)			$^1\text{H } T_{1\rho}$ of 22% hydrated samples (ms)		
		Collagen	Elastin	Coll / El	Collagen	Elastin	Coll / El
18	C_β (Ala)	4.8 ± 0.3	5.5 ± 0.5	9.4 ± 0.2	2.5 ± 0.5	4.4 ± 0.2	4.4 ± 0.2
		4.0 ± 0.5	5.0 ± 0.5	8.0 ± 0.5	3.0 ± 0.5	5.0 ± 0.5	3.5 ± 3.5
25	$\text{C}_{\beta,\gamma}$ (Pro)	5.0 ± 0.5	5.0 ± 0.5	6.5 ± 0.5	2.6 ± 0.2	5.0 ± 0.5	4 ± 0.5
	C_β (Val)	5.0 ± 0.5	5.0 ± 0.5	7.0 ± 0.5	2.6 ± 0.2 3.0 ± 0.3	5.0 ± 0.5	
43	C_α (Gly)	4.8 ± 0.2	5.0 ± 0.5	6.5 ± 0.5	2.5 ± 0.5	5.0 ± 0.2	3.5 ± 0.5
					2.8 ± 0.2		3.5 ± 0.5
50	C_α (Ala)	5.0 ± 0.5	4.0 ± 0.5	8.0 ± 0.5	3.0 ± 0.5	5.0 ± 0.5	4.0 ± 0.5
		5.0 ± 0.5	4.5 ± 0.5		3.0 ± 0.5		
55	C_α (Glu)	4.0 ± 0.5	n.d.	7.0 ± 0.5	2.5 ± 0.5	5.2 ± 0.2	3.4 ± 0.2
60	C_α (Pro, HyPro)	4.8 ± 0.2	4.0 ± 0.5	n.d.	3.0 ± 0.5	5.5 ± 0.5	3.2 ± 0.2
		2.8 ± 0.2					2.3 ± 0.1
71	C_γ (HyPro)	3.0 ± 0.8	-	7.0 ± 0.5	3.0 ± 0.5	-	3.5 ± 0.5
171-175	Carbonyl (C=O)	5.0 ± 0.5	5.0 ± 0.5	6.0 ± 0.5	3.0 ± 0.5	5.8 ± 0.2	3.0 ± 0.2 3.0 ± 0.5
		4.0 ± 0.5	4.5 ± 0.5	5.0 ± 0.5	2.5 ± 0.5	4.8 ± 0.2	
						5.0 ± 0.5	
						5.0 ± 0.2 4.5 ± 0.5	

obtained from mono-exponential curves. This indicates that there are no domains with different mobilities in the sample and the various residues behave exactly in the same way, independently from the protein they belong to. As a consequence, it is expected that all the protons in the sample have the same $T_{1\rho}$, whereas values varying from 5.0 ± 0.5 to 9.4 ± 0.2 ms are found. Either a not sufficiently efficient mechanism of spin diffusion or an extremely high mobility of the sample, and thus $T_{1\rho}$ higher than the minimum value (Fig. 5.6), might be the causes of the observed behaviour.

Hydrating collagen/elastin samples up to a water content of 22 ± 1 % w/w resulted in faster proton spin-lattice relaxation times in the rotating frame than at 10 ± 1 % w/w hydration. At these conditions, all ^1H $T_{1\rho}$ had similar values of approximately 4 ms, suggesting that spin diffusion equilibrated the relaxation of all protons [17, 48]. In a mixture, like the prepared collagen and elastin one, such a rapid exchange through dipole-dipole interactions indicates that the sample is well-homogenised and all the protons are in contact on a molecular distance [24].

Collagen ^{13}C $T_{1\rho}$

To complement the proton spin-lattice relaxation time measurement, the ^{13}C $T_{1\rho}$ was determined. Differently from the ^1H $T_{1\rho}$, the spin-lattice relaxation times in the rotating frame of the carbon atoms cannot be influenced by spin diffusion effects, because of its low abundance (~1%). It is interesting to note that the ^{13}C spin-lattice relaxation times of different amino acid residues of 10 ± 1 % w/w hydrated collagen revealed substantial differences. As seen from the ^{13}C CP/MAS NMR spectra of collagen, in the carbonyl region, the broad signal is a superposition of three different resonances at 168.2, 170.9 and 174.5 ppm, respectively. Each of these peaks can be described by mono-exponential decays yielding ^{13}C $T_{1\rho}$ values of 51 ± 0.5 , 55 ± 0.5 and 61 ± 0.5 ms, respectively. Values varying between 15 ± 0.5 and 36 ± 0.5 ms were instead observed for the side chain carbons of hydrophobic amino acids (18-71 ppm), thus showing their higher mobility compared to the C-atoms of the carbonyls of the polypeptide (Table 5.5). The lower flexibility of the backbone compared to the side chains of collagen is known [50] and can be attributed to the tight packing of the collagen triple helix preventing motions in CO.

Increasing the water content to 22 ± 1 % w/w induced significantly more mobility in the entire collagen molecule, as witnessed by a sharp decrease in ^{13}C $T_{1\rho}$ for all resonances. In the hydrophobic region, relaxation times as short as 2.0-11.5 ms were found, thus showing the

Table 5.5. Rotating frame spin-lattice carbon relaxation times (^{13}C $T_{1\rho}$) for collagen, elastin and collagen/elastin samples (weight ratio 1:1) having different degrees of hydration. All relaxation data could be satisfactorily described by mono-exponential decays. Multiple values are expressed when a peak could be deconvoluted in more than one Lorentzian lineshape. All the values have a standard deviation of ± 0.5 ms.

Shift (ppm)	Carbon type	^{13}C $T_{1\rho}$ of 10% hydrated samples (ms)			^{13}C $T_{1\rho}$ of 22% hydrated samples (ms)		
		Collagen	Elastin	Coll / El	Collagen	Elastin	Coll / El
18	C_β (Ala)	36.0	39.0	37.0	11.5	28.0	51.5
		24.0	22.0	24.5	8.0	24.0	29.0
25	$\text{C}_{\beta,\gamma}$ (Pro)	17.0	6.0	19.5	4.0	12.0	12.0
	C_β (Val)	15.0	5.0	18.5	2.0 4.0	10.0	10.0
43	C_α (Gly)	20.0	7.0	28.0	4.0	10.0	12.0
50	C_α (Ala)	24.0	15.0	55.5	9.0	15.0	23.0
		35.0	20.0				23.0
55	C_α (Glu)	27.0	13.0	38.5	7.5	19.5	22.0
60	C_α (Pro, HyPro)	35.0	18.0	29.0	10.0	13.0	20.0
71	C_γ (HyPro)	17.0	-	n.d.	9.0	-	9.0
		16.0					
171-175	Carbonyl (C=O)	51.0	37.0	50.0	40.5	55.0	55.0
		55.0	40.0	55.5	27.0	32.0	52.0
		61.0			22.0		

high mobility of these side chains. At this water content, long relaxation times of 11.5 ± 0.5 ms are found for the C_β of Ala at 17.7 ppm (Table 5.5). This is thought to be due to the restricted possibility for rotation of the CH_3 groups because of steric hindrance, since the collagen triple helix is more tightly packed than a regular helix in other proteins [19]. In all cases mono-exponential decays described the relaxation behaviour, indicating that different structures in the

molecules are well interdispersed. This is important especially in the carbonyl region, where three different spin-lattice relaxation times in the rotating frame varying between 22.0 ± 0.5 and 40.5 ± 0.5 ms are measured. Each of them may be indicative for one of the different structures present in the molecule. In particular, it is expected that the mobility of the triple-helical portions will be less influenced by the addition of water and thus have long $T_{1\rho}$ of 40.0 ms.

Elastin ^{13}C $T_{1\rho}$

The ^{13}C $T_{1\rho}$ values of main chain and side chain carbon atoms of elastin at low hydration levels of 10 ± 1 % w/w, revealed that elastin appears to be more mobile than collagen under the same conditions (Table 5.5). This is consistent with the observation that even at low concentrations, water confers high conformational flexibility to elastin [51, 52]. In contrast to other globular proteins, which respond to hydration by structural ordering, even very low percentages of water in elastin results in high mobility. The strong hydration dynamics of elastin suggests that the protein has an open structure that allows water to induce considerable motion. A similar dynamic response to hydration has also been observed in glycogen, a highly branched polysaccharide with a large void volume [10]. In the present study, very mobile groups having relaxation times of approximately 5.0-7.0 ms were found in the hydrophobic region of 10 ± 1 % w/w hydrated elastin for the C_{α} of Gly and $C_{\beta,\gamma}$ of Pro at 25-43 ppm. Comparable relaxation times of 5.0 ms were found for the same groups in samples of insoluble elastin [48]. The carbonyl groups have relaxation times of 37.0-40.0 ms (Table 5.5). The signal from the carbonyl group originates from overlapping peaks at 172-175 ppm, thus underlining the different conformations (*i.e.* α -helix, β -sheet, random unfolded structures) present in this protein. In particular, it is known that in proteins the presence of a peak centred at 172.5-173 ppm, is indicative of extensive β -strands [48]. This is consistent with previous solid-state NMR studies on hydrated insoluble elastin, as well as with circular dichroism results [18]. Slightly different $T_{1\rho}$ values are observed for the differently organized portions of the molecule. In all cases mono-exponential decays are obtained, indicating that no separate domains are present in elastin.

Increasing the water content to 22 ± 1 % w/w, resulted in longer relaxation times for all the groups except the C_{α} of Pro and HyPro, C_{β} of Ala and portions of the carbonyl groups for which mobility increased at the higher hydration level (Table 5.5). These results are consistent with the hydrophobicity of elastin, which results in slightly increased mobility at higher

hydration levels of 22 ± 1 % w/w, for the groups that can interact with water. The longer relaxation times observed for the C_β of Ala may derive from restrictions of the motions of this atom due to its hydrophobicity and subsequent reluctance of interacting with water. As for the carbonyl groups, increasing the water content results in longer $T_{1\rho}$ values for certain portions, probably more organized, like the α -helical or β -sheets.

Collagen/elastin ^{13}C $T_{1\rho}$

A broader range of ^{13}C $T_{1\rho}$ relaxation times was found for the collagen/elastin sample (Table 5.5). At lower hydration levels of 10 ± 1 % w/w, the long relaxation times of approximately 50.0-55.0 ms for the carbonyl carbon atoms at approximately 170 ppm suggested that the backbone mobility was highly restricted in both the disordered and ordered portion of the molecule. The lower ^{13}C $T_{1\rho}$ values of the carbon atoms of the aliphatic amino acid residues (18.5-38.5 ms) showed that these atoms are more mobile than the carbons in the carbonyls. However, the relaxation times measured in this region are longer than those observed in the single proteins before mixing. The only exception to this general trend is observed for the C_β of Ala, having a spin-lattice relaxation time in the rotating frame of 24.5-37 ms, comparable to that observed in collagen or in elastin. Another interesting feature is the equilibration of the ^{13}C $T_{1\rho}$ of C_α of Ala to one single value of 55.5 ms, as compared to the two separate ones found in the two proteins. This suggests that in the mixture, there is a high degree of homogeneity and the C_α of Ala residues belonging to the two different proteins cannot be distinguished.

Increasing the water content to 22 ± 1 % w/w resulted in a slight stabilization of the backbone of collagen/elastin samples, whereas the ^{13}C $T_{1\rho}$ of all other carbon atoms (except C_β from Ala) decreased as compared to the values measured at 10 ± 1 % w/w hydration (Table 5.4). The observed longer $T_{1\rho}$ of C_β of Ala suggests that the mobility of the side chains of Ala is restricted by hydrophobic interactions.

We have recently reported that in a mixture of freeze-dried insoluble collagen and insoluble elastin, collagen tends to enwrap and bridge different elastin fibres together. This results in alignment of the fibres of the two proteins in the same spatial direction in the assembly [35]. The presence of interactions between collagen and elastin was investigated by ^{13}C CP/MAS NMR. Though the simultaneous presence of the two proteins does not induce any detectable

conformational or local order change in collagen or elastin, it affects significantly the mobility of the different amino acid residues of the two components.

Variations in the hydration level strongly affect the ^1H $T_{1\rho}$ of hydrophilic collagen, whereas the proton spin-lattice relaxation times in the rotating frame of elastin are hardly influenced by this, thus illustrating its hydrophobic nature. The higher hydrophilicity of collagen as compared to elastin was further verified by the difference of the ^{13}C $T_{1\rho}$ values for the two proteins at 22 ± 1 % w/w. Collagen had lower ^{13}C $T_{1\rho}$ than those measured for elastin under the same conditions.

Mixing collagen and elastin together also influenced the mobility of the separate components, as anticipated by ^{13}C CP/MAS NMR spectra and confirmed by analyses of the relaxation times. In all cases, the presence of separate domains with only one particular structure (*i.e.* α -helix or β -sheets) can be excluded, because the spin-lattice relaxation in the rotating frame can be described by mono-exponential decays. Moreover, the values of T_{1S} are not significantly different for collagen and collagen/elastin samples at 10 ± 1 % w/w hydration. In collagen/elastin mixtures both proton and carbon $T_{1\rho}$ are higher than those obtained for the separate components, illustrating the presence of interactions between the two proteins. In particular, at 10 ± 1 and at 22 ± 1 % w/w, the measured values for the ^{13}C $T_{1\rho}$ show reduced mobility of hydrophobic amino acid side chains of collagen/elastin as compared to the proteins alone. This is thought to depend on the presence of hydrophobic interactions. Similar increases in relaxation times were in fact observed in collagen after mineralization [53] or in elastin after deposition of hydrophobic ligands, such as cholesterol and esters [54]. In the same way, also the relaxation times of the hydrophilic amino acid residues increase after mixing of collagen and elastin, thus illustrating the formation of hydrogen bonds between different portions of the two proteins.

Conclusions.

In this study, ^{13}C CP/MAS NMR has been used to investigate the nature of the interactions occurring between soluble collagen and soluble elastin at two different hydration levels. To our knowledge this has not been reported before. The simultaneous presence of both proteins did not induce any detectable conformational or local order change in collagen or elastin and yielded specimens in which the two proteins were homogeneously mixed. This was verified by the cross-relaxation times and by the uniform $T_{1\rho}$ values, which could be described with mono-

exponential decays in collagen/elastin samples. Both proton and carbon T_{1ρ} values were higher in the mixture as compared to the separate components, indicating lower mobility and occurrence of hydrogen bonding and hydrophobic interactions between the two proteins.

In vivo, the presence of both collagen and elastin is often necessary for the functionality of a tissue or organ. The particular assembly of proteins investigated in this study is different from that encountered *in vivo*, where collagen and elastin are not interdispersed in aggregates.

Acknowledgments.

H.Th.B. van Moerkerk and T. van Kuppevelt (Department of Biochemistry 194, University of Medical Centrum Nijmegen, The Netherlands) are kindly acknowledged for performing the amino acid analyses.

References.

1. Faury, G., Function-structure relationship of elastic arteries in evolution: from microfibrils to elastin and elastic fibres. *Pathol. Biol.*, 2001. 49(4): 310-325.
2. Lee, C.H., Singla, A., and Lee, Y., Biomedical applications of collagen. *Inter. J. Pharm.*, 2001. 221(1-2): 1-22.
3. Hafemann, B., Ensslen, S., Erdmann, C., Niedballa, R., Zuhlke, A., Ghofrani, K., and Kirkpatrick, C., Use of a collagen/elastin-membrane for the tissue engineering of dermis. *Burns*, 1999. 25(5): 373-384.
4. Lefebvre, F., Gorecki, S., Bareille, R., Amedee, J., Bordenave, L., and Rabaud, New artificial connective matrix-like structure made of elastin solubilized peptides and collagens: elaboration, biochemical and structural properties. *Biomaterials*, 1992. 13(1): 28-33.
5. Goissis, G., Suzigan, S., Parreira, D.R., Maniglia, J.V., Braile, D.M., and Raymundo, S., Preparation and characterization of collagen-elastin matrices from blood vessels intended as small diameter vascular grafts. *Artif. Organs*, 2000. 24(3): 217-223.
6. Nimni, M.E., Collagen: molecular structure and biomaterial properties, in *Encyclopedia handbook of biomaterials and bioengineering materials*, Deheler, M., Editor. 1995: New York. 1229-1243.

7. Orgel, J.P.R.O., Miller, A., Irving, T.C., Fischetti, R.F., Hammersley, A.P., and Wess, T.J., The in situ supermolecular structure of type I collagen. *Structure*, 2001. 9(11): 1061-1069.
8. Urry, D.W., Ohnishi, T., Long, M.M., and Mitchell, L.W., Studies on the conformation and interactions of elastin: nuclear magnetic resonance of the polyhexapeptide. *Int. J. Peptide Proteins Res.*, 1975. 7: 367-378.
9. Debelle, L. and Tamburro, A.M., Elastin: molecular description and function. *Int. J. Biochem. Cell Biol.*, 1999. 31(2): 261-272.
10. Yao, X.L., Conticello, V.P., and Hong, M., Investigation of the dynamics of an elastin-mimetic polypeptide using solid-state NMR. *Magn. Reson. Chem.*, 2004. 42: 267-275.
11. Schaefer, J., Stejskal, E.O., Brewer, C.F., Keiser, H.D., and Sternlicht, H., Cross polarization ^{13}C nuclear magnetic resonance spectroscopy of collagen. *Arch. Biochem. Biophys.*, 1978. 190(2): 657-661.
12. Renou, J.P., Bonnet, M., Bieliki, G., Rochdi, A., and Gatellier, P., NMR study of collagen-water interactions. *Biopolymers*, 1994. 34: 1615-1626.
13. Consonni, R., Santomo, L., Tenni, R., Longhi, R., and Zetta, L., Conformational study of a collagen peptide by H-1 NMR spectroscopy: observation of the N-14-H-1 spin-spin coupling of the Arg guanidinium moiety in the triple-helix structure. *Febs Letters*, 1998. 436(2): 243-246.
14. Brodsky, B. and Ramshaw, J.A.M., The collagen triple-helix structure. *Matrix Biol.*, 1997. 15(8-9): 545-554.
15. Melacini, G., Bonvin, A.M.J.J., Goodman, M., Boelens, R., and Kaptein, R., Hydration dynamics of the collagen triple helix by NMR. *J. Mol. Biol.*, 2000. 300(5): 1041-1049.
16. Martino, M., Coviello, A., and Tamburro, A.M., Synthesis and structural characterization of poly(LGGVG), an elastin-like polypeptide. *Intern. J. Biol. Macromolecules*, 2000. 27(1): 59-64.
17. Perry, A., Stype, M.P., Tenn, B.K., and Kumashiro, K.K., Solid-state ^{13}C NMR reveals effects of temperature and hydration on elastin. *Biophys. J.*, 2002. 82: 1086-1095.
18. Kumashiro, K.K., Kurano, T.L., Niemczura, W.P., Martino, M., and Tamburro, A.M., ^{13}C CPMAS NMR studies of the elastin-like polypeptide (LGGVG)_n. *Biopolymers*, 2003. 70(2): 221-226.
19. Reichert, D., Pascui, O., deAzevedo, E.R., Bonagamba, T.J., Arnold, K., and Huster, D., A solid-state NMR study of the fast and slow dynamics of collagen fibrils at varying hydration levels. *Magn. Reson. Chem.*, 2004. 42: 276-284.

20. Stejskal, E.O. and Memory, J.D., High resolution NMR in the solid state. Fundamentals of CP/MAS, Oxford University Press. 1994.
21. Schaefer, J., Sefcik, M.D., Stejskal, E.O., and McKay, R.A., Carbon-13 T_{1ρ} experiments on solid polymers having tightly spin-coupled protons. *Macromolecules*, 1984. 17: 1118-1124.
22. Serrano, P.J., van Duynhoven, J.P.M., Gaymans, R.J., and Hulst, R., Morphology of alternating poly(ester amide)s based on 1,4-butylene established by ¹³C solid-state NMR relaxation measurements. *Macromolecules*, 2002. 35: 8013-8019.
23. Sefcik, M.D., Schaefer, J., Stejskal, E.O., and McKay, R.A., Analysis of the room-temperature molecular motions of poly(ethylene terephthalate). *Macromolecules*, 1980. 13: 1132-1137.
24. Dickinson, L.C., Yang, H., Chu, C.W., Stein, R.S., and Chien, J.C.W., Limits to compatibility in poly(x-methylstyrene)/poly(2,6-dimethylphenylene oxide) blends by NMR. *Macromolecules*, 1987. 20: 1757-1760.
25. Armitage, I.M., Huber, H., Pearson, H., and Roberts, J.D., Nuclear magnetic resonance spectroscopy. Carbon-13 spin-lattice relaxation time measurements of amino acids. *Proc. Natl. Acad. Sci.*, 1974. 71(5): 2096-2097.
26. Miclet, E., Williams, D.C., Clore, G.M., Bryce, D.L., Boisbouvier, J., and Bax, A., Relaxation-optimized NMR spectroscopy of methylene groups in proteins and nucleic acids. *J. Am. Chem. Soc.*, 2004. 126(34): 10560-10570.
27. Holmgren, K.S., Taylor, K.M., Bretscher, L.E., and Raines, R.T., Code for collagen's stability deciphered. *Nature*, 1998. 392.
28. Li, B., Alonso, D.O., Bennion, B.J., and Daggett, V., Hydrophobic hydration is an important source of elasticity in elastin-based biopolymers. *J. Am. Chem. Soc.*, 2001. 123(48): 11991-11998.
29. Detken, A., Hardy, E.H., Ernst, M., and Meier, B.H., Simple and efficient decoupling in magic-angle spinning solid-state NMR: the XiX scheme. *Chem. Phys. Lett.*, 2002. 356(3-4): 298-304.
30. Huster, D., Schiller, J., and Arnold, K., Comparison of collagen dynamics and isolated fibrils by solid-state in articular cartilage NMR Spectroscopy. *Magn. Reson. Med.*, 2002. 48(4): 624-632.
31. Saito, H. and Tabeta, R., A high-resolution ¹³C-NMR study of collagen like polypeptides and collagen fibrils in solid state studied by the cross-polarization magic

- angle-spinning method. Manifestation of conformation-dependent ^{13}C chemical shifts and application to conformational characterization. *Biopolymers*, 1984. 23: 2279-2297.
32. Pretsch-Clerc, Seibl, and Simon, Tables of spectral data for structure determination of organic compounds. 2nd ed, Springer-Verlag. 1989.
 33. Kricheldorf, H.R. and Muller, D., Secondary structure of peptides:15. A ^{13}C NMR CP/MAS study of solid elastin and proline-containing copolyesters. *Inter. J. Biol. Macromol.*, 1984. 6: 145.
 34. Saito, H. and Yokoi, M., A ^{13}C NMR study on collagens in the solid state: hydration/dehydration-induced conformational change of collagen and detection of internal motions. *J. Biochem.*, 1992. 111: 376-382.
 35. Buttafoco, L., Engbers-Buijtenhuijs, P., Poot, A.A., Dijkstra, P.J., Daamen, W.F., van Kuppevelt, T.H., Vermes, I., and Feijen, I., First steps towards tissue engineering of small diameter blood vessels: preparation of flat scaffolds of collagen and elastin by means of freeze drying. *Submitted to J. Biomed. Mat. Res.*
 36. Sandberg, L.B., Soskel, N.T., and Leslie, J.G., Elastin structure, biosynthesis, and relation to disease states. *N. Engl J Med.*, 1981. 304(10): 566-579.
 37. Mammi, M., Gotte, L., and Pezzin, G., Evidence for order in the structure of alpha-elastin. *Nature*, 1968. 220(165): 371-373.
 38. Boland, E.D., Matthews, J.A., Pawlowski, K.J., Sompson, D.G., Wnek, G.E., and Gary, L., Electrospinning collagen and elastin: preliminary vascular tissue engineering. *Front. Biosci.*, 2004. 9: 1442-1432.
 39. Buttafoco, L., Kolkman, N.G., Engbers-Buijtenhuijs, P., Poot, A.A., Dijkstra, P.J., Vermes, I., Feijen, J., Electrospinning of collagen and elastin for tissue engineering applications. *Submitted to Biomaterials.*
 40. Lin, C.L., Kao, H.M., Wu, R.R., and Kuo, P.L., Multinuclear solid-state NMR, DSC and conductivity studies of solid polymer electrolytes based on polyurethane/poly(dimethylsiloxane) segmented copolymers. *Macromolecules*, 2002. 35(8): 3083-3096.
 41. Hou, W.H., Chen, C.Y., Wang, C.C., and Huang, Y.H., The effect of different lithium salts on conductivity of comb-like polymer electrolyte with chelating functional group. *Electrochim. Acta*, 2003. 48(6): 679-690.
 42. Nishiyama, N., Asakura, T., Suzuki, K., Horie, K., and Nemoto, K., Effects of a structural-change in collagen upon binding to conditioned dentin studied by C-13 NMR. *J. Biomed. Mat. Res.*, 1995. 29(1): 107-111.

43. Yang, Z., Liivak, O., Seidel, A., LaVerde, G., Zax, D.B., and Jelinski, L.W., Supercontraction and backcone dynamics in spider silk: ¹³C and ²H NMR studies. *J. Am. Chem. Soc.*, 2000. 122: 9019-9025.
44. Simmons, A., Ray, E., and Jelinski, L.W., Solid-state C-13 NMR of nephila-clavipes dragline silk establishes structure and identity of crystalline regions. *Macromolecules*, 1994. 27(18): 5235-5237.
45. Wang, J.X., Parkhe, A.D., Tirrell, D.A., and Thompson, L.K., Crystalline aggregates of the repetitive polypeptide {(AlaGly)₃GluGly(GlyAla)₃GluGly}₁₀: Structure and dynamics probed by C-13 magic angle spinning nuclear magnetic resonance spectroscopy. *Macromolecules*, 1996. 29(5): 1548-1553.
46. De Guzzi Plepis, A.M., Goissis, G., and Das-Gupta, D.K., Dielectric and pyroelectric characterization of anionic and native collagen. *Polym. Eng. Sci.*, 1996. 36(24): 2932-2938.
47. Marzec, E., The dielectric-relaxation time of collagen over a wide temperature-range. *J. Mat. Sci.*, 1995. 30(20): 5237-5240.
48. Kumashiro, K.K., Kim, M.S., Kaczmarek, S.E., Sandberg, L.B., and Boyd, C.D., ¹³C Cross-polarization/magic angle spinning NMR studies of alfa-elastin preparations show retention of overall structure and reduction of mobility with a decreased number of cross-links. *Biopolymers*, 2001. 59: 266-275.
49. Kumashiro, K.K., Schmidt-Rohr, K., Murphy, O.J., Ouellette, K.L., Cramer, W.A., and Thompson, L.K., A novel tool for probing membrane protein structure: Solid-state NMR with proton spin diffusion and X-nucleus detection. *J. Am. Chem. Soc.*, 1998. 120(20): 5043-5051.
50. Torchia, D.A., Batchelder, L.S., Fleming, W.W., Jelinski, L.W., Sarkar, S.K., and Sullivan, C.E., Mobility and function in elastin and collagen. *Ciba Found. Symp.*, 1993. 93: 98-115.
51. Rousseau, R., Schreiner, E., Kohlmeyer, A., and Marx, D., Temperature-dependent conformational transitions and hydrogen-bond dynamics of the elastin-like octapeptide GVG(VPGVG): a molecular-dynamics study. *Biophys. J.*, 2004. 86: 1393-1407.
52. Fleming, W.W., Sullivan, C.E., and Torchia, D.A., Characterization of molecular motions in ¹³C-labeled aortic elastin by ¹³C-¹H magnetic double resonance. *Biopolymers*, 1980. 19(3): 597-617.
53. Sarkar, S.K., Sullivan, C.E., and Torchia, D.A., Solid state ¹³C NMR study of collagen molecular dynamics in hard and soft tissues. *J. Biol. Chem.*, 1983. 258(16): 9762-9767.

54. Lillie, M.A. and Gosline, J.M., Effects of lipids on elastin's viscoelastic properties. *Biopolymers*, 2002. 64(3): 127-138.

Chapter 6

Development of a Bioreactor for Tissue Engineering of Small-Diameter Blood Vessels: Design of a Pulsatile Flow System*.

If we knew what we were doing it wouldn't be research.

(A.Einstein)

Abstract.

A pulsatile flow bioreactor for tissue engineering of small-diameter blood vessels was developed. The bioreactor consists of four vessels mounted in four parallel chambers. Culture medium can be perfused through the vessels inside the chambers using a peristaltic pump. The closed-circuit system was pressurised to 100 mmHg. This set up allows pulsatile flow (120 beats/min) and fluctuation of pressure inside the vessels between approximately 80 and 120 mmHg, simulating physiological conditions. Two types of vessels were used to further characterize the system. Vessels were either made of non-porous silicone rubber or of porous collagen/elastin crosslinked with N-(3-dimethylaminopropyl)-N'-ethylcarbodiimide (EDC) and N-hydroxysuccinimide (NHS). The latter scaffolds were seeded with smooth muscle cells (SMC) and cultured in the bioreactor up to 14 d.

The flow rate in the vessels increased linearly with the number of beats/min. At an average flow rate of 9.6 ml/min, an average wall shear rate of 61 s^{-1} was reached, comparable to the

* L. Buttafoco¹, P. Engbers-Buijtenhuijs^{1,2}, A.A. Poot¹, P.J. Dijkstra¹, I. Vermes^{1,2} and J. Feijen¹

Submitted to Biotech. Bioeng.

¹ Department of Polymer Chemistry and Biomaterials, Faculty of Science and Technology and Institute of Biomedical Technology (BMTI), University of Twente, Enschede, P.O. Box 217, 7500 AE, The Netherlands.

² Hospital Group Medisch Spectrum Twente, Department of Clinical Chemistry, P.O. Box 50.000, 7500 KA Enschede, The Netherlands.

lower wall shear rates in the human carotid artery (60-775 s⁻¹). Increasing the flow rate from 3 to 9.6 ml/min leads to an increase of Reynolds numbers from 29 to 96, which is also in the same range as found for the carotid artery. Pressures were monitored proximal and distal to the vessels and outside the vessels in the chambers. After 1 d of culture of SMC on crosslinked collagen/elastin scaffolds in the bioreactor, no significant differences were measured between the average pressures over the wall and along the length of the tube. After 14 d of culture, the average pressure inside the vessel was 14 mmHg higher than the average pressure outside the vessel, which is caused by decreased permeability of the tube after longer culture times. A versatile bioreactor for vascular tissue engineering, able to accommodate a broad range of vessel sizes, easy to handle, clean and maintain was thus developed. Moreover, this system can be used as a valuable *in vitro* model to study the effects of physical forces on (developing) tissues and to predict the response of tissue-engineered constructs once implanted *in vivo*.

Introduction.

Tissue engineering is a discipline that applies the principles of engineering and life sciences for the development of biological substitutes that can restore, maintain or improve tissue functions. For this reason, polymeric scaffolds, which function as temporary templates with adequate mechanical properties to prevent failure of the constructs during dynamic culture, have been developed. The ideal engineered scaffold should degrade and resorb at a controlled rate, to match cell proliferation, extra-cellular matrix (ECM) production and tissue ingrowth *in vitro* and/or *in vivo*. Finally, the resulting tissue should mimic the biomechanical characteristics of the natural tissue [1].

Vascular tissue engineering deals with creating functional blood vessels *in vitro*, either to treat (cardio-)vascular diseases or to develop models to study vascular biology [2]. Most vascular tissue engineering strategies aim at creating grafts mimicking the three-layered structure of a natural blood vessel. One strategy to create these biological substitutes is to use cells seeded in porous scaffolds. Various tissue engineering approaches have been proposed, using either natural [3-6] or synthetic [7-9] materials, but many challenges still have to be overcome before a suitable vascular replacement is available [10]. In the past, either vascular cell culture models [11, 12] or animal models [13, 14] have been used to evaluate the effects of chemical and mechanical stimuli on cell proliferation, phenotype, alignment, migration and ECM production. However, the proper phenotype of cells and mechanical stimuli for cell organisation and development of the desired ECM structure are often lacking in cell culture models [15]. These

characteristics are more easily accomplished in animal models, but, in this case, it is not possible to study the effect of distinct factors (*e.g.* growth factors) or to vary the hemodynamics.

With the development of bioreactors, advantages of both cell culture and animal models were combined. Bioreactors are generally defined as devices in which biological and/or biochemical processes develop under closely monitored and tightly controlled environmental and operating conditions [16]. For tissue engineering of blood vessels, numerous research groups have designed their own bioreactors. In particular, spinner flasks and rotating bioreactors have been developed to enhance mass transfer of nutrients, oxygen and waste products [17]. In the spinner flask bioreactor, culture medium is flowing continuously around immobile scaffolds. During seeding, cells are transported to and into the scaffold by convection. The flow of the medium enhances mass transfer but may also generate turbulent eddies. These could be detrimental for the development of the new tissue, since a turbulent flow generally prevents a homogeneous distribution of oxygen and nutrients throughout the construct [18].

Rotating bioreactors provide the constructs with a dynamic culture environment, laminar flow and high mass transfer rates. However, these systems are often complex, expensive or not capable of reproducing physiological hemodynamics [16, 17]. Other bioreactors [9, 19-22] have been manufactured to mimic the physiological conditions of the human vasculature and to investigate the role of single factors. The most detailed analysis of such a bioreactor is reported by Conklin *et al.* [15], who described a system able to generate a pulsatile flow by means of a cam-driven syringe, a peristaltic pump and a compliance chamber. Physiological haemodynamics could thus be simulated and the effect of different factors, like shear stress or pressure, was evaluated on intact vascular tissue for up to 48 h. All these studies demonstrated that an environment resembling *in vivo* conditions may promote both the development of constructs with sufficient mechanical strength to be implanted and the modulation of appropriate cellular functions. However, the optimal bioreactor set up and culture conditions for the development of a functional arterial graft remain to be elucidated and the biggest challenge remains how to grow three-dimensional structures that contain more than a few layers of SMC [23].

The objective of this study is to develop a bioreactor for tissue engineering of small-diameter blood vessels. Such a bioreactor should be suitable to develop functional tissue-engineered vascular grafts from constructs incorporating living human vascular smooth muscle cells (SMC) embedded in scaffolds composed of natural proteins and/or synthetic

polymers. These constructs should be ultimately lined with endothelial cells (EC) to provide a living, responsive and non-thrombogenic blood conduit. In order to reach this aim, a compact and relatively inexpensive bioreactor, adapted from the system devised by Bardy *et al.* [24] and Perrée *et al.*[25], was developed in our laboratories. In this bioreactor, physiologic-like flow and pressure were mimicked. The flow dynamics of the system were characterized using either a silicone tube or a porous tubular scaffold of insoluble collagen and insoluble elastin as vessel. The flow conditions in the bioreactor were compared to those experienced *in vivo*. Moreover, the system was set up to culture SMC-seeded porous tubular scaffolds and thus to investigate the response of these constructs to dynamic loading.

Materials and Methods.

Bioreactor system.

A pulsatile flow system was designed for tissue engineering of small-diameter vascular grafts (Figure 6.1). A peristaltic roller-pump (Watson Marlow Sci-Q-323, Brussels, Belgium) was used to pump fluid from a custom-made three-port glass fluid reservoir via highly distensible silicone tubing (Watson Marlow, Brussels, Belgium, 3.2 mm ID x 6.4 mm OD) to four custom-made glass chambers and back to the fluid reservoir.

Approximately three-quarters of the fluid reservoir (60 ml) were filled with culture medium, while air filled the remaining volume. The air acts as a source of oxygen for the cells during culturing and is used to achieve the desired pressure. A pressure of 100 mmHg was applied to the fluid reservoir and regulated by means of an electronically controlled Venturi valve (T5200-50, Fairchild Company, Winston-Salem, NC, USA). The applied pressure was monitored proximal and distal to the vessels as well as outside the vessels in the glass chambers by pressure sensors (Edwards Lifesciences LLC, Unterschleissheim, GmbH, Instrumentation Department, Academic Medical Centre of Amsterdam, The Netherlands), and a scope meter (Fluke 199BM scopemeter, Adquipment Medical B.V., Hellevoetsluis, The Netherlands) throughout the duration of the experiment. The pressure sensors were calibrated at atmospheric pressure (0 mmHg) and 100 mmHg above atmospheric pressure before every experiment by a pneumatictransducer tester (DALE20, DALE technology, Carson city, NV, USA). Alternatively, pressure signals were displayed by an oscilloscope (DATEX cardiocap II, Helsinki, Finland). Two valves (DATEX, Helsinki, Finland) preventing a back flow of the culture medium, were inserted at the proximal and distal position of the chambers, in order to

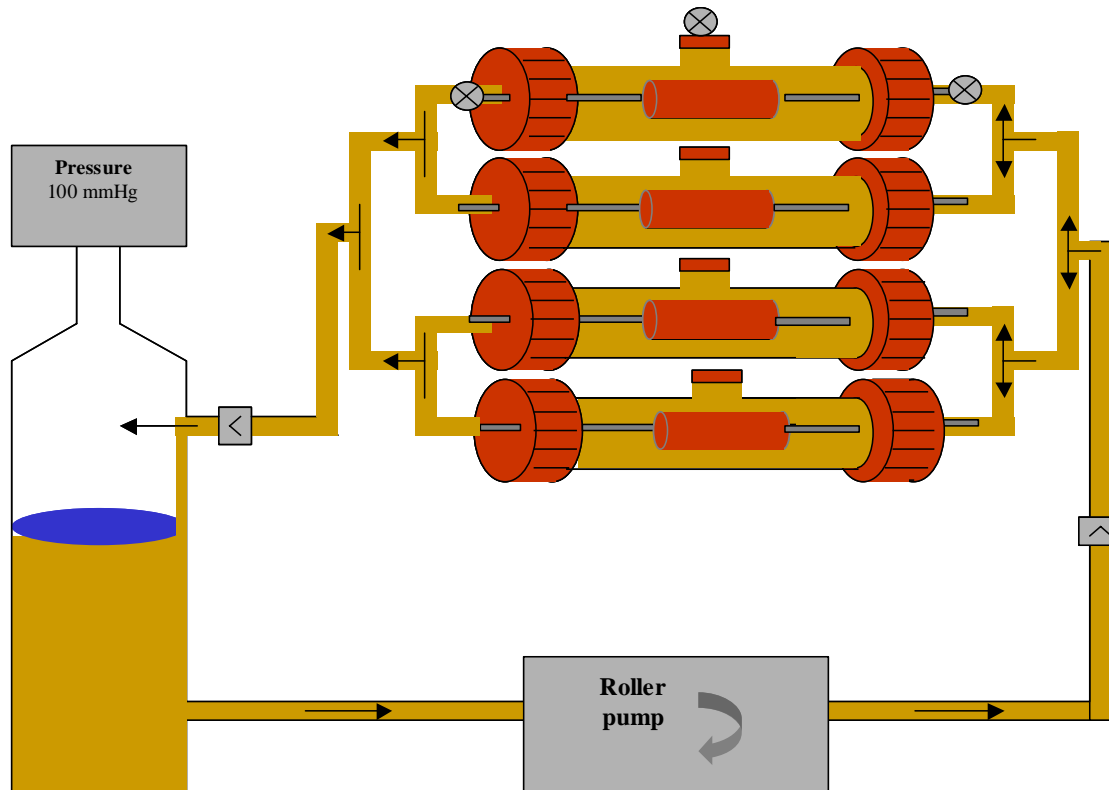


Figure 6.1. Schematic representation of the bioreactor used in this study. The vessels were mounted in four parallel chambers filled with fluid. The chambers were connected through silicone tubing to the peristaltic pump and the fluid reservoir, respectively. Fluid was perfused through the vessels inside the flow chambers. A pressure of 100 mmHg was applied to the fluid reservoir (\triangle represents a pressure sensor, \otimes represents a valve).

obtain a more accurate reproduction of the pressure wave-forms experienced by blood vessels *in vivo* during ventricular systole and diastole. In this particular design, four chambers could be placed in a single incubator in parallel with respect to each other, all driven by a single pump. Silicone tubing (Watson Marlow, Brussels, Belgium, 3.2 mm ID x 6.4 mm OD) was cannulated and tied on both ends with sutures (Ethicon Mersilene, Johnson & Johnson Intl., St. Stevens-Woluwe, Belgium) to thin-walled stainless-steel tubes having an outside diameter of 3 mm, which matches the inside diameter of the used vessels at physiological pressure. Alternatively, porous tubular scaffolds of insoluble collagen type I from bovine Achilles tendon and insoluble elastin from equine ligamentum nuchae (porosity 94%, average pore size 131 μm , ID 3 mm, OD 6 ± 1 mm) were used as vessel. Prior to use, these scaffolds were crosslinked with a carbodiimide N-(3-dimethylaminopropyl)-N'-ethylcarbodiimide (EDC) in combination with N-hydroxysuccinimide (NHS), as previously described [26]. SMC isolated

from human umbilical vein [27], were seeded on the crosslinked collagen/elastin scaffolds (10^7 cells/scaffold) by means of a filtration seeding procedure. The cells were dynamically cultured in the bioreactor for 1 up to 14 d.

During analyses, the vessels were mounted inside the chambers and these were connected to the silicone tubing by Discifix connectors (Discifix-3 and Discifix-5, B. Braun, Melsungen, AG, Germany). The outside of the vessels was in contact with culture medium in the chambers (ca. 20 ml). The fluid reservoir, the chambers containing the vascular grafts and the pressure sensors were placed in humidified atmosphere inside an incubator at 37 °C and 5% CO₂ (CleanAir Techniek bv, Woerden, The Netherlands). A peristaltic roller pump (Watson Marlow, Brussel, Belgium) inserted between the proximal side of the flow chambers and the fluid reservoir, generated pressure pulses in the system (30-120 beats/min). Vessels of various lengths and diameters could be accommodated in this system and cultured for extended periods of time. Vessels with a length of approximately 4 cm were used for the experiments described in this paper.

Flow dynamics.

Simplified model of an artery.

In order to make an estimation of the flow characteristics in the vessels, several major simplifications have been made. It is assumed that:

- the vessels are straight, non-porous, rigid tubes, with a smooth luminal surface;
- entrance effects are neglected;
- the flow inside the vessels is steady.

The flow dynamics of the system were studied using PBS instead of culture medium as a solvent. However, the reported results are also valid if culture medium is used, since the two fluids have a relative viscosity of 1.05.

Flow rate. The flow rate (φ) inside the vessels was determined experimentally, by measuring the volume of fluid collected from the silicone tubing mounted in each chamber during 1 min. The measurements were repeated 3 times.

Nature of the flow. The nature of the flow (laminar or turbulent) inside the vessels was evaluated by calculating the Reynolds number (Re) [28]:

$$\text{Re} = \frac{d * \bar{V} * \rho}{\mu} \quad (6.1)$$

where d is the internal diameter of the vessel (0.3 cm), ρ the density (1 g/cm³) and μ the viscosity of PBS (0.719 centipoise at 37 °C). The mean velocity (\bar{V}) was calculated from the flow rate ($\varphi = (\bar{V} * \pi * d^2) / 4$).

Shear rate. The wall shear rate ($\dot{\gamma}$) was calculated from the following equation [28]:

$$\dot{\gamma} = \frac{4 * \varphi}{\pi * r^3} \quad (6.2)$$

where r is the radius of the vessel.

Shear stress. The wall shear stress (τ) was calculated from [29]:

$$\tau = \frac{4 * \mu * \varphi}{\pi * r^3} \quad (6.3)$$

Wall stress. The wall stress was calculated from [28]:

$$\text{Wall stress} = \frac{\bar{\Delta P} * r}{\text{Thickness}_{\text{wall}}} \quad (6.4)$$

where $\bar{\Delta P}$ is the average trans-wall pressure difference. This was calculated by subtracting the value of the mean pressure measured outside the vessel in the chamber from the mean pressure at the entrance of the vessel. The mean pressure was calculated by adding one third of the pulse pressure to the diastolic pressure (see below). The pulse pressure is the difference between systolic and diastolic pressure. No attenuation of the pressure wave because of the dissipative

mechanisms associated with the viscoelastic materials comprising the vessel wall was considered [30].

Results and Discussion

Bioreactors can be defined as devices in which biological and/or biochemical processes can be performed under controlled environmental conditions [16]. *In vivo* the blood vessel wall is continuously exposed to two types of haemodynamic forces: a tensile stress, which has a perpendicular, a circumferential and a longitudinal component relative to the vessel wall and a tractive force, caused by blood flow, parallel to the longitudinal axis of the vessel and determined by vessel geometry and fluid viscosity [31]. Mechanical stimuli contribute to induce orientation of both smooth muscle cells (SMC) [22, 32] and endothelial cells (EC) [33] and enhance ECM production and tissue formation thus yielding a more functional construct [34, 35].

In the current study, a sophisticated but simple bioreactor, adapted from the system devised by Bardy *et al.* [24] and Perrée *et al.* [25] was designed to improve the spatial distribution and organisation of the cells in porous tubular scaffolds for tissue engineering of small-diameter blood vessels. In this system, the vessels were cannulated inside glass chambers and connected through highly distensible silicone tubing to a peristaltic roller pump and to a fluid reservoir. In contrast to the flow system of Bardy *et al.* and Perrée *et al.*, four chambers placed in parallel were used in this study (Fig. 6.1). The peristaltic roller pump generated a continuous pulsatile flow through the lumen of the vessels. Moreover, in contrast to the former flow system, the glass chambers had no open connection to the air during perfusion.

In order to verify whether the haemodynamic forces present in the vessels are similar to those in arteries *in vivo* and thus to prove the applicability of this system for tissue engineering of blood vessels, the flow dynamic properties were estimated using the simplifications mentioned above. Blood vessels normally consist of a number of different materials and cells, arranged in a complex manner. About 70% of the walls of the arteries consists of water, whereas the rest is constituted by a mesh of fibres (*e.g.* collagen and elastin) with (visco)elastic properties. However, in order to describe the system developed in our laboratories with the equations available in literature, the vessels were assumed to be long, straight, rigid tubes, with a smooth and non-porous inner surface. Although the equations describing such tubes cannot account for the complexity of the cardiovascular system, they provide a good starting point [36].

Experimentally, it was found that increasing the rotational speed of the pump from 30 to 120 beats/min resulted in a linear increase of the average flow rate from 3.0 to 9.6 ml/min per vessel (Figure 6.2). No differences were observed in the flow recorded for each of the four parallel vessels. The measured flow rates are much lower than in the human carotid artery (5-35 ml/s) [38, 39]. However, it has been documented that mechanical stimulation in the form of a periodic stretch is the main factor influencing the orientation of SMC and the synthesis of ECM components [22, 37]. Therefore it was considered to be more important to mimic the pressure pulses in a native artery rather than the flow rate. In the developed set up, flow rate and pulsations cannot be controlled independently. However, use of two separate pumps to control the flow and the pressure pulses can easily solve this problem.

In the carotid artery, a waveform analogous to that shown in figure 6.3a is present. The systolic (120 mmHg) and diastolic (80 mmHg) pressure are the maximum and minimum pressure, respectively. The mean pressure (93 mmHg) is the average pressure throughout the cardiac cycle. It can be calculated by adding one third of the pulse pressure to the diastolic pressure. The pulse pressure is the difference between systolic and diastolic pressure. The possibility to reproduce these natural conditions in the vessels of the bioreactor is advantageous since it is known that dynamic mechanical conditioning induces SMC orientation in tissue-engineered constructs [40, 41]. When a silicone tube is used as vessel in our system and the rotational speed of the pump is set at 120 beats/min, the pressure in a position proximal to the vessel oscillates between 46 and 144 mmHg ($\bar{P} = 78$ mmHg) (Fig. 6.3b).

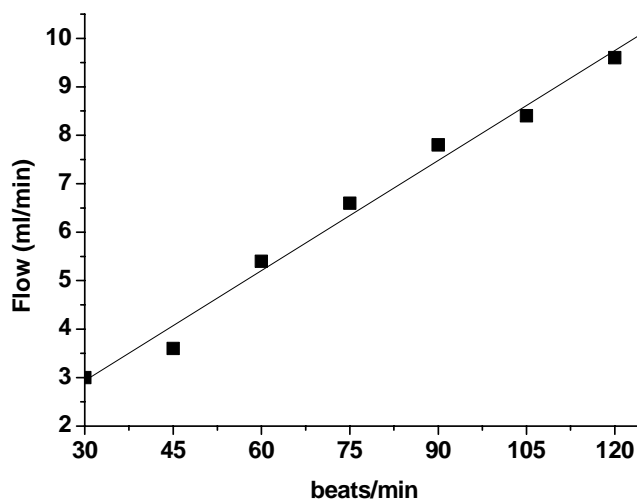


Figure 6.2. Dependence of the flow rate inside the vessels on the number of beats/min.

No significant pressure drop is observed along the length of the vessel ($\overline{\Delta P} = 4$ mmHg), since a pressure of 48-127 mmHg ($\overline{P} = 74$ mmHg) is found at the distal position. Though the measured values are different from those in a natural artery of a healthy subject (80-120 mmHg) [42], it is possible to reproduce a pressure waveform in the flow system similar to the natural one. Since the bioreactor described in this paper is a closed system, the pressure in the vessels mounted in the four separate chambers was the same.

In a human carotid artery, Reynolds numbers vary from 2 up to 560, depending on whether the values are calculated at the diastole or at the systole or whether the vessels have some atherosclerotic plaques [43]. In vessels with a diameter of 6 mm, a length of 20 cm and a mean blood velocity of 3.6 cm/s the Reynolds number is 72 [30]. Under the conditions described, Reynolds numbers vary between 29 (30 beats/min) and 96 (120 beats/min).

These values indicate that the flow is laminar ($Re < 2100$ [28]), a condition necessary to have efficient and homogeneous transfer of oxygen and nutrients to the three-dimensional construct. This transfer can be limited under static culture conditions, where the transport of nutrients and oxygen can only take place through diffusion [40]. Reduced nutrients and oxygen transfer to three-dimensional constructs is generally one of the main problems to be addressed in tissue engineering of blood vessels [16].

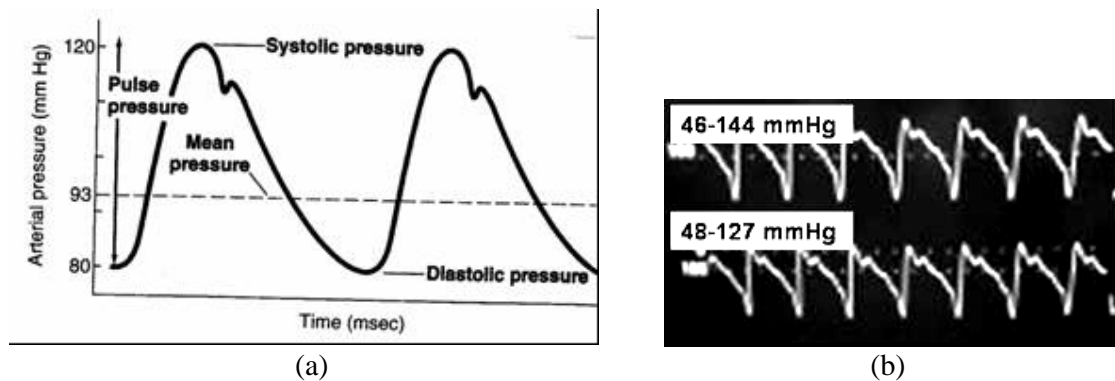


Figure 6.3. (a) Pressure waveform characteristic of the blood flow in the carotid artery. The mean pressure is the average pressure throughout the cardiac cycle; it equals diastolic pressure + $1/3$ pulse pressure. Pulse pressure is the difference between systolic and diastolic pressure; (b) Pressure waveform obtained in the pulsatile flow bioreactor, at an average pressure of 100 mmHg and 120 beats/min, with a silicone tube as vessel. Top and bottom curves: position proximal and distal to the vessel, respectively.

Under the conditions described above (120 beats/min, flow rate = 9.6 ml/min), the average wall shear rate is 61 s^{-1} , a value fitting the lower range of shear rates found in the human carotid artery ($60\text{-}775 \text{ s}^{-1}$) [44]. Changes of the vessel diameter and flow rate as a consequence of the pulsatile blood flow will influence this value causing its continuous variation.

Also the values of wall shear stress are important in tissue engineering of blood vessels, since wall shear stress is known to influence the biochemistry of endothelial cells [45] and the permeability of the arterial wall to macromolecules. *In vivo*, the different vessels adapt their internal diameter to blood flow, thus achieving minimal expenditure of energy for transportation of blood [45]. Under physiological circumstances, the mean wall shear stress varies from 10 to 26 dyne/cm^2 , from the aorta to the capillaries, respectively [46]. Mean wall shear stresses decrease with age due to the age-dependent increase in the diameter of blood vessels [47, 48]. In the system described in this study, the values of wall shear stress increase from 0.13 dyne/cm^2 at 30 beats/min to 0.43 dyne/cm^2 at 120 beats/min. Values down to $5 \cdot 10^{-4} \text{ dyne/cm}^2$ are known to enhance cell viability and proliferation [49]. Moreover, low-shear-stress preconditioning of tissue-engineered vascular grafts has been proven to be a successful method to enhance retention of seeded endothelial cells *in vitro* [50].

Arterial wall stress is another significant parameter in determining the properties of a vessel during arterial development and is dependent on the transmural pressure and on the mechanical properties of the vessel wall [51]. In a carotid artery, an average wall stress of $93 \cdot 10^3 \text{ dyne/cm}^2$ can be estimated considering a mean arterial pressure of 70 mmHg [52], an inner diameter of 4 mm and an outer diameter of 6 mm. As a consequence of the pulsatile blood flow, the vessel is continuously dilated and contracted. The transmural pressure, the inner and outer diameter of the vessel and the wall thickness determine the stress exercised on the wall of the vessel. In a closed system as described here, a difference in pressure observed along the length or across the wall of a vessel can be related to its porosity as well as to its elasticity. When silicone tubing is used as a vessel, the values of pressure recorded at the entrance, at the exit of the vessel and in the area surrounding it, in the flow chamber, are 46-144 mmHg, 48-127 mmHg and 63 mmHg, respectively (Fig. 6.3b). No significant pressure drop ($\overline{\Delta P} = 5 \text{ mmHg}$, $\overline{P}_{\text{entrance}} = 79 \text{ mmHg}$; $\overline{P}_{\text{exit}} = 74 \text{ mmHg}$) is present along the length of the vessel, whereas a maximum $\overline{\Delta P}$ of 16 mmHg is present across the wall of the silicone tube. The difference in pressure observed between the inner and outer side of the vessel is due to the lack of porosity of the silicone tube. The maximal trans-wall pressure of 16 mmHg resulted in an average wall

stress of $21 \cdot 10^3$ dyne/cm², much lower than that estimated for a human carotid artery. This low wall stress might contribute to prevent bursting of a scaffold once cultured in the bioreactor.

The pressures were measured under the same conditions (flow rate = 9.6 ml/min per vessel, 120 beats/min) with EDC/NHS crosslinked porous tubular scaffolds of collagen/elastin. In previous work, we have shown that crosslinking of collagen/elastin structures with EDC/NHS results in relatively stiff materials [26]. Moreover, it has been reported that the physical properties of a scaffold change in time during SMC culture [53]. After 1 d of culture with SMC under dynamic conditions, no significant differences in pressure were observed along the length or over the wall of the crosslinked collagen/elastin constructs ($P_{\text{entrance}} = 80\text{-}91$ mmHg; $P_{\text{exit}} = 81\text{-}91$ mmHg; $P_{\text{outside}} = 84\text{-}93$ mmHg). The high porosity of the vessels (94%) ensures equilibration of the pressure to an average value of 85 ± 2 mmHg, thus preventing attenuation of the pressure pulses. The absence of a trans-wall pressure difference in this particular case, most probably prevented the scaffolds from bursting. On the contrary, after 14 d of culture in such a dynamic environment, SMC have migrated and grown throughout the porous construct. SMC are responsible for the ability of a blood vessel to contract and to relax, thus enhancing the elasticity of the vessel [53]. Moreover, as a consequence of the presence of SMC, the porosity of the constructs decreases. Both these effects were visible in the pressure values recorded. A pressure of 61-124 mmHg was found at the entrance of the construct (Fig. 6.4), but due to the acquired elasticity and the decreased porosity of the construct, a pressure of 49-105 mmHg was measured in the environment around the construct in the flow chamber ($\overline{\Delta P}_{\text{wall}} = 14$ mmHg, $\overline{P}_{\text{entrance}} = 82$ mmHg, $\overline{P}_{\text{outside vessel}} = 68$ mmHg). This corresponds to an average wall stress of $19 \cdot 10^3$ dyne/cm², comparable to that observed with the silicone tube.

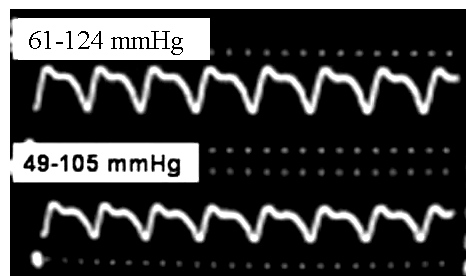


Figure 6.4. Pressure waveform obtained in the pulsatile flow bioreactor, at an average pressure of 100 mmHg and at 120 beats/min, with an EDC/NHS crosslinked porous tubular scaffold of collagen and elastin (weight ratio 1:1) cultured for 14 d with SMC. Top curve proximal position, bottom curve outside the vessel in the chamber.

Pressure values 51-102 mmHg, similar to those outside the vessel in the flow chamber, were found at the exit of the construct ($\overline{\Delta P}_{\text{length}} = 14$ mmHg, $\overline{P}_{\text{exit}} = 68$ mmHg). Evidently the attenuation of the pulse occurred partly through the wall and not along the length of the scaffold.

A suitable bioreactor for tissue engineering of small-diameter blood vessels has been developed. Further experiments are currently being performed to analyse the physical and biological properties of the collagen/elastin constructs and of SMC-seeded hybrid structures of poly(1,3-trimethylene carbonate)co(D,L-lactide) and insoluble collagen, cultured in the bioreactor.

Conclusions.

The bioreactor described in the current study is versatile and functional, being able to accommodate a broad range of vessel sizes, easy to handle, clean and maintain. Moreover, the possibility to disconnect the chambers from the bioreactor permits to seed the scaffolds *in situ*, reducing the risks associated with handling and transferring the constructs between different systems. The scaffolds can be accessed singularly, thus permitting to correct eventual anomalies in one of the vessels without affecting other samples. Continuous observation of the vessels is possible through the glass chamber walls by direct vision, thus allowing immediate detection of any macroscopic evidence of bacterial or fungal contamination throughout the culture period.

The flow dynamic properties of this bioreactor have been roughly estimated using silicone tubing as a vessel at an average pressure of 100 mmHg and 120 beats/min. Under these conditions, a flow rate of 9.6 ml/min in each vessel results in an average wall shear rate of 61 s^{-1} , comparable to that in the carotid artery. Pressure waveforms are also similar to arterial waveforms. In contrast, values of average wall stress and wall shear stress are lower than *in vivo*. This may be advantageous in terms of structural stability of the cultured vessel as well as cell viability and proliferation. Physical and biological characterization of SMC-seeded porous tubular scaffolds cultured in the bioreactor is currently being performed.

Use of ultrasound equipment can permit accurate and continuous monitoring of the pulsatile flow inside the vessels and of their change in diameter. A system as the one described above could also serve as a valuable *in vitro* model to study the effects of physical forces on (developing) tissues and to predict the response of the tissue-engineered constructs once implanted *in vivo*.

Acknowledgement

J. Perrée and T.G. van Leeuwen (Academic Medical Centre, University of Amsterdam, Laser Center, Amsterdam, The Netherlands) are kindly acknowledged for their help in the design of this equipment. B.H.L. Betlem and C. Kruit (Process Dynamics and Control Group, Faculty of Science and Technology, University of Twente, Enschede, The Netherlands) are thanked for the interesting discussions.

References

1. Langer, R. and Vacanti, J.P., Tissue Engineering. *Science*, 1993. 260(5110): 920-926.
2. Seifalian, A.M., Giudiceandrea, A., Schmidt-Rixen, T. and Hamilton G., Non compliance: the silent acceptance of a villain, in Tissue engineering of vascular prosthetic grafts, G.H.P. Zilla P., Editor. 1999. 621.
3. L'Heureux, N., A completely biological tissue-engineered human blood vessel. *Faseb J.*, 1998. 12(1): 47-56.
4. Campbell, J.H., Efendy, J.L. and Campbell, G.R., Novel vascular graft grown within recipient's own peritoneal cavity. *Circ. Res.*, 1999. 85(12): 1173-1178.
5. Bader, A., Steinhoff, G. and Strobl, K., Engineering of human vascular aortic tissue based on a xenogenic starter matrix. *Transplant.*, 2000. 70(1): 7-14.
6. Weinberg, C.B. and Bell, E., A blood vessel model constructed from collagen and cultured vascular cells. *Science*, 1986. 231: 397-400.
7. Mooney, D.J., Mazzoni, C.L., Breuer, C., McNamara, K., Hern, D., Vacanti, J.P. and Langer, R., Stabilized polyglycolic acid fibre-based tubes for tissue engineering. *Biomaterials*, 1996. 17(2): 115-124.
8. Hoerstrup, S.P., Zund, G., Sodian, R., Schnell, A.M., Grunenfelder, J. and Turina, M., Tissue engineering of small caliber vascular grafts. *E. J. Cardio-Thorac. Surg.*, 2001. 20(1): 164-169.
9. Niklason, L.E., Gao, J., Abbott, W.M., Hirschi, K.K., Houser, S., Marini, R. and Langer, R., Functional arteries grown in vitro. *Science*, 1999. 284(5413): 489-493.
10. Mitchell, S.L. and Niklason, L.E., Requirements for growing tissue-engineered vascular grafts. *Cardiovasc. Pathol.*, 2003. 12(2): 59-64.
11. Campbell, J.H. and Campbell, G.R., Culture techniques and their applications to studies of vascular smooth-muscle. *Clin. Sci.*, 1993. 85(5): 501-513.

12. Jaffe, E.A., Nachman, R.L., Bedker, C.G. and Minik, C.R., Culture of human endothelial cells derived from umbilical veins. *J. Clin. Invest.*, 1973. 52: 2756.
13. Kallmes, D.F., Lin, H.B., Fujiwara, N.H., Short, J.G., Hagspiel, K.D., Li, S.T. and Matsumoto, A.H., Dr. Gary J. Becker young investigator award: comparison of small-diameter type 1 collagen stent-grafts and PTFE stent-grafts in a canine model-work in progress. *J. Vasc. Intervent. Radiol.*, 2001. 12(10): 1127-1133.
14. Campbell, J.H., Walker, P., Chue, W.L., Daly, C., Cong, H.L., Xiang, L. and Campbell, G.R., Body cavities as bioreactors to grow arteries. *Inter. Congress Series*, 2004. 1262: 118-121.
15. Conklin, B.S., Surowiec, S.M., Lin, P.H. and Chen, C., A simple physiologic pulsatile perfusion system for the study of intact vascular tissue. *Med. Eng. Phys.*, 2000. 22(6): 441-449.
16. Martin, I., Wendt, D. and Heberer, M., The role of bioreactors in tissue engineering. *Trends Biotechnol.*, 2004. 22(2): 80-86.
17. Nasserri, B.A., Pomerantseva, I., Kaazempur-Mofrad, M.R., Sutherland, F.W.H., Perry, T., Ochoa, E., Thompson, C.A., Mayer, J.E., Oesterle, S.N. and Vacanti, J.P., Dynamic rotational seeding and cell culture system for vascular tube formation. *Tissue Eng.*, 2003. 9(2): 291-299.
18. Wendt, D., Marsano, A., Jakob, M., Heberer, M. and Martin, I., Oscillating perfusion of cell suspensions through three-dimensional scaffolds enhances cell seeding efficiency and uniformity. *Biotechnol. Bioeng.*, 2003. 84(2): 205-214.
19. Surowiec, S.M., Conklin, B.S., Li, J.S., Lin, P.H., Weiss, V.J., Lumsden, A.B. and Chen, C., A New Perfusion Culture System Used to Study Human Vein. *J. Surg. Res.*, 2000. 88(1): 34-41.
20. Papadaki, M. and Eskin, S.G., Effects of fluid shear stress on gene regulation of vascular cells. *Biotechnol. Prog.*, 1997. 13(3): 209-221.
21. Seliktar, D., Nerem, R.M. and Galis, Z.S., Mechanical strain-stimulated remodeling of tissue-engineered blood vessel constructs. *Tissue Eng.*, 2003. 9(4): 657-666.
22. Kanda, K. and Matsuda, T., Mechanical stress-induced orientation and ultrastructural change of smooth muscle cells cultured in three-dimensional collagen lattices. *Cell Transplant.*, 1994. 3(6): 481-492.
23. Zandonella, C., Tissue engineering: the beat goes on. *Nature*, 2003. 421: 884-886.

24. Bardy, N., Karillon, G.J., Merval, R., Samuel, J.L. and Tedgui, A., Differential effects of pressure and flow on DNA and protein synthesis and on fibronectin expression by arteries in a novel organ-culture system. *Circ. Res.*, 1995. 77(4): 684-694.
25. Perree, J., van Leeuwen, T.G., Keridongo, R., Spaan, J.A.E. and van Bavel, E., Function and structure of pressurized and perfused porcine carotid artery. Effect of in vivo balloon angioplasty. *Am. J. Pathol.*, 2003. 163(5): 1743-1750.
26. Buttafoco, L., Engbers-Buijtenhuijs, P., Poot, A.A., Dijkstra, P.J., Daamen, W.F., van Kuppevelt, T.H., Vermes.I. and Feijen, J., First steps towards tissue engineering of small-diameter blood vessels: preparation of flat scaffolds of collagen and elastin by means of freeze-drying. *Submitted to J. Biomed. Mat. Res.*
27. Buijtenhuijs, P., Buttafoco, L., Poot, A.A., Dijkstra, P.J., deVos, R.A.I., Sterk, L.M.T., Geelkerken, B.R.H., Feijen. J. and Vermes.I., Tissue engineering of blood vessels: characterisation of smooth muscle cells for culturing on collagen and elastin based scaffolds. *Biotechnol. Appl. Biochem.*, 2004. 9(2): 141-149.
28. Foust, A.S., Wenzel, L.A., Clump, C.W., Maus, L. and Andersen, L.B., Principles of unit operations. 2nd ed. Vol. 1. 1980, New York: Wiley.
29. Greenwald, S.E. and Berry, C.L., Improving vascular grafts: the importance of mechanical and haemodynamic properties. *J. Pathol.*, 2000. 190(3): 292-299.
30. Caro, C.G., Pedley, T.J., Schroter, R.C. and Seed. W.A., The systemic arteries, in *The mechanics of the circulation*, J.W.A. Ltd., Editor. 1978, Oxford University Press. 243-349.
31. Gan, L.M., Sjogren, L.S., Doroudi, R. and Jern, S., A new computerized biomechanical perfusion model for ex vivo study of fluid mechanical forces in intact conduit vessels. *J. Vasc. Res.*, 1999. 36(1): 68-78.
32. Kanda, K. and Matsuda, T., Behavior of arterial wall cells cultured on periodically stretched substrates. *Cell Transplant.*, 1993. 2(6): 475-484.
33. Davies, P., Haemodynamic influences on vascular remodelling. *Transpl. Immunol.*, 1997. 5(4): 243-245.
34. Seliktar, D., Black, R.A., Vito, R.P. and Nerem, R.M., Dynamic mechanical conditioning of collagen-gel blood vessel constructs induces remodeling in vitro. *Ann. Biomed. Eng.*, 2000. 28(4): 351-362.
35. Stegemann, J.P. and Nerem, R.M., Phenotype modulation in vascular tissue engineering using biochemical and mechanical simulation. *Ann. Biomed. Eng.*, 2003. 31: 391-402.

36. Whitmore, R.L., The circulating system, in *Rheology of the circulation*, A.Wheaton, Editor. 1968, Pergamon Press Ltd. 17-34.
37. Stegemann, J.P. and Nerem, R.M., Altered response of vascular smooth muscle cells to exogenous biochemical stimulation in two- and three-dimensional culture. *Exp. Cell Res.*, 2003. 283(2): 146-155.
38. Papathanasopoulou, P., Zhao, S., Koehler, U., Robertson, M.B., Long, Q., Hoskins, P., Xu, Y. and Marshall, I., MRI measurements of time-resolved wall shear stress vectors in a carotid bifurcation model, and comparison with CFD predictions. *J. Mag. Reson.*, 2003. 17: 153-162.
39. Kaazempur-Mofrad, M.R., Isasi, A.G., Younis, H.F., Chan, R.C., Hinton, D.P., Sukhova, G., LaMuraglia, G.M., Lee, R.T. and Kamm, R.D., Characterization of the atherosclerotic carotid bifurcation using MRI, finite element modeling, and histology. *Ann. Biomed. Eng.*, 2004. 32(7): 932-946.
40. Carrier, R.L., Papadaki, M., Rupnick, M., Schoen, F.J., Bursac, N., Langer, R., Freed, L.E. and Vunjak-Novakovic, G., Cardiac tissue engineering: cell seeding, cultivation parameters, and tissue construct characterization. *Biotechnol. Bioeng.*, 1999. 64(5): 580-589.
41. Lee, A.A., Graham, D.A., Dela, C.S., Ratcliffe, A. and Karlon, W.J., Fluid shear stress-induced alignment of cultured vascular smooth muscle cells. *J. Biomech. Eng.*, 2002. 124(1): 37-43.
42. Stock, U.A. and Vacanti, J.P., Cardiovascular physiology during fetal development and implications for tissue engineering. *Tissue Eng.*, 2001. 7(1): 1-7.
43. Bale-Glickman, J., Selby, K., Saloner, D. and Savas, O., Experimental flow studies in exact-replica phantoms of atherosclerotic carotid bifurcations under steady input conditions. *J. Biomech. Eng.-Trans. ASME*, 2003. 125(1): 38-48.
44. Stokholm, R., Oyre, S., Ringgaard, S., Flaagoy, H., Paaske, W.P. and Pedersen, E.M., Determination of wall shear rate in the human carotid artery by magnetic resonance techniques. *E. J. Vasc. Endovasc. Surg.*, 2000. 20(5): 427-433.
45. Samijo, S.K., Willigers, J.M., Barkhuysen, R., Kitslaar, P.J.E.H.M., Reneman, R.S., Brands, P.J. and Hoeks, A.P.G., Wall shear stress in the human common carotid artery as function of age and gender. *Cardiovas. Res.*, 1998. 39(2): 515-522.
46. Labarbera, M., Principles of design of fluid transport-systems in zoology. *Science*, 1990. 249(4972): 992-1000.

47. Perktold, K., Thurner, E. and Kenner, T., Flow and stress characteristics in rigid walled and compliant carotid-artery bifurcation models. *Med. Biol. Eng. Comput.*, 1994. 32(1): 19-26.
48. Duncan, D.D., Bargeron, C.B., Borchardt, S.E., Deters, O.J., Gearhart, S.A., Mark, F.F. and Friedman, M.H., The effect of compliance on wall shear in casts of a human aortic bifurcation. *J. Biomech. Eng. Trans. ASME*, 1990. 112(2): 183-188.
49. Porter, B., Zauel, R., Stockman, H., Guldberg, R. and Fyhrie, D.P.D., 3-D computational modeling of media flow through scaffolds in a perfusion bioreactor. *J. Biomech.*, 2004. *In Press*.
50. Baguneid, M., Murray, D., Salacinski, H.J., Fullert, B., Hamilton, G., Walker, M. and Seifailian, A.M., Shear-stress preconditioning and tissue-engineering-based paradigms for generating arterial substitutes. *Biotechnol. Appl. Biochem.*, 2004. 39: 151-157.
51. Wentzel, J.J., Kloet, J., Andhyiswara, I., Oomen, J.A.F., Schuurbiers, J.C.H., de Smet, B., Post, M.J., de Kleijn, D., Pasterkamp, G., Borst, C., Slager, C.J. and Krams, R., Shear-stress and wall-stress regulation of vascular remodeling after balloon angioplasty - Effect of matrix metalloproteinase inhibition. *Circulation*, 2001. 104(1): 91-96.
52. Fung, Y.C., Mechanical properties and active remodeling of blood vessels, in *Biomechanics. Mechanical Properties of Living Tissues*, Springer, Editor. 1999.
53. Bank, A.J. and Kaiser, D.R., Smooth muscle relaxation - Effects on arterial compliance, distensibility, elastic modulus, and pulse wave velocity. *Hypertension*, 1998. 32(2): 356-359.

Chapter 7

Dynamic versus Static Smooth Muscle Cell Culture in Tubular Collagen/Elastin Matrices for Vascular Tissue Engineering*.

*Great things are not done by impulse,
but by a series of small things brought together.*

(V. van Gogh)

Abstract.

Tubular scaffolds of collagen and elastin (weight ratio 1:1) with interconnected pores were prepared by freeze drying and successively stabilized by crosslinking with N-(3-dimethylaminopropyl)-N'-ethylcarbodiimide hydrochloride (EDC) and N-hydroxysuccinimide (NHS) in the presence or absence of a Jeffamine spacer (J230). For crosslinked as well as uncrosslinked samples, porosities of 90% and average pore sizes of 131-151 μm were determined. Smooth muscle cells (SMC) were cultured on the (crosslinked) tubular scaffolds under pulsatile flow at 120 beats/min, with pressures varying from approximately 80 to 120 mmHg. All the constructs were capable of withstanding cyclic mechanical strain without cracking or suffering permanent deformation. No mechanical support was needed during culturing to prevent the vessels from bursting. After 7 d of culture, SMC were homogeneously distributed throughout the uncrosslinked and EDC/NHS

* Buttafoco L.¹, Engbers-Buijtenhuijs P.^{1,2}, Poot A.A.¹, Dijkstra P.J.¹, Vermes I.^{1,2}, Feijen J.¹

Submitted to Biomaterials

¹ Department of Polymer Chemistry and Biomaterials, Faculty of Science and Technology and Institute of Biomedical Technology (BMTI), University of Twente, Enschede, P.O. Box 217, 7500 AE, The Netherlands,

² Department of Clinical Chemistry, Medical Spectrum Twente Hospital, Enschede, P.O. Box 50000, 7500 KA, The Netherlands.

crosslinked constructs. In contrast, hardly any cell was observed on the luminal side of J230/EDC/NHS crosslinked matrices. Considering the better mechanical performance of EDC/NHS crosslinked matrices compared to non-crosslinked constructs after 7 d of culture, SMC were dynamically cultured on the former scaffolds for 14 d. During this period, the high strain stiffness of the constructs increased more than two times, to 38.0 ± 2.0 kPa, whereas the low strain stiffness doubled to 8 ± 2 kPa. The yield stress and yield strain were 30 ± 10 kPa and 120 ± 20 %, respectively. Histology and SEM showed SMC homogeneously distributed throughout the EDC/NHS crosslinked collagen/elastin constructs and collagen fibres partially oriented in the circumferential direction.

Introduction.

The development of a functional small-diameter vascular graft has long been a “holy grail”. Although some successful solutions are available for large-diameter vessels (inner diameter > 6 mm) [1-3], the occurrence of thrombosis is still the main problem encountered in small-diameter blood vessel reconstructions. In order to develop a suitable small-diameter vascular prosthesis, research has been directed to tissue-engineered constructs. Up to now, either synthetic or natural occurring materials have been used as scaffolds in attempts to successfully engineer a vascular graft. Biodegradable synthetic materials have been used, because they are relatively easy to process and often match the required mechanical properties [4, 5]. Many polylactide- or polyglycolide-based scaffolds have thus been produced [4, 6-9], but achieving the necessary compliance, cell adhesion, proliferation and matrix synthesis is still a challenge [10].

The use of polymers also present in the wall of natural blood vessels may obviate some of these problems, especially in terms of cell adhesion. However, tissue-engineered collagen-based vascular grafts matching the desired mechanical properties, especially in terms of compliance and burst strength, have not been developed yet [11-13]. In non-compliant grafts, the transmission of pulsatile wave energy to the downstream vasculature is hampered.

Our aim is to develop a functional tissue-engineered small-diameter blood vessel based on polymers present in the vascular wall, extracellular matrix components and human cells. In this study, insoluble collagen type I from bovine Achilles tendon and insoluble elastin from horse neck ligament were used to prepare tubular scaffolds. In nature, collagen is one of the main components of blood vessels. Collagen fibres are essential to maintain the structural integrity of arteries [14]. Introduction of elastin in collagenous vessels, can result in enhanced elasticity

and compliance [15]. At physiological pressures, elastin prevents vascular creep [16]. In previous work, we have shown that, after 20 cycles up to 10% of strain, non-porous scaffolds containing both elastin and collagen have a degree of strain recovery of 70 ± 5 %, much higher than that recorded for collagen films (42 ± 6 %) under the same conditions [17]. Moreover, this protein is also involved in the control of smooth muscle cell (SMC) functions [18]. The ability of SMC to contract and relax is essential to ensure maintenance of the vascular tone [19].

In this study, porous tubular scaffolds of collagen and elastin were prepared by freeze drying and successively stabilized by crosslinking with a water-soluble carbodiimide, N-(3-dimethylaminopropyl)-N'-ethylcarbodiimide hydrochloride (EDC) and N-hydroxysuccinimide (NHS), in the presence or absence of a Jeffamine spacer. After morphological and mechanical characterization, scaffolds were cultured with SMC for different time periods in a pulsatile flow bioreactor [20]. Scaffolds cultured under static conditions were used as control. The effects of the culture conditions on the morphology and mechanical properties of the resulting constructs were monitored.

Materials and Methods.

All chemicals and materials were purchased from Sigma & Aldrich (Zwijndrecht, The Netherlands) unless otherwise stated.

Preparation of tubular porous structures.

Insoluble collagen type I derived from bovine Achilles tendon (University of Nijmegen, The Netherlands, purification procedure as in [21]) and insoluble elastin derived from equine ligamentum nuchae (University of Nijmegen, The Netherlands; purification procedure as in [22]) were mixed in 0.25 M acetic acid in order to obtain a suspension containing 1% w/v of each of the components. The resulting suspension was homogenised first with a Philips Blender for 4 min and then for 15 min at 4 °C with an Ultra-Turrax T25 (IKA Labortechnik, Staufen, Germany). The suspension was degassed at 0.1 mbar (Edwards, oil vacuum pump), poured in glass tubular moulds having an outer diameter of 6 ± 1 mm and an inner diameter of 3 mm and then frozen at -18 °C. The cooling rate was not controlled. After freezing, samples were freeze-dried for 24 h.

Crosslinking.

Freeze-dried collagen/elastin tubes were crosslinked with a water-soluble carbodiimide in the presence or absence of a Jeffamine spacer (J230). Ethanol/water (40% v/v) was used as solvent in all the described reactions.

Carboxylic acid groups of collagen and elastin were activated by N-(3-dimethylaminopropyl)-N'-ethylcarbodiimide hydrochloride (EDC) in the presence of N-hydroxysuccinimide (NHS). This combination limits the occurrence of secondary reactions and induces crosslinking with free primary amine groups [23]. Tubular freeze-dried scaffolds (OD = 6 ± 1 mm, ID = 3 mm, length = 3 cm) were incubated (215 ml per gram of sample) for 30 min at room temperature in a 2-morpholinoethane sulfonic acid (MES) buffer (0.05 M, pH 5.5) using ethanol/water (40% v/v) as solvent. Crosslinking was carried out in the same MES buffer containing EDC (2.3 g) and NHS (0.56 g) per gram of collagen/elastin (molar ratio of EDC/NHS = 2.5). The reaction was performed for 2 h at room temperature. After removal of the crosslinking solution, samples were incubated for 2 h in 0.1 M sodium phosphate (pH = 7.4). A further washing step was performed with ethanol/water (40% v/v). The total incubation time was 2 h, during which ethanol/water was exchanged every 30 min. Finally the samples were rinsed for 10 min with demineralised MilliQ water. The crosslinked matrices were frozen at -18 °C, and subsequently freeze-dried for 24 h.

Crosslinking reactions in the presence of poly(propylene glycol)-bis-(2-aminopropyl ether) (J230) were performed by first incubating the freeze-dried scaffolds for 30 min in a MES buffer (0.05M, pH 5.5 in ethanol/water (40% v/v)) containing J230 (0.062 M) at room temperature. Subsequently, EDC (5.75 g/g of protein) and NHS (1.38 g/g of protein) were added and crosslinking was performed overnight at room temperature (molar ratio of J230 : EDC : NHS = 2.1 : 1 : 0.4). The samples were rinsed with sodium phosphate (0.1M, pH 7.4) and ethanol/water (40% v/v) and then freeze-dried as described above.

Morphology.

The morphology of the porous scaffolds was studied by SEM (Leo Gemini 1550 FEG-SEM apparatus). Prior to analyses, scaffolds were sputter-coated with gold using a Polaron E 5600 sputter coater, in order to prevent surface charging.

Further characterization was performed by micro-computer tomography (μ CT). The scaffolds were scanned without additional sample preparation using a desktop μ CT (μ CT-40, Scanco Medical, Bassersdorf, Switzerland) at a resolution of 6 μ m in all three spatial

dimensions (X-Ray voltage 45 KV). The morphology of the three-dimensional scaffolds was evaluated directly without model assumptions regarding structural aspects of the scaffolds. Pore voxels were defined as voxels corresponding to the void space and polymer voxels as voxels corresponding to the polymer phase. To determine the pores size, pores are completely filled with modelled spheres of different diameters. The pore diameter assigned to a pore voxel is the diameter of the largest sphere (still containing that pore voxel) that fits inside the pore. The average pore size was calculated by averaging the product of the pore voxels with their assigned pore diameter over the total amount of pore voxels, according to the formula [24]:

$$\text{Average pore size} = \frac{\sum_i (\text{pore voxel}_i \times \text{pore size}_i)}{\sum_i \text{pore voxel}_i} \quad (7.1)$$

Pore size, accessible surface area and accessible surface volume were also evaluated as previously described [24].

Chemical and physical properties.

Thermal analyses.

The denaturation temperature of (crosslinked) collagen/elastin samples was measured by DSC (DSC 7, Perkin Elmer, Norwalk, CT). Samples of approximately 5-10 mg were swollen overnight in 50 μl of PBS (pH 7.4) in high-pressure pans and heated from 20 $^{\circ}\text{C}$ to 90 $^{\circ}\text{C}$ at a heating rate of 10 $^{\circ}\text{C}/\text{min}$. A sample containing 50 μl of PBS (pH 7.4) was used as a reference. The onset of the endothermic peak, which indicates denaturation of the collagen triple helix, was recorded as the denaturation temperature.

Primary amine group content.

Samples of approximately 5 mg were incubated for 30 min in an aqueous solution of NaHCO_3 (1 ml, 4% w/v). Then a solution of 2,4,6-trinitrobenzenesulfonic acid (TNBS) (1 ml, 0.5% w/v, in the same aqueous NaHCO_3 solution) was added and the mixture was incubated at 40 $^{\circ}\text{C}$ for 2 h. After the addition of HCl (3 ml, 6 M) samples were hydrolysed at 60 $^{\circ}\text{C}$ for 90 min. The reaction mixture was diluted with demineralised MilliQ water (5 ml) and cooled to room temperature. The absorbance at 420 nm was measured using a Varian Cary 300 Bio spectrophotometer. A blank was prepared using the same procedure, except that HCl was

added prior to the TNBS solution. The absorbance was correlated to the concentration of free amino groups using a calibration curve obtained with glycine (stock solution: glycine (10 mg) in an aqueous NaHCO₃ solution (100 ml, 4% w/v)).

Mechanical properties.

Tensile measurements in the radial direction were performed at 37 °C after equilibrating the specimens (OD = 6 ± 1 mm, ID = 3 mm, length = 7 mm) for 30 min in PBS (pH= 7.4). Samples were mounted on rigid supports in such a way that one side of each support projected through the lumen of the tube [25]. The supports were clamped to a Zwick (Z020, Ulm, Germany) tensile tester, equipped with a 10 N load cell. Measurements of stress response to a constant strain rate of 1 mm/min were performed. Stress was calculated by dividing the force generated during extension by the initial cross-sectional area. Prior to analyses, samples were preconditioned by performing 10 cycles up to 15% strain. After 10 cycles no more hysteresis was observed.

The resulting stress-strain data were used to calculate the stiffness, the yield stress and the yield strain for each of the scaffold types. At higher strains the contribution of the collagen fibres to the stiffness of the specimens was evaluated. In blood vessels, at strains less than 20% the elastic fibres dominate the mechanical behaviour, whereas above 20% alignment of collagen fibres occurs [26]. Therefore the slopes of the linear portions of the stress-strain curves for elongations lower than 1% and in the range of 40 to 45% strain, were used to calculate the low and higher strain stiffness, respectively. The higher strain stiffness is referred to as high strain stiffness.

Integrity of the scaffolds in vitro.

The integrity of non-cultured (crosslinked) collagen/elastin scaffolds after incubation in culture medium (Dulbecco's Modified Eagle's Medium containing 10% v/v human serum, 10% v/v foetal bovine serum, 50 U/ml penicillin and 50 µg/ml streptomycin) was evaluated using different methods.

In the first approach, the loss in weight was monitored after incubating samples of 5-10 mg in 1 ml of culture medium at 37 °C and 5 % CO₂ for 1, 3, 7 and 14 d. Samples were rinsed 3 times with MilliQ water, the samples were freeze-dried to constant weight and subsequently weighed.

The mechanical properties of tubular (crosslinked) collagen/elastin specimens incubated for 1, 3, 7 and 14 d in culture medium at 37 °C and 5% CO₂ were also analysed as described above. Stiffness was calculated at strains lower than 1 %. The results were compared with the mechanical properties of (crosslinked) collagen/elastin scaffolds measured at day 0.

Smooth muscle cell culture.

Smooth muscle cells (SMC) were isolated from human umbilical veins by a collagenase digestion method as previously described [27]. Sub-confluent cultures of SMC (passage 5 to 9) were harvested by trypsinisation (2 min, 0.125% trypsin/0.05% EDTA) after which cells were resuspended in culture medium (Dulbecco's Modified Eagle's Medium containing 10% v/v human serum, 10% v/v foetal bovine serum, 50 U/ml penicillin and 50 µg/ml streptomycin). Cells were counted with a Bürker hemacytometer, diluted in 20 ml culture medium and successively seeded on (crosslinked) collagen/elastin scaffolds at a final density of approximately 10⁷ cells/scaffold. Before seeding, the (crosslinked) scaffolds (length 4 cm, ID = 3 mm, OD = ca. 6 mm) were disinfected by incubation for approximately 10 min in ethanol/water (70% v/v), followed by rinsing in PBS.

After overnight incubation in culture medium at 37 °C, the scaffolds were mounted in glass chambers and seeded by a filtration seeding procedure from the lumen of the scaffolds. Briefly, the cell suspension (10⁷ cells in 20 ml) was infused in the lumen with two syringes from both ends of the scaffold and filtered through the wall (Fig. 7.1).

The seeded matrices were placed in an incubator (37 °C and 5% CO₂) and rotated 90 ° along the longitudinal axis every 30-60 min for the first 2.5 h to promote homogeneous adhesion of the cells floating in the culture medium to the scaffolds. After 1 d, the chambers containing the seeded scaffolds were mounted in a bioreactor operating at 37 °C and 5% CO₂ [20] (Fig. 7.2). This system consists of four parallel chambers connected through silicone tubing (Watson Marlow, Brussels, Belgium, 3.2 mm ID x 6.4 mm OD) to a fluid reservoir containing culture medium. A pulsatile flow was generated by a peristaltic pump (Watson Marlow Sci-Q-323) placed proximal to the vessels. A pressure of 100 mmHg was applied to the culture medium reservoir and regulated by an electronically controlled Venturi valve (T5200-50, Fairchild Company, Winston-Salem, NC, USA). Pulsations were gradually increased from 30 to 120 beats/min after 3 d of culture, yielding a volumetric flow rate of 9.6 ml/min in each vessel and pressures in the range of 80-120 mmHg at the proximal connections of the flow chambers. The pressure was monitored in the distal and proximal position of the specimens as well as in

the chambers by pressure sensors (Edwards Lifesciences LLC, Unterschleissheim, GmbH, Germany). Pressure signals were displayed with the use of a pressure transducer (Instrumentation Department, Academic Medical Centre of Amsterdam, The Netherlands), and of a scope-meter (Fluke 199BM scopemeter, Adquiment Medical B.V., Hellevoetsluis, The Netherlands) throughout the duration of the experiment. The cells were dynamically cultured for 1, 3, 7 or 14 d in culture medium, which was refreshed every 2 d.

SMC-seeded scaffolds cultured under static conditions for the same time periods (1, 3, 7 and 14 d) were used as controls.

Characterization of the tissue engineered constructs.

At predetermined time periods (1, 3, 7 and 14 d), the tissue engineered constructs were disconnected from the bioreactor and characterized in terms of mechanical properties, morphology and histology.

Morphology and histology.

The morphology of the cultured scaffolds was investigated by means of scanning electron microscopy (SEM). Tubular samples having a length of approximately 3 mm were rinsed in PBS and incubated in formalin (4% v/v) overnight. The scaffolds were then incubated in a graded series of ethanol, freeze-dried overnight and then analysed as described above.

For histological evaluation, cultured scaffolds containing SMC were fixed with formalin (4% v/v), impregnated with paraffin, cut into transverse sections and stained using the Elastic von Gieson (EG) method at the Laboratory of Pathology Oost Nederland according to standard procedures. Using this method, collagen was stained pink, elastin black and the nuclei of the cells brown.

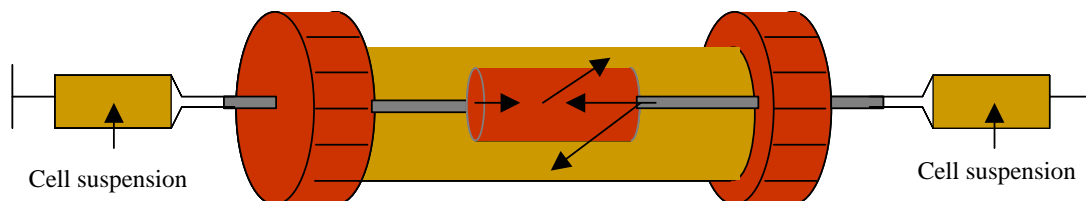


Figure 7.1. Schematic representation of the procedure used for cell seeding. After the tubular scaffolds were mounted in the chambers, the cell suspension was infused with two syringes from both luminal openings of the tubular scaffold through its wall, as indicated by arrows.

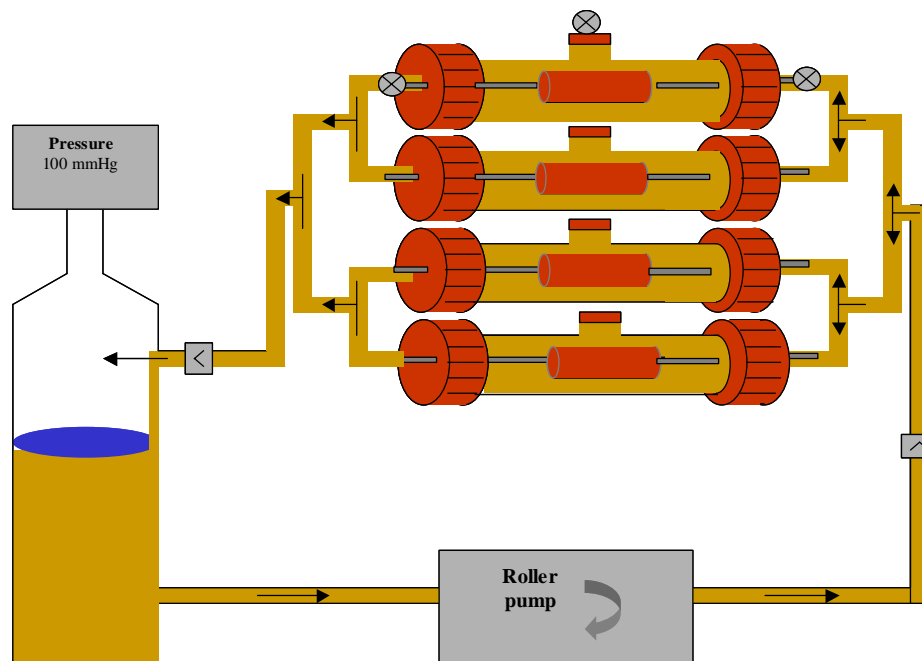




Figure 7.2. Schematic representation of the set up of the bioreactor used in this study. The SMC-seeded (crosslinked) collagen/elastin structures were mounted in four parallel chambers filled with culture medium. The chambers were connected through silicone tubing to the peristaltic pump and the culture medium reservoir, respectively. Culture medium was perfused through the cell-seeded scaffolds inside the chambers. A pressure of 100 mmHg was applied to the culture medium reservoir ( represents the pressure sensor,  represents the liquid valve).

Mechanical analyses.

The mechanical properties of cultured (crosslinked) collagen/elastin constructs were measured and compared to those of non-cultured scaffolds. Measurements of stress response to a constant strain rate of 1 mm/min were performed on 0.7 cm long samples, immediately after their removal from the bioreactor, as described above. Prior to analyses, samples were preconditioned by performing 10 cycles up to 15% strain. After 10 cycles no more hysteresis was observed. The resulting stress-strain data were used to calculate stiffness, yield stress and yield strain.

Results and Discussion.

Porous tubular structures with an inner diameter of 3 mm and an outer diameter of approximately 6 mm were produced by freeze drying collagen/elastin suspensions at $-18\text{ }^{\circ}\text{C}$.

Crosslinking was performed to improve the mechanical properties of the materials and to increase their resistance to fragmentation due to loss of fibres. Based on earlier results with flat scaffolds of insoluble collagen and elastin, ethanol/water (40% v/v) was chosen as solvent for all crosslinking reactions [17]. A carbodiimide (EDC) in combination with a succinimide (NHS), were used to form stable crosslinks between carboxylic acid groups and amine groups in the matrix [28]. As previously reported [17], the occurrence of crosslinking was measured by the increase of the denaturation temperature of the materials from $48\text{ }^{\circ}\text{C}$ up to $75\text{--}80\text{ }^{\circ}\text{C}$ and by the decrease in the free amino group content from $110 \pm 20\text{ nmol/mg}$ to $25 \pm 1\text{ nmol/mg}$. When crosslinking was performed in the presence of J230, an increase in free amino group content to $127 \pm 3\text{ nmol/mg}$ was observed. This increase must be due to the presence of non-reacted amine groups of J230 (dangling groups).

The morphology of (crosslinked) collagen/elastin tubular scaffolds was evaluated by SEM (Fig. 7.3a,b), μCT (Fig. 7.4) and gravimetry. The average pore size of the scaffolds was not

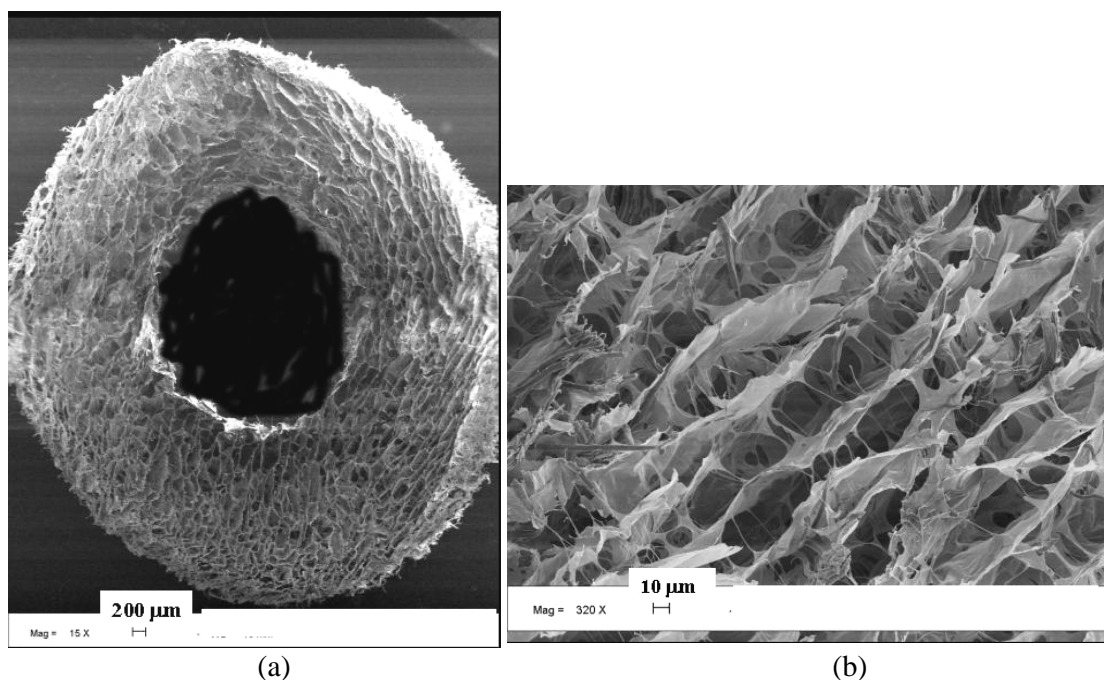


Figure 7.3. SEM pictures of a tubular porous structure of native collagen/elastin (weight ratio 1:1) prepared by means of freeze drying at $-18\text{ }^{\circ}\text{C}$. The scale bar is 200 μm (a) and 10 μm (b).

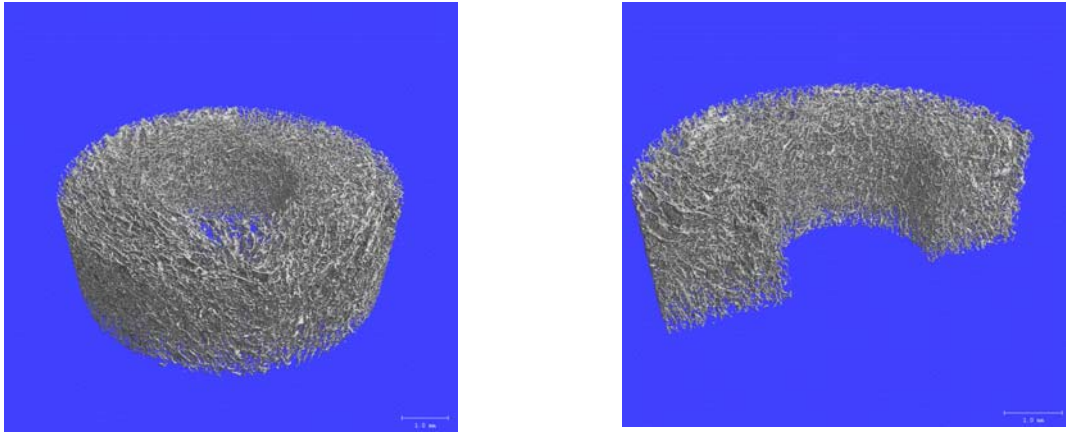


Figure 7.4. 3D computer generated images of porous tubular scaffolds of native collagen/elastin (weight ratio 1:1) prepared by means of freeze drying at -18°C . The scale bar is 1 mm.

significantly altered by crosslinking and values of $143\ \mu\text{m}$ (native sample), $131\ \mu\text{m}$ (EDC/NHS crosslinked samples) and $151\ \mu\text{m}$ (J230/EDC/NHS crosslinked specimens) were obtained by μCT (Fig. 7.5). A homogeneous distribution of pores is observed throughout the scaffolds. This also allows an equal distribution of cells throughout the construct [29], thus establishing the basis for uniform tissue regeneration [30].

The porosity was also not influenced by crosslinking and values of approximately 90% were calculated by gravimetry for all the (crosslinked) samples, whereas values of 95, 94 and 93% were obtained by μCT for the uncrosslinked scaffolds and for the samples crosslinked with EDC/NHS in the absence or presence of J230, respectively (Fig. 7.6a). However, these latter

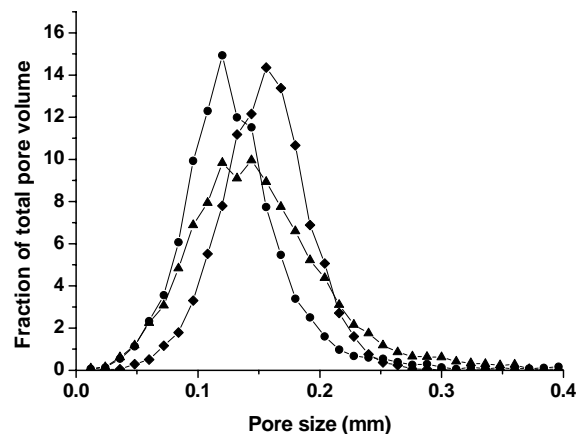


Figure 7.5. Fraction of total pore volume vs. pore size of porous (crosslinked) tubular collagen/elastin samples (weight ratio 1:1) prepared by means of freeze drying at -18°C . (♦) native scaffold; (●) EDC/NHS crosslinked scaffold; (▲) J230/EDC/NHS crosslinked scaffold.

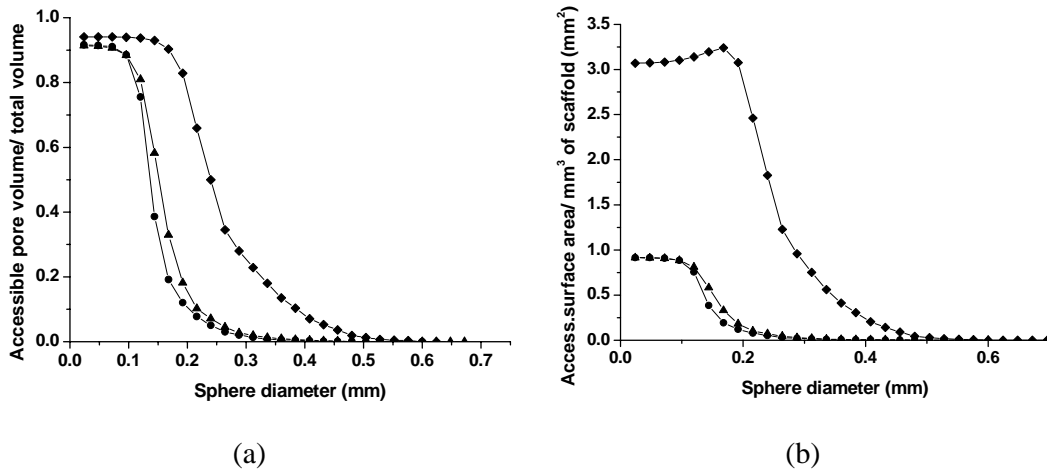


Figure 7.6. (a) Accessible pore volume per total volume and (b) accessible surface area per mm^3 of scaffold for simulated spheres with variable diameters. Porous (crosslinked) collagen/elastin scaffolds (weight ratio 1:1) prepared by means of freeze drying at -18°C . (♦) native scaffold; (●) EDC/NHS crosslinked scaffold; (▲) J230/EDC/NHS crosslinked scaffold.

values are only indicative of the real porosity of the scaffolds, since the total volume available used for calculation of the porosity is based on μCT results and thus excludes pores with sizes smaller than $6\ \mu\text{m}$. The morphological characteristics of these scaffolds are ideal for tissue engineering of blood vessels, since porosities of approximately 90% and pore sizes of $100\ \mu\text{m}$ are known to be sufficient to ensure exchange of nutrients and oxygen and migration of SMC [31].

Crosslinking substantially altered the interconnectivity between the pores and the available surface area for cell adhesion (Fig. 7.6a,b). It has been reported that SMC from aortic tissue in suspension at 37°C have a length of $54.5 \pm 1.5\ \mu\text{m}$ and a diameter of $7.5 \pm 0.3\ \mu\text{m}$ and that an optimal pore size for SMC migration is $100\ \mu\text{m}$ [31]. In crosslinked matrices, more than 80% of the pore volume is still accessible for SMC and approximately $1\ \text{mm}^2$ of surface area per mm^3 of scaffold is available for cellular adhesion.

Stress-strain profiles in the radial direction revealed that all the vessels exhibited a “toe” region, followed by a relatively linear region until the maximum load was reached (Fig. 7.7) [11]. A similar behaviour is observed for natural blood vessels [32]. At low strains (<20% [26]) most of the collagen fibres are slack and not straight. All the stress is then taken up by elastin fibres. As the strain increases, the collagen fibres extend and increasingly take up the stress. Since the latter fibres are much stiffer than the elastin fibres, at higher strain an

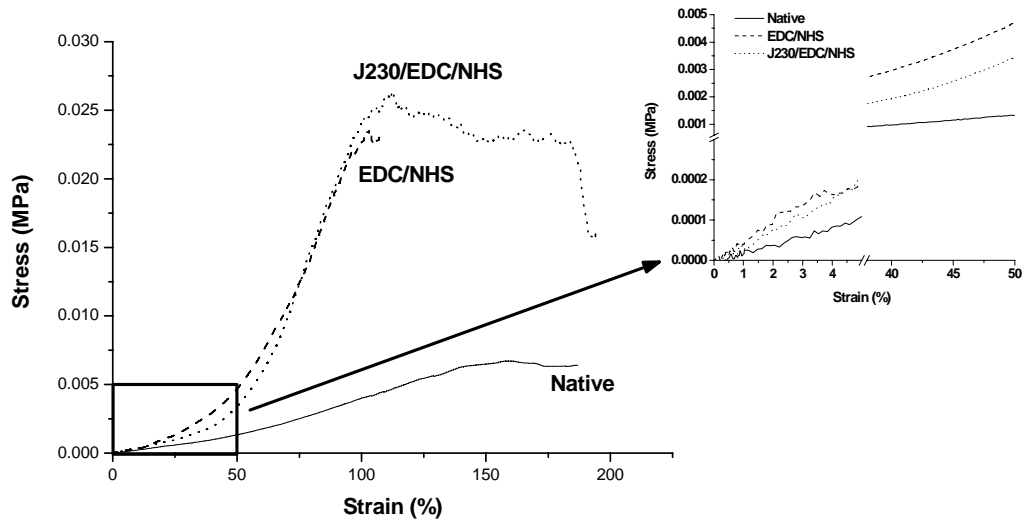


Figure 7.7. Representative stress-strain curves of (crosslinked) porous tubular collagen/elastin scaffolds (weight ratio 1:1) prepared by means of freeze drying at -18°C . Analyses were performed at 37°C , in the radial direction on samples swollen in PBS for 30 min, after preconditioning the specimens with 10 cycles up to 15% strain.

increase in the stiffness of the wall of blood vessels is observed [33]. The radial (low and high strain) stiffness and the yield stress of all crosslinked specimens were significantly higher than those of uncrosslinked samples (Table 7.1). Uncrosslinked scaffolds showed a yield strain of $160 \pm 20\%$. As expected [12], crosslinking resulted in decreased yield strains ($100 \pm 10\%$ for EDC/NHS and $130 \pm 10\%$ for J230/EDC/NHS).

Table 7.1. Mechanical properties of (crosslinked) porous tubular collagen/elastin scaffolds (weight ratio 1:1). Measurements were performed at 37°C after equilibrating the samples for 30 min in PBS. The stiffness at low strain was calculated for strains lower than 1%; the stiffness at high strain was calculated between 40 and 45% strain ($n = 4 \pm s.d.$).

Crosslinking method	Stiffness at low strain (kPa)	Stiffness at high strain (kPa)	Yield stress (kPa)	Yield strain (%)
None	2.10 ± 0.01	3.4 ± 0.6	10 ± 1	160 ± 20
EDC/NHS	4.0 ± 0.1	15.0 ± 1.0	20 ± 1	100 ± 10
J230/EDC/NHS	3.3 ± 0.1	13.0 ± 0.5	30 ± 1	130 ± 10

After incubation in culture medium at 37 °C and 5% CO₂ for a maximum of 14 d, all crosslinked scaffolds retained more than 93% of their original weight, whereas uncrosslinked samples lost 13% of their weight (Fig. 7.8a). The decrease in weight can be related to the loss of fibres from the scaffolds, which is inhibited in crosslinked samples due to formation of intramolecular crosslinks by treatment with (J230)/EDC/NHS [36]. This trend is in agreement with the observed variations in terms of yield stress (Fig. 7.8b). Samples with loose fibres during incubation will have lower yield stress. In contrast to the other analysed parameters, the stiffness at low strain decreases substantially already after 1 d of incubation in culture medium (Fig. 7.8c). It is known that elastin is responsible for the mechanical behaviour of blood vessels

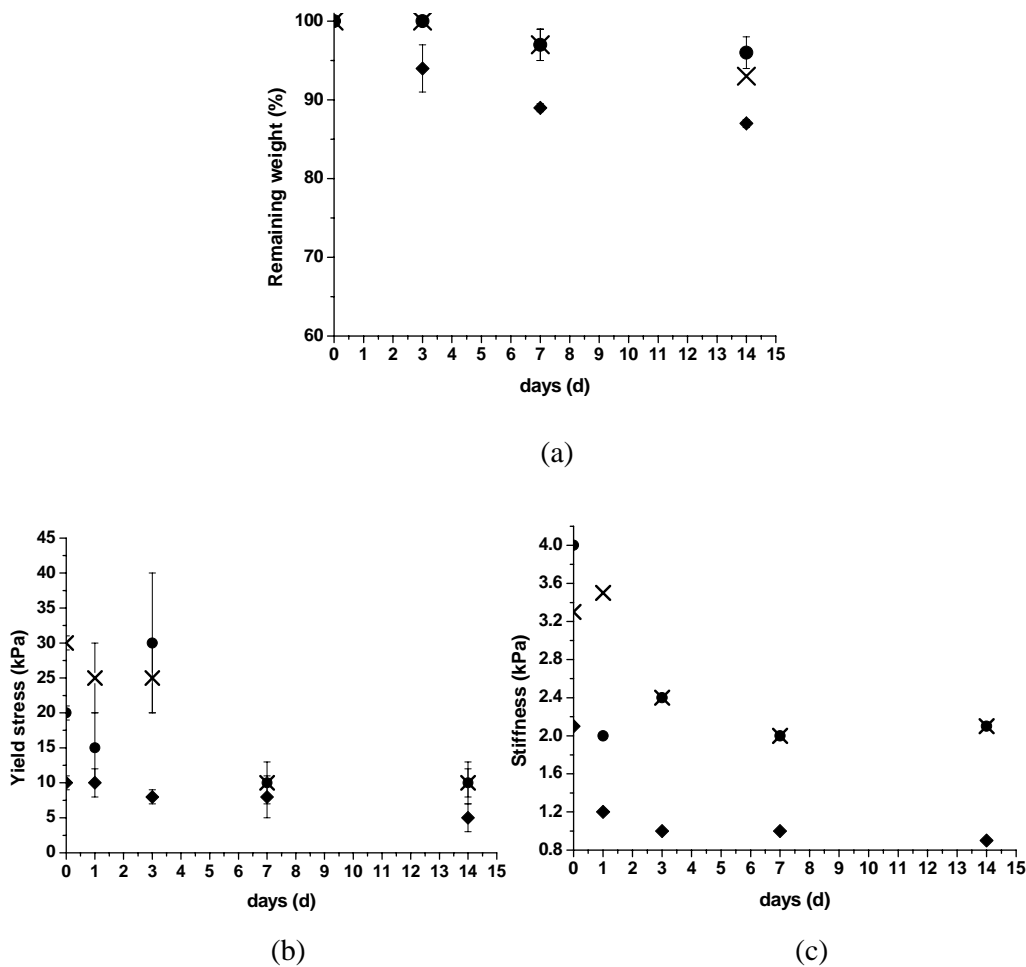


Figure 7.8. (a) Percentage of remaining weight; (b) yield stress and (c) stiffness at strains lower than 1% of (crosslinked) collagen/elastin (weight ratio 1:1) scaffolds after incubation in culture medium for 1, 3, 7 and 14 d. (◆) native scaffold; (●) EDC/NHS crosslinked scaffold; (X) J230/EDC/NHS crosslinked scaffold.

at low strains [26] and we have reported that in freeze-dried collagen/elastin samples, collagen fibres are distributed around the fibres of elastin [17]. As a consequence, the applied load will be partially distributed between the collagen and elastin fibres. Incubation in culture medium may interfere with the interactions between collagen and elastin, eventually disrupting them. Under these conditions, only the fibres of elastin withstand the load, thus explaining the observed decrease in stiffness at low strain already after 1 d.

To obtain a homogeneous distribution of cells in the scaffolds, the cell suspension was perfused from both luminal openings through the scaffold wall as illustrated in Figure 7.

It has been reported that filtration seeding procedures promote an even distribution of cells throughout a porous vascular graft, due to the direct perfusion of SMC through the scaffold [37, 38]. Cells were allowed to adhere on the scaffolds for 1 d, after which the tubular constructs were cultured under pulsatile flow at an average pressure 100 mmHg. The flow rate increased from 3.0 to 9.6 ml/min by increasing the pulses from 30 to 120 beats/min in 3d. Continuous exposure to a periodic change in vessel circumference and stress pulsations on the wall of the vessels are known to accelerate the orientation of SMC and the production of collagen fibre bundles [39]. Tailoring the culture conditions for tissue engineering of blood vessels is also important for control of mass transport. Reduced mass transport is generally one of the greatest challenges to be addressed in cell culture. The bioreactor used in this study, ensures the development of a dynamic laminar flow (Reynolds numbers between 29 and 96 [20]), which effectively contributes to a homogeneous diffusion of nutrients (*i.e.* glucose), gases (*i.e.* oxygen and CO₂) and metabolic end products (*i.e.* lactate) in the medium and in the constructs during culture [30].

All the constructs were capable of withstanding cyclic mechanical strain without cracking or suffering permanent deformation. Up to now, a silicone tube in the lumen of the vessel has been an essential requirement to ensure support and prevent excessive expansion during mechanical stimulation [40]. The improvement in mechanical properties of the scaffolds obtained by combining collagen and elastin, the crosslinking procedure and the specific conditions for dynamic culturing [20] all ensured the structural stability of the constructs during culture.

Histology showed that SMC were predominantly present on the adventitial side of statically cultured vessels (Fig. 7.9a), whereas culturing of native collagen/elastin scaffolds for 7 d under dynamic conditions resulted in a homogeneous distribution of SMC throughout the constructs (Fig. 7.9c). The presence of cells in the culture medium around the vessels, in the bioreactor chambers immediately after seeding can explain the observed distribution of cells. During the

first hours of culturing, SMC still floating in the culture medium can adhere on the adventitial side of the vessels. Only due to the effect of the pulses, SMC migrate from the adventitial side, through the construct till the luminal side. SEM analyses of the luminal side of the former constructs indeed showed an open structure without cells (Fig. 7.9b). In contrast, the luminal side of native collagen/elastin constructs cultured for 7 d under dynamic conditions was completely covered with cells (Fig. 7.9d). The same pattern was observed after culturing of EDC/NHS crosslinked collagen/elastin scaffolds under static or dynamic conditions. When a

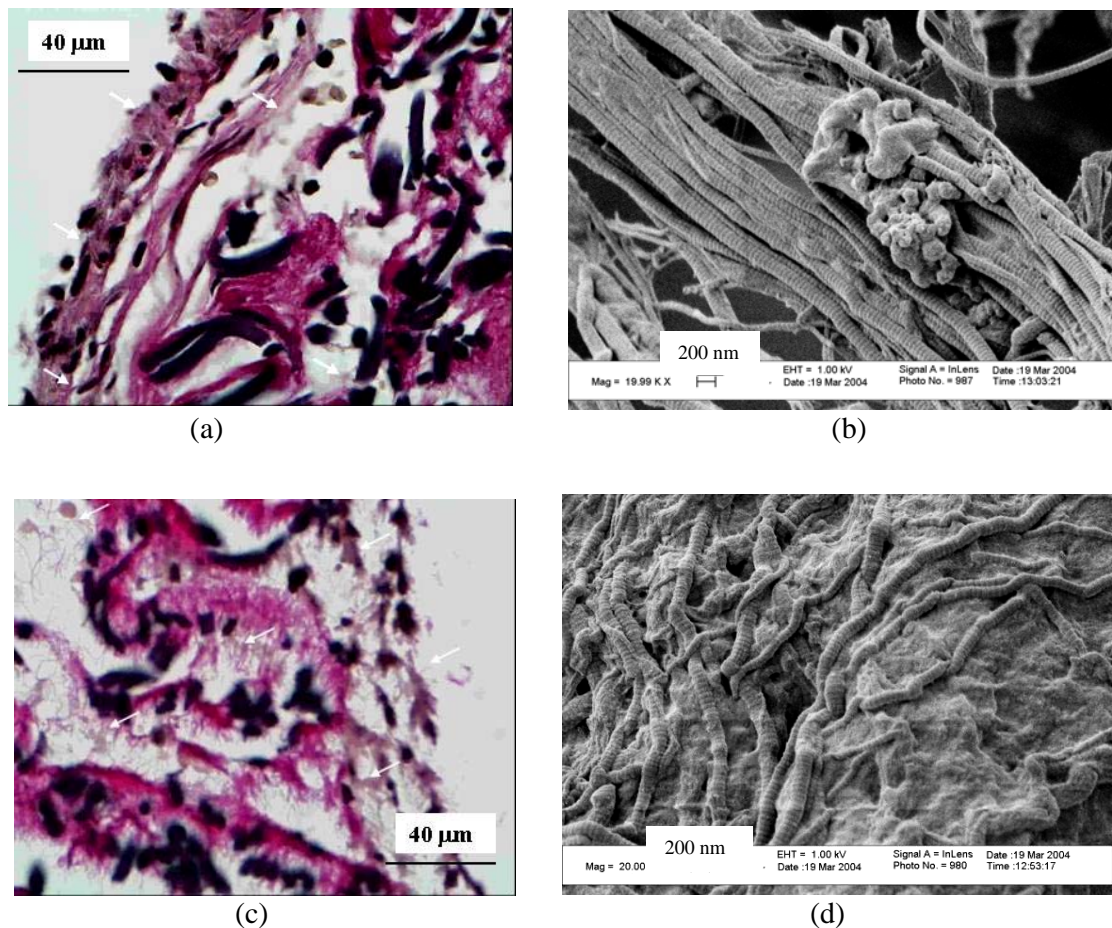


Figure 7.9. Images of native porous tubular collagen/elastin scaffolds (weight ratio 1:1) cultured with SMC for 7 days. (a) Histology of statically cultured constructs. Adventitial side and cross-section; (b) SEM picture of statically cultured constructs, luminal section. Scale bar is 200 nm; (c) histology of dynamically cultured constructs. Adventitial side and cross-section; (d) SEM picture of dynamically cultured constructs, luminal side. Scale bar is 200 nm. SMC are indicated by arrows.

diamine spacer was introduced during crosslinking, hardly any cell was observed on the luminal side of the constructs under dynamic culture conditions. Cells were instead present on the adventitial side of these constructs (data not shown). Maybe cells adhere less due to the presence of the diamine, compared to uncrosslinked or EDC/NHS crosslinked tubular structures, thus explaining the lower extent of cell migration. Application of cyclic mechanical strain during SMC culture, led to an enhancement in the mechanical performance of the engineered tissues over time. After 7 d of culture of native collagen/elastin scaffolds under static conditions, the presence of SMC did not alter the mechanical properties of the original scaffolds in terms of low strain stiffness and yield strain, but resulted in weaker constructs. However, the stiffness measured at higher strains of 40-45% increased five times during static culture (Table 7.1 and 7.2). Since the high strain stiffness is mostly determined by collagen fibres [32], the observed trend might suggest that new collagen fibres were produced. This effect was much more evident when culture was performed under dynamic conditions, since high strain stiffness increased approximately ten times during culture. The improvement in mechanical properties (i.e. stiffness and strength) observed for dynamically cultured vessels is in agreement with the results reported for synthetic polymers [41] and for collagen gels [40]. In general, the better overall mechanical performance of dynamically vs. statically cultured constructs can be related to the higher density of cells and ECM components of dynamically stimulated constructs as compared to statically cultured vessels.

After 7 d of culture under static conditions, EDC/NHS crosslinked constructs exhibited a higher low strain stiffness than before culture (10.0 ± 0.5 kPa vs. 4.0 ± 0.1 kPa), whereas no significant change in high strain stiffness was observed. As compared to non-cultured EDC/NHS crosslinked scaffolds, both low and high strain stiffness doubled when the culture was performed for 7 d under dynamic conditions (Table 7.1 and 7.2). As observed for non-crosslinked collagen/elastin matrices, this suggests an increase in the collagen content of the constructs during culture.

Static culture of SMC for 7 d on scaffolds crosslinked in the presence of a Jeffamine spacer, J230, did not induce any significant change in low and high strain stiffness as well as yield stress, as compared to the same scaffolds before culture. However, a higher elongation at yield of 200 ± 20 % vs. 130 ± 30 % was found. A comparable increase in elongation at yield was

Table 7.2. Mechanical properties of (crosslinked) porous tubular collagen/elastin scaffolds (weight ratio 1:1) after culture with SMC for 7 d under dynamic or static conditions. Measurements were performed at 37 °C after equilibrating the samples for 30 min in PBS. The stiffness at low and high strain was calculated for strains lower than 1% and between 40 and 45%, respectively ($n = 3 \pm s.d.$).

Culture environment	Crosslinking method	Stiffness at low strain (kPa)	Stiffness at high strain (kPa)	Yield stress (kPa)	Yield strain (%)
Static	None	2.00 ± 0.01	18.0 ± 1.0	4.0 ± 0.1	160 ± 10
	EDC/NHS	10.0 ± 0.5	16.0 ± 1.0	15 ± 1	160 ± 30
	J230/EDC/NHS	3.8 ± 0.1	11.0 ± 6.0	20 ± 10	200 ± 20
Dynamic	None	10.0 ± 0.01	35.0 ± 1.0	20 ± 10	220 ± 20
	EDC/NHS	10.0 ± 0.01	35.0 ± 1.0	40 ± 10	130 ± 30
	J230/EDC/NHS	10.0 ± 0.01	15.0 ± 0.9	50 ± 20	230 ± 20

observed when culture was performed under dynamic conditions. In this case, the low strain stiffness increased to 10.0 ± 0.01 kPa as compared to 3.3 ± 0.1 kPa for non-cultured scaffolds. In contrast to the other constructs, yield stress and high strain stiffness of J230/EDC/NHS crosslinked collagen/elastin matrices did not increase during dynamic culturing, thus suggesting that no ECM production occurred (Table 7.1 and 7.2).

Considering the better ability to withstand load of crosslinked scaffolds as compared to native structures, the former were further evaluated. In particular, EDC/NHS crosslinked collagen/elastin constructs showed better results in terms of SMC growth and distribution as compared to J230/EDC/NHS matrices and were thus selected to monitor the changes in the morphological and mechanical properties of the constructs with culture time. The same experiments as described above were performed for 1, 3 and 14 d.

After 1 d of static or dynamic culture of EDC/NHS crosslinked collagen/elastin scaffolds, yield stress and yield strain were not significantly different as compared to non-cultured scaffolds (Table 7.1 and 7.3) After dynamic culture for 1 d, high strain stiffness increased from 15 ± 1.0 kPa to 27 ± 2.0 , whereas under static conditions high strain stiffness did not increase. Low strain stiffness of the samples increased from 4.0 ± 0.1 kPa to 13 ± 1 kPa and 6 ± 1 kPa after static or dynamic culture, respectively. The lower values of stiffness observed under

Table 7.3. Mechanical properties of EDC/NHS crosslinked porous tubular collagen/elastin scaffolds (weight ratio 1:1) after culture with SMC for different time periods under dynamic or static conditions. Measurements were performed at 37 °C after equilibrating the samples for 30 min in PBS. The stiffness at low and high strain was calculated for strains lower than 1% and between 40 and 45%, respectively ($n = 3 \pm s.d.$).

Culture environment	Culture time (d)	Stiffness at low strain (kPa)	Stiffness at high strain (kPa)	Yield stress (kPa)	Yield strain (%)
Static	1	13 ± 1	16.0 ± 1.0	25 ± 5	90 ± 20
	3	2 ± 1	7.0 ± 3.0	15 ± 5	138 ± 3
	7	10.0 ± 0.5	18.0 ± 1.0	15 ± 1	160 ± 30
	14	4 ± 1	31.0 ± 2.0	10 ± 1	140 ± 20
Dynamic	1	6 ± 1	27.0 ± 2.0	20 ± 1	110 ± 20
	3	4 ± 1	10.0 ± 5.0	20 ± 10	120 ± 30
	7	10.0 ± 0.01	35.0 ± 1.0	40 ± 10	130 ± 30
	14	8 ± 2	38.0 ± 2.0	30 ± 10	120 ± 20

dynamic conditions may be due to a weakening effect of the pulsatile flow, since, at this time period, SMC have not yet proliferated into the constructs, thus filling their pores.

Increasing the culture time to 3 d did not alter in a significant way the mechanical properties of the EDC/NHS crosslinked collagen/elastin scaffolds cultured in a dynamic environment, except for the high strain stiffness, which decreased from 27.0 ± 2.0 kPa to 10.0 ± 5.0 kPa. Constructs cultured under static conditions were less stiff and strong after 3 d as compared to 1 d of culture (Table 7.3). This is in agreement with the trend observed studying the structural integrity of the unseeded scaffolds after incubation in culture medium (Fig. 7.8b-c).

EDC/NHS crosslinked collagen/elastin samples cultured with SMC for 14 d under static conditions showed lower yield stresses than constructs cultured for 7 d in the same environment. On the contrary, the yield stress of EDC/NHS crosslinked collagen/elastin samples did not change from 7 to 14 d of culture under dynamic conditions (Table 7.3). Low strain stiffness decreased under both culture conditions, increasing the culture time from 7 to 14 d. This decrease in stiffness might be determined by elastin and SMC, since these are the components mostly influencing the stiffness at low strain. However, the reasons behind this decrease in stiffness are not clearly understood yet.

Significant changes were also found in terms of high strain stiffness. Culturing EDC/NHS crosslinked collagen/elastin scaffolds for 14 d under static conditions yielded constructs with a high strain stiffness of 31.0 ± 2.0 kPa, almost twice the value after 7 d of culture. For constructs cultured under dynamic conditions, an even higher stiffness of 38.0 ± 2.0 kPa was measured at strains between 40 and 45 %. During culture, the composition and morphology of the constructs vary, thus accounting for the increase in high strain stiffness. In particular, the observed increase in stiffness, more substantial for dynamically than for statically cultured constructs, might be due to the formation of preferentially oriented collagen fibres. Circumferentially oriented fibre layers are known to improve the performance of tubular composite polymeric structures [42]. In arteries, the circumferential architecture of collagen allows distension at relatively low pressures and prevents the vessel from being overstretched at high pressures [43]. Moreover, it has been reported that mechanical stress loading on SMC embedded in collagen matrices [44, 45] or on segments of decellularized porcine carotid artery [46] yields constructs in which the orientation of cells and collagen fibres is similar to that of the natural arterial media.

In order to verify whether dynamic stimulation had any effect on the morphology of the developed constructs, histological and SEM analyses were performed. After 14 d of culture under dynamic conditions, SMC were homogeneously distributed through the EDC/NHS crosslinked collagen/elastin constructs (Fig. 7.10a), whereas SMC were found mostly on the adventitial side of statically cultured vessels (Fig. 7.10b). Moreover, dynamic culture

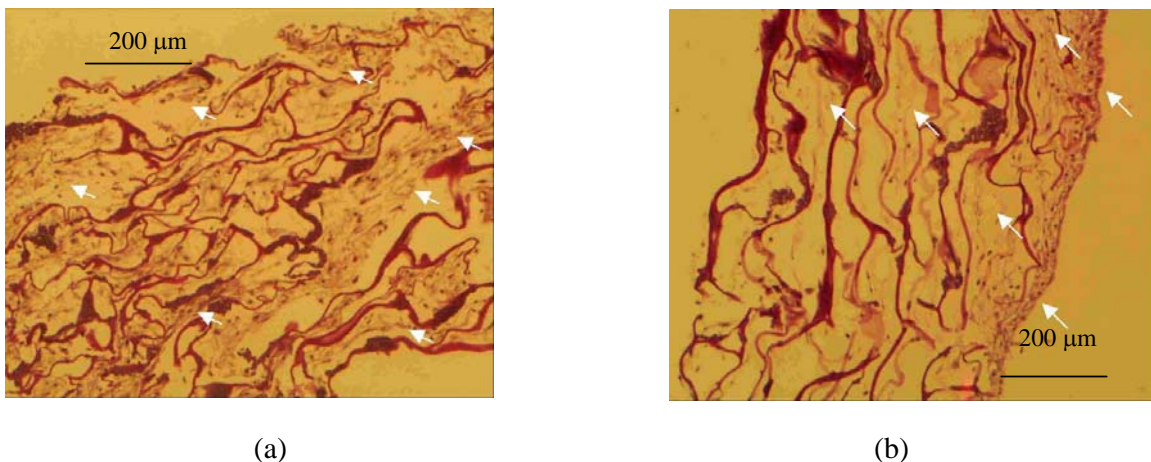


Figure 7.10. Histological sections of EDC/NHS crosslinked collagen/elastin constructs (weight ratio 1:1) cultured with SMC for 14 d under dynamic (a) or static (b) conditions. Magnification is 100X. SMC are indicated by arrows.

conditions yielded collagen fibres partially oriented in the circumferential direction on the adventitial and luminal surface of the constructs (Fig. 7.11a). Only randomly oriented collagen fibres were visible on statically cultured vessels (Fig. 7.11b). This is in agreement with previously reported data.

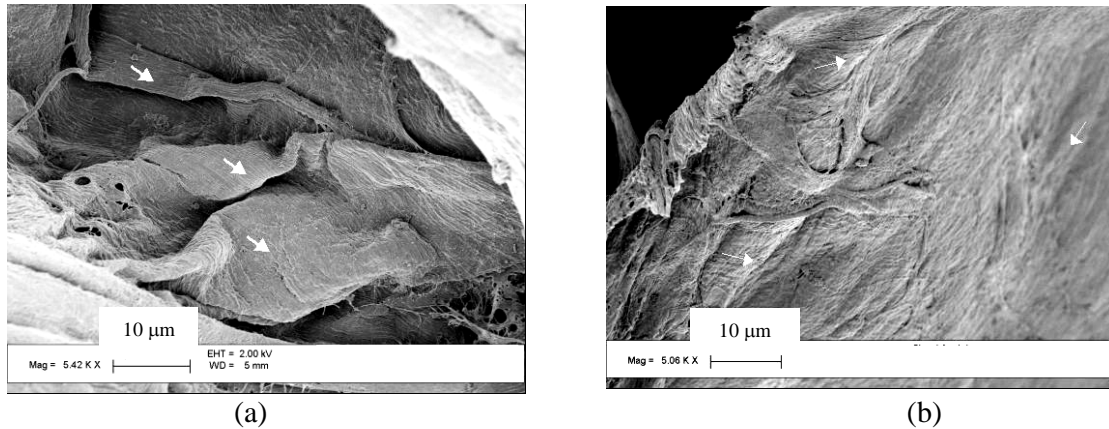


Figure 7.11. SEM image of EDC/NHS crosslinked collagen/elastin constructs (weight ratio 1:1) cultured for 14 d with SMC. Under dynamic conditions (a) a preferential direction of alignment of collagen fibres is visible; under static conditions (b) no preferential alignment is visible. Scale bar is 10 µm in both images. Arrows indicate the direction of alignment of collagen fibres.

Conclusions.

Tubular scaffolds based on insoluble collagen and insoluble elastin were prepared, crosslinked and cultured with SMC under dynamic conditions at arterial pressure. No support was needed in the (crosslinked) constructs to preserve their structural stability during dynamic culturing, which yielded scaffolds having higher (low and high strain) stiffness and more uniform SMC distribution than static controls. Already after 7 d, cells were present throughout the vessels cultured under dynamic conditions, with EDC/NHS crosslinked constructs showing the best mechanical performance. Culturing these constructs for 14 d under dynamic conditions yielded engineered vessels with a uniform distribution of SMC and partially oriented collagen fibres. Longer culture times and introduction of a luminal monolayer of endothelial cells, might provide constructs suitable for *in vivo* testing.

Acknowledgments.

R. de Vos and L. Sterks are kindly acknowledged for performing the histological analyses. M. Smithers is thanked for the SEM images. W.H. Daamen, H.Th.B. van Moerkerk and T. van Kuppevelt (Department of Biochemistry 194, NCMLS, University Medical Centrum Nijmegen, The Netherlands) are acknowledged for providing collagen and elastin for this study.

References.

1. Auguste, K.I., Quinones-Hinojosa, A. and Lawton, M.T., The tandem bypass: subclavian artery-to-middle cerebral artery bypass with dacron and saphenous vein grafts. Technical case report. *Surg. Neurol.*, 2001. 56(3): 164-169.
2. Johansen, K.H. and Watson, J.C., Dacron femoral-popliteal bypass grafts in good-risk claudicant patients. *Am. J. Surg.*, 2004. 187(5): 580-584.
3. Harrison, J.H., Synthetic materials as vascular prostheses: II. A comparative study of nylon, dacron, orlon, ivalon sponge and teflon in large blood vessels with tensile strength studies. *Am. J. Surg.*, 1958. 95(1): 16-24.
4. Hoerstrup, S.P., Zund, G., Sodian, R., Schnell, A.M., Grunenfelder, J. and Turina, M., Tissue engineering of small caliber vascular grafts. *E. J. Cardio-Thorac. Surg.*, 2001. 20(1): 164-169.
5. Ratcliffe, A., Tissue engineering of vascular grafts. *Matrix Biol.*, 2000. 19: 353-357.
6. Pennings, A.J., Knol, K.E., Leenslag, J.W. and Van der Lei, B., A two-ply artificial blood vessel of polyurethane and poly(L-lactide). *Colloid Polym. Sci.*, 1990. 268: 2-11.
7. Kobashi, T. and Matsuda, T., Fabrication of branched hybrid vascular prostheses. *Tissue Eng.*, 1999. 5(6): 515-524.
8. Niklason, L.E., Gao, J., Abbott, W.M., Hirschi, K.K., Houser, S., Marini, R. and Langer, R., Functional arteries grown in vitro. *Science*, 1999. 284(5413): 489-493.
9. Soldani, G., Panol, G., Saskaen, H.F., Goddard, M.B. and Galletti, P.M., Small diameter polyurethane polydimethylsiloxane vascular prostheses made by a spraying, phase-inversion process. *J. Mater. Sci.-Mater. Med.*, 1992. 3(2): 106-113.
10. Nerem, R.M. and Ensley, A.E., The tissue engineering of blood vessels and the heart. *Am. J. Transplant.*, 2004. 4: 36-42.

11. Seliktar, D., Black, R.A., Vito, R.P. and Nerem, R.M., Dynamic mechanical conditioning of collagen-gel blood vessel constructs induces remodeling in vitro. *Ann. Biomed. Eng.*, 2000. 28(4): 351-362.
12. Berglund, J.D., Mohseni, M.M., Nerem, R.M. and Sambanis, A., A biological hybrid model for collagen-based tissue engineered vascular constructs. *Biomaterials*, 2003. 24(7): 1241-1254.
13. L'Heureux, N., A completely biological tissue-engineered human blood vessel. *Faseb J.*, 1998. 12(1): 47-56.
14. Mitchell, S.L. and Niklason, L.E., Requirements for growing tissue-engineered vascular grafts. *Cardiovasc. Pathol.*, 2003. 12(2): 59-64.
15. Nerem, R.M., Critical issues in vascular tissue engineering. *Inter. Congress Series*, 2004. 1262: 122-125.
16. Faury, G., Function-structure relationship of elastic arteries in evolution: from microfibrils to elastin and elastic fibres. *Pathol. Biol.*, 2001. 49(4): 310-325.
17. Buttafoco, L., Engbers-Buijtenhuijs, P., Poot, A.A., Dijkstra, P.J., Daamen, W.F., van Kuppevelt, T.H., Vermes, I. and Feijen, J., First steps towards tissue engineering of small-diameter blood vessels: preparation of flat scaffolds of collagen and elastin by means of freeze drying. *Submitted to J. Biomed. Mat. Res.*
18. Li, D.Y., Brooke, B., Davis, E.C., Mecham, R.P., Sorensen, L.K., Boak, B.B., Eichwald, E. and Keating, M.T., Elastin is an essential determinant of arterial morphogenesis. *Nature*, 1998. 393(6682): 276-280.
19. Ogle, B.M. and Mooradian, D.L., The role of vascular smooth muscle cell integrins in the compaction and mechanical strengthening of a tissue-engineered blood vessel. *Tissue Eng.*, 1999. 5(4): 387-402.
20. Buttafoco, L., Engbers-Buijtenhuijs, P., Poot, A.A., Dijkstra, P.J., Vermes, I. and Feijen, J., Development of a bioreactor for tissue engineering of small-diameter blood vessels: design of a pulsatile flow system. *Submitted to Biotech. Bioeng.*
21. Daamen, W.F., van Moerkerk, H.T.B., Hafmans, T., Buttafoco, L., Poot, A.A., Veerkamp, J.H. and van Kuppevelt, T.H., Preparation and evaluation of molecularly-defined collagen-elastin-glycosaminoglycan scaffolds for tissue engineering. *Biomaterials*, 2003. 24(22): 4001-4009.
22. Daamen, W.F., Hafmans, T., Veerkamp, J.H. and van Kuppevelt, Comparison of five procedures for the purification of insoluble elastin. *Biomaterials*, 2001. 22(14): 1997-2005.

23. Pieper, J.S., Oosterhof, A., Dijkstra, P.J., Veerkamp, J.H. and van Kuppevelt, T.H., Preparation and characterization of porous crosslinked collagenous matrices containing bioavailable chondroitin sulphate. *Biomaterials*, 1999. 20(9): 847-858.
24. Hildebrand, T. and Ruegseggen, A., A new method for the model independent assessment of thickness in three-dimensional images. *J. Microsc.*, 1997. 185: 67-75.
25. Girton, T.S., Oegema, T.R. and Tranquillo, R.T., Exploiting glycation to stiffen and strengthen tissue equivalents for tissue engineering. *J. Biomed. Mat. Res.*, 1999. 46(1): 87-92.
26. Silver, F.H. and Christiansen, D.L., *Biomaterials Science and Biocompatibility*, ed. Springer. 1999.
27. Buijtenhuijs, P., Buttafoco, L., Poot, A.A., Dijkstra, P.J., deVos, R.A.I., Sterk, L.M.T., Geelkerken, B.R.H., Feijen. J. and Vermes.I., Tissue engineering of blood vessels: characterisation of smooth muscle cells for culturing on collagen and elastin based scaffolds. *Biotechnol. Appl. Biochem.*, 2004. 9(2): 141-149.
28. Dijkstra, P.J., Olde Damink, L. and Feijen. J., Chemical stabilization of collagen based biomaterials. *Cardiovasc. Pathol.*, 1993. 5(5): 295.
29. Kim, B.S., Putnam, A.J., Kulik, t.J. and Mooney, D.J., Optimizing seeding and culture methods to engineer smooth muscle tissue on biodegradable polymer matrices. *Biotechnol. Bioeng.*, 1998. 57: 46-54.
30. Martin, I., Wendt, D. and Heberer, M., The role of bioreactors in tissue engineering. *Trends in Biotechnol.*, 2004. 22(2): 80-86.
31. Yannas, I.V., Tissue regeneration templates based on collagen-glycosaminoglycan copolymers. *Adv. Pol. Sci.*, 1995. 122(26): 219-244.
32. Fung, Y.C., Mechanical properties and active remodeling of blood vessels, in *Biomechanics. Mechanical Properties of Living Tissues*, Springer, Editor. 1999.
33. Oliver, J.J. and Webb, D.J., Noninvasive assessment of arterial stiffness and risk of atherosclerotic events. *Arterioscler. Thromb. Vasc. Biol*, 2003. 23(4): 554-566.
34. Tredget, E.E., Forsyth, N., Ujifriedland, A., Chambers, M., Ghahary, A., Scott, P.G., Hogg, A.M. and Burke, J.F., Gas-chromatography mass-spectrometry determination of O-18(2) in O-18-labeled 4-hydroxyproline for measurement of collagen-synthesis and intracellular degradation. *J. Chromatogr.-Biomed. Appl.*, 1993. 612(1): 7-19.
35. Yoo, B.S., Yoon, J., Ko, J.Y., Lee, K.H., Ahn, M.S., Lee, S.H., Hwang, S.O. and Choe, K.H., The serum hydroxyproline level, a maker for collagen, is a biochemical marker in patients with vulnerable plaque or plaque disruption. *Eur. Heart J.*, 2002. 23: 84-84.

36. Damink, L.H.H.O., Dijkstra, P.J., van Luyn, M.J.A., van Wachem, P.B., Nieuwenhuis, P. and Feijen, J., In vitro degradation of dermal sheep collagen cross-linked using a water-soluble carbodiimide. *Biomaterials*, 1996. 17(7): 679-684.
37. Li, Y., Ma, T., Kniss, D.A., Lasky, L.C. and Yang, S.T., Effects of filtration seeding on cell density, spatial distribution, and proliferation in nonwoven fibrous matrices. *Biotechnol. Prog.*, 2001. 17(5): 935-944.
38. van Wachem, P.B., Stronck, J.W.S., Koers-Zuideveld, R., Dijk, F. and Wildevuur, C.R.H., Vacuum cell seeding: a new method for the fast application of an evenly distributed cell layer on porous vascular grafts. *Biomaterials*, 1990. 11(8): 602-606.
39. Hirai, J. and Matsuda, T., Self-organized, tubular hybrid vascular tissue composed of vascular cells and collagen for low-pressure-loaded venous system. *Cell Transplant.*, 1995. 4(6): 597-608.
40. Seliktar, D., Nerem, R.M. and Galis, Z.S., Mechanical strain-stimulated remodeling of tissue-engineered blood vessel constructs. *Tissue Eng.*, 2003. 9(4): 657-666.
41. Kim, B.S., Nikolovski, J., Bonadio, J. and Mooney, D.J., Cyclic mechanical strain regulates the development of engineered smooth muscle tissue. *Nature Biotechnol.*, 1999. 17: 979--983.
42. Krikanov, A.A., Composite pressure vessels with higher stiffness. *Comp. Struct.*, 2000. 48(1-3): 119-127.
43. Driessen, N.J.B., Wilson, W., Bouten, C.V.C. and Baaijens, F.P.T., A computational model for collagen fibre remodelling in the arterial wall. *J. Theor. Biol.*, 2004. 226(1): 53-64.
44. Kanda, K. and Matsuda, T., Mechanical stress-induced orientation and ultrastructural change of smooth muscle cells cultured in three-dimensional collagen lattices. *Cell Transplant.*, 1994. 3(6): 481-492.
45. Stegemann, J.P. and Nerem, R.M., Altered response of vascular smooth muscle cells to exogenous biochemical stimulation in two- and three-dimensional culture. *Exp. Cell Res.*, 2003. 283(2): 146-155.
46. Conklin, B.S., Surowiec, S.M., Lin, P.H. and Chen, C., A simple physiologic pulsatile perfusion system for the study of intact vascular tissue. *Med. Eng.Phys.*, 2000. 22(6): 441-449.

Chapter 8

Preparation of Porous Hybrid Structures Based on P(DLLAcoTMC) and Collagen for Tissue Engineering of Small-Diameter Blood Vessels*.

*Engineering is the professional art of
applying science to the optimum conversion of natural resources
to the benefit of man.*
(R.J. Smith)

Abstract.

Poly (D,L,lactide)co(1,3-trimethylene carbonate) (P(DLLAcoTMC)) containing 83 mol% DLLA was used to produce matrices suitable for tissue engineering of small-diameter blood vessels. The copolymer was processed into tubular structures with a porosity of approximately 98% by melt spinning and fibre winding, thus obviating the need of organic solvents that may compromise subsequent cell culture. Unexpectedly, incubation in culture medium at 37 °C, resulted in disconnection of the contact points between the polymer fibres. To improve the structural stability of these P(DLLAcoTMC) scaffolds, a collagen microsp sponge was formed inside the pores of the synthetic matrix by dip coating and freeze drying. Hybrid structures with a porosity of 97% and an average pore size of 102 µm were obtained. Structural stability was preserved during incubation in culture medium at 37 °C.

* Buttafoco L.¹, Boks N.P.¹, Engbers-Buijtenhuijs P.², Grijpma D.W.¹, Poot A.A.¹, Dijkstra P.J.¹, Vermes I.^{1,2}, Feijen J.¹

Submitted to J. Biomed. Mat. Res.

¹ Department of Polymer Chemistry and Biomaterials, Faculty of Science and Technology and Institute of Biomedical Technology (BMTI), University of Twente, Enschede, P.O. Box 217, 7500 AE, The Netherlands.

² Department of Clinical Chemistry, Medical Spectrum Twente Hospital, Enschede, P.O.Box 50000, 7500 KA, The Netherlands.

Smooth muscle cells (SMC) were seeded in these hybrid scaffolds and subsequently cultured under pulsatile flow conditions in a bioreactor at 120 beats/min and a pressure of 80-120 mmHg. After 7 d of culture in a dynamic environment viable SMC were homogeneously distributed throughout the constructs, which were five times stronger and stiffer than non-cultured scaffolds. Values for yield stress (2.8 ± 0.6 MPa), stiffness (1.6 ± 0.4 MPa) and yield strain (120 ± 20 %) were comparable to those of the human artery mesenterica.

Introduction.

Although artificial blood vessels prepared from Dacron or Teflon are successfully being used for large-diameter vascular reconstructions, there still is no functional synthetic vascular graft available for small-diameter (inner diameter < 6 mm) applications. To solve this problem, various tissue engineering approaches have been proposed, using either natural [1-4] or synthetic materials [5-7].

The extracellular matrix protein collagen type I is one of the main components of natural blood vessels. It is synthesized and secreted by cells present in the vascular wall, such as smooth muscle cells (SMC) and fibroblasts. Collagen provides cellular attachment sites as well as tensile strength of the vascular wall [8]. Until now, however, vascular tissue engineering using collagen type I scaffolds has been unsuccessful because of inappropriate mechanical properties of the obtained constructs [1, 9, 10].

By combining collagen with elastin, the mechanical properties of scaffolds for vascular tissue engineering can be improved. Elastin, another extracellular matrix protein, confers elasticity to the vascular wall, enabling it to stretch and recoil without tearing [11]. In previous work, it has been shown that incorporation of insoluble elastin in insoluble collagen type I matrices improves the degree of strain recovery and the elongation at yield of the scaffolds [12, 13]. Currently, crosslinked porous tubular structures of collagen type I and elastin are successfully used as substrate for SMC culture under pulsatile flow conditions at physiological pressure, without any additional mechanical support of the tubes [14]. However, the use of elastin has certain disadvantages in terms of scarce availability and high costs due to laborious purification procedures.

Hybrid scaffolds of synthetic polymers in combination with collagen may alternatively be used for vascular tissue engineering. A hybrid structure would benefit from suitable mechanical properties and low costs of the synthetic polymer as well as appropriate cellular interactions

due to the collagen [15, 16]. For this application flexible polymers, unlike the commonly used lactide- and/or glycolide-based polymers, are needed. Therefore, a copolymer of D,L-lactide (DLLA) and trimethylene carbonate (TMC), P(DLLAcoTMC), was selected in this study to prepare porous tubular matrices. In a second step, a collagen microsphere was formed inside the synthetic matrix. In previous studies, we have reported on the synthesis and properties of P(DLLAcoTMC) polymers as well as their application in heart tissue engineering [17, 18].

In the present work, P(DLLAcoTMC) was processed by melt spinning and fibre winding into porous tubular structures. This approach obviates the need of organic solvents that may compromise subsequent cell culture. To our knowledge, preparation of tubular scaffolds for tissue engineering by melt spinning of P(DLLAcoTMC) has not been reported before. By varying processing parameters (temperature of the viscous melt, rotational and longitudinal speed of the collecting mandrel, collecting distance), tubes with different morphological and mechanical characteristics were prepared. To improve cellular interactions, the tubes were dipped in a suspension of collagen type I and subsequently freeze-dried. The resulting hybrid structures were seeded with SMC and cultured under dynamic conditions in a bioreactor developed in our laboratories. Finally, the morphology and mechanical properties of the resulting constructs were analysed.

Materials and methods.

All chemicals and materials were purchased from Sigma Aldrich (Zwijndrecht, The Netherlands) unless otherwise stated.

Copolymer synthesis.

Prior to use, D,L-lactide (DLLA) (Purac Biochem, Gorinchem, The Netherlands) was recrystallized from dry toluene under argon atmosphere. Approximately 35 g of 1,3-trimethylene carbonate (TMC) (Boehringer Ingelheim, Germany) and 50 g of DLLA were charged in freshly silanized glass ampoules and $2 \cdot 10^{-4}$ moles stannous octoate per mole of monomer were added. The ampoules were heat-sealed under vacuum and the mixtures were polymerized at 130 ± 2 °C for 3 d.

The obtained copolymers were purified by dissolution in chloroform, filtration through a sintered glass filter and precipitation in methanol. The copolymers were dried in vacuum at room temperature for 1-2 weeks.

Copolymer analyses.

The composition of the copolymers was determined using nuclear magnetic resonance (NMR) spectroscopy. ^1H -NMR spectra were recorded using a Varian Inova 300 MHz; CDCl_3 (Merck, Germany) was used as solvent.

Molecular weights of the copolymers were determined by gel permeation chromatography (GPC) (Waters Model 510 pump, HP Ti-Series 1050 autosampler and Waters Model 410 Differential Refractometer) using a Viscotec H502 Viscometer Detector and 10^5 - 10^4 - 10^3 -500 Å Waters Ultra-Styrigel columns placed in series. Chloroform was used as eluent at a flow rate of 1.5 ml/min. Narrow polystyrene standards were used for calibration.

Thermal properties of the copolymers were determined by differential scanning calorimetry (DSC) (DSC 7, Perkin Elmer, Norwalk, CT). Copolymer samples of approximately 10 mg were heated from 25 °C to 150 °C at a rate of 10 °C/min, quenched to -80 °C and then heated in a second scan to 150 °C at a rate of 10 °C/min. The data presented were measured during the second heating scan. The glass transition temperature (T_g) was taken at the inflection point of the heat capacity change.

Preparation of porous tubular scaffolds.

P(DLLAcoTMC) was charged into a Kayness Galaxy V capillary rheometer and heated to 200-220 °C for 5-10 min. The viscous melts were then extruded through a stainless steel capillary (inner diameter 0.5 mm; length 2.2 cm) with a plunger at a speed of 2.5 mm/min. The spun fibres were wound on a rotating glass mandrel (outer diameter ca. 3 mm) with a reciprocating longitudinal speed in the range of 0.056 to 0.11 m/s and a rotational speed of 0.148 m/s (Fig. 8.1a). To facilitate removal of the tubes, the glass rod was covered with Teflon tape. To improve fusion between the spun fibres, an lamp (Philips, infraphil HP 3616, The Netherlands) was positioned close to the air gap between the spinneret and the rotating mandrel. This resulted in a temperature in the environment surrounding the spun fibres of approximately 55 °C during winding. Scaffolds with an average wall thickness of 1.5 or 3.5 mm were prepared, depending on the spinning time.

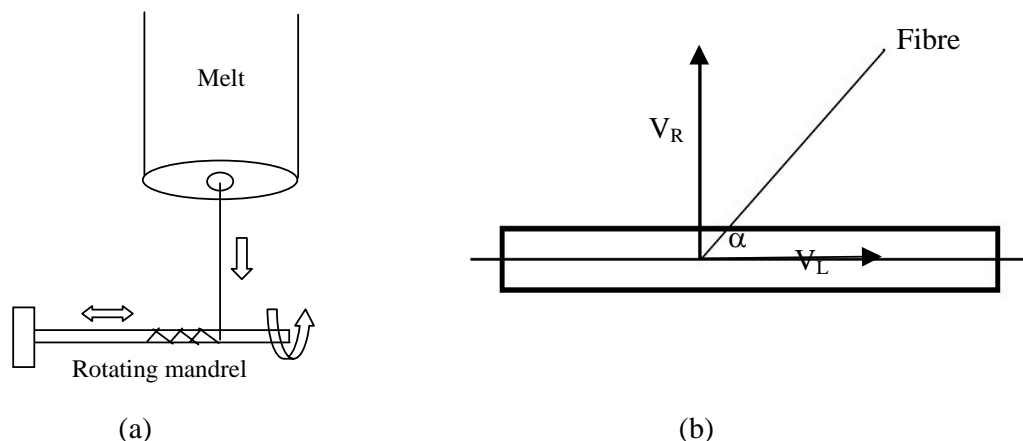


Figure 8.1. (a) Set up of the melt spinning equipment; (b) schematic representation of the winding angle (α).

Theoretical winding angles were calculated using the following equation:

$$\tan \alpha = V_R / V_L \quad (8.1)$$

where V_R is the rotational velocity, V_L the longitudinal velocity and α the angle between the fibre and the longitudinal axis of the tube (Fig. 8.1b).

Preparation of hybrid P(DLLAcoTMC)-collagen structures.

A 1% (w/v) suspension of insoluble collagen type I derived from bovine Achilles tendon (University of Nijmegen, The Netherlands, purification procedure as in [19]) was prepared by swelling overnight in 0.05 M acetic acid at 6 °C. The suspension was homogenised first with a Philips Blender for 4 min at 4 °C and then for 15 min at 4 °C with an Ultra-Turrax T25 (IKA Labortechnik). The suspension was filtered through a 20 denier nylon filter (average pore size 30 μm) and degassed at 0.1 mbar.

Melt spun copolymer tubes (without glass mandrel) were dipped three times in the 1% (w/v) collagen suspension for 10 s. The hybrid structures were then frozen at -18 °C and subsequently freeze-dried.

Characterization of melt spun P(DLLAcoTMC) tubes and hybrid structures.*Copolymer analyses.*

After processing the polymers into tubular structures, DSC and GPC were employed to evaluate the effect of the processing temperature and residence time in the melt chamber on the thermal properties and molecular weight of the copolymer.

Morphology, pore size and porosity.

The average pore size was theoretically calculated applying the model described by Leidner *et al.* [20]. According to this model the pore size was defined as the distance between two fibres located on the same plane (Fig. 8.2a). The average pore size can be calculated from the pore fraction of the fibres:

$$V_f = \frac{\Pi d_f}{4(p + d_f)d_f} = \frac{\rho_{scaffold}}{\rho_{polymer}} \quad (8.2)$$

where V_f is the volume fraction of the fibres, d_f the average diameter of the fibre, p the average pore size and $\rho_{scaffold}$, and $\rho_{polymer}$ are the densities in g/cm^3 of the scaffold (porous P(DLLAcoTMC) structure) and of the non-porous P(DLLAcoTMC) polymer (1.29 g/cm^3). From this equation, the average pore size is:

$$p = \left(\frac{\Pi}{4V_f} - 1 \right) d_f \quad (8.3)$$

The value of the average pore sizes from this model was compared to the experimental average pore size measured using scanning electron microscopy (SEM) (Leo Gemini 1550 FEG-SEM). Before analyses the specimens were carefully flattened on the sample holders to eliminate the effect of the curvature of the tubular scaffolds. Measurements were performed always in the same direction, parallel to the axis of the tube, by averaging diameters of at least ten pores taken at random between two fibres located on the same plane. Fig. 8.2b shows a representative SEM image used for the calculation of the pore size. SEM analysis was also

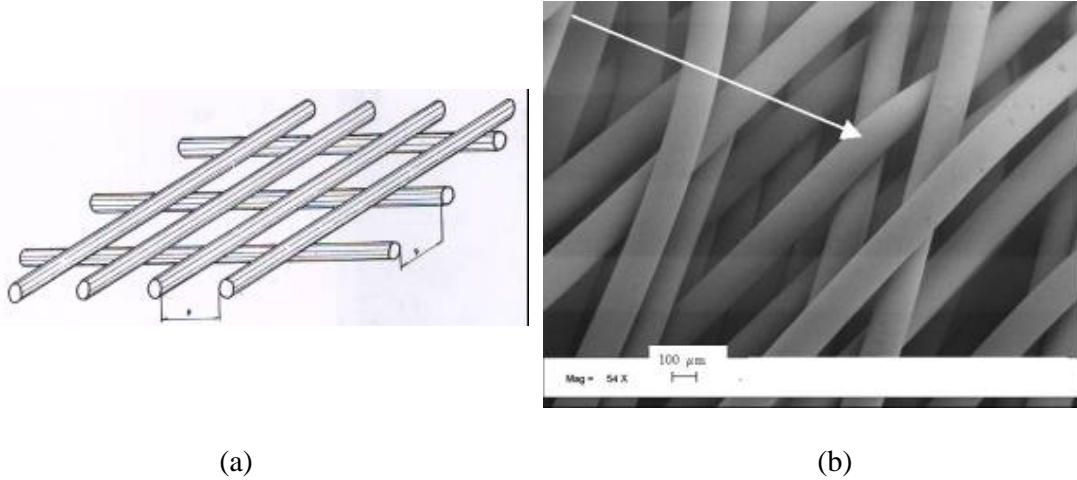


Figure 8.2. (a) Scheme of the model developed to evaluate the theoretical average pore size (p); (b) representative SEM image of a sample of P(DLLAcoTMC) for determination of the pore size of the scaffolds. Before analyses, the P(DLLAcoTMC) specimens were carefully flattened on the sample holder to eliminate the effect of the curvature of the tubular scaffolds. Measurements were always performed in the same direction, parallel to the axis of the tube, as indicated by the arrow.

used to calculate the average diameter of the spun fibres, by averaging the diameter of at least 20 fibres taken at a random. Exactly the same procedure was used to determine the pore size of P(DLLAcoTMC)-collagen hybrid samples using SEM. For this calculation also the pores formed by collagen were taken into account. To prevent surface charging, collagen-containing scaffolds were sputter-coated with gold using a Polaron E 5600 sputter coater, prior to analysis. Experimental winding angles were also determined from SEM images, by averaging the winding angles of 15 fibres taken at random. The obtained results were compared with theoretical winding angles.

The porosity (p) of the scaffolds was determined gravimetrically using the following equations:

$$p = [1 - (\rho_{\text{scaffold}} / \rho_{\text{polymer}})] * 100 \quad (8.4)$$

$$p_{\text{hybrid}} = p - [(g_{\text{coll}} / V_{\text{tube}}) / \rho_{\text{coll}}] * 100 \quad (8.5)$$

where ρ_{scaffold} , ρ_{polymer} and ρ_{coll} are the densities in g/cm^3 of the scaffold (porous P(DLLAcoTMC) structure), the non-porous P(DLLAcoTMC) polymer (1.29 g/cm^3) and

collagen (1.60 g/cm^3) [15], respectively. The mass of collagen added to the tube is g_{coll} , ρ_{hybrid} is the porosity of the hybrid scaffold and V_{tube} the volume of the tubular structure (ID = 3 mm; OD = 6 mm; length = 3-4 cm).

Further morphological characterization was performed by micro-computed tomography (μCT). The scaffolds were analysed without additional sample preparation using a desktop μCT ($\mu\text{CT-40}$, Scanco Medical, Bassersdorf, Switzerland) at a resolution of $6 \mu\text{m}$ in the three spatial dimensions (X-Ray voltage 45 kVp). The morphology of the three-dimensional scaffolds was evaluated directly without model assumptions for the structure. Porosity, pore size, accessible pore volume and accessible surface area were determined as previously described [21].

Mechanical properties.

To evaluate the mechanical properties of the scaffolds in the radial direction, samples were mounted on rigid supports in such a way that one side of each support projected through the lumen of the tube [22]. The supports were clamped to a Zwick (Z020, Ulm, Germany) tensile tester, equipped with a 500 N load cell. Measurements of stress response to a constant strain rate of 1 mm/min were performed on 0.7 cm long samples with an inner diameter of 3 mm and an outer diameter of approximately 6 mm. Stress was calculated by dividing the force generated during extension by the initial cross-sectional area. Prior to measuring, samples were preconditioned to account for small changes in the orientation of the fibres due to handling, by performing 10 cycles up to 15% strain, after which no more hysteresis was observed.

Tensile measurements in the radial direction were performed both on dry samples at room temperature and after equilibrating the specimens for 30 min in phosphate-buffered saline (PBS) at $37 \text{ }^\circ\text{C}$.

Smooth muscle cell culture.

Smooth muscle cells (SMC) were isolated from human umbilical veins by a collagenase digestion method as previously described [23]. Sub-confluent cultures of SMC were harvested by trypsinisation (2 min, 0.125% trypsin/0.05% EDTA) after which the cells were resuspended in culture medium (Dulbecco's Modified Eagle's Medium containing 10% (v/v) human serum, 10% (v/v) foetal bovine serum, 50 U/ml penicillin and 50 $\mu\text{g/ml}$ streptomycin). Cells were

counted with a Bürker hemacytometer and subsequently seeded onto hybrid P(DLLAcoTMC)-collagen tubular structures (length 1.5-2 cm, ID 3 mm, OD ca. 6 mm) at a density of 10^6 cells/scaffold. The scaffolds were mounted in glass chambers and seeded by means of a filtration procedure, during which the cell suspension was infused in the lumen with two syringes from both ends of the scaffolds and filtered through the wall (Fig. 8.3). The seeded matrices were placed in an incubator (37 °C and 5% CO₂) and rotated 90° along the longitudinal axis every 30-60 min for the first 4 h to promote homogeneous adhesion of the cells floating in the culture medium to the scaffolds. After 1 d, the flow chambers containing the seeded scaffolds were mounted in a bioreactor operating at 37 °C and 5% CO₂ [24]. This system consists of four parallel chambers connected through silicone tubing to a fluid reservoir containing culture medium (Fig. 8.4). Pulses are generated by a peristaltic pump (Watson Marlow Sci-Q-323) placed proximal to the vessels. A pressure of 100 mm Hg is applied to the culture medium reservoir and regulated by an electronically controlled Venturi valve (T5200-50, Fairchild Company, Winston-Salem, NC, USA). Pulsations were gradually increased from 30 to 120 beats/min after 3 d of culture, corresponding to a volumetric flow rate of approximately 10 ml/min/vessel and pressures in the range of 80-120 mmHg at the proximal connections of the chambers.

The bioreactor was operated for 7 d; the culture medium was refreshed every 2-3 d. SMC-seeded hybrid scaffolds were also cultured for 7 d under static conditions. After culturing, the constructs were analysed by SEM.

The mechanical properties were determined at 37 °C on samples equilibrated in PBS as described above.

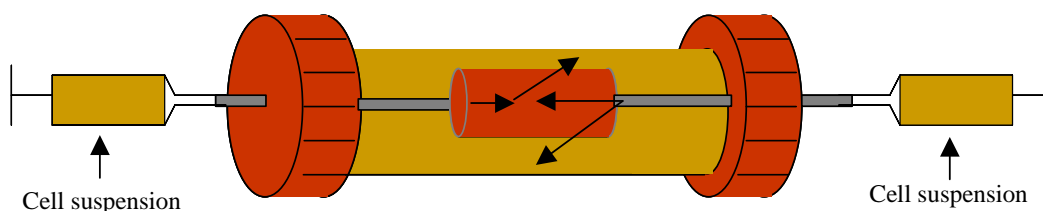


Figure 8.3. Schematic representation of the procedure used for cell seeding. After the tubular scaffolds were mounted in the chambers, the cell suspension was infused with two syringes from both luminal openings of the tubular scaffold through its wall, as indicated by arrows.

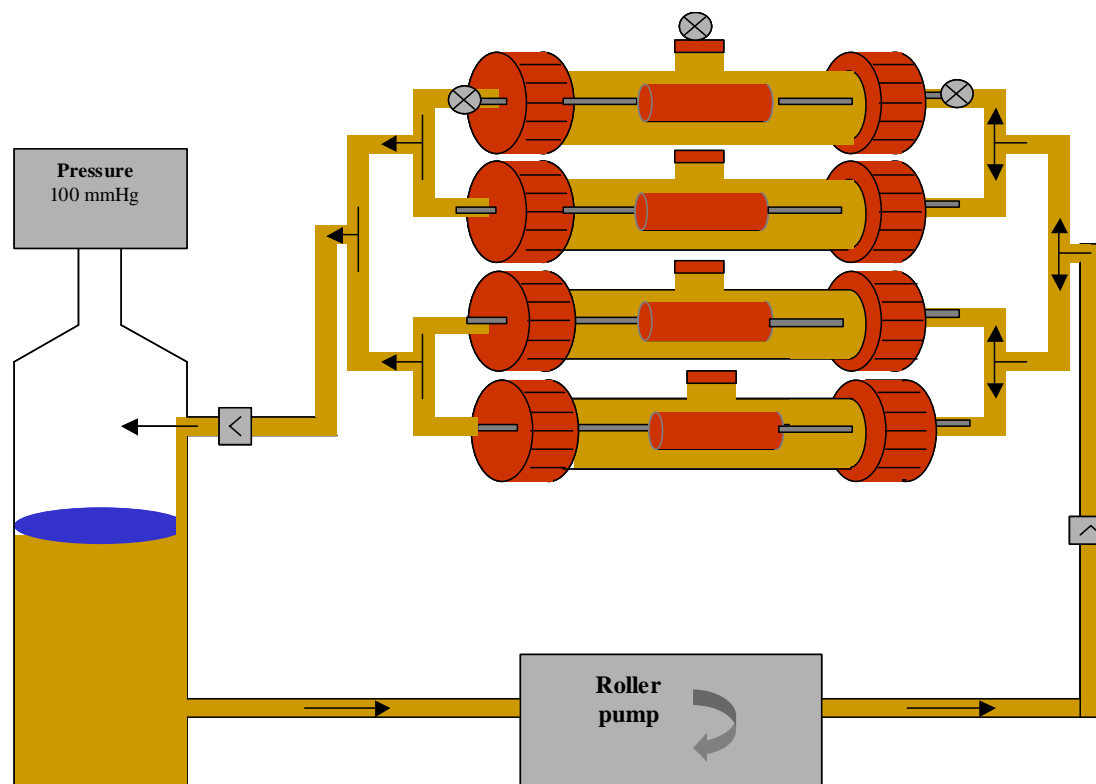


Figure 8.4. Schematic representation of the bioreactor used in this study. The SMC-seeded hybrid structures were mounted in four parallel chambers filled with culture medium. The chambers were connected through silicone tubing to the peristaltic pump and the culture medium reservoir, respectively. Culture medium was perfused through the cell-seeded hybrid scaffolds inside the chambers. A pressure of 100 mmHg was applied to the fluid reservoir.

Results and discussion.

Vascular tissue engineering using scaffolds prepared from natural materials like collagen, has been unsuccessful because of inappropriate mechanical properties of the obtained constructs [1, 9, 10]. Synthetic polymers such as poly(lactic acid), poly(glycolic acid) and their copolymers also have important drawbacks in terms of incompatible mechanical properties. In a previous study, flexible high molecular weight polymers based on D,L-lactide and trimethylene carbonate P(DLLAcoTMC) were synthesized and applied in heart tissue engineering [17, 18]. In the present study, P(DLLAcoTMC) with a molar ratio of 83:17 was used to prepare porous tubular structures by means of melt spinning and fibre winding. Subsequently, a collagen type I microsponge was formed inside the three-dimensional synthetic scaffolds to improve adhesion and proliferation of seeded smooth muscle cells.

Chemical characterization of the copolymers.

A copolymer of D,L-lactide and TMC P(DLLAcoTMC) containing 83 mol% DLLA, with an average molecular weight, \overline{M}_n , of $1.4 \cdot 10^5$ (PDI = 1.8) was synthesized as described in the Materials and Methods. The obtained copolymer is a relatively rigid material in the glassy state at room temperature (E-modulus of compression moulded films is approximately 1900 MPa [17], $T_g = 45$ °C) and has a density of 1.29 g/cm^3 .

Preparation and characterization of porous tubular structures.

P(DLLAcoTMC) (83 mol% DLLA) was used to prepare porous tubular structures by melt spinning and fibre winding. An extrusion speed of 2.5 mm/min and a temperature of the melt of 200 °C allowed continuous spinning of the copolymer and minimized the residence time in the melt chamber to 42-55 min. Under these conditions substantial degradation of the copolymer could be prevented, as verified by the constant value of the extrusion force (10 N) throughout the duration of the spinning process and by the \overline{M}_n of the copolymer before and after spinning ($1.4 \cdot 10^5$ vs. $1.1 \cdot 10^5$, respectively).

The diameter of all distinct P(DLLAcoTMC) tubular structures in the dry state was monitored for 142 d at room temperature. No changes in the original dimensions were observed during this time period since the glass transition temperature of the samples (45 °C) is above room temperature. Table 8.1 gives an overview of the morphological and mechanical characteristics of porous P(DLLAcoTMC) tubular structures with different winding angles.

Samples with experimental winding angles of 33 ± 1 , 40 ± 5 and 51 ± 2 ° were not able to retain their original structures when subjected to an external stress, because of the poor interconnectivity between the fibres. In these scaffolds, the fibres were oriented almost parallel to each other and to the longitudinal axis of the tube. As a consequence, fibres in the specimens were easily displaced from their original position during removal of the tubular scaffolds from the collecting mandrel, leading to large differences between the theoretical and the experimental winding angles and average pore size. Although mechanical properties of the tubes could not be directly related to the experimental winding angles for the reasons described above (Table 8.1), samples with an experimental winding angle of 51 ± 2 ° seemed to have the best mechanical performance. Moreover, a better agreement between theoretical and experimental average pore size was found for these latter specimens. This may suggest that tubes with a winding angle of 51 ± 2 ° can, at least partially, retain their original structure

Table 8.1. Morphological and mechanical characteristics of porous tubes of P(DLLAcoTMC) spun at different reciprocating longitudinal speeds. Measurements were performed at room temperature on dry samples (unless otherwise stated). All specimens had an average wall thickness of approximately 1.5 mm and a length of 0.7 cm. ($n = 3 \pm s.d.$).

Sample	Theoretical Winding Angle (°)	Experimental Winding Angle (°)	Porosity (%)	Experimental Pore Size ** (µm)	Theoretical Pore Size + (µm)	Stiffness (KPa)	Yield stress (MPa)	Yield strain (%)
L12*	54.1	33 ± 1	80 ± 2	150 ± 50	200 ± 50	200 ± 50	0.16 ± 0.04	61 ± 1
L11*	61.0	40 ± 5	80 ± 2	310 ± 120	420 ± 40	90 ± 40	0.18 ± 0.06	60 ± 10
L10*	69.3	51 ± 2	78 ± 3	270 ± 90	280 ± 20	250 ± 100	0.24 ± 0.06	55 ± 5
L10* (PBS, T = 37 °C)	69.3	51 ± 2	78 ± 3	270 ± 90	280 ± 20	10 ± 10	0.09 ± 0.06	90 ± 70

* Reciprocating longitudinal speeds L10 = 0.056 m/s; L11 = 0.08 m/s and L12 = 0.11 m/s. Rotational speed was 0.148 m/s for all samples.

** Pore sizes from SEM analyses

+ Pore size from model of Leidner *et al.* [20]

during handling. Tubular structures prepared with this experimental winding angle were therefore used for further experiments.

In order to evaluate the mechanical behaviour of these tubes in an environment similar to that experienced *in vivo*, their mechanical properties were also measured at 37 °C after equilibration in PBS (Table 8.1). The stiffness and yield stress decreased from 250 ± 100 to 10 ± 10 KPa and from 0.24 ± 0.06 to 0.09 ± 0.06 MPa, respectively, for the dry samples as compared to the PBS swollen samples (Table 8.1). This decrease in stiffness and yield strength may be due to the lower glass transition temperature of the copolymer after swelling in PBS (39 °C vs. 45 °C in the dry state).

To improve mutual fibre binding, the tubes were spun with additional heating of the fibres in the air gap between the spinneret and the rotating mandrel, using an IR lamp. The temperature in the air gap around the spun fibres was approximately 55 °C, well above the glass transition temperature of the polymer. In this way, scaffolds with well-fused connected fibres were obtained (Fig. 8.5). This procedure resulted in a smaller difference between the experimental (62 ± 3 °) and the theoretical winding angle (69.3 °), as well as in an increased yield stress (0.3 ± 0.2 MPa vs. 0.09 ± 0.06 MPa) of samples swollen in PBS and analysed at 37 °C (Tables 8.1 and 8.2)

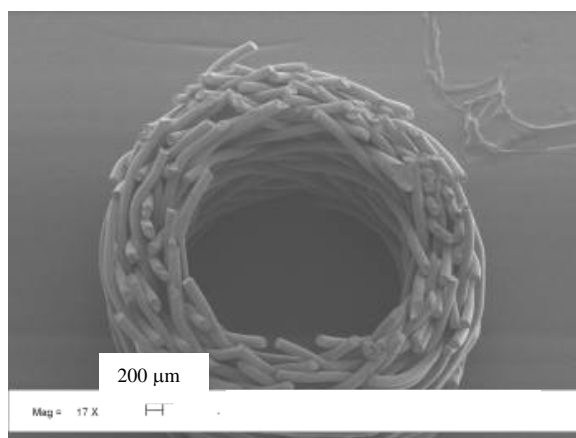


Figure 8.5. SEM image of a melt-spun porous tubular structure of *P(DLLAcoTMC)* containing 83 mol% DLLA. Fibres leaving the melt chamber were heated with an infrared lamp. Experimental winding angle is 62 ± 3 °. Scale bar is 200 μm.

Table 8.2. Morphological and mechanical characteristics of porous tubes of P(DLLAcoTMC) (and collagen). Measurements were performed at 37 °C on specimens equilibrated for 30 min in PBS. All tubular structures were spun with heating of the fibres in the air gap with an IR lamp. All the specimens had an average wall thickness of approximately 1.5 mm (unless otherwise stated) and a length of 0.7 cm ($n = 3 \pm s.d.$).

Sample	Theoretical winding angle (°)	Experimental winding angle (°)	Porosity (%)	Pore size** (µm)	Stiffness (KPa)	Yield stress (MPa)	Yield strain (%)
L10*	69.3	62 ± 3	98 ± 1	300 ± 150	0.01 ± 0.01	0.3 ± 0.2	90 ± 30
L10* (wall thickn. 3.5 mm)	69.3	62 ± 3	98 ± 0	300 ± 150	180 ± 90	0.7 ± 0.1	90 ± 30
L10* (+ collagen)	69.3	62 ± 3	97 ± 1	102 ± 98	290 ± 40	0.5 ± 0.2	63 ± 9

** Pore sizes from SEM analyses.

Increasing the wall thickness from 1.5 to 3.5 mm yielded samples with improved stiffness (180 ± 90 KPa vs. 0.01 ± 0.01 kPa) and yield stress (0.7 ± 0.1 MPa vs. 0.3 ± 0.2 MPa). Independent of the use of an IR lamp during processing and wall thickness, all wet specimens tested at 37 °C had a yield strain of approximately 90% (Tables 8.1 and 8.2).

Increasing the wall thickness of the samples from 1.5 to 3.5 mm also did not alter in a significant way the range of pore size (307 ± 207 μ m vs. 193 ± 93 μ m). Also the overall porosity was not influenced by the wall thickness of the scaffolds and values of 98% were found for specimens with an experimental winding angle of 62 ± 3 °, which were spun with an elevated temperature in the air gap (Table 8.2).

Unexpectedly, when incubated overnight in culture medium containing serum at 37 °C and 5% CO₂, these scaffolds collapsed due to the loss of the connections between the fibres. Since identical porous tubular structures were not destabilized after overnight incubation at 37 °C in PBS, it was hypothesized that the disconnection of contact points between the fibres was due to protein adsorption from the culture medium onto the synthetic polymer matrix [25]. This implies that, despite the presence of an IR lamp in the air gap between the spinneret and the collecting mandrel, the different fibres were connected only by adhesion, whereas there was not any interpenetration of molecules from one spun fibre to the next.

Preparation and characterization of hybrid structures.

In order to improve the structural stability of the melt spun tubular scaffolds, a collagen microsp sponge with interconnected pore structure was formed in the pores of the tubular P(DLLAcoTMC) matrix, by means of dipping the matrices into a collagen type I suspension and subsequent freeze drying. In this way, 4-6 wt% of collagen was incorporated in the scaffolds. Collagen was present both on the outer and on the inner surface of the tubular structures (Fig. 8.6). In particular, a thin layer of collagen is present on top of the synthetic fibres. This can enhance cell adhesion. Contact of collagen with the synthetic polymer matrix may also have a beneficial effect on the mechanical stability of the scaffolds. Moreover, the formation of a fibrous network inside a porous structure may increase the available surface area for cell attachment.

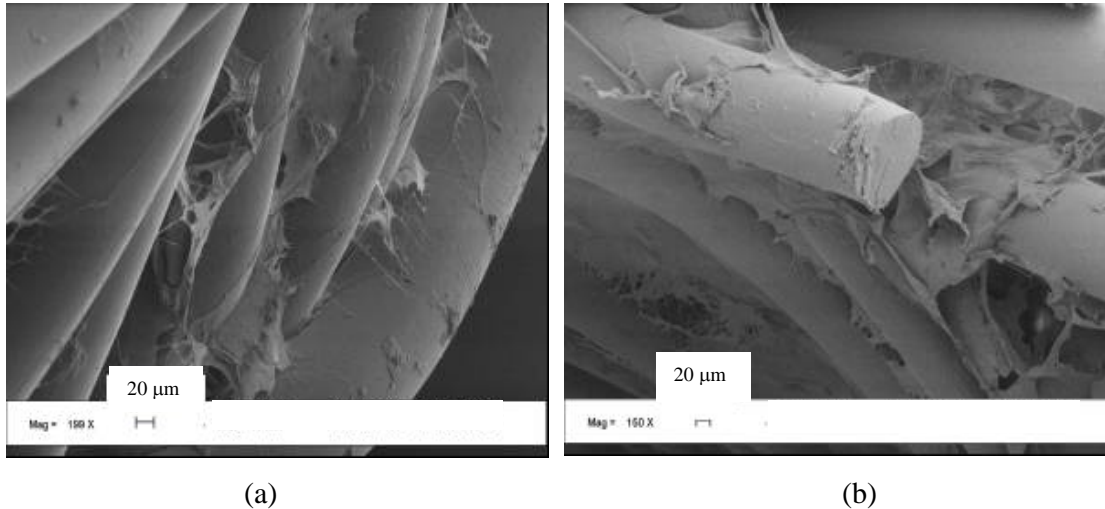


Figure 8.6. SEM images of a hybrid scaffold of P(DLLAcoTMC) dip-coated with type I collagen. Approximately 4-6 wt% collagen has been incorporated. A collagen microsphere is visible both on the outer surface (a) and on the inner surface (b). Fibres leaving the melt chamber were heated with an infrared lamp. Experimental winding angle is $62 \pm 3^\circ$. The collagen sponge was formed by freeze drying. The scale bar is 20 μm in both images.

The overall porosity determined by gravimetry was not significantly altered by the addition of collagen (Table 8.2). On the contrary, addition of collagen to the P(DLLAcoTMC) scaffolds and subsequent freeze-drying caused the pore size distribution to shift from 100-514 μm to a lower range of 5-200 μm , as measured by SEM. The average pore size after incorporation of collagen was $102 \pm 98 \mu\text{m}$, which is still sufficient to allow SMC migration inside the three-dimensional scaffolds [26].

The morphological characteristics of the P(DLLAcoTMC)-collagen hybrid scaffolds determined by gravimetry and SEM were compared with those obtained by μCT analysis. The average pore size determined by SEM was comparable to that of 107 μm obtained from μCT analysis (Fig. 8.7). On the contrary, the available resolution (6 μm) prevented an accurate determination of the porosity by μCT analysis (53%).

The accessible pore volume for a simulated sphere with a diameter of 100 μm was more than 50% of the total pore volume (Fig. 8.8a), indicating the presence of interconnected pores permitting significant migration of cells as well as transport of oxygen and nutrients throughout the three-dimensional matrix. For the same simulated sphere diameter, the accessible surface area was 75% of the available total surface area (Fig. 8.8b).

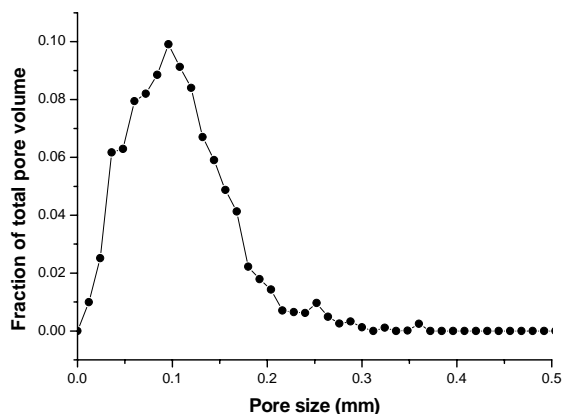
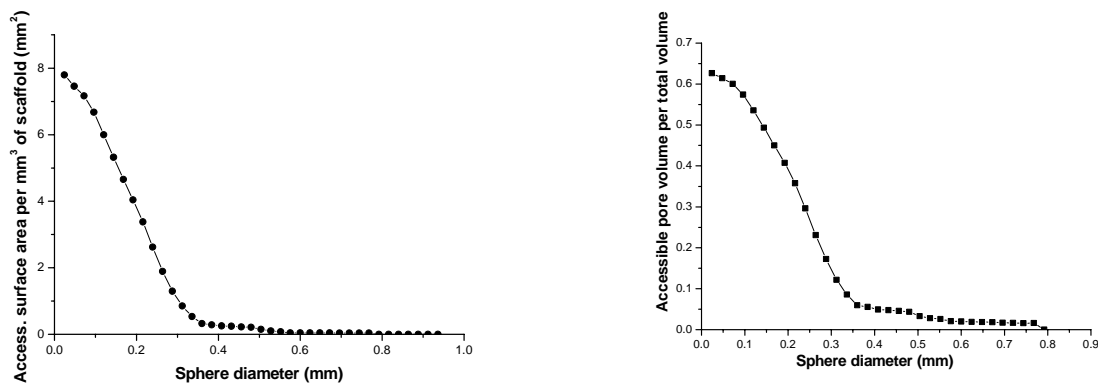


Figure 8.7. Pore size distribution derived from μ CT analysis of a hybrid scaffold of P(DLLAcoTMC) and collagen (83 mol% DLLA; 4-6 wt% collagen). Fibres leaving the melt chamber were heated with an infrared lamp. Experimental winding angle is $62 \pm 3^\circ$.



(a)

(b)

Figure 8.8. (a) Accessible pore volume (normalized to the total volume) and (b) accessible surface area (normalized to the total volume) vs. simulated sphere diameter for a hybrid scaffold of P(DLLAcoTMC) and collagen (83 mol% DLLA; 4-6 wt% collagen). Fibres leaving the melt chamber were heated with an infrared lamp. Experimental winding angle is $62 \pm 3^\circ$.

Formation of a collagen microsponge inside P(DLLAcoTMC) porous tubular scaffolds yielded reinforced structures. Compared to wet scaffolds without collagen, the hybrid structures were stiffer (290 ± 40 KPa vs. 0.01 ± 0.01 kPa) and showed slightly lower elongations at yield

($63 \pm 9 \%$ vs. $90 \pm 30 \%$) (Table 8.2). Formation of collagen microsponges in the pores of synthetic scaffolds has already been reported to improve the mechanical properties of and the cell adhesion on polylactides and polyglycolides [15, 27]. This reinforcement, especially in terms of stiffness, may be due to the possibility to disperse stresses over a more extensive area when smaller pores are formed inside a porous structure with larger pore sizes [28]. Significant stress concentration normally occurs in the weak locations of the pore walls if only larger pores are present. When smaller pores are formed, a part of the stress is distributed also on the pore walls between the big and small pores, thus reinforcing the overall structure.

The presence of a collagen microsp sponge in the porous tubular matrix also resulted in improved structural stability of the scaffolds during incubation in culture medium at $37\text{ }^{\circ}\text{C}$ and $5\% \text{ CO}_2$. This might be due to the swelling of the P(DLLAcoTMC) fibres in the acidic collagen suspension during dipping and successive freeze-drying, resulting in improved fibre binding. Moreover, the presence of collagen at the connections between the fibres may have prevented protein adsorption from the culture medium, leading to improved structural stability of the hybrid scaffolds.

Cell culture.

Hybrid P(DLLAcoTMC)-collagen scaffolds with an experimental winding angle of $62 \pm 3^{\circ}$, were seeded with SMC and cultured in a bioreactor built in our laboratories [24]. The constructs maintained their structural stability during culturing. After 7 d of culture under dynamic conditions, the SMC were viable and could be observed by SEM on the inner and outer surface as well as in the cross-section of the three-dimensional porous scaffolds. SMC were covered with abundant collagen, which might have been produced by the cells during the culture period (Fig. 8.9a,b).

Compared with non-seeded scaffolds, culturing with SMC for 7 d under dynamic conditions yielded stronger constructs (yield stress $2.8 \pm 0.6 \text{ MPa}$ vs. $0.5 \pm 0.2 \text{ MPa}$) having a higher elongation at yield (yield strain $120 \pm 20 \%$ vs. $63 \pm 9 \%$). Also the stiffness of the constructs was higher than that of the non-seeded scaffolds ($1.6 \pm 0.4 \text{ MPa}$ vs. $90 \pm 40 \text{ KPa}$) (Fig. 8.10).

These results were compared with those obtained with analogous SMC-seeded scaffolds cultured for 7 d under static conditions. SEM analyses revealed that SMC grew on the outer surface of the statically cultured scaffolds, but were hardly present in their cross section (Fig. 8.11a,b). SMC were also partially covered with collagen fibres, though less than observed

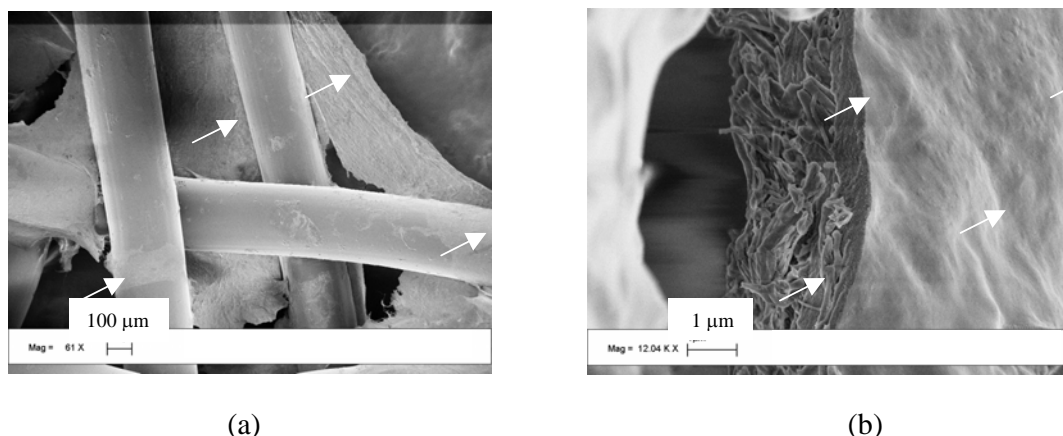


Figure 8.9. SEM images of a hybrid scaffold of P(DLLAcoTMC) and collagen (83 mol% DLLA; 4-6 wt% collagen) cultured with SMC under dynamic conditions for 7d. As indicated by arrows, a layer of collagen and possibly SMC is visible on and in between the synthetic fibres. (a) Inner surface of the construct (scale bar 100 μm); (b) detail of the cross-section of a multi layer of SMC and collagen interspersed with each other (scale bar is 1 μm).

in the presence of flow. Also the overall cell density was lower than in dynamically cultured scaffolds. The improved ability of SMC to adhere and proliferate in a dynamic environment is in agreement with data presented in literature [29, 30].

Dynamically cultured scaffolds were slightly stronger than scaffolds cultured under static conditions, which had a yield stress of 2.0 ± 0.2 MPa, whereas yield strain (115 ± 15 %) and stiffness (1.8 ± 0.9 MPa) were similar (Fig. 8.10). These values are comparable with the radial mechanical properties of healthy human artery mesenterica (approximate age 60 ys), which were measured in our laboratories in exactly the same way. In agreement with data reported in literature for the carotid and the mammary artery [31, 32], stiffness of several MPa and elongation at yield of approximately 100% were found. Obviously, the latter values will vary if different arteries are considered. For example, muscular arteries, like the carotid, will have higher stiffness and lower elongation at yield than elastic vessels, like the mammary artery [32].

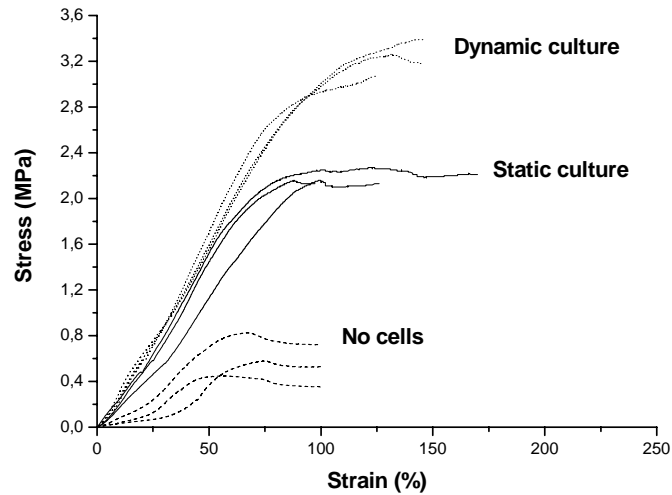


Figure 8.10. Comparison of stress-strain curves of hybrid scaffolds of *P(DLLAcoTMC)* and collagen (83 mol% DLLA; 4-6 wt% collagen) incubated in culture medium for 7 d without cells (dashed line) or cultured for 7 d under static (solid line) or dynamic (dotted line) conditions. Measurements were performed on PBS-equilibrated samples at 37 °C ($n = 3$).

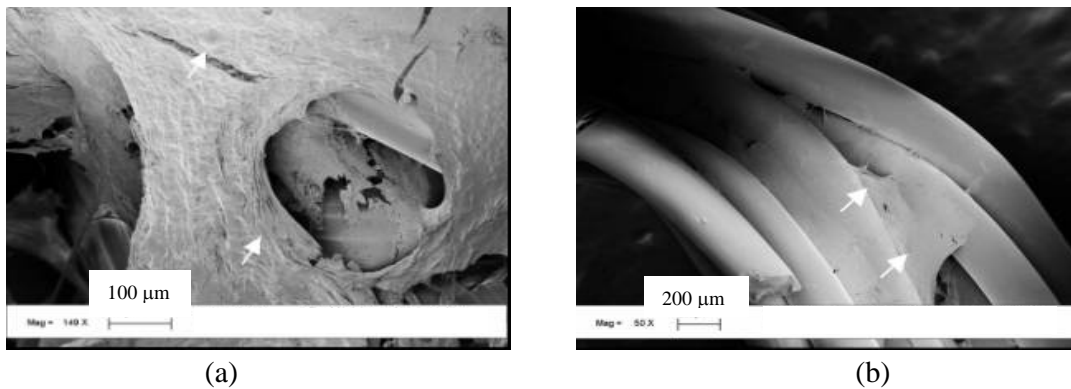


Figure 8.11. SEM images of a hybrid scaffold of *P(DLLAcoTMC)* and collagen (83 mol% DLLA; 4-6 wt% collagen) cultured with SMC under static conditions for 7d. (a) Collagen and possibly cells are present on the outer surface (scale bar is 100 µm); (b) a few cells are visible in the cross-section of the construct, especially on the collagen fibres between the synthetic fibres (scale bar is 200 µm).

Conclusions.

In this study, P(DLLAcoTMC) containing 83 mol% DLLA was used to produce matrices potentially useful in tissue engineering of small-diameter blood vessels. The copolymer was processed into highly porous tubular structures by melt spinning and fibre winding. This approach obviates the need of organic solvents that may compromise subsequent cell culture. A collagen microsp sponge with interconnected pores was formed in the pores of the P(DLLAcoTMC) porous tubular structure. The hybrid scaffolds of synthetic polymer and collagen possessed higher stiffness than the synthetic polymer alone. Moreover, hybridisation with collagen conferred structural stability to three-dimensional synthetic scaffolds at 37 °C in culture medium, which permitted SMC seeding and culturing in dynamic conditions (120 beats/min at arterial pressure). Dynamically cultured constructs revealed SMC homogeneously distributed throughout the wall. These constructs had improved mechanical properties compared to specimens cultured without mechanical stimulation. It is concluded that dynamically cultured hybrid constructs can be used as base structures for tissue engineering of small-diameter blood vessels, since their mechanical properties were comparable to those of the human artery mesenterica.

Acknowledgments.

H.Th.B. van Moerkerk and T. van Kuppevelt (Department of Biochemistry 194, NCLMS, University Medical Centrum Nijmegen, The Netherlands) are acknowledged for providing collagen for this study.

References.

1. Weinberg, C.B. and Bell, E., A blood vessel model constructed from collagen and cultured vascular cells. *Science*, 1986. 231: 397-400.
2. L'Heureux, N., Paquet, S., Labbe, R., Germain, L., and Auger, F.A., A completely biological tissue-engineered human blood vessel. *Faseb J.*, 1998. 12(1): 47-56.
3. Campbell, J.H., Efendy, J.L., and Campbell, G.R., Novel vascular graft grown within recipient's own peritoneal cavity. *Circ. Res.*, 1999. 85(12): 1173-1178.
4. Bader, A., Steinhoff, G., and Strobl, K., Engineering of human vascular aortic tissue based on a xenogenic starter matrix. *Transplant.*, 2000. 70(1): 7-14.

5. Mooney, D.J., Mazzoni, C.L., Breuer, C., McNamara, K., Hern, D., Vacanti, J.P., and Langer, R., Stabilized polyglycolic acid fibre-based tubes for tissue engineering. *Biomaterials*, 1996. 17(2): 115-124.
6. Niklason L.E., Gao J., Abbott W.M., Hirschi K.K., Houser S., Marini R., and R., L., Functional arteries grown in vitro. *Science*, 1999. 284(5413): 489-493.
7. Hoerstrup, S.P., Zund, G., Sodian, R., Schnell, A.M., Grunenfelder, J., and Turina, M.I., Tissue engineering of small caliber vascular grafts. *E. J. Cardio-Thorac. Surg.*, 2001. 20(1): 164-169.
8. Fung, Y.C., Mechanical properties and Active Remodeling of Blood Vessels, in *Biomechanics. Mechanical Properties of Living Tissues*. 1993, Springer Ed.: New York. 321-391.
9. Kanda, K. and Matsuda, T., Mechanical stress-induced orientation and ultrastructural change of smooth muscle cells cultured in three-dimensional collagen lattices. *Cell Transplant.*, 1994. 3(6): 481-492.
10. Seliktar, D., Nerem, R.M., and Galis, Z.S., Mechanical strain-stimulated remodeling of tissue-engineered blood vessel constructs. *Tissue Eng.*, 2003. 9(4): 657-666.
11. Debelle, L. and Tamburro, A.M., Elastin: molecular description and function. *Int. J. Biochem. Cell Biol.*, 1999. 31(2): 261-272.
12. Buttafoco, L., Engbers-Buijtenhuijs, P., Poot, A.A., Dijkstra, P.J., Daamen, W.F., van Kuppevelt, T.H., Vermes.I., and Feijen, J., First steps towards tissue engineering of small-diameter blood vessels: preparation of flat scaffolds of collagen and elastin by means of freeze-drying. *Submitted to J. Biomed. Mat. Res.*
13. Daamen, W.F., van Moerkerk, H.T.B., Hafmans, T., Buttafoco, L., Poot, A.A., Veerkamp, J.H., and van Kuppevelt, T.H., Preparation and evaluation of molecularly-defined collagen-elastin-glycosaminoglycan scaffolds for tissue engineering. *Biomaterials*, 2003. 24(22): 4001-4009.
14. Buttafoco, L., Engbers-Buitenhuijs, P., Poot, A.A., Dijkstra, P.J., Vermes, I. and Feijen, J., Dynamic versus static smooth muscle cells culture in tubular collagen/elastin matrices for vascular tissue engineering. *Submitted to Biomaterials*.
15. Chen, G.P., Ushida, T., and Tateishi, T., A biodegradable hybrid sponge nested with collagen microsponges. *J. Biomed. Mat. Res.*, 2000. 51(2): 273-279.
16. Berglund, J.D., Mohseni, M.M., Nerem, R.M., and Sambanis, A., A biological hybrid model for collagen-based tissue engineered vascular constructs. *Biomaterials*, 2003. 24(7): 1241-1254.

17. Pego, A.P., Poot, A.A., Grijpma, D.W., and Feijen, J., Physical properties of high molecular weight 1,3-trimethylene carbonate and D,L-lactide copolymers. *J. Mater. Sci.-Mater. Med.*, 2003. 14(9): 767-773.
18. Pego, A.P., Siebum, B., van Luyn, M.J.A., Gallego, X.I., van Seijen, Y., Poot, A.A., Grijpma, D.W., and Feijen, J., Preparation of degradable porous structures based on 1,3-trimethylene carbonate and D,L-lactide (co)polymers for heart tissue engineering. *Tissue Eng.*, 2003. 9(5): 981-994.
19. Pieper, J.S., Oosterhof, A., Dijkstra, P.J., Veerkamp, J.H., and van Kuppevelt, T.H., Preparation and characterization of porous crosslinked collagenous matrices containing bioavailable chondroitin sulphate. *Biomaterials*, 1999. 20(9): 847-858.
20. Leidner, J., Wong, E.W., MacGregor, D.C., and Wilson, G.J., A novel process for the manufacturing of porous grafts: process description and product evaluation. *J. Biomed. Mat. Res.*, 1983. 17(2): 229-247.
21. Claase, M.B., de Riekerink, M.B., de Bruijn, J.D., Grijpma, D.W., Engbers, G.H.M., and Feijen, J., Enhanced bone marrow stromal cell adhesion and growth on segmented poly(ether ester)s based on poly(ethylene oxide) and poly(butylene terephthalate). *Biomacromolecules*, 2003. 4(1): 57-63.
22. Girton, T.S., Oegema, T.R., and Tranquillo, R.T., Exploiting glycation to stiffen and strengthen tissue equivalents for tissue engineering. *J. Biomed. Mat. Res.*, 1999. 46(1): 87-92.
23. Buijtenhuijs, P., Buttafoco, L., Poot, A.A., Daamen, W.F., van Kuppevelt, T.H., Dijkstra, P.J., de Vos, R.A.I., Sterk, L.M.T., Geelkerken, B.R.H., Feijen, J., and Vermes, I., Tissue engineering of blood vessels: characterization of smooth-muscle cells for culturing on collagen-and-elastin-based scaffolds. *Biotechnol. Appl. Biochem.*, 2004. 39: 141-149.
24. Buttafoco, L., Engbers-Buijtenhuijs, P., Poot, A.A., Dijkstra, P.J., Vermes, I., Feijen, J., Development of a bioreactor for tissue engineering of small-diameter blood vessels: design of a pulsatile flow system. *Submitted to Biotech. Bioeng.*
25. Denizli, F.K. and Guven, O., Competitive adsorption of blood proteins on gamma-irradiated-polycarbonate films. *J. Biomater. Sci.-Polym. Ed.*, 2002. 13(2): 127-139.
26. Yannas, I.V., Tissue regeneration templates based on collagen-glycosaminoglycan copolymers. *Adv. Pol. Sci.*, 1995. 122(26): 219-244.
27. Chen, G.P., Ushida, T., and Tateishi, T., Fabrication of PLGA-collagen hybrid sponge. *Chem. Lett.*, 1999(7): 561-562.

28. Han, F., Cheng, H., Wang, J., and Wang, Q., Effect of pore combination on the mechanical properties of an open cell aluminum foam. *Scripta Materialia*, 2004. 50(1): 13-17.
29. Kim, B.S. and Mooney, D.J., Scaffolds for engineering smooth muscle under cyclic mechanical strain conditions. *J. Biomech. Eng.*, 2000. 122: 210-215.
30. Matsuda, T. and Miwa, H., A hybrid vascular model biomimicking the hierarchic stuture of the arterial wall: neointimal stability and neoarterial regeneration process under arterial circulation. *J. Thorac.Cardiovasc. Surg.*, 1995. 110(4): 988-997.
31. Ozolanta, I., Tetere, G., Purinya, B., and Kasyanov, V., Changes in the mechanical properties, biochemical contents and wall structure of the human coronary arteries with age and sex. *Med. Eng. Phys.*, 1998. 20(7): 523-533.
32. van Andel, C.J., Pistecky, P.V., and Borst, C., Mechanical properties of porcine and human arteries: implications for coronary anastomotic connectors. *Ann. Thorac. Surg.*, 2003. 76(1): 58-64.

Summary

Atherosclerotic vascular disease, including peripheral and coronary artery disease, is the main cause of morbidity and mortality in the Western society. Although synthetic blood vessel prostheses are successfully being used for large-diameter vascular reconstructions, until now no functional small-diameter (< 6 mm) artificial vascular graft is available. Autologous veins and arteries are currently being used as vessel substitutes, but limitations in arteries supply and compliance mismatch are some of their main drawbacks encountered in this approach. Therefore, tissue engineering of small-diameter vascular grafts is an expanding area of research.

Tissue engineering is an interdisciplinary field that applies the principles of engineering and life sciences towards the reconstruction or development of biological substitutes that restore, maintain or improve tissue functions. The aim of the work described in this thesis is to tissue engineer small-diameter blood vessels from porous tubular scaffolds based on the extracellular matrix protein collagen in combination with either natural or synthetic materials. Human vascular smooth muscle cells (SMC) were cultured in these scaffolds in a pulsatile flow bioreactor developed in our laboratories.

Chapter 2 gives an overview of the different approaches to tissue engineer small-diameter blood vessels and find a solution to the problem of atherosclerosis. Many scaffolds based on synthetic polymers, like poly(α -hydroxy acids) (*e.g.* poly(glycolic acid) or poly(lactic acid)) and their copolymers, have been developed for this purpose. The use of synthetic polymers has certain advantages as compared to natural ones, in terms of control of the properties of the material and of the scaffold (*e.g.* strength, degradation, porosity and microstructure). However, achieving the necessary cell adhesion, proliferation and extracellular matrix deposition is still a challenge. Moreover, polymer degradation products may alter the local cellular environment and thus cell function, preventing the development of a proper vascular graft. Protein-based scaffolds, especially prepared from collagen, have also been used for vascular tissue engineering, because of their biocompatibility and biodegradability. Unfortunately, despite many efforts to improve the mechanical properties of tissue-engineered small-diameter blood vessels based on collagen, the use of these constructs is still limited due to their poor mechanical integrity.

In the present programme, the possibility to improve the mechanical properties of collagen scaffolds by incorporation of the extracellular matrix protein elastin was investigated. Furthermore, hybrid scaffolds of poly(D,L-lactide)co(1,3-trimethylene carbonate) and collagen were developed. Such hybrid structures are attractive based on both the suitable mechanical properties of the copolymer and the appropriate cellular interactions of collagen.

Matrices of insoluble collagen type I and insoluble elastin have improved mechanical properties (*i.e* elongation at yield and degree of total strain recovery) as compared to collagen structures (**chapter 3**). Flat scaffolds of these two proteins prepared by freeze drying have porosities between 90 and 98 % and pore sizes of 130-340 μm , depending on the collagen to elastin weight ratio used. It was found that the use of a ratio of collagen to elastin of 1:1 is most suitable in terms of mechanical properties. In order to further match the requirements needed for *in vitro* smooth muscle cells (SMC) culture, the scaffolds were crosslinked. Crosslinking of collagen/elastin matrices either in water or in ethanol/water (40% v/v) was carried out using a carbodiimide (EDC) in combination with a succinimide (NHS), in the presence or absence of a Jeffamine (J230) or by reaction with butanediol diglycidylether (BDGE) followed by treatment with EDC/NHS. Crosslinking with EDC/NHS or J230/EDC/NHS results in matrices with improved mechanical properties as compared to non-crosslinked matrices, whereas sequential crosslinking with BDGE and EDC/NHS yields very fragile scaffolds. Ethanol/water is used as the preferred solvent during crosslinking due to its ability to retain porous open structures, on which SMC could be successfully cultured.

Electrospinning was explored as an alternative technique to prepare porous scaffolds from soluble collagen type I, soluble elastin and mixtures of the two proteins (**chapter 4**). Non-woven meshes were successfully spun from aqueous solutions of these proteins, thus avoiding the use of organic solvents. In all cases addition of PEO ($M_w = 8 \cdot 10^6$) and NaCl is necessary to obtain continuous fibres. The voltage needed to continuously spin the fibres is dependent on the composition of the starting solution, but always between 10 and 25 kV. The morphology of the produced fibres is influenced by the composition of the spun solutions. For example, increasing the collagen to elastin weight ratio from 2:1 to 1:3 results in an increase in the diameter of the fibres from 220 to 600 nm. Collagen/elastin meshes were stabilized by crosslinking in ethanol/water (70% v/v) with EDC/NHS. This treatment affords materials with high thermal stability ($T_d = 79$ °C) and does not alter their original morphology. Moreover, after the

crosslinking procedure, PEO and NaCl are fully leached out. A confluent layer of SMC could be formed on top of flat electrospun scaffolds after 14 d of culture under stationary conditions.

Since spinning collagen and elastin together affords fibres in which the single components could not be distinguished by SEM, the possible interactions occurring in collagen/elastin assemblies were investigated by solid-state ^{13}C cross-polarization magic angle spinning (CP/MAS) NMR (**chapter 5**). Freeze-dried samples of soluble collagen, elastin or collagen/elastin (weight ratio 1:1) were analysed at two degrees of hydration (10 ± 1 and 22 ± 1 %), since water is known to have an essential role in the structure and properties of both proteins. The simultaneous presence of both the proteins does not induce any detectable conformational change in collagen or elastin. In all cases the spin-lattice relaxation times in the rotating frame ($T_{1\rho}$) found for all protons in collagen/elastin samples could be obtained from mono-exponential curves. This indicates that there are no domains with different mobilities in the sample and the various residues behave exactly in the same way, independently from the protein they belong to. Carbon $T_{1\rho}$ values are instead higher in the mixture, indicating lower mobility of the collagen/elastin assembly as compared to the separate components and occurrence of hydrogen bonding and hydrophobic interactions between the two proteins.

In vivo, orientation of vascular cells is induced by the dynamic environment to which these are exposed. A pulsatile flow bioreactor was developed in our laboratories in which arterial pressures (80-120 mmHg) and pulses (120 beats/min) can be established (**chapter 6**). The system was characterized in terms of flow dynamical properties by using either a silicone tube or an EDC/NHS crosslinked collagen/elastin freeze-dried tubular scaffold as vessel. The flow rate increases linearly with the number of applied pulses. Mean wall shear rates of 61 s^{-1} and Reynolds numbers of 20-96, in the same range as those found in the human carotid artery are obtained. The values of the Reynolds number indicate that the flow is laminar, thus ensuring an efficient transfer of nutrients and oxygen through the three-dimensional construct. The increase of the average pressure drop from 0 to approximately 14 mmHg over the wall and along the length of EDC/NHS crosslinked collagen/elastin constructs, during 14 d of culture with SMC indicate that the porosity of the constructs decreases during the culture period.

The effects of culturing SMC on (crosslinked) collagen/elastin porous tubular scaffolds for different time periods under dynamic conditions were also evaluated in terms of morphological and mechanical properties of the constructs (**chapter 7**). No mechanical support is needed during

culturing to prevent the (crosslinked) vessels from bursting. After 7 d of culture, SMC are homogeneously distributed throughout the (EDC/NHS crosslinked) constructs. In contrast, after 7 d, hardly any cell is observed on the luminal side of J230/EDC/NHS crosslinked matrices. Further analyses with the EDC/NHS crosslinked scaffolds revealed that, after 14 d of culture, the high strain stiffness of the constructs increases more than two times, up to 38 ± 2.0 MPa, whereas the low strain stiffness doubles to 8 ± 2 kPa as compared to initial mechanical properties. The yield stress is 30 ± 10 kPa and the elongation at yield 120 ± 20 %. The latter value is comparable to that found for the human artery mesenterica. SEM analyses and histology reveal the presence of SMC throughout the constructs and of collagen fibres partially oriented in the circumferential direction.

Hybrid scaffolds of natural and synthetic polymers were investigated as a suitable alternative for tissue engineering of small-diameter blood vessels (**chapter 8**). In this way, suitable mechanical properties are ensured by the synthetic material, whereas interaction with cells is favoured by the natural component. Poly(D,L-lactide)co (1,3-trimethylene carbonate) (P(DLLAcoTMC)) containing 83 mol% DLLA was used for this purpose. The copolymer was processed into tubular structures with a porosity of approximately 98% by melt spinning and fibre winding, thus obviating the need of organic solvents that may compromise subsequent cell culture. A collagen micro sponge was formed inside the pores of these P(DLLAcoTMC) scaffolds, by dip coating in an insoluble collagen type I suspension and successive freeze drying. Hybrid scaffolds with a porosity of 97% and an average pore size of approximately 102 μm are obtained. After 7 d of culture in a dynamic environment viable SMC are homogeneously distributed throughout the constructs, which are five times stronger and stiffer than non-cultured scaffolds. Values for yield stress (2.8 ± 0.6 MPa), stiffness (1.6 ± 0.4 MPa) and yield strain (120 ± 20 %) are comparable to those of the human artery mesenterica.

The research conducted in this thesis shows promising results for application of collagen-based constructs in tissue engineering of small-diameter blood vessels. Many aspects still have to be investigated, including the formation of an endothelial cell layer on the luminal side of the constructs.

Samenvatting

Atherosclerotische vaataandoeningen, van zowel perifere als coronaire arteriën, vormen de hoofdoorzaak van ziekte en sterfte in de Westerse samenleving. Hoewel synthetische bloedvatprothesen goed voldoen voor vasculaire reconstructies met een grote diameter, is er thans nog geen goed functionerende vaatprothese met een kleine diameter (< 6 mm) beschikbaar. Autologe venen en arteriën worden veel gebruikt voor vervanging van bloedvaten. Aan deze benadering zijn echter ook nadelen verbonden zoals beperkte beschikbaarheid en afwijkende compliantie van deze vaten. Om deze redenen vormt *tissue engineering* van bloedvatprothesen met een kleine diameter een groeiend onderzoeksgebied.

Tissue engineering is een interdisciplinaire tak van wetenschap waarin de principes van zowel technische als levenswetenschappen worden toegepast voor de constructie of ontwikkeling van biologische vervangingsmaterialen voor het herstellen, handhaven of verbeteren van weefselfuncties. Het doel van het werk beschreven in dit proefschrift was het vervaardigen van geschikte poreuze buisvormige structuren, gebaseerd op het extracellulaire matrixeiwit collageen in combinatie met andere natuurlijke of synthetische materialen, voor *tissue engineering* van bloedvaten met een kleine diameter. Humane vasculaire gladde spiercellen werden vervolgens in deze matrices gekweekt in een door ons ontwikkelde bioreactor, waarin de constructen werden geperfundeed met een pulserende stroom van kweekmedium.

In **hoofdstuk 2** wordt een overzicht gegeven van de verschillende benaderingen voor het vervaardigen van bloedvaten met een kleine diameter middels *tissue engineering*. Vele matrices gebaseerd op synthetische polymeren zoals poly(α -hydroxyzuren), bijvoorbeeld poly(glycolzuur) of poly(melkzuur), en de hiervan afgeleide copolymeren zijn voor dit doel ontwikkeld. Het gebruik van synthetische polymeren heeft bepaalde voordelen ten opzichte van natuurlijke materialen, met betrekking tot controle van de eigenschappen van het materiaal en van de matrix (bijvoorbeeld sterkte, degradatie, porositeit en microstructuur). Adhesie en proliferatie van cellen alsmede depositie van extracellulaire matrixeiwitten in deze matrices zijn echter niet optimaal. Bovendien kunnen degradatieproducten van de polymeren de lokale cellulaire omgeving en daarmee de celfunctie veranderen, waardoor de juiste ontwikkeling van een bloedvat wordt

belemmerd. Matrices gebaseerd op eiwitten, met name collageen, worden ook gebruikt voor vasculaire *tissue engineering*, vanwege hun biocompatibiliteit en biodegradeerbaarheid. Ondanks vele inspanningen is het echter nog niet gelukt om uitgaande van matrices gebaseerd op collageen, bloedvaten te vervaardigen met voldoende mechanische eigenschappen.

In het huidige project is de mogelijkheid onderzocht om de mechanische eigenschappen van collageen matrices te verbeteren middels incorporeren van het extracellulaire matrixeiwit elastine. Bovendien zijn hybride matrices ontwikkeld, bestaande uit een copolymeer van D,L-lactide en 1,3-trimethyleencarbonaat alsmede collageen. Deze hybride matrices hebben attractieve eigenschappen, omdat de geschikte mechanische eigenschappen van het copolymeer worden gecombineerd met de goede cellulaire interacties van het collageen.

Matrices bestaande uit onoplosbaar collagen type I en onoplosbaar elastine hebben betere mechanische eigenschappen (rek bij breuk en behoud van afmetingen na herhaalde elongatie) dan collageen structuren (**hoofdstuk 3**). Vlakke matrices van deze twee eiwitten vervaardigd middels vriesdrogen, hebben porositeiten tussen 90 en 98 % en porie-grootten van 130-340 μm , afhankelijk van de collageen:elastine verhouding. Een collageen:elastine ratio van 1:1 (w/w) is het meest geschikt met betrekking tot de mechanische eigenschappen. Deze matrices werden gecrosslinkt om ze geschikter te maken voor het kweken van gladde spiercellen. Collageen/elastine matrices werden gecrosslinkt in water of ethanol/water (40 % v/v) gebruikmakend van een carbodiimide (EDC) in combinatie met een succinimide (NHS), in de aanwezigheid van een Jeffamine (J230) of door reactie met butaandioldiglycidylether (BDGE) gevolgd door behandeling met EDC/NHS. Crosslinken met EDC/NHS of J230/EDC/NHS resulteert in matrices met betere mechanische eigenschappen dan ongecrosslinkte matrices, terwijl achtereenvolgende crosslinking met BDGE en EDC/NHS zeer fragiele matrices oplevert. Ethanol/water wordt bij voorkeur gebruikt als medium voor het crosslinken, omdat dan een open poreuze structuur wordt gehandhaafd, geschikt voor het kweken van gladde spiercellen.

Electrospinnen is onderzocht als alternatieve techniek voor het vervaardigen van poreuze matrices van oplosbaar collageen type I, oplosbaar elastine en mengsels van de twee eiwitten (**hoofdstuk 4**). *Non-woven* netwerken werden gesponnen uit waterige oplossingen van deze eiwitten, dus zonder gebruik van organische oplosmiddelen. Toevoegen van PEO ($M_w = 8 \cdot 10^6$) en NaCl is noodzakelijk voor het verkrijgen van continue vezels. Het benodigde voltage voor het spinnen van continue vezels is afhankelijk van de samenstelling van de te spinnen oplossing, maar altijd tussen

10 en 25 kV. De morfologie van de geproduceerde vezels is tevens afhankelijk van de samenstelling van deze oplossing. Verandering van de collageen:elastine ratio (w/w) van 2:1 tot 1:3 resulteert bijvoorbeeld in een toename van de diameter van de vezels van 220 tot 600 nm. Collageen/elastine netwerken werden gestabiliseerd door crosslinken met EDC/NHS in ethanol/water (70 % v/v). Deze behandeling resulteert in matrices met een hoge thermische stabiliteit ($T_d = 79$ °C) zonder verandering van de oorspronkelijke morfologie. Bovendien worden tijdens de wasstappen na afloop van de crosslinkingsprocedure, PEO en NaCl geheel weg gewassen. Een confluerende laag gladde spiercellen kon worden gevormd op vlakke gesponnen matrices na 14 d kweken onder stationaire omstandigheden.

Omdat in de gesponnen collageen/elastine vezels de afzonderlijke componenten niet konden worden onderscheiden door middel van SEM, werden de mogelijke interacties in collageen/elastine structuren onderzocht met behulp van vaste stof ^{13}C *cross-polarization magic angle spinning* (CP/MAS) NMR (**hoofdstuk 5**). Gevriesdroogde structuren van collageen, elastine en collageen/elastine (1:1 w/w) werden geanalyseerd bij twee vochtgehaltenes (10 ± 1 en 22 ± 1 %), omdat water van grote invloed is op de structuur en eigenschappen van beide eiwitten. De gelijktijdige aanwezigheid van beide eiwitten induceert geen detecteerbare veranderingen in de conformatie van collageen of elastine. De spin relaxatie tijden ($T_{1\rho}$) van alle protonen in collageen/elastine structuren konden worden bepaald uit mono-exponentiële curven. Dit is een aanwijzing dat er geen domeinen zijn met een verschillende mobiliteit en dat de verscheidene residuen zich exact hetzelfde gedragen, onafhankelijk van het eiwit waartoe ze behoren. Koolstof $T_{1\rho}$ waarden zijn echter hoger in het mengsel, hetgeen duidt op een lagere mobiliteit in de collageen/elastine structuur in vergelijking met de afzonderlijke componenten, waarschijnlijk ten gevolge van waterstofbruggen en hydrofobe interacties tussen beide eiwitten.

De oriëntatie van vaatwandcellen wordt *in vivo* beïnvloed door de dynamische omstandigheden waaraan de cellen onderhevig zijn. Er werd een bioreactor ontwikkeld waarin kweekmedium pulserend (120 slagen/min) wordt rondgepompt onder arteriële drukken (80-120 mmHg) door 4 parallelle bloedvatconstructen (**hoofdstuk 6**). De rheologische eigenschappen van het systeem werden gekarakteriseerd, gebruikmakend van siliconrubber buisjes of buisvormige EDC/NHS gecrosslinkte gevriesdroogde matrices van onoplosbaar collageen/elastine. De stroomsnelheid neemt lineair toe met het aantal pulsen. Gemiddelde afschuifnelheden aan de wand van 61 s^{-1} en Reynolds getallen van 20-96 zijn van dezelfde orde van grootte als die van de humane

halsslagader. De Reynolds getallen duiden op laminaire stroming, hetgeen efficiënt transport van voedingsstoffen en zuurstof naar het drie-dimensionale construct bevordert. Een toename van het gemiddelde drukverschil van 0 tot 14 mmHg gemeten over de wand en over de lengte van EDC/NHS gecrosslinkte collageen/elastine matrices gedurende 14 dagen kweken met gladde spiercellen, duidt er op dat de porositeit van de constructen afneemt gedurende de kweekperiode.

De effecten van het kweken van gladde spiercellen in (gecrosslinkte) poreuze buisvormige collageen/elastine matrices gedurende verschillende tijdsintervallen onder dynamische omstandigheden zijn ook onderzocht met betrekking tot morfologische en mechanische eigenschappen van de constructen (**hoofdstuk 7**). Gedurende het kweken is er geen mechanische ondersteuning nodig om scheuren van de (gecrosslinkte) vaten tegen te gaan. Na 7 dagen kweken zijn de gladde spiercellen homogeen verdeeld over de (EDC/NHS gecrosslinkte) constructen. Na dezelfde periode worden er echter nauwelijks cellen waargenomen aan de binnenzijde van J230/EDC/NHS gecrosslinkte matrices. Uit verder onderzoek met de EDC/NHS gecrosslinkte matrices bleek dat na 14 d kweken de stijfheid bij relatief grote mate van rek van de constructen meer dan tweevoudig toeneemt tot 38 ± 2.0 kPa, terwijl de stijfheid bij kleine elongatie verdubbelt tot 8 ± 2 kPa in vergelijking met de oorspronkelijke mechanische eigenschappen. De kracht bij breuk bedraagt 30 ± 10 kPa en de rek bij breuk 120 ± 20 %. De laatste waarde is vergelijkbaar met die van de humane darmslagader. Uit SEM analyse en histologie blijkt dat er collageen vezels partieel georiënteerd zijn in de omtrekriching en dat de gladde spiercellen aanwezig zijn in het gehele construct.

Hybride structuren van natuurlijke en synthetische polymeren zijn onderzocht als alternatieve matrices voor *tissue engineering* van bloedvaten met een kleine diameter (**hoofdstuk 8**). Volgens deze benadering worden geschikte mechanische eigenschappen gewaarborgd door het synthetische materiaal, terwijl interacties met cellen worden bevorderd door de natuurlijke component. Een copolymeer van D,L-lactide en 1,3-trimethyleencarbonaat (P(DLLAcoTMC)) bevattende 83 mol% DLLA werd hiervoor gebruikt. Buisvormige structuren met een porositeit van 98 % werden vervaardigd middels spinnen van gesmolten copolymeer gevolgd door het winden van vezels, dus zonder gebruik van organische oplosmiddelen die een negatief effect kunnen hebben op het kweken van cellen. Een microspons van collageen werd gevormd in de poriën van deze P(DLLAcoTMC) matrices, middels dipcoaten in een suspensie van onoplosbaar collageen type I gevolgd door vriesdrogen. Aldus werden hybride matrices met een porositeit van 97 % en een

gemiddelde porie-grootte van 102 μm verkregen. Na 7 d kweken onder dynamische omstandigheden hebben de gladde spiercellen zich homogeen verdeeld over de constructen, die 5 maal sterker en stijver zijn dan niet-gekweekte matrices. Waarden van de kracht bij breuk (2.8 ± 0.6 MPa), stijfheid (1.6 ± 0.4 MPa) en rek bij breuk (120 ± 20 %) zijn vergelijkbaar met die van de humane darmslagader.

Uit het onderzoek beschreven in dit proefschrift zijn veelbelovende resultaten voortgekomen voor toepassing van constructen gebaseerd op collageen voor *tissue engineering* van bloedvaten met een kleine diameter. Vele aspecten moeten echter nog worden onderzocht, zoals de vorming van een monolaag endotheelcellen op de binnenzijde van de constructen.

Sommario

La principale causa di paralisi e mortalità nel mondo occidentale è rappresentata dall'arteriosclerosi e da patologie vascolari a carico delle arterie coronarie o del sistema arterioso periferico. Attualmente la pratica medica consente l'applicazione di protesi sintetiche per la ricostruzione di vasi sanguigni con un diametro maggiore di 6 mm. Al contrario, nessun impianto protesico è attualmente disponibile se il diametro del vaso sanguigno da ricostruire è inferiore ai 6 mm. L'utilizzo di arterie e vene è possibile in alcuni casi, ma questo approccio presenta numerose limitazioni tra cui lo scarso numero di arterie disponibili e la difficoltà ad ottenere tessuti con elasticità paragonabile a quella fisiologica.

L'ingegneria tissutale è un campo interdisciplinare di ricerca che consiste nell'applicazione dei principi dell'ingegneria unitamente a quelli delle scienze chimiche, fisiche, biologiche e naturali per la ricostruzione o lo sviluppo di sostituti biologici atti a riparare, prolungare o migliorare le funzioni dei vari tessuti. Pertanto l'ingegneria tissutale rappresenta uno dei più promettenti campi di ricerca per lo sviluppo di nuovi materiali quali sostituti artificiali o parzialmente artificiali dei vasi sanguigni. Il lavoro di ricerca presentato in questa tesi si inserisce in questo contesto ed ha come scopo lo sviluppo di vasi sanguigni di piccolo diametro a partire da matrici porose tubulari, costituite da collagene, una proteina della matrice extracellulare, e da altri materiali naturali e/o sintetici. Inoltre, al fine di valutare le proprietà funzionali e di biocompatibilità delle matrici preparate, cellule muscolari lisce (SMC), derivanti dall'apparato vascolare umano, sono state coltivate sui supporti preparati in presenza di un flusso pulsante, in un bioreattore sviluppato nei nostri laboratori.

Il **capitolo 2** offre una panoramica generale dei diversi approcci utilizzati fino ad oggi per la realizzazione di vasi sanguigni di piccolo diametro. A tale scopo sono state usate numerose matrici a base di polimeri sintetici, come i poli(α -idrossi acidi), ad esempio il poli(acido glicolico) o il poli(acido lattico) ed i loro copolimeri. L'impiego di materiali sintetici presenta dei vantaggi significativi rispetto all'utilizzo di materiali di origine naturale, in quanto riduce significativamente la possibilità del contagio e dei fenomeni dovuti al rigetto, nonché permette un migliore controllo delle proprietà del materiale stesso e della matrice risultante (per esempio in termini di forza meccanica, degradazione, porosità e microstruttura). D'altra parte però, la matrice sintetica più difficilmente favorisce l'adesione e proliferazione cellulare nonché la deposizione di matrice extracellulare, fattori essenziali per garantire la funzionalità in vivo.

Inoltre, i prodotti di degradazione del polimero possono alterare il contesto biologico e quindi la funzione cellulare, limitando o impedendo lo sviluppo di un vaso sanguigno funzionale. Anche matrici costituite principalmente da proteine, specialmente collagene, sono state usate per l'ingegneria dei vasi sanguigni, grazie alla loro biocompatibilità e biodegradabilità. Sfortunatamente, però, i vasi sanguigni sviluppati a partire da collagene presentano scarse proprietà meccaniche e non possono ancora essere utilizzati a causa della loro spiccata fragilità. In questo lavoro di tesi viene presentato uno studio volto alla possibilità di migliorare le proprietà meccaniche di matrici di collagene grazie all'incorporazione di elastina, una proteina normalmente presente nella matrice extracellulare in condizioni fisiologiche. Inoltre, sono descritte anche matrici ibride di collagene e copolimeri di D-L lattato e 1,3-trimetilen carbonato. La potenzialità di queste matrici ibride è legata sia alle buone proprietà meccaniche garantite dalla presenza del copolimero sia alla elevata compatibilità in termini di adesione cellulare dovuta al collagene.

Proprietà meccaniche (specialmente in termini di allungamento a rottura e grado di recupero dell'allungamento iniziale) migliori rispetto a quelle osservate in matrici di solo collagene sono state trovate in matrici costituite da collagene insolubile di tipo I e da elastina insolubile (**capitolo 3**). Matrici piatte di questa natura, preparate tramite liofilizzazione sono risultate avere una porosità compresa tra 90 e 98% e pori di dimensioni comprese tra 130-340 μm , a seconda del rapporto in peso tra il collagene e l'elastina usata. In particolare, è stato verificato che un rapporto in peso di 1:1 tra il collagene e l'elastina consente di ottenere le migliori proprietà meccaniche. Matrici così ottenute sono state reticolate nel tentativo di soddisfare ancor meglio i requisiti per la coltura in vitro di cellule muscolari lisce. La reticolazione è stata portata a termine in acqua o in etanolo diluito con acqua (40 %v/v), grazie all'aggiunta di reticolanti sintetici, quali N-(3-dimetil amminopropil)-N'-etil carbodiimmide idrocloruro (EDC) e N-idrossi succinimide (NHS) in presenza o meno di una jaffamina (J230) o, alternativamente, con etere diglicidico butandiolo (BDGE) seguito da trattamento con EDC/NHS. La reticolazione con EDC/NHS o con J230/EDC/NHS determina un miglioramento delle proprietà meccaniche delle matrici rispetto a prima della reticolazione, mentre il trattamento con BDGE seguito da EDC/NHS rende le matrici molto fragili. Il miglior solvente durante la reticolazione è risultato l'etanolo tecnico in quanto consente di mantenere costante il diametro dei pori nelle matrici di collagene ed elastina. La presenza di pori è essenziale in quanto stimola l'adesione e garantisce la possibilità di coltivare con successo SMC.

La produzione di fibre in seguito all'applicazione di un campo elettrico, o elettrospinning, è stata scelta come metodo alternativo per la produzione di matrici porose a partire da

collagene solubile di tipo I ed elastina solubile (**capitolo 4**). Filati non tessuti sono stati ottenuti a partire da soluzioni acquose di queste proteine, evitando cosí l'uso di solventi organici. L'aggiunta di poli(ossi etilene) (PEO) (peso molecolare $8 \cdot 10^6$) e di cloruro di sodio (NaCl) si é rivelata sempre necessaria per ottenere fibre in modo continuo. Il voltaggio necessario per produrre fibre in modo continuo é risultato dipendente dalla composizione della soluzione iniziale, ma sempre compreso tra 10 e 25 kV. Anche la morfologia delle fibre prodotte é determinata dalla composizione della soluzione iniziale, i.e un aumento del rapporto in peso tra il collagene e l'elastina da 2:1 a 3:1 provoca un aumento del diametro delle fibre da 220 a 660 nm.

Le matrici di collagene e elastina cosí ottenute, sono state stabilizzate attraverso la reticolazione in acqua e etanolo (40 % v/v) con EDC/NHS. Questo trattamento consente l'ottenimento di materiali con una migliore stabilitá termica ($T_d = 79$ °C) e non altera la loro morfologia iniziale. Inoltre, la reticolazione garantisce la eliminazione di PEO e NaCl. Dopo 14 giorni di coltura in condizioni stazionarie, é stato possibile osservare la formazione di uno strato omogeneo di SMC su matrici piatte di collagene e elastina prodotte mediante l'elettrospinning.

Poiché dopo la produzione di fibre, tecniche di microscopia elettronica a scansione (SEM) non sono in grado di discriminare tra residui di collagene e di elastina, la natura delle interazioni eventualmente presenti tra le due proteine nelle fibre é stata investigata mediante spettroscopia ^{13}C -NMR allo stato solido, usando la cross-polarizzazione e l'angolo magico di rotazione (CP/MAS) (**capitolo 5**). Campioni liofilizzati di collagene, elastina o collagene ed elastina solubili (rapporto in peso 1:1) sono stati analizzati a due diversi livelli di idratazione (10 ± 1 e 22 ± 1 %). L'acqua riveste infatti un ruolo fondamentale nella struttura e nelle proprietá di entrambe le proteine. La presenza contemporanea di collagene ed elastina non induce nessun visibile cambiamento nella conformazione di nessuna delle due proteine. In tutti i casi, il tempo di rilassamento spin-reticolo nella rotating frame ($T_{1\rho}$) dei protoni dei campioni di collagene ed elastina puó essere ottenuto da curve monoesponenziali. Questo indica che nei campioni non ci sono domini caratterizzati da diversa mobilitá e che i vari residui si comportano esattamente nella stessa maniera indipendentemente dalla proteina alla quale appartengono. Al contrario, i valori di $T_{1\rho}$ relativi agli atomi di carbonio sono risultati piú elevati nelle miscele di collagene e elastina, indicando la loro minore mobilitá se paragonati con i due componenti proteici separati. Tale aumento é anche indicativo della possibile presenza di legami idrogeno e di interazioni idrofobiche tra le due proteine.

In vivo, l'orientamento delle cellule vascolari é indotto dall'ambiente dinamico a cui sono esposte. Nei nostri laboratori, é stato sviluppato un bioreattore con un flusso pulsatile, grazie al quale é stato possibile riprodurre condizioni molto simili a quelle fisiologiche sia in termini di pressione arteriosa (80-120 mmHg) che di ritmo di pulsazioni (120 battiti/min) (**capitolo 6**). Tale sistema é stato caratterizzato in termini di proprietá fluido dinamiche usando come vaso sanguigno o un tubo di silicone o una matrice tubulare liofilizzata di collagene ed elastina. É stato cosí possibile verificare che il flusso cresce con l'aumentare delle pulsazioni. Il valore medio della velocitá di flusso lungo la parete é 61 s^{-1} ed il numero di Reynolds varia tra 20 e 96, valori assai vicini a quelli misurati per la carotide degli essere umani. I valori del numero di Reynolds indicano che il flusso é laminare, il che assicura un trasporto efficiente dei nutrienti e dell'ossigeno nella matrice tridimensionale. L'aumento della caduta di pressione da 0 a circa 10 mmHg attraverso la parete o nella lunghezza di un vaso sanguigno costituito da collagene ed elastina reticolati con EDC/NHS, durante 14 gg di coltura con SMC, indica che la porositá dell'arteria prodotta diminuisce nel tempo.

Gli effetti della lunghezza e delle condizioni (stazionarie o dinamiche) della coltura di SMC su matrici tubulari (reticolate) di collagene ed elastina sono stati valutati in termini di proprietá meccaniche e morfologiche delle matrici (**capitolo 7**). Nessun supporto meccanico é stato necessario per impedire la rottura di matrici (reticolate). Dopo 7 gg di coltura, le SMC sono risultate distribuite omogeneamente sulla superficie e all'interno delle matrici (reticolate con EDC/NHS). Al contrario, quasi nessuna cellula puó essere osservata dopo 7 gg di coltura, sul lato luminale di matrici reticolate con J230/EDC/NHS. Ulteriori analisi delle matrici reticolate con EDC/NHS ha mostrato che, dopo 14 gg di coltura, ad alte percentuali di allungamento, la durezza/rigiditá delle matrici ha raggiunto valori dell'ordine degli $8 \pm 2 \text{ kPa}$, raddoppiati quindi rispetto ai valori iniziali. Lo sforzo a rottura é $30 \pm 10 \text{ kPa}$, mentre l'allungamento a rottura é $120 \pm 20 \%$. Quest'ultimo valore é paragonabile a quello misurato per un'arteria mesenterica umana. Analisi di microscopia elettronica a scansione e di istologia hanno mostrato la presenza di SMC attraverso tutta la matrice e di fibre di collagene parzialmente orientate circolarmente. Matrici ibride di polimeri naturali e sintetici sono state studiate come una possibile alternativa per la realizzazione di vasi sanguigni di diametro piccolo (**capitolo 8**). In questo modo, é possibile ottenere matrici con proprietá meccaniche soddisfacenti grazie alla presenza del materiale sintetico e, allo stesso tempo, l'interazione con le cellule é favorita dal componente naturale. Poli(D, L-lattato-co-1,3-trimetilene carbonato) [P(DLLAcoTMC)] contenente l'83% molare di DLLA é stato usato per questo scopo. Il copolimero é stato processato in strutture

tubulari aventi una porosità di circa 98% mediante melt spinning, una tecnica basata sulla produzione di fibre a partire dal fuso polimerico. Questo metodo garantisce la produzione di fibre in assenza di solventi organici che potrebbero compromettere la successiva coltura cellulare. Al momento della produzione, le fibre sono state avvolte intorno ad una bacchetta rotante che si muove anche in senso longitudinale, permettendo così la formazione di strutture tubulari porose. Una spugna microporosa di collagene è stata poi introdotta nei pori della matrice di P(DLLAcoTMC), attraverso immersione in una sospensione di collagene insolubile di tipo I e successiva liofilizzazione. In questo modo, sono state ottenute matrici ibride con una porosità del 97% e una dimensione media dei pori di 102 μm . Dopo 7 gg di coltura in un ambiente dinamico, SMC vitali sono risultate presenti in modo omogeneo in tutta la matrice. Questa è cinque volte più forte e più rigida che delle matrici prive di cellule. I valori ottenuti per la forza a rottura (2.8 ± 0.6 MPa), la rigidità (1.6 ± 0.4 MPa) e l'allungamento a rottura (120 ± 20 %) sono paragonabili con quelli misurati per l'arteria mesenterica umana.

La ricerca condotta in questa tesi porta a risultati promettenti per l'applicazione di matrici basate sul collagene nell'ingegneria di vasi sanguigni di piccolo diametro. Tuttavia, molti aspetti devono ancora essere investigati. La possibilità di formare uno strato di cellule endoteliche sul lato luminale dei vasi così prodotti è uno di questi.

Curriculum vitae

Laura Buttafoco was born on the 14th of December in Rome, Italy. In 1993 she obtained the Proficiency in English of the University of Cambridge (Great Britain). In the same year, she passed the State exams for the Scientific Liceum and entered the University La Sapienza in Rome to study Industrial Chemistry. The last two years of her university studies were mostly focused in Biotechnology. In 2000 she obtained her degree *magna cum laude*, with the dissertation “Crosslinking of Collagen-Based Materials for Neuron Regeneration” completed in cooperation with the Polymer Chemistry and Biomaterials groups in the University of Twente (Enschede, The Netherlands) where she worked during a 6-months Erasmus grant. Thereafter, she joined this latter same group to pursue her Ph.D. degree under the supervision of Prof. Dr. J. Feijen and Prof. Dr. I. Vermes. The aim and the results of her project, “Collagen-Based Scaffolds for Tissue Engineering of Small-Diameter Blood Vessels” are described in this thesis.